



日中笹川医学奨学金制度
第42期（学位取得コース）

報 告 書

2020年4月～2022年3月

公益財団法人 日中医学協会

目 次

| No. | 氏名 | 所属機関 | 研究先 | 指導責任者 | 頁数 |
|-----|--------------------------------|---|---------------------------------|---------|--------|
| G1 | 趙 景敏 チヨウ ケイミン (論文博士) | 吉林大学中日聯誼医院 | 福島県立医科大学 | 伊藤 浩 | ……P1 |
| | | 主治医師 | 放射線医学講座 | 教授 | |
| | | 研究テーマ：脳神経画像を用いた虚血性脳血管障害の治療効果・予後評価の研究 | | | |
| G2 | 焦 丹丹 シヨウ タンタン (課程博士) | 河南科技大学第一附属医院 | 筑波大学大学院人間総合科学研究科 | 安梅 勅江 | ……P35 |
| | | 主管護師 | 国際発達ケア：エンパワメント科学研究室 | 教授 | |
| | | 研究テーマ：地域在住慢性疾患高齢者の機能維持の支援方法の解明 | | | |
| G3 | 張 碧航 チヨウ ヒキコウ (課程博士) | 中南大学湘雅医院 | 自治医科大学 | 吉村 浩太郎 | ……P94 |
| | | 大学院生 | 外科学講座 | 教授 | |
| | | 研究テーマ：幹細胞培養上清成分を用いた再生医療の開発 | | | |
| G4 | 劉 霄 リュウ ショウ (課程博士) | 慶應義塾大学医学部 | 慶應義塾大学医学部・医学研究科 | 根岸 一乃 | ……P100 |
| | | 大学院生 | 眼科学教室 | 教授 | |
| | | 研究テーマ：東アジア人におけるABCA4関連網膜症の臨床的・分子遺伝学的調査 | | | |
| G5 | 孟 華川 モウ カン (課程博士) | 中日友好医院院 | 国際医療福祉大学大学院 | 島崎 謙治教授 | ……P174 |
| | | 通訳（日本プロジェクト担当） | 医療福祉経営専攻 医療経営管理分野 医学研究科 医学専攻 | 桐生 茂教授 | |
| | | 研究テーマ：遠隔医療の導入効果及び推進方策(副題)日本の遠隔画像診断の中国への展開を中心に | | | |
| G6 | 翟 達 チキ タツ (課程博士) | 長崎大学大学院 | 長崎大学原爆後障害医療研究所 | 李 桃生 | ……P180 |
| | | 大学院生 | 幹細胞生物学研究分野 | 教授 | |
| | | 研究テーマ：メカノストレスが癌細胞に与える影響と機序 | | | |

日中笹川医学奨学金制度(学位取得コース)評価書

論文博士：指導教官用



第 42 期

研究者番号： G4201

作成日： 2022 年 3 月 1 日

| | | | | | | |
|-----------|---|-----|----|-------------------------------|------|--------------|
| 氏名 | Zhao Jingmin | 趙景敏 | 性別 | M | 生年月日 | 1987. 02. 25 |
| 所属機関(役職) | 吉林大学中日聯誼医院神経内科(主治医師) | | | | | |
| 研究先(指導教官) | 福島県立医科大学放射線医学講座(伊藤浩教授) | | | | | |
| 研究テーマ | 脳神経画像を用いた虚血性脳血管障害の治療効果・予後評価の研究 Investigation of pathophysiology of ischemic cerebrovascular diseases using neuroimaging techniques | | | | | |
| 専攻種別 | <input checked="" type="checkbox"/> 論文博士 | | | <input type="checkbox"/> 課程博士 | | |

研究者評価(指導教官記入欄)

| 成績状況 | 優 良 可 不可 | 取得単位数 |
|---------------|--|---|
| | | 取得単位数/取得すべき単位数総数 |
| 学生本人が行った研究の概要 | (優) | |
| 総合評価 | <p>1) 核医学的分子イメージング手法を用いた脳神経機能損傷の評価法の開発 びまん性軸索損傷(DAI)ラットモデル作成に成功した。DAI発生24時間後、神経学的重症度スコア(NSS)の低下、¹⁸F-FDG PETの脳画像における脳糖代謝の低下が認められた。またDAIラットの脳病理組織において、脳損傷のバイオマーカーのAmyloid precursor protein (APP)の陽性所見が認められた。</p> <p>2) 自然衰弱超高齢マウスにおける脳糖代謝異常・インシュリン耐性発生について、核医学的分子イメージング手法を用いて、超高齢マウス(96週齢)における全身及び脳局所の糖代謝変化の評価を行うと同時に漢方薬・人参養栄湯が超高齢マウスの糖代謝異常・インシュリン耐性に対する改善作用効果の評価を行った。その結果、超高齢マウスにおいて、核医学的分子イメージング手法を用いて、加齢に伴うインシュリン耐性による各臓器、特に脳局所の糖代謝が低下したこと、さらに人参養栄湯が脳インシュリン耐性(糖代謝低下)を改善できる可能性を明らかにした。</p> <p>【良かった点】 1) DPAラットモデル作成に成功し、世界で初めて核医学的分子イメージングを用いたDPAの評価法の開発を試み、ポジティブな結果を得られ、今後の発展に繋がったこと。 2) 世界で初めて、自然衰弱超高齢(96週齢)マウス(ヒト70歳高齢相当)の全身及び脳局所における糖代謝変化を評価すると同時に、漢方薬・人参養栄湯による超高齢マウスの糖代謝異常・インシュリン抵抗の改善効果を評価し、短期間で研究成果を2篇の論文にまとめて発表できたこと。</p> <p>【改善すべき点】 DAIラットモデル作成において、DAIモデルの成功率と再現性を向上させるためには、DAIモデル作成装置の改善とが必要であると思う。しかし、これには高いコストがかかる。¹⁸F-FDG PET画像解析法と病理組織学的評価においても更なる検討が必要であると思う。</p> <p>【今後の展望】 DAIラットモデルにおける、骨髄間質細胞(BMSC)の移植治療を展開すること、BMSCの移植治療によるDAIラットの脳機能障害の改善を¹⁸F-FDG PET等核医学的分子イメージング手法を用いて実証できることを大いに期待する。</p> | |
| 学位取得見込 | | すでにインパクトファクターが4を超えた英文雑誌に2篇論文と症例報告英文論文を発表した。また本学の論文博士に係る学識認定試験(外国語)にも合格しているので、在学期間中に博士学位申請を行って、学位取得の見込みが十分あったが、新型コロナウイルス拡大のため、博士学位申請を見送った。2022年中の学位取得を目指す。 |
| 評価者(指導教官名) | | 伊藤 浩 |

日中笹川医学奨学金制度(学位取得コース)報告書 研究者用



第42期

研究者番号: G4201

作成日: 2022年3月1日

| | | | | | |
|---|---|-------------------------------------|------|--------------------------|-------------------|
| 氏名 | Zhao Jingmin | 趙景敏 | 性別 | M | 生年月日 1987. 02. 25 |
| 所属機関(役職) | 吉林大学中日聯誼医院神経内科(主治医師) | | | | |
| 研究先(指導教官) | 福島県立医科大学放射線医学講座(伊藤浩教授) | | | | |
| 研究テーマ | 脳神経画像を用いた虚血性脳血管障害の治療効果・予後評価の研究 Investigation of pathophysiology of ischemic cerebrovascular diseases using neuroimaging techniques | | | | |
| 専攻種別 | 論文博士 | <input checked="" type="checkbox"/> | 課程博士 | <input type="checkbox"/> | |
| 1. 研究概要(1) | | | | | |
| 1) 目的(Goal) Exploring changes of glucose metabolism by ¹⁸ F-FDG PET in diffuse axonal injury (DAI) rat model | | | | | |
| 2) 戦略(Approach) | | | | | |
| ① Make the rat DAI model | | | | | |
| ② Perform the ¹⁸ F-FDG PET imaging | | | | | |
| ③ Perform the neurological assessments | | | | | |
| ④ Perform the immunohistochemical analysis | | | | | |
| 3) 材料と方法(Materials and methods) | | | | | |
| We used Marmarou's weight drop model for this study. In this model, the energy of impact is applied via a 500g steel block that falls freely from a designated height through a Plexiglas tube. The rat skull is exposed by a midline incision. A stainless steel disc is mounted on the skull midline between the lambda and the bregma to prevent skull fracture. The rats are then placed on a foam bed and subjected to the impact by dropping the steel block onto the stainless steel disc. After palinesthesia, neurological severity score (NSS) is determined. We used the modified Morris Water Maze (MWM) test in a blind manner to investigate learning and memory processes in rats. Then ¹⁸ F-FDG PET was carried out before and 24 hours after making DAI model. The blood glucose level measured every time before ¹⁸ F-FDG PET. After the last scan, the rats were sacrificed 90min after ¹⁸ F-FDG injection. The brains were removed, stored in 10% paraformaldehyde for 24 hours, then chaged into the 1% paraformaldehyde for several days. After formalin-fixed and paraffin-embedded, 4-μm-thick coronal sections of brain tissue were used for immunohistochemical staining and analysis. Each section was treated with antibodies against β-APP. | | | | | |
| 4) 実験結果(Results) | | | | | |
| Compared with before the injury, the weight of rat dropped significantly after the injury. ¹⁸ F-FDG PET images showed that glucose metabolism was reduced in animals with DAI after 24 hours. The overall curve shows a downward trend. Neurological severity score (NSS) was reduced in animals with DAI after 24h. APP positive injured axons were found in DAI rat model. | | | | | |
| 5) 考察(Discussion) | | | | | |
| The tracer used in microPET, 2-[¹⁸ F]-fluoro-2-deoxy-D-glucose (¹⁸ F-FDG), is a well-known radiotracer that has frequently been used as a marker of brain glucose metabolism. Because the glucose is the primary fuel source under normal conditions in the adult, the level of glucose utilization correlates with the degree of neuronal activity. We found that ¹⁸ F-FDG PET images showed that glucose metabolism was reduced in APP positive DAI rat model and neurological severity score (NSS) was reduced in animals with DAI after 24 hours. These results demonstrate that injury-induced hypometabolism in the brain at the acute stage of DAI were correlated with neural dysfunctions. We need to further study and expand the sample size to confirm this result. | | | | | |
| 6) 参考文献(References) | | | | | |
| [1] J. Li, L. Gu, D.F. Feng, F. Ding, G. Zhu, and J. Rong. Exploring temporospatial changes in glucose metabolic disorder, learning, and memory dysfunction in a rat model of diffuse axonal injury. J Neurotrauma 2012;29:2635-2646. | | | | | |
| [2] M.M. van Eijck, G.G. Schoonman, J. van der Naalt, J. de Vries, and G. Roks. Diffuse axonal injury after traumatic brain injury is a prognostic factor for functional outcome: a systematic review and meta-analysis. Brain Inj 2018;32:39 | | | | | |
| [3] W. Zheng, C. Ma, L. Kong, X. Chen, and W. Fan. Detecting diffuse axonal injury in rat brainstems by diffusion tensor imaging and AQP4 expression. Biomed Mater Eng 2015;26(Suppl 1):S1169-1175. | | | | | |
| [4] V.E. Johnson, W. Stewart, M.T. Weber, D.K. Cullen, R. Siman, and D.H. Smith. SNTF immunostaining reveals previously undetected axonal pathology in traumatic brain injury. Acta Neuropathol 2016;131:115-135. | | | | | |

1. 研究概要(2)

1) 目的(Goal)

The aim of this study is to evaluate the effect of Ninjin'yoeito (NYT) on regional brain glucose metabolism in aged wild-type mice.

2) 戦略(Approach)

- ① Evaluate organ glucose metabolism by ^{18}F -FDG accumulation with insulin loading in aged mice compared with young normal mice.
- ② Evaluate the regional brain glucose metabolism by ^{18}F -FDG accumulation with insulin loading in aged mice compared with young normal mice.
- ③ Evaluate the effect of Ninjin'yoeito (NYT) on regional brain glucose metabolism by ^{18}F -FDG autoradiography with insulin loading in aged mice.

3) 材料と方法(Materials and methods)

In the first step, each animal was initially anesthetized with 4% isoflurane in air and maintained via spontaneous ventilation with 2% isoflurane in air. ^{18}F -FDG (11.5 MBq/0.1 ml) was injected into the tail vein. Ninety minutes later, the animals were sacrificed and their organs were excised. The radioactivity of organs, muscle, heart, lungs, spleen, pancreas, white adipose tissue (superior pole of epididymis), testes, stomach, small intestine, large intestine, kidneys, liver, brown adipose tissue (between the shoulder blades), and brain were determined with a gamma counter. In the second step, eight-week-old and 96-week-old male mice ($n = 6$, each group) were assigned to the control and insulin-loaded groups, then perform the ^{18}F -FDG autoradiography. In the third step, after 12 weeks of feeding NYT, mice were assigned to the control and insulin-loaded groups and received an intraperitoneal injection of human insulin (2 U/kg body weight) 30 minutes prior to ^{18}F -FDG injection. Ninety minutes after the injection, brain autoradiography was performed.

4) 実験結果(Results)

In the untreated groups, the levels of ^{18}F -FDG accumulation in the blood, plasma, muscle, lungs, spleen, pancreas, testes, stomach, small intestine, kidneys, liver, brain, and brain regions, namely, the cortex, striatum, thalamus, and hippocampus, were all significantly higher in the aged mice. The treated group showed lower ^{18}F -FDG accumulation levels in the pancreas and kidneys, as well as in the cortex, striatum, thalamus, and hippocampus in the aged mice than the untreated groups, whereas higher ^{18}F -FDG accumulation levels were observed in those in the young mice. After insulin loading, the ^{18}F -FDG accumulation showed negative changes in the cortex, striatum, thalamus, and hippocampus in the control group, whereas positive changes were observed in the NYT-treated group.

5) 考察(Discussion)

These results demonstrate that insulin loading decreases effect on ^{18}F -FDG accumulation levels in some organs of the aged mice. In the young mice group, the levels of ^{18}F -FDG accumulation in the cortex, striatum, and hippocampus significantly increased after insulin loading. Compared with the young group, the levels of ^{18}F -FDG accumulation in the striatum, thalamus and hippocampus in the aged group did not markedly change after insulin loading. In contrast, the level of ^{18}F -FDG accumulation in the cortex significantly decreased after insulin loading in the aged group. Aging is associated with reductions in the levels of both insulin and its receptor in the brain, which may even cause the brain to be in the state of insulin resistance. Ninjin'yoeito could improve the glucose metabolism dysfunction in brain regions in aged mice. Ninjin'yoeito may potentially reduce insulin resistance in the brain regions in aged mice, thereby preventing age-related brain diseases.

6) 参考文献(References)

- [1] C. Kudoh, R. Arita, M. Honda, T. Kishi, Y. Komatsu, H. Asou, and M. Mimura. Effect of ninjin'yoeito, a Kampo (traditional Japanese) medicine, on cognitive impairment and depression in patients with Alzheimer's disease: 2 years of observation. *Psychogeriatrics* 2016;16:85-92.
- [2] S. Suzuki, F. Aihara, M. Shibahara, and K. Sakai. Safety and Effectiveness of Ninjin'yoeito: A Utilization Study in Elderly Patients. *Front Nutr* 2019;6:14.
- [3] G.M. Martin, The biology of aging: 1985-2010 and beyond. *Faseb J* 2011;25: 3756-3762.
- [4] J. Xiao, J. Weng, L. Ji, W. Jia, J. Lu, Z. Shan, J. Liu, H. Tian, Q. Ji, Z. Yang, and W. Yang. Worse pancreatic β -cell function and better insulin sensitivity in older Chinese without diabetes. *J Gerontol A Biol Sci Med Sci* 2014;69:463-170.
- [5] B. Cholerton, L.D. Baker, and S. Craft. Insulin resistance and pathological brain ageing. *Diabet Med* 2011;28:1463-1475.
- [6] W.A. Banks, J.B. Jaspán, and A.J. Kastin, Effect of diabetes mellitus on the permeability of the blood-brain barrier to insulin. *Peptides* 18 (1997) 1577-84.
- [7] G.J. Biessels, L.P. van der Heide, A. Kamal, R.L. Bley, and W.H. Gispen. Ageing and diabetes: implications for brain function. *Eur J Pharmacol* 2002;441:1-14.
- [8] H.N. Frazier, K.L. Anderson, S. Maimaiti, A.O. Ghoweri, S.D. Kraner, G.J. Popa, K.K. Hampton, M.D. Mendenhall, C.M. Norris, R.J. Craven, and O. Thibault. Expression of a Constitutively Active Human Insulin Receptor in Hippocampal Neurons Does Not Alter VGCC Currents. *Neurochem Res* 2019;44:269-280.
- [9] E.M. Rhea, and W.A. Banks, Role of the Blood-Brain Barrier in Central Nervous System Insulin Resistance. *Front Neurosci* 2019;13:521.
- [10] L.M. Voipio-Pulkki, P. Nuutila, M.J. Knuuti, U. Ruotsalainen, M. Haaparanta, M. Teräs, U. Wegelius, and V.A. Koivisto. Heart and skeletal muscle glucose disposal in type 2 diabetic patients as determined by positron emission tomography. *J Nucl Med* 1993;34:2064-2067.

2. 執筆論文 Publication of thesis ※記載した論文を添付してください。Attach all of the papers listed below.

| | | | | | | |
|---------------------------|---|------------------------|---------------|-----------------------|----------------|---------|
| 論文名 1 Title | Evaluation of Effect of Ninjin'yoeito on Regional Brain Glucose Metabolism by ¹⁸ F-FDG Autoradiography With Insulin Loading in Aged Mice | | | | | |
| 掲載誌名 Published journal | FRONTIERS IN NUTRITION | | | | | |
| | 2021 年 5 月 | 8 巻(号) | 657663 頁 ~ | 頁 | 言語 Language | English |
| 第1著者名 First author | Zhao, Jingmin | 第2著者名 Second author | Imai, Ryota | 第3著者名 Third author | Ukon, Naoyuki | |
| その他著者名 Other authors | Shimoyama, Saki; Tan, Chengbo; Maejima, Yuko; Omiya, Yuji; Takahashi, Kazuhiro; Nan, Guangxian; Zhao, Songji; Ito, Hiroshi; Shimomura, Kenju | | | | | |
| 論文名 2 Title | Evaluation of organ glucose metabolism by ¹⁸ F-FDG accumulation with insulin loading in aged mice compared with young normal mice | | | | | |
| 掲載誌名 Published journal | SCIENTIFIC REPORTS | | | | | |
| | 2021 年 4 月 | 11(1) 巻(号) | 7421 頁 ~ | 頁 | 言語 Language | English |
| 第1著者名 First author | Zhao, Jingmin | 第2著者名 Second author | Chengbo Tan | 第3著者名 Third author | Ryota Imai | |
| その他著者名 Other authors | Naoyuki Ukon; Saki Shimoyama; Yuko Maejima; Yuji Omiya; Kazuhiro Takahashi; Hiroshi Ito; Guangxian Nan; Songji Zhao; Kenju Shimomura | | | | | |
| 論文名 3 Title | Bilateral Medial Medullary Infarction Accompanied by Cerebral Watershed Infarction: A case report | | | | | |
| 掲載誌名 Published journal | Journal of Radiology Case Reports | | | | | |
| | 2020 年 4 月 | 14 (4) 巻(号) | 1 頁 ~ | 7 頁 | 言語 Language | English |
| 第1著者名 First author | Jingmin Zhao | 第2著者名 Second author | Guangxian Nan | 第3著者名 Third author | Guangxun Shen | |
| その他著者名 Other authors | Songji Zhao; Hiroshi Ito | | | | | |
| 論文名 4 Title | | | | | | |
| 掲載誌名 Published journal | | | | | | |
| | 年 月 | 巻(号) | 頁 ~ | 頁 | 言語 Language | |
| 第1著者名 First author | | 第2著者名 Second author | | 第3著者名 Third author | | |
| その他著者名 Other authors | | | | | | |
| 論文名 5 Title | | | | | | |
| 掲載誌名 Published journal | | | | | | |
| | 年 月 | 巻(号) | 頁 ~ | 頁 | 言語 Language | |
| 第1著者名 First author | | 第2著者名 Second author | | 第3著者名 Third author | | |
| その他著者名 Other authors | | | | | | |

3. 学会発表 Conference presentation ※筆頭演者として総会・国際学会を含む主な学会で発表したものを記載してください

※Describe your presentation as the principal presenter in major academic meetings including general meetings or international meetings

| | | | | |
|-----------------------|--|-------------|--|--|
| 学会名 Conference | 第68回米国核医学・分子イメージング学会 (SNMMI2021 Annual Meeting) | | | |
| 演題 Topic | Evaluation of effect of Ninjin'yoeito on regional brain glucose metabolism by ¹⁸ F-FDG autoradiography with insulin loading in superaged mice | | | |
| 開催日 date | 2021 年 6 月 11 日 | 開催地 venue | Virtual Edition | |
| 形式 method | <input type="checkbox"/> 口頭発表 Oral <input checked="" type="checkbox"/> ポスター発表 Poster | 言語 Language | <input type="checkbox"/> 日本語 <input checked="" type="checkbox"/> 英語 <input type="checkbox"/> 中国語 | |
| 共同演者名 Co-presenter | Zhao J; Imai R; Ukon N; Shimoyama S; Tan C; Maejima Y; Omiya Y; Takahashi K; Nan G; Zhao S; Ito H; Shimomura K | | | |
| 学会名 Conference | 第61回日本核医学会学術総会 | | | |
| 演題 Topic | ¹⁸ F-FDG ARGを用いた超高齢マウスの局所脳代謝に対する人参栄養湯の効果評価 | | | |
| 開催日 date | 2021 年 11 月 4 日 | 開催地 venue | 名古屋 | |
| 形式 method | <input checked="" type="checkbox"/> 口頭発表 Oral <input type="checkbox"/> ポスター発表 Poster | 言語 Language | <input checked="" type="checkbox"/> 日本語 <input type="checkbox"/> 英語 <input type="checkbox"/> 中国語 | |
| 共同演者名 Co-presenter | 趙景敏; 今井亮太; 右近直之; 下山彩希; 前島裕子; 大宮雄司; 高橋和弘; 南光賢; 趙松吉; 下村健寿; 伊藤浩 | | | |
| 学会名 Conference | | | | |
| 演題 Topic | | | | |
| 開催日 date | 年 月 日 | 開催地 venue | | |
| 形式 method | <input type="checkbox"/> 口頭発表 Oral <input type="checkbox"/> ポスター発表 Poster | 言語 Language | <input type="checkbox"/> 日本語 <input type="checkbox"/> 英語 <input type="checkbox"/> 中国語 | |
| 共同演者名 Co-presenter | | | | |
| 学会名 Conference | | | | |
| 演題 Topic | | | | |
| 開催日 date | 年 月 日 | 開催地 venue | | |
| 形式 method | <input type="checkbox"/> 口頭発表 Oral <input type="checkbox"/> ポスター発表 Poster | 言語 Language | <input type="checkbox"/> 日本語 <input type="checkbox"/> 英語 <input type="checkbox"/> 中国語 | |
| 共同演者名 Co-presenter | | | | |

4. 受賞(研究業績) Award (Research achievement)

| | | | |
|------------------|---------------|----------------------|-----|
| 名称 Award name | 国名 Country | 受賞年 Year of award | 年 月 |
| 名称 Award name | 国名 Country | 受賞年 Year of award | 年 月 |

5. 本研究テーマに関わる他の研究助成金受給 Other research grants concerned with your research theme

| | |
|--------------------------|---|
| 受給実績 Receipt record | <input type="checkbox"/> 有 <input type="checkbox"/> 無 |
| 助成機関名称 Funding agency | |
| 助成金名称 Grant name | |
| 受給期間 Supported period | 年 月 ~ 年 月 |
| 受給額 Amount received | 円 |
| 受給実績 Receipt record | <input type="checkbox"/> 有 <input type="checkbox"/> 無 |
| 助成機関名称 Funding agency | |
| 助成金名称 Grant name | |
| 受給期間 Supported period | 年 月 ~ 年 月 |
| 受給額 Amount received | 円 |

6. 他の奨学金受給 Another awarded scholarship

| | |
|---------------------------|---|
| 受給実績 Receipt record | <input type="checkbox"/> 有 <input type="checkbox"/> 無 |
| 助成機関名称 Funding agency | |
| 奨学金名称 Scholarship name | |
| 受給期間 Supported period | 年 月 ~ 年 月 |
| 受給額 Amount received | 円 |

7. 研究活動に関する報道発表 Press release concerned with your research activities

※記載した記事を添付してください。Attach a copy of the article described below

| | | | |
|--------------------------|--|--------------------------|--------------------------|
| 報道発表 Press release | <input checked="" type="checkbox"/> 有 <input type="checkbox"/> 無 | 発表年月日 Date of release | 1)2021年5月24日 2)2021年6月9日 |
| 発表機関 Released medium | 福島県立医科大学 | | |
| 発表形式 Release method | ・新聞 ・雑誌 ・Web site ・記者発表 ・ <input checked="" type="checkbox"/> その他(大学Web NEWS(研究成果)) | | |
| 発表タイトル Released title | 1)高齢マウスと若齢マウスにおける臓器糖代謝の評価:インシュリン負荷による18F-FDGの取り込みの潜在力の比較 2)高齢マウスの局所脳糖代謝に対する人参栄養湯の効果:インシュリン負荷による18F-FDG オートラジオグラフィーの画像手法を用いた評価 | | |

8. 本研究テーマに関する特許出願予定 Patent application concerned with your research theme

| | | | |
|----------------------------------|---|--------------------|--|
| 出願予定 Scheduled | <input type="checkbox"/> 有 <input type="checkbox"/> 無 | 出願国 Application | |
| 出願内容(概要) Application contents | | | |

9. その他 Others

| |
|--|
| |
|--|

指導責任者(記名) 伊藤 浩



OPEN

Evaluation of organ glucose metabolism by ^{18}F -FDG accumulation with insulin loading in aged mice compared with young normal mice

Jingmin Zhao^{1,2,8}, Chengbo Tan^{3,4,8}, Ryota Imai^{5,6}, Naoyuki Ukon⁴, Saki Shimoyama⁴, Yuko Maejima⁵, Yuji Omiya⁶, Kazuhiro Takahashi⁴, Hiroshi Ito^{2,4}, Guangxian Nan¹✉, Songji Zhao^{4,7}✉ & Kenju Shimomura⁵

It is important to determine the functional changes of organs that occur as a result of aging, the understanding of which may lead to the maintenance of a healthy life. Glucose metabolism in healthy bodies is one of the potential markers used to evaluate the changes of organ function. Thus, information about normal organ glucose metabolism may help to understand the functional changes of organs. [^{18}F]-Fluoro-2-deoxy-2-D-glucose (^{18}F -FDG), a glucose analog, has been used to measure glucose metabolism in various fields, such as basic medical research and drug discovery. However, glucose metabolism changes in aged animals have not yet been fully clarified. The aim of this study is to evaluate changes in glucose metabolism in organs and brain regions by measuring ^{18}F -FDG accumulation and ^{18}F -FDG autoradiography with insulin loading in aged and young wild-type mice. In the untreated groups, the levels of ^{18}F -FDG accumulation in the blood, plasma, muscle, lungs, spleen, pancreas, testes, stomach, small intestine, kidneys, liver, brain, and brain regions, namely, the cortex, striatum, thalamus, and hippocampus, were all significantly higher in the aged mice. The treated group showed lower ^{18}F -FDG accumulation levels in the pancreas and kidneys, as well as in the cortex, striatum, thalamus, and hippocampus in the aged mice than the untreated groups, whereas higher ^{18}F -FDG accumulation levels were observed in those in the young mice. These results demonstrate that insulin loading decreases effect on ^{18}F -FDG accumulation levels in some organs of the aged mice. Therefore, aging can increase insulin resistance and lead to systemic glucose metabolism dysfunction.

With a globally aging population, the health issues caused by aging and age-related diseases have become inevitable challenges for all countries. Understanding the functional changes of organs that occur as a result of aging is essential to prevent these age-related diseases, including Alzheimer's disease (AD), Parkinson's disease (PD), dementia, stroke, peripheral neuropathy, macular degeneration, cataracts, senile deafness, diabetes mellitus, osteoporosis, osteoarthritis, atherosclerosis, prostatic hyperplasia, and even cancer¹. In particular, the metabolism of glucose as an energy source has been regarded as a potential indicator for these disorders.

Under tight hormonal control by insulin, glucose homeostasis is maintained by a balance among glucose ingestion, utilization, and production². As age advances, glucose homeostasis tends to gradually become disrupted, giving rise to type 2 diabetes (T2D) and cardiovascular diseases^{3–5}. Insulin resistance is one of the major mechanisms underlying abnormal glucose tolerance⁶. Recognition of abnormal glucose metabolism in the elderly

¹Department of Neurology, China-Japan Union Hospital of Jilin University, 126 XianTai Street, Changchun 130031, Jilin, China. ²Department of Radiology and Nuclear Medicine, Fukushima Medical University, Fukushima, Japan. ³Department of Neurosurgery, Shanghai East Hospital, Tongji University School of Medicine, Shanghai, China. ⁴Advanced Clinical Research Center, Fukushima Global Medical Science Center, Fukushima Medical University, Fukushima 960-1295, Japan. ⁵Department of Bioregulation and Pharmacological Medicine, Fukushima Medical University, Fukushima, Japan. ⁶Tsumura Kampo Research Laboratories, Kampo Research & Development Division, Tsumura & Co., Ibaraki, Japan. ⁷Basic Medical College of Jilin University, Changchun, China. ⁸These authors contributed equally: Jingmin Zhao and Chengbo Tan. ✉email: nangx@jlu.edu.cn; zhao-s@fmu.ac.jp

| | Young group | | Aged group | |
|---------------|-----------------|----------------------------|-----------------------------|----------------------------|
| | Control (n = 5) | Insulin (n = 5) | Control (n = 5) | Insulin (n = 4) |
| Body weight | 22.0 ± 0.9 | 22.2 ± 1.2 | 30.04 ± 0.8 ^{####} | 31.9 ± 2.4 ^{####} |
| Blood glucose | 91.4 ± 9.9 | 24.0 ± 6.8 ^{####} | 95.0 ± 13.6 | 22.3 ± 3.9 ^{####} |

Table 1. Body weight (g) and blood glucose concentration (mg/dl) in organ ¹⁸F-FDG accumulation study. Data in parentheses are mean ± SD. Control, control group; Insulin, insulin-loaded group. ^{####}*P* < 0.0001 vs control value. ^{####}*P* < 0.0001 vs young groups in control and insulin-loaded groups.

| | Young groups | | Aged groups | |
|--|-----------------|-----------------|-------------------------------|-------------------------------|
| | Control (n = 5) | Insulin (n = 5) | Control (n = 5) | Insulin (n = 4) |
| Muscle | 0.128 ± 0.019 | 0.116 ± 0.019 | 0.136 ± 0.023 | 0.125 ± 0.036 |
| Heart | 0.088 ± 0.008 | 0.093 ± 0.007 | 0.132 ± 0.013 ^{***} | 0.129 ± 0.007 ^{**} |
| Lung | 0.115 ± 0.010 | 0.105 ± 0.009 | 0.160 ± 0.013 ^{***} | 0.155 ± 0.013 ^{**} |
| Spleen | 0.049 ± 0.004 | 0.047 ± 0.006 | 0.086 ± 0.018 ^{**} | 0.067 ± 0.013 [*] |
| Pancreas | 0.091 ± 0.023 | 0.099 ± 0.027 | 0.163 ± 0.018 ^{***} | 0.173 ± 0.016 ^{**} |
| White adipose tissue (superior pole of epididymis) | 0.070 ± 0.014 | 0.081 ± 0.014 | 0.141 ± 0.055 [*] | 0.185 ± 0.055 ^{**} |
| Testis | 0.086 ± 0.007 | 0.079 ± 0.011 | 0.097 ± 0.003 [*] | 0.096 ± 0.007 [*] |
| Stomach | 0.110 ± 0.008 | 0.119 ± 0.009 | 0.164 ± 0.011 ^{####} | 0.181 ± 0.011 ^{####} |
| Small intestine | 0.825 ± 0.042 | 0.891 ± 0.092 | 1.224 ± 0.021 ^{####} | 1.343 ± 0.126 ^{####} |
| Large intestine | 0.115 ± 0.010 | 0.111 ± 0.010 | 0.129 ± 0.012 | 0.138 ± 0.013 ^{**} |
| Kidney | 0.264 ± 0.005 | 0.277 ± 0.014 | 0.433 ± 0.022 ^{####} | 0.476 ± 0.086 ^{**} |
| Liver | 0.885 ± 0.029 | 0.895 ± 0.063 | 1.134 ± 0.073 ^{####} | 1.125 ± 0.240 |
| Brown adipose tissue (between the shoulder blades) | 0.053 ± 0.006 | 0.049 ± 0.011 | 0.057 ± 0.013 | 0.062 ± 0.013 |
| Brain | 0.331 ± 0.016 | 0.330 ± 0.014 | 0.345 ± 0.017 | 0.340 ± 0.023 |

Table 2. Weights of organs in mice (g). Data in parentheses are mean ± SD. Control, control group; Insulin, insulin-loaded group. ^{*}*P* < 0.05, ^{**} *P* < 0.01, ^{***} *P* < 0.001, ^{####} *P* < 0.0001 vs young groups in control and insulin-loaded groups.

is important in implementing age-appropriate preventive and therapeutic strategies. It is widely accepted that aging is accompanied by an increase in insulin resistance^{7,8}. This age-related insulin resistance has been variously attributed to several factors, including mitochondrial dysfunctions, reduced lean muscle mass and elevated adiposity, hormonal changes, increased oxidative stress, inflammation, and reduced physical activity^{9–14}. However, these studies do not provide insights into organ-specific differences in insulin resistance.

The glucose analog [¹⁸F]-Fluoro-2-deoxy-2-d-glucose (¹⁸F-FDG), a molecular imaging probe, is widely used in nuclear medicine for evaluating tissue glucose utilization and glucose metabolism^{15–17}. Although ¹⁸F-FDG accumulation has been investigated in various fields, such as basic medical research and drug discovery, changes in glucose metabolism evaluated using ¹⁸F-FDG in aged animals have not yet been fully clarified. Determining whether ¹⁸F-FDG distribution is associated with aging could provide insight into metabolic changes and help to prevent age-related diseases.

Therefore, in this study, we attempted to clarify the changes in glucose metabolism that occur with aging by comparing ¹⁸F-FDG accumulation levels after insulin loading in aged and young wild-type mice.

Results

Organ ¹⁸F-FDG accumulation experiment in control groups. The body weight and blood glucose level were determined in young and aged mice groups (Table 1).

The weight of organ level was determined in young and aged mice groups (Table 2). The levels of organ ¹⁸F-FDG accumulation were determined in young and aged mice groups (Table 3). The body weight of the aged mice was significantly higher than that of the young mice (Table 1). The blood glucose concentration was not significantly different between two groups (Table 1). The weights of the heart, lungs, spleen, pancreas, white adipose tissue, testes, stomach, small intestine, kidneys and liver were significantly higher in the aged mice than in the young mice (Table 2). Apart from the white adipose tissue, brown adipose tissue, large intestine, and heart, the levels of ¹⁸F-FDG uptake in the blood, plasma, muscle, lungs, spleen, pancreas, testes, stomach, small intestine, kidneys, liver and brain were all significantly higher in the aged mice than in the young mice (Table 3).

Changes in ¹⁸F-FDG accumulation level in organs. In the young mice group, the levels of ¹⁸F-FDG uptake in the muscle, heart, pancreas, white adipose tissue, stomach, kidneys, brown adipose tissue, and brain significantly increased after insulin loading. In contrast, the levels of ¹⁸F-FDG uptake in the blood, plasma,

| | Young groups | | Aged groups | |
|--|-----------------|-------------------|-----------------|-------------------|
| | Control (n = 5) | Insulin (n = 5) | Control (n = 5) | Insulin (n = 4) |
| Blood | 0.019 ± 0.002 | 0.010 ± 0.000**** | 0.033 ± 0.002 | 0.012 ± 0.002**** |
| Blood plasma | 0.015 ± 0.002 | 0.007 ± 0.001**** | 0.027 ± 0.003 | 0.010 ± 0.002**** |
| Muscle | 0.016 ± 0.003 | 0.052 ± 0.005**** | 0.028 ± 0.007 | 0.057 ± 0.019* |
| Heart | 0.473 ± 0.253 | 1.538 ± 0.211**** | 0.479 ± 0.259 | 1.551 ± 0.406** |
| Lung | 0.112 ± 0.013 | 0.102 ± 0.014 | 0.147 ± 0.011 | 0.108 ± 0.023* |
| Spleen | 0.095 ± 0.011 | 0.064 ± 0.008** | 0.141 ± 0.021 | 0.072 ± 0.012*** |
| Pancreas | 0.053 ± 0.005 | 0.077 ± 0.015* | 0.072 ± 0.010 | 0.063 ± 0.004 |
| White adipose tissue (superior pole of epididymis) | 0.007 ± 0.002 | 0.031 ± 0.003**** | 0.010 ± 0.004 | 0.033 ± 0.008*** |
| Testis | 0.133 ± 0.011 | 0.024 ± 0.003**** | 0.185 ± 0.014 | 0.035 ± 0.005**** |
| Stomach | 0.077 ± 0.009 | 0.137 ± 0.010**** | 0.104 ± 0.018 | 0.195 ± 0.064* |
| Small intestine | 0.105 ± 0.014 | 0.084 ± 0.014 | 0.147 ± 0.019 | 0.088 ± 0.020** |
| Large intestine | 0.187 ± 0.012 | 0.153 ± 0.023* | 0.202 ± 0.034 | 0.154 ± 0.027 |
| Kidney | 0.057 ± 0.006 | 0.133 ± 0.033*** | 0.084 ± 0.010 | 0.080 ± 0.046 |
| Liver | 0.032 ± 0.002 | 0.016 ± 0.002**** | 0.060 ± 0.010 | 0.025 ± 0.008*** |
| Brown adipose tissue (between the shoulder blades) | 0.050 ± 0.009 | 0.289 ± 0.065**** | 0.051 ± 0.012 | 0.252 ± 0.099** |
| Brain | 0.370 ± 0.037 | 0.488 ± 0.036*** | 0.488 ± 0.059 | 0.551 ± 0.190 |

Table 3. Organ ^{18}F -FDG accumulation in mice (%ID/g/kg). Data in parentheses are mean ± SD. Control, control group; Insulin, insulin-loaded group. * $P < 0.05$, ** $P < 0.01$, *** $P < 0.001$, **** $P < 0.0001$ vs control value.

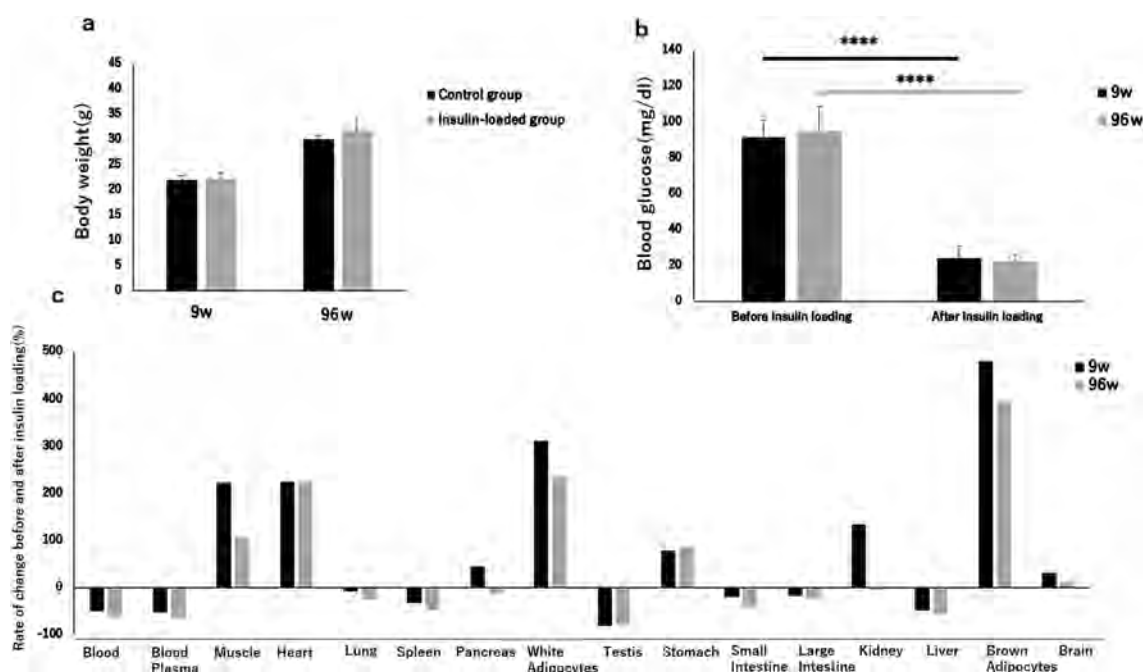


Figure 1. Body weight (a), blood glucose concentration (b), and rate of ^{18}F -FDG uptake changes (c) in organs in young and aged control and insulin-loaded groups. **** $P < 0.0001$.

spleen, testes, large intestine, and liver significantly decreased after insulin loading (Table 3). On the other hand, in the aged mice group, the levels of ^{18}F -FDG uptake in the muscle, heart, white adipose tissue, stomach, and brown adipose tissue significantly increased after insulin loading. However, the levels of ^{18}F -FDG uptake in blood, plasma, spleen, testes, and liver were significantly decreased after insulin loading (Table 3). Compared with the young mice group, the levels of ^{18}F -FDG uptake in the pancreas, kidneys and brain did not exhibit observable changes after insulin loading in the aged mice group. In contrast, those in the lungs and small intestine significantly decreased after insulin loading (Table 3).

The body weight showed no significant difference between control and insulin-loaded groups in both young and aged mice (Table 1, Fig. 1a). When the blood glucose concentration decreased and displayed as “low” after insulin loading, we defined this blood glucose concentration as 20 mmol/dl which is the detection limit of blood glucose meter. After insulin loading, the blood glucose concentration significantly decreased in both young and

| | Young group | | Aged group | |
|---------------|-----------------|----------------------------|----------------------------|----------------------------|
| | Control (n = 6) | Insulin (n = 6) | Control (n = 6) | Insulin (n = 6) |
| Body weight | 21.4 ± 1.0 | 22.0 ± 0.7 | 31.8 ± 1.5 ^{****} | 29.7 ± 1.9 ^{****} |
| Blood glucose | 97.8 ± 17.2 | 21.5 ± 3.7 ^{****} | 102.5 ± 9.5 | 22.5 ± 6.1 ^{****} |

Table 4. Body weight (g) and blood glucose concentration (mg/dl) in brain ¹⁸F-FDG autoradiography study. Data are shown in parentheses (mean ± SD). Control, control group; Insulin, insulin-loaded group. ^{****}*P* < 0.0001 vs control value. ^{****}*P* < 0.0001 vs young groups in control and insulin-loaded groups.

| | Young group | | Aged group | |
|-------------|-----------------|-------------------------------|-----------------|-----------------|
| | Control (n = 6) | Insulin (n = 6) | Control (n = 6) | Insulin (n = 6) |
| Cortex | 0.013 ± 0.002 | 0.017 ± 0.002* | 0.020 ± 0.003 | 0.015 ± 0.004* |
| Striatum | 0.020 ± 0.002 | 0.024 ± 0.002 ^{***} | 0.028 ± 0.003 | 0.026 ± 0.005 |
| Thalamus | 0.018 ± 0.002 | 0.020 ± 0.002 | 0.025 ± 0.002 | 0.021 ± 0.007 |
| Hippocampus | 0.012 ± 0.001 | 0.016 ± 0.001 ^{****} | 0.018 ± 0.002 | 0.015 ± 0.003 |

Table 5. ¹⁸F-FDG accumulation in brain regions in mice (%ID/p/kg). Data are shown in parentheses (mean ± SD). Control, control group; Insulin, insulin-loaded group. **P* < 0.05, ^{***}*P* < 0.001, ^{****}*P* < 0.0001 vs control value.

aged mice groups (Table 1, Fig. 1b). The rate of ¹⁸F-FDG uptake level change in the control and insulin-loaded groups was assessed according to the following formula: [(mean level of ¹⁸F-FDG uptake in insulin-loaded group – mean level of ¹⁸F-FDG uptake in control group)/mean level of ¹⁸F-FDG uptake in control group] × 100%. In these mice, the rates of change in the muscle, heart, white adipose tissue, stomach, brown adipose tissue, and brain showed positive changes, whereas those in the blood, plasma, lungs, spleen, testes, small intestine, large intestine, and liver showed negative changes (Fig. 1c). Moreover, the rates of change in the pancreas and kidneys showed positive changes in the young mice but negative changes in the aged mice (Fig. 1c). Regarding these positive changes, the rate of change in the muscle in the young mice was higher than that in the aged mice (223.3% vs 107.9%), as well as brain (31.6% vs 13.0%), white adipose tissue (313.1% vs 235.6%) and brown adipose tissue (482.9% vs 394.6%) (Fig. 1c).

Brain ¹⁸F-FDG autoradiographic experiment in control groups. The body weight and blood glucose concentration were determined in the young and aged mice (Table 4). The levels of ¹⁸F-FDG uptake in brain regions were determined in the young and aged mice (Table 5). The body weight of the aged mice was significantly higher than that of the young mice (*P* < 0.0001) (Table 4, Fig. 2a). The blood glucose concentration was not significantly different between the two groups (Table 4, Fig. 2b). The levels of ¹⁸F-FDG accumulation in the cortex, striatum, thalamus, and hippocampus were all significantly higher in the aged mice than in the young mice (*P* < 0.001) (Table 5, Fig. 2c).

Changes in ¹⁸F-FDG accumulation level in brain regions. The levels of ¹⁸F-FDG accumulation in brain regions in the insulin-loaded young and aged mice were determined and compared with those in the control young and aged groups (Table 5). In the brain, the levels of ¹⁸F-FDG accumulation in the cortex, striatum, and hippocampus significantly increased after insulin loading in the young group (Table 5, Fig. 3a). Compared with the young group, the levels of ¹⁸F-FDG accumulation in the striatum, thalamus and hippocampus did not show observable changes after insulin loading in the aged group (Table 5, Fig. 3b). In contrast, the level of ¹⁸F-FDG accumulation in the cortex significantly decreased after insulin loading in the aged group (Table 5, Fig. 3b).

The body weight showed no significant difference between control and insulin-loaded groups in both young and aged mice (Table 4, Fig. 4a). When the blood glucose concentration decreased and displayed as “low” after insulin loading, we defined this blood glucose concentration as 20 mmol/dl which is the detection limit of blood glucose meter. After insulin loading, the blood glucose concentration significantly decreased in both young and aged groups (Table 4, Fig. 4b). The rate of ¹⁸F-FDG accumulation level change in the control and insulin-loaded groups was assessed according to the following formula: [(mean level of ¹⁸F-FDG accumulation in insulin loaded group – mean level of ¹⁸F-FDG accumulation in control group)/mean level of ¹⁸F-FDG accumulation in control group] × 100%. The ¹⁸F-FDG accumulation level showed positive changes in the cortex, striatum, thalamus, and hippocampus in the young group, whereas negative changes were observed in those in aged group (Fig. 4c).

Discussion

Alterations in glucose homeostasis are enhanced with age and can be linked to T2D, cardiocerebrovascular injury, and other age-related diseases¹⁸. To clarify the changes in glucose metabolism with aging, we examined and compared the body weight, blood glucose concentration, and ¹⁸F-FDG accumulation level in each organ

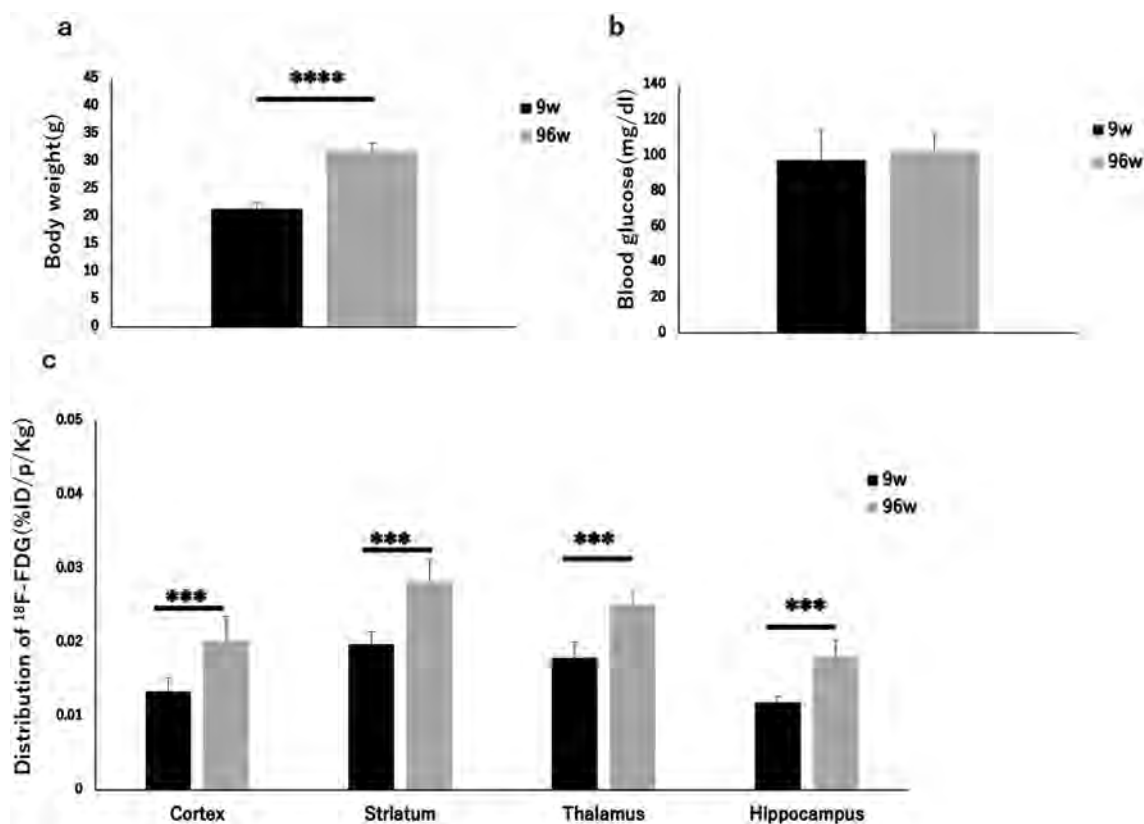


Figure 2. Body weight (a), blood glucose concentration (b), and ¹⁸F-FDG distribution (c) in brains in young and aged control groups. *** $P < 0.001$, **** $P < 0.0001$.

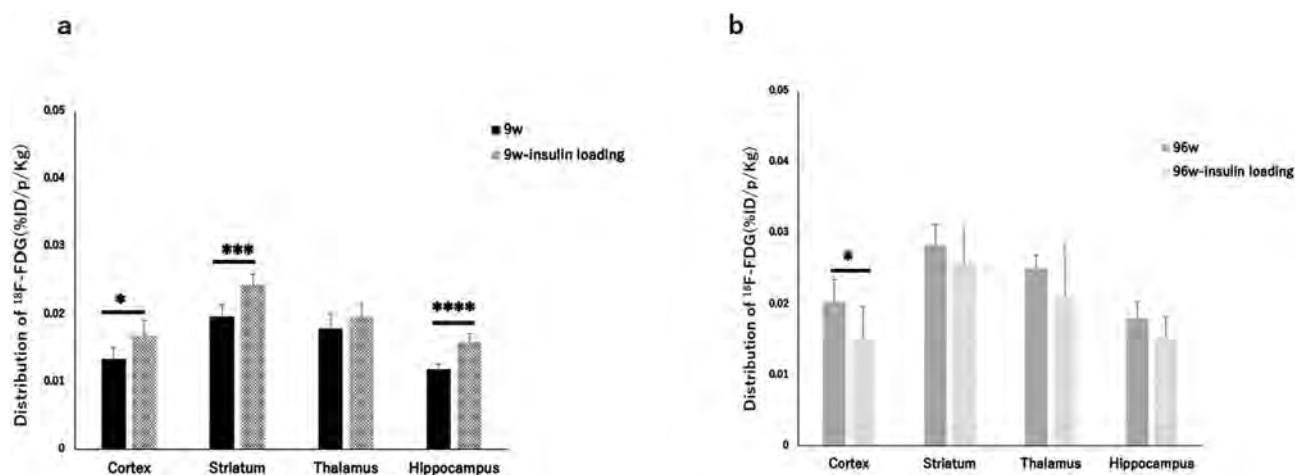


Figure 3. ¹⁸F-FDG distribution in brains with and without insulin loading in young and aged groups. * $P < 0.05$, *** $P < 0.001$, **** $P < 0.0001$.

between the aged and young mice. The age range of aged mice is defined as 18–24 months¹⁹. On the basis of his standard, we chose the 96-week-old male C57BL/6J mice as the aged group.

In this study, the body weight of the aged mice was markedly higher than that of the young mice. Previous studies have indicated that the progressive decline in insulin action with age can be attributed largely to gradual increases in the degree of relative obesity and the number of sites of fat deposition. In addition, insulin resistance is associated with sarcopenia and an accompanying relative increase in fat mass^{20,21}. In a longitudinal study of over 4500 healthy individuals, Lindstrom and Tuomilehto²² and Salmon²³ showed that the likelihood of patients aged 55–64 years developing drug-treated diabetes was roughly equivalent to patients with a BMI > 30. Since muscle is a crucial variable in determining the efficacy of glucose uptake, a decrease in muscle mass leads to a simultaneous decrease in glucose disposal rate^{24,25}. Although the mechanisms underlying the link between insulin resistance and fat deposition have not yet been fully elucidated, it has been suggested that because of both an

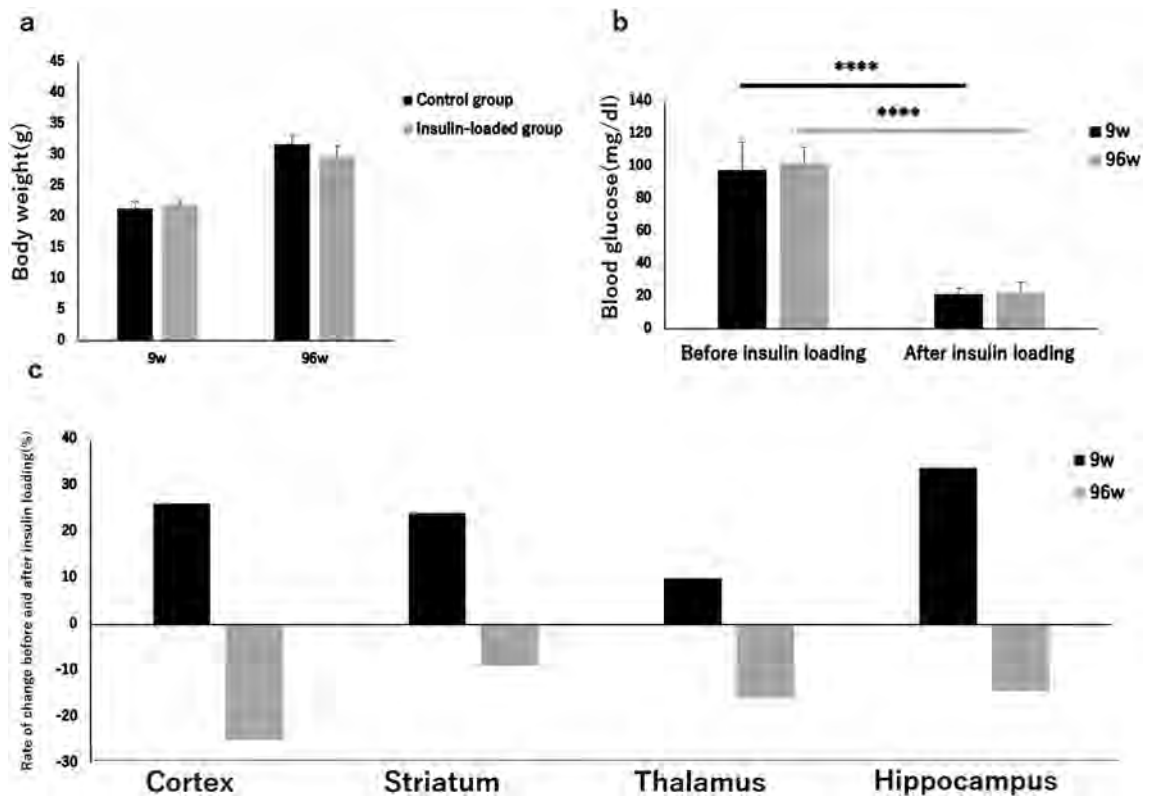


Figure 4. Body weight (a), blood glucose concentration (b), and rate of ¹⁸F-FDG accumulation changes (c) in brains in young and aged control and insulin-loaded groups. **** $P < 0.0001$.

increased level of the β -adrenoceptor pathway and a reduced $\alpha 2$ -adrenoceptor component level, visceral adipose tissue shows a high lipolytic response to catecholamine, exposing the liver to high free fatty acid concentrations, which in turn induces insulin resistance^{25–28}. In this study, after insulin loading, the muscle ¹⁸F-FDG uptake rate of aged mice was significantly lower than that of young mice (107.9% vs 223.3%). The organ weight of the white adipose tissue was significantly higher in the aged mice than in the young mice. In aged mice, the increase in adipose tissue weight may lead to insulin resistance to decrease glucose uptake level in the muscle.

In all the insulin-loaded groups, the levels of ¹⁸F-FDG uptake in the muscle, heart, white adipose tissue, stomach, and brown adipose tissue were significantly higher than in all the control groups. Glucose transporter type 4 (Glut-4), which is an insulin-regulated glucose transporter, is primarily expressed in several tissues, including adipocytes, as well as the skeletal and cardiac muscles^{29,30}. An excessively high blood insulin concentration leads to a series of signal cascades, including the autophosphorylation of the insulin cell surface receptor, the activation of receptor tyrosine kinase, the tyrosine phosphorylation of insulin receptor substrates 1 and 2, the activation of phosphatidylinositol 3-kinase, and the activation of protein kinase B and its downstream mediator AS160. These signal cascades eventually induce the translocation of a large quantity of Glut-4 from intracellular vesicles to the plasma membrane^{31,32}. Thus, hyperinsulinemia markedly increases the level of glucose uptake in adipocytes and the skeletal and cardiac muscles.

In all the insulin-loaded groups, the levels of ¹⁸F-FDG uptake in the blood, plasma, spleen, testes, and liver were significantly lower than those in all the control groups. Previous studies ascribed the reduced ¹⁸F-FDG uptake in tumors and inflammatory lesions with insulin-induced hypoglycemia to the effects of insulin, which shifts ¹⁸F-FDG from the original area to insulin-sensitive organs^{33,34}. This insulin effect may also explain the reduced ¹⁸F-FDG accumulation in insulin-insensitive organs with insulin-induced hypoglycemia.

In the control groups, excluding the heart, white adipose tissue, brown adipose tissue, and large intestine, the levels of ¹⁸F-FDG accumulation in the blood, plasma, muscle, lungs, spleen, pancreas, testes, stomach, small intestine, kidneys, liver, and brain were all significantly higher in the aged mice than that in the young mice. However, the blood glucose concentration was not significantly different between the young and aged control groups. Previous comparative studies have shown that C3H and CBA mice were among the most susceptible among all inbred mouse strains to hepatocarcinogenesis whereas the C57BL/6, A, BALB/c, and DBA/2 strains are relatively resistant, SWR/J mice were the most susceptible to lung tumor whereas the C57BR/cdJ, C57BL/6J, P/J, and SM/J strains were relatively resistant³⁵. We observed no tumors in any organs of aged mice in this study. Hyperinsulinemia has been implicated in the progression of obesity, insulin resistance, and T2D. Elevated insulin levels can be a cause and consequence of obesity and insulin resistance^{36–38}. Hyperinsulinemia, which is inevitably associated with insulin resistance, also appears to negatively affect kidney function via the induction of glomerular hyperfiltration and increase in vascular permeability³⁹. In this study, the levels of ¹⁸F-FDG uptake in the kidneys in the young insulin-loaded group were significantly higher than those in the young control group.

Compared with the young group, the levels of ^{18}F -FDG uptake in kidneys in the aged group did not markedly change after insulin loading. Moreover, the levels of ^{18}F -FDG uptake in the kidneys showed positive changes in the young mice, but negative changes were observed in the aged mice after insulin loading. As mentioned above, insulin-induced hypoglycemia shifts ^{18}F -FDG from the original area to insulin-sensitive organs^{33,34}. This insulin effect may also explain the reduced ^{18}F -FDG uptake in the kidneys in the aged mice, because the decreased insulin sensitivity of the kidneys leads to the shift of ^{18}F -FDG to insulin-sensitive organs. These findings suggest that there were obstacles in glucose metabolism in the kidneys in aged mice. On the other hand, this insulin resistance in old mice negatively affects kidney function, which leads to the excretion disorders of ^{18}F -FDG, and subsequently to higher levels of ^{18}F -FDG accumulation in organs of elderly mice. Kidney dysfunction is a major cause of morbidity and mortality, whose prevalence is rising worldwide mainly because of the aging of populations⁴⁰. However, the epidemics of abnormalities associated with insulin resistance⁴¹ might play a role in the increase in the prevalence of kidney dysfunction⁴². Insulin receptor substrate 1 plays a key role in insulin signaling and action in several organs including the kidneys⁴³. Among the genes involved in the insulin signaling pathway is the gene encoding transmembrane glycoprotein ectonucleotide pyrophosphatase phosphodiesterase 1, which binds to and inhibits the insulin receptor and subsequent downstream insulin signaling and action in both cultured cells and animal models⁴⁴. We consider that aging could induce insulin resistance through abnormal-insulin-signaling-related genes, and ultimately lead to glucose intolerance and kidney dysfunction. On the other hand, although there is convincing evidence that the kidney is an insulin-regulating organ, in which insulin regulates various functions, similar to traditional target organs, it is unclear whether the kidney is affected by insulin resistance in whole or in part⁴⁵. The insulin receptor exists in two isoforms A and B, which are formed due to exclusion (isoform A) or inclusion (isoform B) of exon 11 of the insulin receptor gene. Insulin receptor-A is ubiquitously expressed, whereas insulin receptor-B is expressed largely in the classically insulin-sensitive tissues of liver, skeletal muscle and adipose tissue. Interestingly, insulin receptor-B is also expressed abundantly in the kidney⁴⁶. According to a literature review, insulin receptor-A may increase with aging, thereby contributing to insulin resistance, insulin receptor-B downregulation may contribute to insulin resistance in aging⁴⁷. According to the above literature, we consider that aging could down-regulate insulin receptor B and up-regulate insulin receptor A, leading to a decrease in insulin sensitivity in the kidneys.

In addition, after insulin loading, the brain glucose uptake rate in old mice was significantly lower than that in young mice (13.0% vs 31.6%). To more specifically evaluate the changes in glucose metabolism in the brain, we carried out ^{18}F -FDG autoradiography to evaluate the ^{18}F -FDG accumulation in brain regions after insulin loading in aged and young wild-type mice. We found that the levels of ^{18}F -FDG accumulation in the cortex, striatum, thalamus, and hippocampus were all significantly higher in the aged mice than in the young mice. However, the blood glucose concentration was not significantly different between the young and aged groups. This is consistent with the finding that the levels of ^{18}F -FDG uptake in the brain were significantly higher in the aged mice than in the young mice in the study on the ^{18}F -FDG distribution in organs. In the young mice group, the levels of ^{18}F -FDG accumulation in the cortex, striatum, and hippocampus significantly increased after insulin loading. Compared with the young group, the levels of ^{18}F -FDG accumulation in the striatum, thalamus and hippocampus in the aged group did not markedly change after insulin loading. In contrast, the level of ^{18}F -FDG accumulation in the cortex significantly decreased after insulin loading in the aged group. Aging is associated with reductions in the levels of both insulin and its receptor in the brain, which may even cause the brain to be in the state of insulin resistance^{48–51}. Cholerton et al.⁴⁹ indicated that chronic high levels of insulin and insulin resistance may exert a negative effect on several body systems, including the central nervous system, for some time prior to the onset of diabetes. There is increasing support to the idea that such early insulin abnormalities may be associated with the initiation of the cascade of the AD pathology in some individuals, years or even decades before the first clinical dementia symptoms are manifest⁴⁹. Bingham et al.¹⁶ demonstrated an enhanced cerebral glucose metabolism that was particularly pronounced in the cortex following the administration of a low dose of insulin. The basis for brain-region-specific insulin effects on glucose metabolism may be attributable to the distribution of GLUTs^{52,53}. Insulin-sensitive GLUTs 4 and 8 are selectively distributed in the brain, and insulin increases the levels of brain GLUT 4 expression and translocation⁵⁴. In this study, ^{18}F -FDG accumulation showed positive changes in the cortex, striatum, thalamus, and hippocampus in the young mice, whereas negative changes were observed in those in the aged mice after insulin loading. These indicate that the insulin sensitivity of these brain regions might gradually decrease with age and lead to age-related brain diseases such as AD and PD. The characteristics of glucose metabolism in the localized brain regions of these aged mice can be used to develop therapeutic models for age-related brain diseases.

The limitation of our study was the lack of insulin sensitivity assays, such as the intraperitoneal glucose tolerance test (IPGTT), intraperitoneal insulin tolerance test (IPITT), and plasma insulin measurements.

Conclusions

In summary, we demonstrated that aging can induce insulin resistance and lead to dysfunction of systemic glucose metabolism. Insulin resistance could affect glucose metabolism and eventually cause age-related diseases. On the basis of findings, ameliorating this dysfunction may be a good preventive and therapeutic strategy for age-related diseases.

Methods

Preparation of animal models. The entire experimental protocols were approved by the Laboratory Animal Care and Use Committee of Fukushima Medical University (approval number 30021) and performed in accordance with the Guidelines for Animal Experiments at Fukushima Medical University. The study was also carried out in compliance with the ARRIVE guidelines. Eight-week-old and 96-week-old male C57BL/6J mice

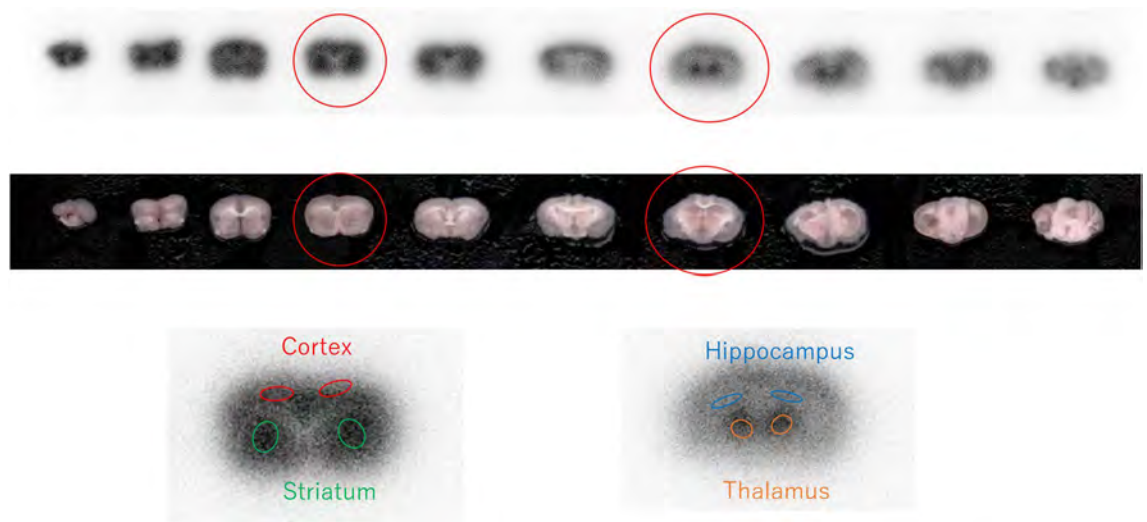


Figure 5. Brain ^{18}F -FDG autoradiography image. ROIs were placed on ^{18}F -FDG ARG image to cover the cortex, striatum, hippocampus, and thalamus on the left and right hemispheres. The cortex is encircled in red, the striatum in green, the hippocampus in blue, and the thalamus in orange.

were purchased from Charles River Laboratories Japan, Inc. (Yokohama, Japan) and maintained in a specific-pathogen-free animal experiment facility. The room temperature was maintained between 23 and 25 °C, and the relative humidity was maintained between 45 and 55%. The institutional laboratory housing provided a 12-h light/dark cycle and met all the criteria of the Association for Assessment and Accreditation of Laboratory Animal Care (AAALAC) International (<http://www.aaalac.org/>)⁵⁵. All animals were fasted overnight and then divided into four subgroups: young control group, aged control group, young insulin-loaded group, and aged insulin-loaded group.

Organ ^{18}F -FDG accumulation study. Eight-week-old and 96-week-old male mice ($n=5$, each group) were assigned to the control and insulin-loaded groups. Those in the insulin-loaded groups were intraperitoneally injected with human insulin (2 U/kg body weight, Eli Lilly & Co., Kobe) 30 min prior to ^{18}F -FDG injection. We excluded one of the 96-week-old mice in the insulin-loaded group because the blood glucose level did not decrease after insulin loading. Each animal was initially anesthetized with 4% isoflurane in air and maintained via spontaneous ventilation with 2% isoflurane in air. ^{18}F -FDG (11.5 MBq/0.1 ml) was injected into the tail vein. Ninety minutes later, the animals were sacrificed and their organs were excised. The organs (muscle, heart, lungs, spleen, pancreas, white adipose tissue (superior pole of epididymis), testes, stomach, small intestine, large intestine, kidneys, liver, brown adipose tissue (between the shoulder blades), and brain) and blood samples (blood and plasma) were weighed, and their radioactivity was determined with a gamma counter (WIZARD² 2480; PerkinElmer, USA). After decay correction, the percentage of injected dose per gram of tissue was obtained and normalized to the animal weight [%ID/g tissue/kg body weight (%ID/g/kg)]. Blood samples for glucose concentration measurement were obtained from the control group and insulin-loaded groups.

Brain ^{18}F -FDG autoradiography study. Eight-week-old and 96-week-old male mice ($n=6$, each group) were assigned to the control and insulin-loaded groups. Those in the insulin-loaded groups received an intraperitoneal injection of human insulin (2 U/kg body weight, Eli Lilly & Co., Kobe) 30 min prior to ^{18}F -FDG injection. Each animal was initially anesthetized with 4% isoflurane in air and maintained via spontaneous ventilation with 2% isoflurane in air. ^{18}F -FDG (11.5 MBq/0.1 ml) was injected into the tail vein. Ninety minutes later, the animals were sacrificed, then brains were rapidly removed, placed in Brain Matrix (Stoelting Co, USA) and cut into coronal slices (2 mm/slice) to obtain 8–9 coronal slices that were exposed to a phosphor imaging plate (Fuji Imaging Plate BAS-SR 2025 for ^{18}F ; Fuji Photo Film Co., Ltd., Tokyo, Japan) with a set of calibrated standards⁵⁶. This autoradiographic exposure was performed overnight to detect the distribution of ^{18}F -FDG. Autoradiography images were analyzed using a computerized imaging analysis system (raytest, CR35, Version 2.1.0, Straubenhardt, Germany) with the image analysis software AIDA (Version 5.1 SP2, Straubenhardt, Germany). To determine brain radioactivity concentration, the cortex, striatum, thalamus and hippocampus were defined using Aida Image Analyzer software. The regions of interests (ROIs), namely, the cortex, striatum, thalamus, and hippocampus in the left and right hemispheres in all mice were marked on the same anatomical plane with reference to the corresponding brain coronal slices (Fig. 5). The radioactivity in each ROI was determined per unit area, the percentage of injected dose per pixel of the cortex, striatum, thalamus, and hippocampus was obtained and normalized to the animal weight [%ID/pixel/kg body weight (%ID/p/kg)]. Finally, the average of the left and right values around each of the four regions was obtained. Blood samples for glucose concentration measurement were obtained from the control and insulin-loaded mice groups.

Statistical analyses. All data are expressed as mean \pm standard deviation. Statistical analyses were performed using the unpaired Student's *t* test to evaluate the significance of differences between the young and aged mice in body weight, organ weights, blood glucose concentration, and ^{18}F -FDG distribution, as well as between the control group and insulin-loaded group both in the young and aged mice groups. Significance was assumed at $P < 0.05$.

Data availability

The data generated and/or analyzed in this study are available from the corresponding author on reasonable request.

Received: 1 December 2020; Accepted: 17 March 2021

Published online: 01 April 2021

References

- Martin, G. M. The biology of aging: 1985–2010 and beyond. *FASEB J.* **25**, 3756–3762. <https://doi.org/10.1096/fj.11-1102.ufm> (2011).
- van den Beld, A. W. *et al.* The physiology of endocrine systems with ageing. *Lancet Diabetes Endocrinol.* **6**, 647–658. [https://doi.org/10.1016/s2213-8587\(18\)30026-3](https://doi.org/10.1016/s2213-8587(18)30026-3) (2018).
- Broughton, D. L. & Taylor, R. Review: Deterioration of glucose tolerance with age: The role of insulin resistance. *Age Ageing* **20**, 221–225. <https://doi.org/10.1093/ageing/20.3.221> (1991).
- Yang, W. *et al.* Prevalence of diabetes among men and women in China. *N. Engl. J. Med.* **362**, 1090–1101. <https://doi.org/10.1056/NEJMoa0908292> (2010).
- Fonseca, V. A. Management of diabetes mellitus and insulin resistance in patients with cardiovascular disease. *Am. J. Cardiol.* **92**, 50j–60j. [https://doi.org/10.1016/s0002-9149\(03\)00616-7](https://doi.org/10.1016/s0002-9149(03)00616-7) (2003).
- Xiao, J. *et al.* Worse pancreatic beta-cell function and better insulin sensitivity in older Chinese without diabetes. *J. Gerontol. A Biol. Sci. Med. Sci.* **69**, 463–470. <https://doi.org/10.1093/gerona/glt104> (2014).
- Karakelides, H., Irving, B. A., Short, K. R., O'Brien, P. & Nair, K. S. Age, obesity, and sex effects on insulin sensitivity and skeletal muscle mitochondrial function. *Diabetes* **59**, 89–97. <https://doi.org/10.2337/db09-0591> (2010).
- Jackson, R. A. *et al.* Influence of ageing on glucose homeostasis. *J. Clin. Endocrinol. Metab.* **55**, 840–848. <https://doi.org/10.1210/jcem-55-5-840> (1982).
- Michalakis, K. *et al.* Obesity in the ageing man. *Metabolism* **62**, 1341–1349. <https://doi.org/10.1016/j.metabol.2013.05.019> (2013).
- Atkins, J. L., Whincup, P. H., Morris, R. W. & Wannamethee, S. G. Low muscle mass in older men: The role of lifestyle, diet and cardiovascular risk factors. *J. Nutr. Health Aging* **18**, 26–33. <https://doi.org/10.1007/s12603-013-0336-9> (2014).
- Petersen, K. F. *et al.* Mitochondrial dysfunction in the elderly: Possible role in insulin resistance. *Science* **300**, 1140–1142. <https://doi.org/10.1126/science.1082889> (2003).
- Maggio, M. *et al.* Association of hormonal dysregulation with metabolic syndrome in older women: Data from the InCHIANTI study. *Am. J. Physiol. Endocrinol. Metab.* **292**, E353–358. <https://doi.org/10.1152/ajpendo.00339.2006> (2007).
- Rains, J. L. & Jain, S. K. Oxidative stress, insulin signaling, and diabetes. *Free Radic. Biol. Med.* **50**, 567–575. <https://doi.org/10.1016/j.freeradbiomed.2010.12.006> (2011).
- Singh, T. & Newman, A. B. Inflammatory markers in population studies of aging. *Ageing Res. Rev.* **10**, 319–329. <https://doi.org/10.1016/j.arr.2010.11.002> (2011).
- Voipio-Pulkki, L. M. *et al.* Heart and skeletal muscle glucose disposal in type 2 diabetic patients as determined by positron emission tomography. *J. Nucl. Med.* **34**, 2064–2067 (1993).
- Bingham, E. M. *et al.* The role of insulin in human brain glucose metabolism: An 18fluoro-deoxyglucose positron emission tomography study. *Diabetes* **51**, 3384–3390. <https://doi.org/10.2337/diabetes.51.12.3384> (2002).
- Virtanen, K. A. *et al.* Human adipose tissue glucose uptake determined using [(18)F]-fluoro-deoxy-glucose [(18)F]FDG and PET in combination with microdialysis. *Diabetologia* **44**, 2171–2179. <https://doi.org/10.1007/s001250100026> (2001).
- Reaven, G. M. Banting lecture 1988. Role of insulin resistance in human disease; 1988. *Nutrition* **13**, 65 (1997) ((discussion 64, 66)).
- Flurkey, K., Curren, J. M., & Harrison, D. E. *The mouse in biomedical research* (ed. Fox, J.G.) 637–672 (2007).
- Cefalu, W. T. *et al.* Contribution of visceral fat mass to the insulin resistance of aging. *Metabolism* **44**, 954–959. [https://doi.org/10.1016/0026-0495\(95\)90251-1](https://doi.org/10.1016/0026-0495(95)90251-1) (1995).
- Coon, P. J., Rogus, E. M., Drinkwater, D., Muller, D. C. & Goldberg, A. P. Role of body fat distribution in the decline in insulin sensitivity and glucose tolerance with age. *J. Clin. Endocrinol. Metab.* **75**, 1125–1132. <https://doi.org/10.1210/jcem.75.4.1400882> (1992).
- Lindström, J. & Tuomilehto, J. The diabetes risk score: A practical tool to predict type 2 diabetes risk. *Diabetes Care* **26**, 725–731. <https://doi.org/10.2337/diacare.26.3.725> (2003).
- Salmon, A. B. Oxidative stress in the etiology of age-associated decline in glucose metabolism. *Longev. Healthspan.* **1**, 7. <https://doi.org/10.1186/2046-2395-1-7> (2012).
- Chumlea, W. C., Rhyne, R. L., Garry, P. J. & Hunt, W. C. Changes in anthropometric indices of body composition with age in a healthy elderly population. *Am. J. Hum. Biol.* **1**, 457–462. <https://doi.org/10.1002/ajhb.1310010408> (1989).
- Barbieri, M., Rizzo, M. R., Manzella, D. & Paolisso, G. Age-related insulin resistance: Is it an obligatory finding? The lesson from healthy centenarians. *Diabetes Metab. Res. Rev.* **17**, 19–26. <https://doi.org/10.1002/dmrr.178> (2001).
- Fried, S. K., Leibel, R. L., Edens, N. K. & Kral, J. G. Lipolysis in intraabdominal adipose tissues of obese women and men. *Obes. Res.* **1**, 443–448. <https://doi.org/10.1002/j.1550-8528.1993.tb00026.x> (1993).
- Boden, G. Role of fatty acids in the pathogenesis of insulin resistance and NIDDM. *Diabetes* **46**, 3–10 (1997).
- Mauriège, P. *et al.* Is visceral adiposity a significant correlate of subcutaneous adipose cell lipolysis in men? *J. Clin. Endocrinol. Metab.* **84**, 736–742. <https://doi.org/10.1210/jcem.84.2.5499> (1999).
- MacLean, P. S., Zheng, D., Jones, J. P., Olson, A. L. & Dohm, G. L. Exercise-induced transcription of the muscle glucose transporter (GLUT 4) gene. *Biochem. Biophys. Res. Commun.* **292**, 409–414. <https://doi.org/10.1006/bbrc.2002.6654> (2002).
- Cheng, C. *et al.* Evaluation of organ-specific glucose metabolism by (1)(8)F-FDG in insulin receptor substrate-1 (IRS-1) knockout mice as a model of insulin resistance. *Ann. Nucl. Med.* **25**, 755–761. <https://doi.org/10.1007/s12149-011-0522-y> (2011).
- James, D. E. Targeting of the insulin-regulatable glucose transporter (GLUT-4). *Biochem. Soc. Trans.* **22**, 668–670. <https://doi.org/10.1042/bst0220668> (1994).
- De Tata, V. Age-related impairment of pancreatic Beta-cell function: Pathophysiological and cellular mechanisms. *Front Endocrinol. (Lausanne)* **5**, 138. <https://doi.org/10.3389/fendo.2014.00138> (2014).
- Zhao, S. *et al.* Effects of insulin and glucose loading on FDG uptake in experimental malignant tumours and inflammatory lesions. *Eur. J. Nucl. Med.* **28**, 730–735. <https://doi.org/10.1007/s002590100517> (2001).

34. Torizuka, T., Fisher, S. J. & Wahl, R. L. Insulin-induced hypoglycemia decreases uptake of 2-[F-18]fluoro-2-deoxy-d-glucose into experimental mammary carcinoma. *Radiology* **203**, 169–172. <https://doi.org/10.1148/radiology.203.1.9122387> (1997).
35. Kemp, C. J. & Drinkwater, N. R. Genetic variation in liver tumor susceptibility, plasma testosterone levels, and androgen receptor binding in six inbred strains of mice. *Cancer Res.* **49**, 5044–5047 (1989).
36. Page, M. M. & Johnson, J. D. Mild suppression of hyperinsulinemia to treat obesity and insulin resistance. *Trends Endocrinol. Metab.* **29**, 389–399. <https://doi.org/10.1016/j.tem.2018.03.018> (2018).
37. Shanik, M. H. *et al.* Insulin resistance and hyperinsulinemia: Is hyperinsulinemia the cart or the horse?. *Diabetes Care* **31**(Suppl 2), S262–268. <https://doi.org/10.2337/dc08-s264> (2008).
38. Mehran, A. E. *et al.* Hyperinsulinemia drives diet-induced obesity independently of brain insulin production. *Cell Metab.* **16**, 723–737. <https://doi.org/10.1016/j.cmet.2012.10.019> (2012).
39. De Cosmo, S., Menzaghi, C., Prudente, S. & Trischitta, V. Role of insulin resistance in kidney dysfunction: Insights into the mechanism and epidemiological evidence. *Nephrol. Dial Transplant* **28**, 29–36. <https://doi.org/10.1093/ndt/gfs290> (2013).
40. de Boer, I. H. *et al.* Temporal trends in the prevalence of diabetic kidney disease in the United States. *JAMA* **305**, 2532–2539. <https://doi.org/10.1001/jama.2011.861> (2011).
41. Reaven, G. M. Banting lecture 1988. Role of insulin resistance in human disease. *Diabetes* **37**(1595–1607), 1988. <https://doi.org/10.2337/diab.37.12.1595> (1988).
42. Chen, J. *et al.* The metabolic syndrome and chronic kidney disease in US adults. *Ann. Intern. Med.* **140**, 167–174. <https://doi.org/10.7326/0003-4819-140-3-200402030-00007> (2004).
43. Formoso, G. *et al.* The TRIB3 R84 variant is associated with increased carotid intima-media thickness in vivo and with enhanced MAPK signalling in human endothelial cells. *Cardiovasc. Res.* **89**, 184–192. <https://doi.org/10.1093/cvr/cvq255> (2011).
44. Prudente, S., Morini, E. & Trischitta, V. Insulin signaling regulating genes: Effect on T2DM and cardiovascular risk. *Nat. Rev. Endocrinol.* **5**, 682–693. <https://doi.org/10.1038/nrendo.2009.215> (2009).
45. Artunc, F. *et al.* The impact of insulin resistance on the kidney and vasculature. *Nat. Rev. Nephrol.* **12**, 721–737. <https://doi.org/10.1038/nrneph.2016.145> (2016).
46. Hale, L. J. & Coward, R. J. The insulin receptor and the kidney. *Curr. Opin. Nephrol. Hypertens.* **22**, 100–106. <https://doi.org/10.1097/MNH.0b013e32835abb52> (2013).
47. Belfiore, A. *et al.* Insulin receptor isoforms in physiology and disease: An updated view. *Endocr. Rev.* **38**, 379–431. <https://doi.org/10.1210/er.2017-00073> (2017).
48. Biessels, G. J., van der Heide, L. P., Kamal, A., Bleys, R. L. & Gispen, W. H. Ageing and diabetes: Implications for brain function. *Eur. J. Pharmacol.* **441**, 1–14. [https://doi.org/10.1016/s0014-2999\(02\)01486-3](https://doi.org/10.1016/s0014-2999(02)01486-3) (2002).
49. Cholerton, B., Baker, L. D. & Craft, S. Insulin resistance and pathological brain ageing. *Diabet. Med.* **28**, 1463–1475. <https://doi.org/10.1111/j.1464-5491.2011.03464.x> (2011).
50. Frazier, H. N. *et al.* Expression of a constitutively active human insulin receptor in hippocampal neurons does not alter VGCC currents. *Neurochem. Res.* **44**, 269–280. <https://doi.org/10.1007/s11064-018-2510-2> (2019).
51. Rhea, E. M. & Banks, W. A. Role of the blood-brain barrier in central nervous system insulin resistance. *Front Neurosci.* **13**, 521. <https://doi.org/10.3389/fnins.2019.00521> (2019).
52. Reagan, L. P. *et al.* Localization and regulation of GLUTx1 glucose transporter in the hippocampus of streptozotocin diabetic rats. *Proc. Natl. Acad. Sci. USA* **98**, 2820–2825. <https://doi.org/10.1073/pnas.051629798> (2001).
53. Schulingkamp, R. J., Pagano, T. C., Hung, D. & Raffa, R. B. Insulin receptors and insulin action in the brain: Review and clinical implications. *Neurosci. Biobehav. Rev.* **24**, 855–872. [https://doi.org/10.1016/s0149-7634\(00\)00040-3](https://doi.org/10.1016/s0149-7634(00)00040-3) (2000).
54. Piroli, G. G. *et al.* Corticosterone impairs insulin-stimulated translocation of GLUT4 in the rat hippocampus. *Neuroendocrinology* **85**, 71–80. <https://doi.org/10.1159/000101694> (2007).
55. Oriuchi, N. *et al.* Possibility of cancer-stem-cell-targeted radioimmunotherapy for acute myelogenous leukemia using (211)At-CXCR4 monoclonal antibody. *Sci. Rep.* **10**, 6810. <https://doi.org/10.1038/s41598-020-63557-9> (2020).
56. Zhao, S. *et al.* Biologic correlates of intratumoral heterogeneity in 18F-FDG distribution with regional expression of glucose transporters and hexokinase-II in experimental tumor. *J. Nucl. Med.* **46**, 675–682 (2005).

Acknowledgements

This study was supported by Tsumura & Co.

Author contributions

J.Z. and C.T. designed the study and wrote the manuscript. R.I., N.U., and S.S. performed animal studies. K.T. performed radiolabeling and QC examination. H.I. and J.M. contributed to the interpretation of the results. Y.O., G.N., S.Z. and K.S. critically revised the manuscript for important intellectual content. All authors reviewed the manuscript.

Competing interests

The authors declare no competing interests.

Additional information

Correspondence and requests for materials should be addressed to G.N. or S.Z.

Reprints and permissions information is available at www.nature.com/reprints.

Publisher's note Springer Nature remains neutral with regard to jurisdictional claims in published maps and institutional affiliations.



Open Access This article is licensed under a Creative Commons Attribution 4.0 International License, which permits use, sharing, adaptation, distribution and reproduction in any medium or format, as long as you give appropriate credit to the original author(s) and the source, provide a link to the Creative Commons licence, and indicate if changes were made. The images or other third party material in this article are included in the article's Creative Commons licence, unless indicated otherwise in a credit line to the material. If material is not included in the article's Creative Commons licence and your intended use is not permitted by statutory regulation or exceeds the permitted use, you will need to obtain permission directly from the copyright holder. To view a copy of this licence, visit <http://creativecommons.org/licenses/by/4.0/>.

© The Author(s) 2021



Evaluation of Effect of Ninjin'yoeito on Regional Brain Glucose Metabolism by ^{18}F -FDG Autoradiography With Insulin Loading in Aged Mice

Jingmin Zhao^{1,2}, Ryota Imai^{3,4}, Naoyuki Ukon⁵, Saki Shimoyama⁵, Chengbo Tan^{5,6}, Yuko Maejima⁴, Yuji Omiya³, Kazuhiro Takahashi⁵, Guangxian Nan^{1*†}, Songji Zhao^{5,7*†}, Hiroshi Ito^{2,5} and Kenju Shimomura⁴

OPEN ACCESS

Edited by:

David Vauzour,
University of East Anglia,
United Kingdom

Reviewed by:

Fang Xie,
Fudan University, China
Sophie Lancelot,
Université de Lyon, France

*Correspondence:

Guangxian Nan
nangx@jlu.edu.cn
Songji Zhao
zhao-s@fmu.ac.jp

†These authors have contributed
equally to this work

Specialty section:

This article was submitted to
Nutrition and Brain Health,
a section of the journal
Frontiers in Nutrition

Received: 23 January 2021

Accepted: 16 March 2021

Published: 12 May 2021

Citation:

Zhao J, Imai R, Ukon N,
Shimoyama S, Tan C, Maejima Y,
Omiya Y, Takahashi K, Nan G, Zhao S,
Ito H and Shimomura K (2021)
Evaluation of Effect of Ninjin'yoeito on
Regional Brain Glucose Metabolism
by ^{18}F -FDG Autoradiography With
Insulin Loading in Aged Mice.
Front. Nutr. 8:657663.
doi: 10.3389/fnut.2021.657663

¹ Department of Neurology, China-Japan Union Hospital of Jilin University, Changchun, China, ² Department of Radiology and Nuclear Medicine, Fukushima Medical University, Fukushima, Japan, ³ Tsumura Kampo Research Laboratories, Kampo Research and Development Division, Tsumura & Co., Ibaraki, Japan, ⁴ Department of Bioregulation and Pharmacological Medicine, Fukushima Medical University, Fukushima, Japan, ⁵ Advanced Clinical Research Center, Fukushima Global Medical Science Center, Fukushima Medical University, Fukushima, Japan, ⁶ Department of Neurosurgery, Shanghai East Hospital, Tongji University School of Medicine, Shanghai, China, ⁷ Department of Pathophysiology, Basic Medical College of Jilin University, Changchun, China

Introduction: A recent clinical study revealed that Ninjin'yoeito (NYT) may potentially improve cognitive outcome. However, the mechanism by which NYT exerts its effect on elderly patients remains unclear. The aim of this study is to evaluate the effect of Ninjin'yoeito on regional brain glucose metabolism by ^{18}F -FDG autoradiography with insulin loading in aged wild-type mice.

Materials and Methods: After 12 weeks of feeding NYT, mice were assigned to the control and insulin-loaded groups and received an intraperitoneal injection of human insulin (2 U/kg body weight) 30 min prior to ^{18}F -FDG injection. Ninety minutes after the injection, brain autoradiography was performed.

Results: After insulin loading, the ^{18}F -FDG accumulation showed negative changes in the cortex, striatum, thalamus, and hippocampus in the control group, whereas positive changes were observed in the NYT-treated group.

Conclusions: Ninjin'yoeito may potentially reduce insulin resistance in the brain regions in aged mice, thereby preventing age-related brain diseases.

Keywords: Ninjin'yoeito, glucose metabolism, ^{18}F -FDG autoradiography, age, insulin loading

INTRODUCTION

With a global aging population, health issues caused by aging and age-related diseases have become inevitable challenges to all countries. Understanding the functional changes of organs that occur as a result of aging is essential to prevent age-related diseases, such as Alzheimer's disease (AD) and Parkinson's disease (PD) (1). In particular, the metabolism of glucose as an energy source has been regarded as a potential indicator for these body disorders.

Insulin resistance is one of the major underlying mechanisms in abnormal glucose tolerance (2). Accumulated evidence supports the idea that insulin resistance raises the risk of AD (3) and also correlates with the progression of PD (4). The aged brain has reduced insulin receptor expression levels, diminished insulin transport into the central nervous system, and may even experience insulin resistance (3–7). Therefore, reducing brain insulin resistance is one of the key points to prevent aging-related brain diseases.

Ninjin'yoeito (NYT, Ren-Shen-Yang-Rong-Tang) is a traditional Japanese medicine (Kampo medicine) and a multicomponent formulation composed of 12 crude drug extracts from ginseng, Japanese angelica roots, peony roots, *rehmannia* roots, *Atractylodes* rhizomes, *poria* sclerotium, cinnamon bark, *astragalus* root, *Citrus unshiu* peel, *polygala* roots, *schisandra* fruit, and *Glycyrrhiza*. NYT extract is approved by the Japanese Ministry of Health, Labor and Welfare as a Kampo medicine for the decline in physical strength, fatigue, anorexia, night sweats, cold extremities, and anemia (8). It is also used for individuals with deteriorating physical or psychiatric conditions, particularly among the elderly (9). Ninjin-to is composed of four medicinal herbs, *atractylodes* rhizome, ginseng, glycyrrhiza, and processed ginger, and has been reported to prevent the progression of diabetes mellitus in non-obese diabetic mice (10). Moreover, glucose intolerance in obese mice is alleviated by *astragalus* root through improvement of insulin resistance (11). Interestingly, NYT contains *atractylodes* rhizome, ginseng, and glycyrrhiza, which are components of Ninjin-to preventing the progression of diabetes (10). Furthermore, NYT also contains *astragalus* root, which improves insulin resistance (11). On the other hand, a recent clinical study revealed that NYT may potentially improve cognitive outcome and AD-related depression in patients with AD (8). Therefore, we hypothesize that NYT may potentially improve insulin resistance in the brain.

The glucose analog [¹⁸F]-Fluoro-2-deoxy-2-D-glucose (¹⁸F-FDG), a molecular imaging probe, is widely used in nuclear medicine for evaluating tissue glucose utilization and glucose metabolism (12–14). In this study, we attempted to clarify the effect of Ninjin'yoeito on regional brain glucose metabolism by ¹⁸F-FDG autoradiography (ARG) with insulin loading in aged mice.

MATERIALS AND METHODS

Radiopharmaceutical and Reagent

NYT Extract

NYT is an herbal supplement composed of 12 crude drugs (15). The NYT extract we used was supplied by Tsumura & Co.

¹⁸F-FDG

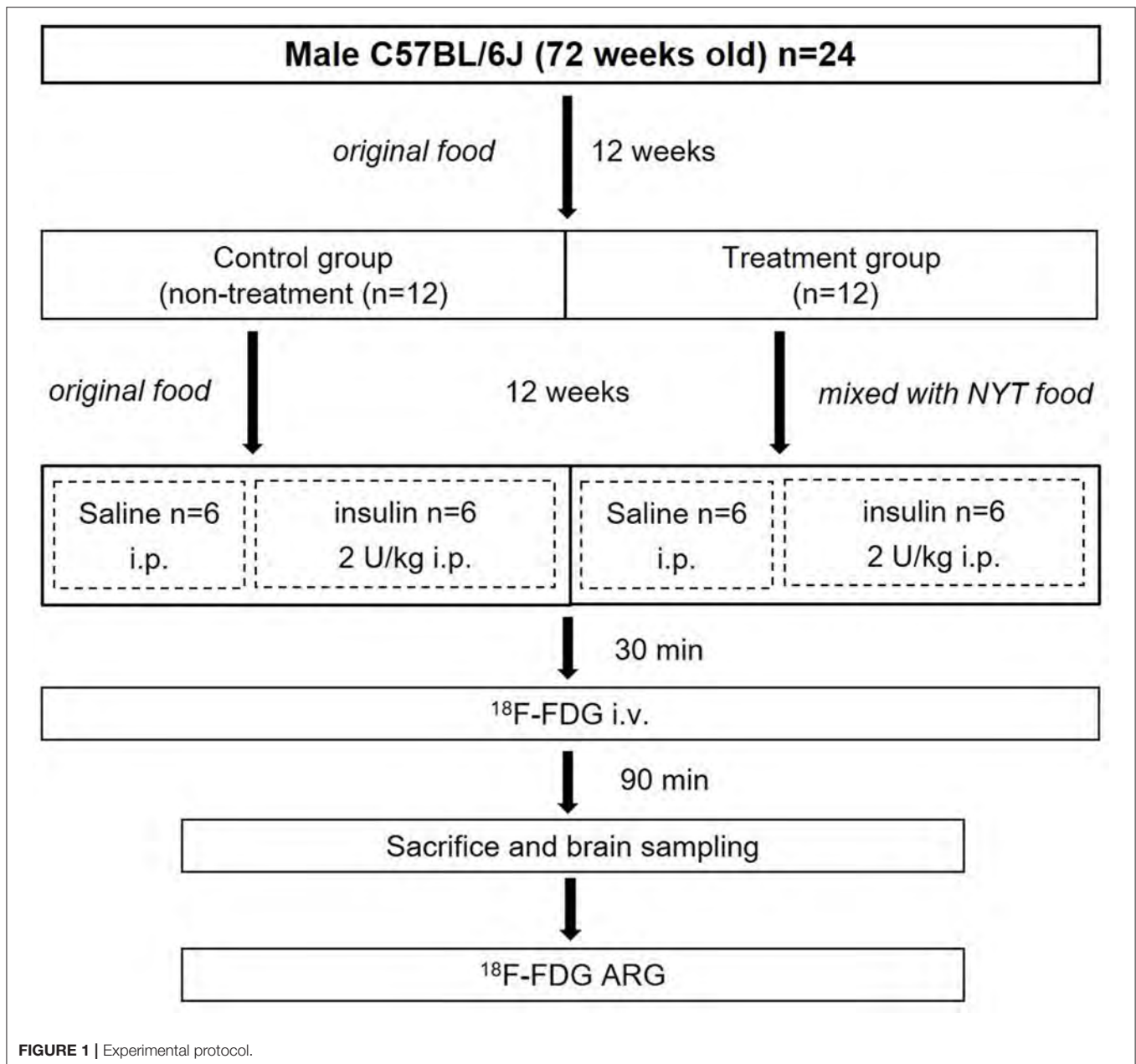
¹⁸F-FDG supplied for clinical PET examinations, and synthesized by standard procedures was obtained from Fukushima Medical University Advanced Clinical Research Center Cyclotron Facility (Fukushima, Japan). The specific activity of ¹⁸F-FDG was about 300 GBq/mmol.

Preparation of Animal Models

The entire experimental protocol was approved by the Laboratory Animal Care and Use Committee of Fukushima Medical University (Approval Number 30021) and performed in accordance with the Guidelines for Animal Experiments at Fukushima Medical University. Male C57BL/6J mice (72 weeks old) ($n = 24$) were purchased from Charles River Laboratories Japan, Inc. (Yokohama, Japan). All mice were housed in a 12 h light/dark cycle at room temperature maintained at 23–25°C and relative humidity at 45–60%. Food and water were provided *ad libitum*, and the treatment and care of animals met all the criteria of the Association for Assessment and Accreditation of Laboratory Animal Care (AAALAC) International (<http://www.aaalac.org/>) (16). The experimental protocol is shown in **Figure 1**. All mice were fed an original diet (CRF-6, ORIENTAL YEAST CO., LTD., Tokyo, Japan). After 12 weeks (84 weeks old), mice were randomly assigned to the control ($n = 12$) and treatment ($n = 12$) groups. The mice in the control group were continued on the original diet (100% CRF-6). The mice in the treatment group were fed the original diet mixed with NYT (97% CRF-6 mixed with 3% NYT, ORIENTAL YEAST CO., LTD., Tokyo, Japan). After 12 weeks (96 weeks old), all mice were fasted overnight and then both the control and treatment groups were further divided two subgroups without and with insulin loading (**Figure 1**).

Brain ¹⁸F-FDG ARG Study

The four subgroups of mice ($n = 6$, each group) were the insulin- and non-insulin-loaded subgroups of the control and treatment groups. The mice in the insulin-loaded subgroups were intraperitoneally injected with human insulin (2 U/kg body weight, Eli Lilly & Co., Kobe) 30 min prior to ¹⁸F-FDG injection. Each animal was initially anesthetized with 3–4% isoflurane in air and maintained *via* spontaneous ventilation with 2% isoflurane in air. ¹⁸F-FDG (11.5 MBq/0.1 ml) was injected into the tail vein. Ninety minutes later, the animals were sacrificed; then their brains were rapidly removed, placed in Brain Matrix (Stoelting Co., USA) and cut into coronal slices (2 mm/slice), from which 9–10 coronal slices were obtained for exposure to a phosphor imaging plate (Fuji Imaging Plate BAS-SR 2025 for ¹⁸F; Fuji Photo Film Co., Ltd., Tokyo, Japan) with a set of calibrated standards (17). This autoradiographic exposure was performed overnight to detect the distribution of ¹⁸F-FDG. ARG images were analyzed using a computerized imaging analysis system (raytest, CR35, Version 2.1.0, Straubenhardt, Germany) with the image analysis software AIDA (Version 5.1 SP2, Straubenhardt, Germany). To determine brain radioactivity concentration, the cortex, striatum, thalamus, and hippocampus were defined using AIDA. The regions of interest (ROIs), namely, the cortex, striatum, thalamus, and hippocampus in the left and right hemispheres in all mice, were marked on the same anatomical plane with reference to the corresponding brain coronal slices (**Figure 2**). The radioactivity concentration in each ROI was determined per unit area, and the percentage of injected dose per pixel of the cortex, striatum, thalamus, and hippocampus was obtained and normalized to the animal weight [%ID/pixel/kg body weight (%ID/p/kg)]. Finally, the average of the left and



right values around each of the four regions was obtained. The rates of change in ¹⁸F-FDG accumulation level before and after insulin loading were assessed using the following formula: [(¹⁸F-FDG uptake level after insulin loading—¹⁸F-FDG uptake level before insulin loading)/¹⁸F-FDG uptake level before insulin loading] × 100%. Blood samples for glucose concentration measurement were obtained from all groups. When the blood glucose concentration decreased and displayed as “low” after insulin loading, we defined this blood glucose concentration as 20 mmol/dl which is the detection limit of blood glucose meter.

Statistical Analyses

All data are expressed as mean ± standard deviation. Statistical analyses were performed using the unpaired Student’s *t*-test to

evaluate the significance of differences between the control and treatment groups in body weight, blood glucose concentration, and ¹⁸F-FDG distribution, as well as between non-insulin and insulin-loaded subgroups both in the control and treatment groups. Significance was assumed at *P* < 0.05.

RESULTS

Brain ¹⁸F-FDG Autoradiographic Experiment in Control and Treatment Groups

The body weight and blood glucose concentration were determined in the control and treatment groups (Table 1).

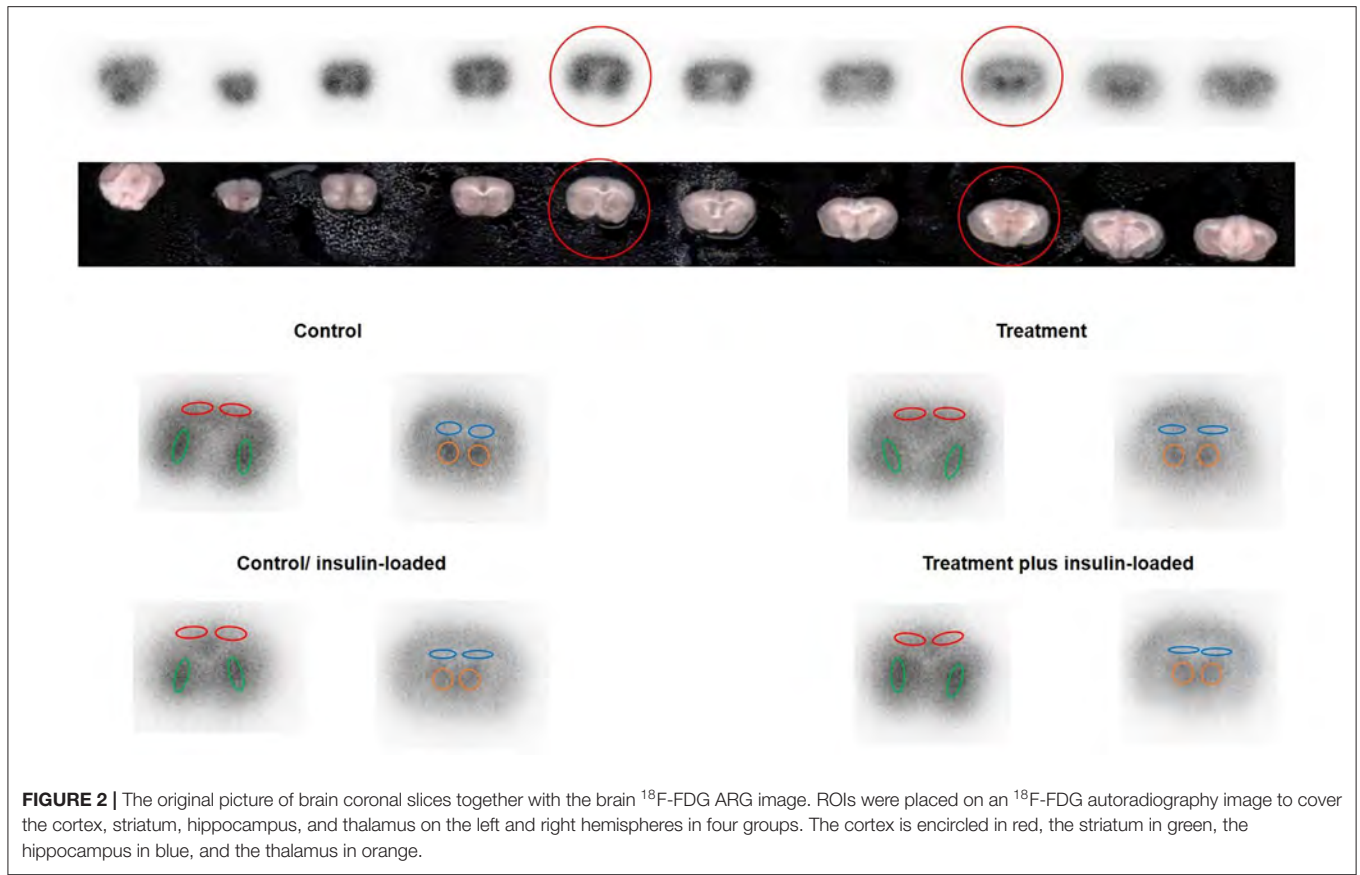


FIGURE 2 | The original picture of brain coronal slices together with the brain ¹⁸F-FDG ARG image. ROIs were placed on an ¹⁸F-FDG autoradiography image to cover the cortex, striatum, hippocampus, and thalamus on the left and right hemispheres in four groups. The cortex is encircled in red, the striatum in green, the hippocampus in blue, and the thalamus in orange.

TABLE 1 | Body weight (g) and blood glucose concentration (mg/dl) in brain ¹⁸F-FDG autoradiography study.

| | Control groups | | Treatment groups | |
|---------------|-------------------------|----------------------|-------------------------|----------------------|
| | Without insulin (n = 6) | With insulin (n = 6) | Without insulin (n = 6) | With insulin (n = 6) |
| Body weight | 35.1 ± 4.1 | 31.6 ± 3.5 | 32.4 ± 1.8 | 32.4 ± 3.0 |
| Blood glucose | 96.5 ± 9.5 | 27.2 ± 16.1**** | 90.8 ± 8.0 | 23.7 ± 6.2**** |

Data are shown in parentheses (mean ± SD).
 Without insulin, no insulin-loaded groups; With insulin, insulin-loaded groups.
 ****P < 0.0001 vs. value in with insulin-loaded group.

The levels of ¹⁸F-FDG accumulation in brain regions were also determined in the control and treatment groups (Table 2). The body weight and blood glucose concentration were not significantly different between these two groups (Table 1). The levels of ¹⁸F-FDG accumulation in the cortex, striatum, thalamus, and hippocampus were also not significantly different between these two groups (Table 2).

Changes in ¹⁸F-FDG Accumulation Level Between Control and Control/Insulin-Loaded Groups

The body weight and blood glucose concentration were determined in the control and control/insulin-loaded groups (Table 1). The levels of ¹⁸F-FDG accumulation in brain regions were also determined in the control and control/insulin-loaded

TABLE 2 | ¹⁸F-FDG accumulation in brain regions in mice (%ID/p/kg).

| | Control groups | | Treatment groups | |
|-------------|-------------------------|----------------------|-------------------------|----------------------|
| | Without insulin (n = 6) | With insulin (n = 6) | Without insulin (n = 6) | With insulin (n = 6) |
| Cortex | 0.019 ± 0.002 | 0.016 ± 0.002* | 0.017 ± 0.003 | 0.018 ± 0.002 |
| Striatum | 0.024 ± 0.004 | 0.024 ± 0.004 | 0.024 ± 0.004 | 0.028 ± 0.002# |
| Thalamus | 0.023 ± 0.002 | 0.021 ± 0.005 | 0.021 ± 0.004 | 0.022 ± 0.003 |
| Hippocampus | 0.016 ± 0.002 | 0.016 ± 0.004 | 0.014 ± 0.002 | 0.017 ± 0.003 |

Data are shown in parentheses (mean ± SD).
 Insulin, insulin-loaded group; Without insulin, no insulin-loaded groups.
 *P < 0.05, vs. value in without insulin-loaded control group.
 #P < 0.05, vs. value in with insulin-loaded control group.

groups (Table 2). The body weight was not significantly different between these two groups (Table 1). After insulin loading, the blood glucose concentration significantly decreased (P < 0.0001) compared with that in the control group (Table 1). The level of ¹⁸F-FDG accumulation in the cortex significantly decreased after insulin loading (P < 0.05; Table 2).

Changes in ¹⁸F-FDG Accumulation Level Between Treatment and Treatment Plus Insulin-Loaded Groups

The body weight and blood glucose concentration were determined in the treatment and treatment plus insulin-loaded groups (Table 1). The levels of ¹⁸F-FDG accumulation in brain

regions were determined in the treatment and treatment plus insulin-loaded groups (Table 2). The body weight was not significantly different between these two groups (Table 1). After insulin loading, the blood glucose concentration significantly decreased compared with that in the treatment group ($P < 0.0001$; Table 1). The levels of ^{18}F -FDG accumulation in the striatum and hippocampus tended to increase trend after insulin loading (Table 2).

Comparison of ^{18}F -FDG Accumulation Level Between Control and Treatment Groups After Insulin Loading

The body weight and blood glucose concentration were not significantly different between the control and treatment plus insulin-loaded groups (Table 1). The levels of ^{18}F -FDG accumulation in the cortex were higher in the treatment group than in the control group after insulin loading. The levels of ^{18}F -FDG accumulation in the striatum were significantly higher in the treatment group than in the control group after insulin loading ($P < 0.05$; Table 2).

Rates of Change in ^{18}F -FDG Accumulation Level Before and After Insulin Loading

The rates of change in ^{18}F -FDG accumulation level before and after insulin loading were assessed using the following formula: $[(^{18}\text{F}\text{-FDG uptake level after insulin loading} - ^{18}\text{F}\text{-FDG uptake level before insulin loading}) / ^{18}\text{F}\text{-FDG uptake level before insulin loading}] \times 100\%$. The ^{18}F -FDG accumulation showed negative changes in the cortex, striatum, thalamus, and hippocampus in the control group, whereas positive changes were observed in the treatment group (Figure 3).

DISCUSSION

To clarify the effect of Ninjin'yoeito on brain glucose metabolism, we examined and compared the ^{18}F -FDG accumulation in brain regions after NYT treatment with insulin loading in aged mice. The ARG method has also been widely used in the quantitative analysis of images of small animal models. ARG imaging plates have a much higher spatial resolution [the Fuji BAS-SR imaging plate is 25–100 μm (17)], than small-animal PET scanners and can visualize the distribution of the radiotracers, within small brain regions and improve the quantification of image analysis of the small brain regions. Therefore, we chose the ARG method to evaluate the effect of NYT on regional brain glucose metabolism in this study.

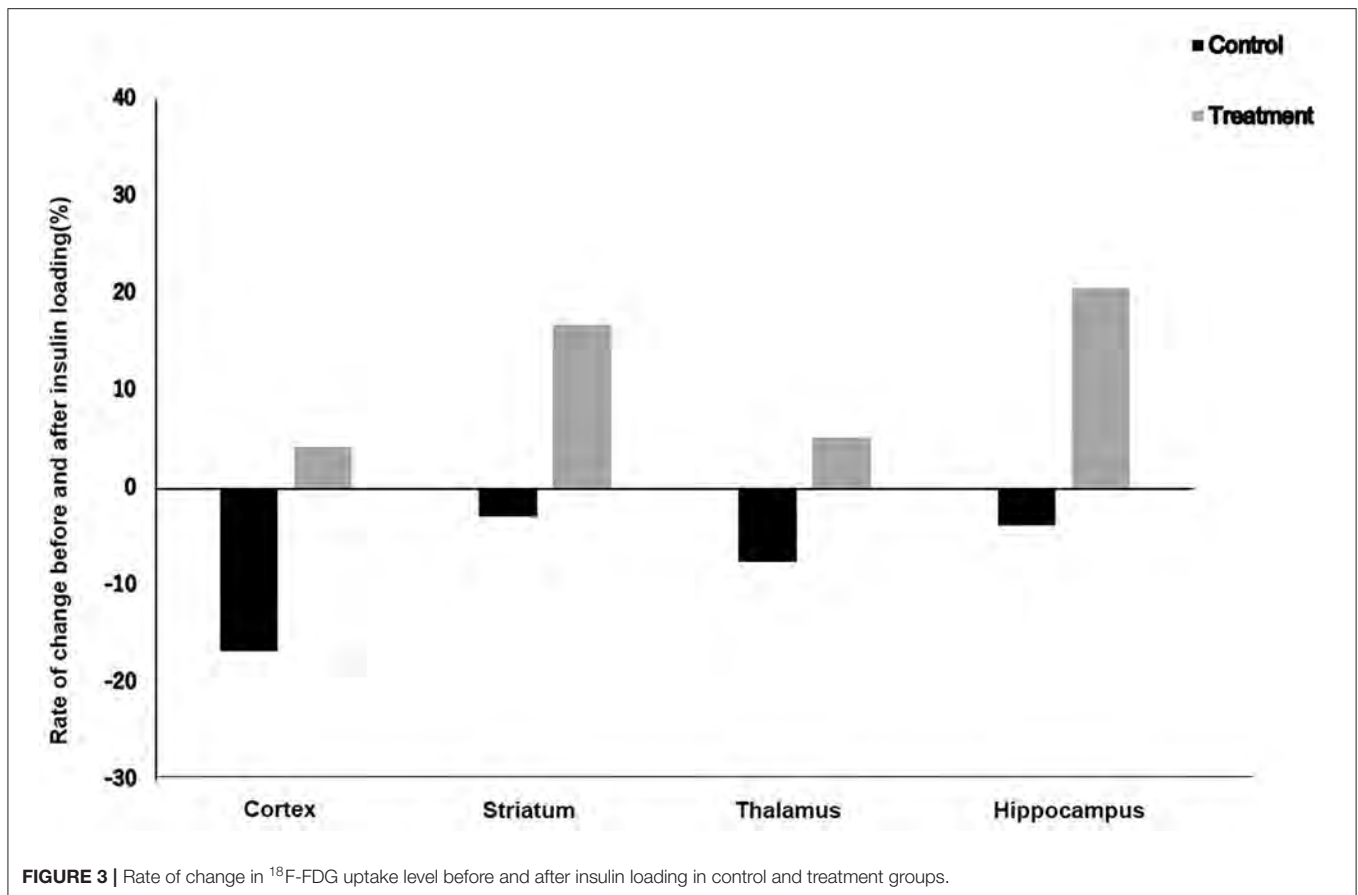
The highest concentration of insulin receptors was observed in neuronal cell bodies of the hippocampus and cerebral cortex (18, 19). Thalamic atrophy was found to start early in life and has a linear association with age; the same study showed that thalamic atrophy correlated with diminished performance on tests of processing speed (20). Effects of both deficient striatal neurogenesis and age-related neurodegeneration within the striatum accumulate, resulting in a progressive decline in the control functions of the basal ganglia, loss of dopaminergic neurons, and occurrence of PD clinical symptoms (21). On the

basis of these studies, we chose the cortex, striatum, thalamus, and hippocampus in the aged brain for analysis in this study.

In this study, the blood glucose concentration and body weight were not significantly different between the control and treatment groups, and between the control and treatment plus insulin-loaded groups. The levels of ^{18}F -FDG accumulation in the cortex, striatum, thalamus, and hippocampus were not significantly different between the control and treatment groups. However, the level of ^{18}F -FDG accumulation in the cortex was higher in the treatment group than in the control group after insulin loading. Moreover, after insulin loading, the levels of ^{18}F -FDG accumulation in the striatum were significantly higher in the treatment group than in the control group. It can be seen from these data that after the insulin loading, the levels of ^{18}F -FDG accumulation were higher in the treatment group than in the control group, especially in the cortex and striatum.

On the other hand, in the control group, the level of ^{18}F -FDG accumulation in the cortex was significantly decreased after insulin loading, whereas no significant difference found in the treatment group. Insulin as a hormone secreted by pancreatic β -cells, which affects the peripheral system, has been well-characterized. Recent evidence has confirmed that active insulin could also be observed in the central nervous system. Despite the debate about whether insulin is synthesized in the adult brain, it is easily transported across the blood–brain barrier to the central nervous system through a process mediated by saturable receptors (22–24). Elevated peripheral insulin levels will sharply increase the brain and cerebrospinal fluid insulin levels, while prolonged peripheral hyperinsulinemia will downregulate the blood–brain barrier insulin receptors and inhibit the transport of insulin to the brain (25, 26). Insulin receptors are situated on the synapses of both neurons and astrocytes (27). Although insulin and insulin receptors are abundant in the brain, they are selectively distributed, with high concentrations in the cerebral cortex, hypothalamus, hippocampus, olfactory bulb, as well as in the amygdala and septum (23, 28–30). In the literature, it is widely accepted that aging is accompanied by an increase in insulin resistance (31, 32). Bingham et al. (13) demonstrated that glucose metabolism in the cerebral cortex increases significantly after treatment with low-dose insulin. The basis for insulin effects on glucose metabolism in regional brains may be due to the distribution of glucose transporter isoforms (GLUTs) (33, 34). The insulin-sensitive GLUTs 4 and 8 are selectively distributed in the brain, and insulin enhances brain GLUT 4 expression and translocation (35). In rats, GLUT 4 is expressed in the cerebellum, sensorimotor cortex, hippocampus, pituitary, and hypothalamus (36–39) and GLUT 8 has been observed to be expressed in the hippocampus and hypothalamus (33).

In this study, after insulin loading, the brain ^{18}F -FDG uptake level in the cortex of aged mice did not increase but decreased in the control group. This result suggests that there was an obstacle in the cortical glucose metabolism in elderly mice. However, in the treatment group, although the ^{18}F -FDG uptake level in the cortex of aged mice did not increase, it did not decrease either. This may be explained by the fact that NYT can improve the insulin resistance of the cortex of aged mice. On the other hand, the ^{18}F -FDG uptake levels in the striatum



and hippocampus of aged mice did not increase after insulin loading in the control group, whereas an increasing trend after insulin loading was observed in the treatment group. This result suggests that NYT may also improve the insulin resistance in the striatum and hippocampus. After insulin loading, the ^{18}F -FDG accumulation showed negative changes in the cortex, striatum, thalamus, and hippocampus in the control group. Previous studies ascribed the reduced ^{18}F -FDG uptake levels in tumors and inflammatory lesions with insulin-induced hypoglycemia to the effect of insulin, i.e., insulin shifts ^{18}F -FDG from the original area to insulin-sensitive organs (40, 41). This insulin effect may also explain the reduced ^{18}F -FDG accumulation level in the control group because of the decreased insulin sensitivity of the brain leading to the shift of ^{18}F -FDG to insulin-sensitive organs. However, in the treatment groups, the ^{18}F -FDG accumulation showed positive changes in the cortex, striatum, thalamus, and hippocampus after insulin loading. It may indicate that NYT may potentially reduce the insulin resistance in the brain regions of aged mice.

A study showed that insulin resistance in the periphery systems in patients with AD positively correlated with brain amyloid β -protein ($\text{A}\beta$) deposition in the frontal and temporal areas (42). Studies have shown that peripheral insulin resistance may precede the accumulation of $\text{A}\beta$ in which midlife Homeostatic Model Assessment for Insulin Resistance

(HOMA-IR) predicted $\text{A}\beta$ aggregation, as assessed by amyloid positron emission tomography 15 years after HOMA-IR was measured (43). In cognitively healthy adults, compared with $\text{A}\beta$ -negative adults, peripheral insulin resistance is also associated with increased levels of $\text{A}\beta$ accumulation within 2 years (44, 45). Brain insulin resistance impairs synaptic integrity, and tau and $\text{A}\beta$ can also interfere with the actions of insulin at synapses (46). Insulin desensitization may be one of the base of PD disease progression. Clinical data demonstrate that around 8–30% of PD patients are diabetic, a significantly higher percentage than that of the age-matched control group (47–50). Previous studies have documented the importance of insulin signaling in the brain (51–53) and proved that insulin signaling is compromised in the brains of PD patients (54–56). Analogs of incretin hormones have been developed to improve insulin signaling in Type 2 diabetes (57, 58). These drugs enhance insulin release and insulin sensitivity. The anti-diabetics in the class of incretin receptor agonists improve symptoms and brain pathology in AD and PD animal models, as well as glucose utilization in AD patients and clinical symptoms in PD patients after their systemic administration (59). The treatment to reduce brain insulin resistance is considered for the treatment of AD and PD.

Hosogi et al. found that NYT improved the serum glucose levels and insulin resistance in STZ-induced diabetic mice (60). This improvement by NYT might be due to the alleviation of

interstitial fluid acidification through the increased expression of SMCT1 in the proximal colon leading to the absorption of butyrate, a pH buffer, *via* epithelial cells of the proximal colon (60). The studies reported by Gonçalves and Martel (61) and Gao et al. (62) revealed the mechanism of NYT-induced improvement of insulin resistance: SMCT1 transports butyrate (61), and butyrate intake prevents insulin resistance in high-fat-diet-fed mice (62). These reports (61, 62) suggest that the elevation of SMCT1 expression prevents the occurrence of insulin resistance by increasing the intake of butyrate. The report by Gao et al. (62) indicates that butyrate treatment improves insulin sensitivity by decreasing the levels of blood lipids such as triglycerides, cholesterol, and total fatty acids, which are as critical factors causing insulin resistance. Therefore, the data showing that NYT reduces local brain insulin resistance in aged mice may provide new options for the treatment of AD and PD.

Small-animal PET as a non-invasive, *in vivo* molecular imaging modality has been widely used for preclinical animal models in research facilities, which provide longitudinal investigation of the same subject and voxel-wise analysis. However, most dedicated small-animal PET scanners are limited by their relatively coarse spatial resolution [typically 1 to 2 mm full width at half-maximum (FWHM)] and therefore cannot reliably define specific regions within the mouse brain (63).

The small-animal PET system (Inveon, PET/SPECT/CT) with a spatial resolution of 1.63 mm was installed in our preclinical facility (64). Prior to this study, we have also evaluated the quantitative analysis of ^{18}F -FDG PET images of the mouse brain. However, owing to the poor spatial resolution of ^{18}F -FDG PET images, it was impossible to accurately define specific regions and set the ROIs at specific regions within the mouse brain. Yang et al. indicated that high-resolution prototype small-animal ^{18}F -FDG PET scanner images showed a much higher spatial resolution and a more detailed structure of the mouse brain (63). However, the dedicated small-animal ^{18}F -FDG PET scanner (Inveon) could not.

The limitations of our study were as follows. The number of animals per group was small. We only performed image analysis of the coronal sections of the mouse brain, and we did not

perform image analysis of the sagittal sections. We consider that more accurate quantitative image information from different sections can be obtained if ARG image analysis of the sagittal sections is performed in this study.

CONCLUSION

In summary, Ninjin'yoeito may potentially reduce insulin resistance in the brain regions in aged mice, thereby preventing age-related brain diseases.

DATA AVAILABILITY STATEMENT

The raw data supporting the conclusions of this article will be made available by the authors, without undue reservation.

ETHICS STATEMENT

The entire experimental protocols were approved by the Laboratory Animal Care and Use Committee of Fukushima Medical University (Approval Number 30021) and performed in accordance with the Guidelines for Animal Experiments at Fukushima Medical University.

AUTHOR CONTRIBUTIONS

JZ designed the study and wrote the manuscript. RI, NU, CT, and SS performed animal studies. YO performed bait prescription. KT performed radiolabeling and QC examination. HI and YM contributed to the interpretation of the results. GN, SZ, and KS critically revised the manuscript for important intellectual content. All authors have reviewed the manuscript.

ACKNOWLEDGMENTS

This study was supported by Tsumura & Co. This study was also supported in part by Japan China Sasakawa Medical Fellowship.

REFERENCES

- Martin GM, The biology of aging: 1985-2010 and beyond. *Faseb J.* (2011) 25:3756–62. doi: 10.1096/fj.11-1102.ufm
- Xiao J, Weng J, Ji L, Jia W, Lu J, Shan Z, et al. Worse pancreatic β -cell function and better insulin sensitivity in older Chinese without diabetes. *J Gerontol A Biol Sci Med Sci.* (2014) 69:463–70. doi: 10.1093/geronol/glt104
- Cholerton B, Baker LD, Craft S. Insulin resistance and pathological brain ageing. *Diabet Med.* (2011) 28:1463–75. doi: 10.1111/j.1464-5491.2011.03464.x
- Banks WA, Jaspán JB, Kastin AJ. Effect of diabetes mellitus on the permeability of the blood-brain barrier to insulin. *Peptides.* (1997) 18:1577–84. doi: 10.1016/S0196-9781(97)00238-6
- Biessels GJ, van der Heide LP, Kamal A, Bleys RL, Gispen WH. Ageing and diabetes: implications for brain function. *Eur J Pharmacol.* (2002) 441:1–14. doi: 10.1016/S0014-2999(02)01486-3
- Frazier HN, Anderson KL, Maimaiti S, Ghoweri AO, Kraner SD, Popa GJ, et al. Expression of a constitutively active human insulin receptor in hippocampal neurons does not alter VGCC currents. *Neurochem Res.* (2019) 44:269–80. doi: 10.1007/s11064-018-2510-2
- Rhea EM, Banks WA. Role of the blood-brain barrier in central nervous system insulin resistance. *Front Neurosci.* (2019) 13:521. doi: 10.3389/fnins.2019.00521
- Kudoh C, Arita R, Honda M, Kishi T, Komatsu Y, Asou H, et al. Effect of ninjin'yoeito, a Kampo (traditional Japanese) medicine, on cognitive impairment and depression in patients with Alzheimer's disease: 2 years of observation. *Psychogeriatrics.* (2016) 16:85–92. doi: 10.1111/psyg.12125
- Suzuki S, Aihara F, Shibahara M, Sakai K. Safety and effectiveness of Ninjin'yoeito: a utilization study in elderly patients. *Front Nutr.* (2019) 6:14. doi: 10.3389/fnut.2019.00014
- Kobayashi T, Song QH, Hong T, Kitamura H, Cyong JC. Preventive effect of Ninjin-to (Ren-Shen-Tang), a Kampo (Japanese traditional) formulation, on spontaneous autoimmune diabetes in non-obese diabetic (NOD) mice. *Microbiol Immunol.* (2000) 44:299–305. doi: 10.1111/j.1348-0421.2000.tb02499.x
- Xu A, Wang H, Hoo RL, Sweeney G, Vanhoutte PM, Wang Y, et al. Selective elevation of adiponectin production by the natural compounds derived from

- a medicinal herb alleviates insulin resistance and glucose intolerance in obese mice. *Endocrinology*. (2009) 150:625–33. doi: 10.1210/en.2008-0999
12. Voipio-Pulkki LM, Nuutila P, Knuuti MJ, Ruotsalainen U, Haaparanta M, Teräs M, et al. Heart and skeletal muscle glucose disposal in type 2 diabetic patients as determined by positron emission tomography. *J Nucl Med*. (1993) 34:2064–7.
 13. Bingham EM, Hopkins D, Smith D, Pernet A, Hallett W, Reed L, et al. The role of insulin in human brain glucose metabolism: an 18fluoro-deoxyglucose positron emission tomography study. *Diabetes*. (2002) 51:3384–90. doi: 10.2337/diabetes.51.12.3384
 14. Virtanen KA, Peltoniemi P, Marjamäki P, Asola M, Strindberg L, Parkkola R, et al. Human adipose tissue glucose uptake determined using [(18)F]-fluoro-deoxy-glucose ([18F]FDG) and PET in combination with microdialysis. *Diabetologia*. (2001) 44:2171–9. doi: 10.1007/s001250100026
 15. Goswami C, Dezaki K, Wang L, Inui A, Seino Y, Yada T. Ninjin'yoeito targets distinct Ca(2+) channels to activate ghrelin-responsive vs. unresponsive NPY neurons in the arcuate nucleus. *Front Nutr*. (2020) 7:104. doi: 10.3389/fnut.2020.00104
 16. Oriuchi N, Aoki M, Ukon N, Washiyama K, Tan C, Shimoyama S, et al. Possibility of cancer-stem-cell-targeted radioimmunotherapy for acute myelogenous leukemia using (211)At-CXCR4 monoclonal antibody. *Sci Rep*. (2020) 10:6810. doi: 10.1038/s41598-020-63557-9
 17. Zhao S, Kuge Y, Mochizuki T, Takahashi T, Nakada K, Sato M, et al. Biologic correlates of intratumoral heterogeneity in 18F-FDG distribution with regional expression of glucose transporters and hexokinase-II in experimental tumor. *J Nucl Med*. (2005) 46:675–82.
 18. Unger J, McNeill TH, Moxley RT, III, White M, Moss A, Livingston JN. Distribution of insulin receptor-like immunoreactivity in the rat forebrain. *Neuroscience*. (1989) 31:143–57. doi: 10.1016/0306-4522(89)90036-5
 19. van Houten M, Posner BI, Kopriwa BM, Brawer JR. Insulin-binding sites in the rat brain: *in vivo* localization to the circumventricular organs by quantitative radioautography. *Endocrinology*. (1979) 105:666–73. doi: 10.1210/endo-105-3-666
 20. Van Der Werf YD, Tisserand DJ, Visser PJ, Hofman PA, Vuurman E, Uylings HB, et al. Thalamic volume predicts performance on tests of cognitive speed and decreases in healthy aging. A magnetic resonance imaging-based volumetric analysis. *Brain Res Cogn Brain Res*. (2001) 11:377–85. doi: 10.1016/S0926-6410(01)00010-6
 21. Błaszczyk JW, Nigrostriatal interaction in the aging brain: new therapeutic target for Parkinson's disease. *Acta Neurobiol Exp (Wars)*. (2017) 77:106–12. doi: 10.21307/ane-2017-041
 22. Banks WA, Jasan JB, Huang W, Kastin AJ. Transport of insulin across the blood-brain barrier: saturability at euglycemic doses of insulin. *Peptides*. (1997) 18:1423–9. doi: 10.1016/S0196-9781(97)00231-3
 23. Baskin DG, Figlewicz DP, Woods SC, Porte D, Jr., Dorsa DM. Insulin in the brain. *Annu Rev Physiol*. (1987) 49:335–47. doi: 10.1146/annurev.ph.49.030187.002003
 24. Baura GD, Foster DM, Porte D, Jr., Kahn SE, Bergman RN, et al. Saturable transport of insulin from plasma into the central nervous system of dogs *in vivo*. A mechanism for regulated insulin delivery to the brain. *J Clin Invest*. (1993) 92:1824–30. doi: 10.1172/JCI116773
 25. Schwartz MW, Figlewicz DF, Kahn SE, Baskin DG, Greenwood MR, Porte D, Jr., Insulin binding to brain capillaries is reduced in genetically obese, hyperinsulinemic Zucker rats. *Peptides*. (1990) 11:467–72. doi: 10.1016/0196-9781(90)90044-6
 26. Wallum BJ, Taborsky GJ, Jr., Porte D, Jr., Figlewicz DP, Jacobson L, Beard JC, et al. Cerebrospinal fluid insulin levels increase during intravenous insulin infusions in man. *J Clin Endocrinol Metab*. (1987) 64:190–4. doi: 10.1210/jcem-64-1-190
 27. Abbott MA, Wells DG, Fallon JR. The insulin receptor tyrosine kinase substrate p58/53 and the insulin receptor are components of CNS synapses. *J Neurosci*. (1999) 19:7300–8. doi: 10.1523/JNEUROSCI.19-17-07300.1999
 28. Havrankova J, Roth J, Brownstein M. Insulin receptors are widely distributed in the central nervous system of the rat. *Nature*. (1978) 272:827–9. doi: 10.1038/272827a0
 29. Havrankova J, Schmechel D, Roth J, Brownstein M. Identification of insulin in rat brain. *Proc Natl Acad Sci USA*. (1978) 75:5737–41. doi: 10.1073/pnas.75.11.5737
 30. Unger JW, Livingston JN, Moss AM. Insulin receptors in the central nervous system: localization, signalling mechanisms and functional aspects. *Prog Neurobiol*. (1991) 36:343–62. doi: 10.1016/0301-0082(91)90015-S
 31. Karakelides H, Irving BA, Short KR, O'Brien P, Nair KS. Age, obesity, and sex effects on insulin sensitivity and skeletal muscle mitochondrial function. *Diabetes*. (2010) 59:89–97. doi: 10.2337/db09-0591
 32. Jackson RA, Blix PM, Matthews JA, Hamling JB, Din BM, Brown DC, et al. Influence of ageing on glucose homeostasis. *J Clin Endocrinol Metab*. (1982) 55:840–8. doi: 10.1210/jcem-55-5-840
 33. Reagan LP, Gorovits N, Hoskin EK, Alves SE, Katz EB, Grillo CA, et al. Localization and regulation of GLUTx1 glucose transporter in the hippocampus of streptozotocin diabetic rats. *Proc Natl Acad Sci USA*. (2001) 98:2820–5. doi: 10.1073/pnas.051629798
 34. Schulingkamp RJ, Pagano TC, Hung D, Raffa RB. Insulin receptors and insulin action in the brain: review and clinical implications. *Neurosci Biobehav Rev*. (2000) 24:855–72. doi: 10.1016/S0149-7634(00)00040-3
 35. Piroli GG, Grillo CA, Reznikov LR, Adams S, McEwen BS, Charron MJ, et al. Corticosterone impairs insulin-stimulated translocation of GLUT4 in the rat hippocampus. *Neuroendocrinology*. (2007) 85:71–80. doi: 10.1159/000101694
 36. Apelt J, Mehlhorn G, Schliebs R. Insulin-sensitive GLUT4 glucose transporters are colocalized with GLUT3-expressing cells and demonstrate a chemically distinct neuron-specific localization in rat brain. *J Neurosci Res*. (1999) 57:693–705.
 37. Brant AM, Jess TJ, Milligan G, Brown CM, Gould GW. Immunological analysis of glucose transporters expressed in different regions of the rat brain and central nervous system. *Biochem Biophys Res Commun*. (1993) 192:1297–302. doi: 10.1006/bbrc.1993.1557
 38. El Messari S, Leloup C, Quignon M, Brisorgueil MJ, Penicaud L, Arluison M. Immunocytochemical localization of the insulin-responsive glucose transporter 4 (Glut4) in the rat central nervous system. *J Comp Neurol*. (1998) 399:492–512
 39. Livingstone C, Lyall H, Gould GW. Hypothalamic GLUT 4 expression: a glucose- and insulin-sensing mechanism? *Mol Cell Endocrinol*. (1995) 107:67–70. doi: 10.1016/0303-7207(94)03423-Q
 40. Zhao S, Kuge Y, Tsukamoto E, Mochizuki T, Kato T, Hikosaka K, et al. Effects of insulin and glucose loading on FDG uptake in experimental malignant tumours and inflammatory lesions. *Eur J Nucl Med*. (2001) 28:730–5. doi: 10.1007/s002590100517
 41. Torizuka T, Fisher SJ, Wahl RL. Insulin-induced hypoglycemia decreases uptake of 2-[F-18]fluoro-2-deoxy-D-glucose into experimental mammary carcinoma. *Radiology*. (1997) 203:169–72. doi: 10.1148/radiology.203.1.9122387
 42. Willette AA, Johnson SC, Birdsill AC, Sager MA, Christian B, Baker LD, et al. Insulin resistance predicts brain amyloid deposition in late middle-aged adults. *Alzheimers Dement*. (2015) 11:504–510.e1. doi: 10.1016/j.jalz.2014.03.011
 43. Ekblad LL, Johansson J, Helin S, Viitanen M, Laine H, Puukka P, et al. Midlife insulin resistance, APOE genotype, and late-life brain amyloid accumulation. *Neurology*. (2018) 90:e1150–7. doi: 10.1212/WNL.0000000000005214
 44. Gomez G, Beason-Held LL, Bilgel M, An Y, Wong DF, Studenski S, et al. Metabolic syndrome and amyloid accumulation in the aging brain. *J Alzheimers Dis*. (2018) 65:629–39. doi: 10.3233/JAD-180297
 45. Kapogiannis D, Mustapic M, Shardell MD, Berkowitz ST, Diehl TC, Spangler RD, et al. Association of extracellular vesicle biomarkers with alzheimer disease in the baltimore longitudinal study of aging. *JAMA Neurol*. (2019) 76:1340–51. doi: 10.1001/jamaneuro.2019.2462
 46. Forner S, Baglietto-Vargas D, Martini AC, Trujillo-Estrada L, LaFerla FM. Synaptic impairment in Alzheimer's disease: a dysregulated symphony. *Trends Neurosci*. (2017) 40:347–57. doi: 10.1016/j.tins.2017.04.002
 47. Hu G, Jousilahti P, Bidel S, Antikainen R, Tuomilehto J. Type 2 diabetes and the risk of Parkinson's disease. *Diabetes Care*. (2007) 30:842–7. doi: 10.2337/dc06-2011
 48. Schernhammer E, Hansen J, Rugebjerg K, Wermuth L, Ritz B. Diabetes and the risk of developing Parkinson's disease in Denmark. *Diabetes Care*. (2011) 34:1102–8. doi: 10.2337/dc10-1333
 49. Cereda E, Barichella M, Pedrolli C, Klersy C, Cassani E, Caccialanza R, et al. Diabetes and risk of Parkinson's disease: a systematic review and meta-analysis. *Diabetes Care*. (2011) 34:2614–23. doi: 10.2337/dc11-1584

50. Miyake Y, Tanaka K, Fukushima W, Sasaki S, Kiyohara C, Tsuboi Y, et al. Case-control study of risk of Parkinson's disease in relation to hypertension, hypercholesterolemia, and diabetes in Japan. *J Neurol Sci.* (2010) 293:82–6. doi: 10.1016/j.jns.2010.03.002
51. Freiherr J, Hallschmid M, Frey WH, II, Brünner YF, Chapman CD, Hölscher C, et al. Intranasal insulin as a treatment for Alzheimer's disease: a review of basic research and clinical evidence. *CNS Drugs.* (2013) 27:505–14. doi: 10.1007/s40263-013-0076-8
52. Ghasemi R, Dargahi L, Haeri A, Moosavi M, Mohamed Z, Ahmadiani A. Brain insulin dysregulation: implication for neurological and neuropsychiatric disorders. *Mol Neurobiol.* (2013) 47:1045–65. doi: 10.1007/s12035-013-8404-z
53. van der Heide LP, Ramakers GM, Smidt MP. Insulin signaling in the central nervous system: learning to survive. *Prog Neurobiol.* (2006) 79:205–21. doi: 10.1016/j.pneurobio.2006.06.003
54. Aviles-Olmos I, Dickson J, Kefalopoulou Z, Djamshidian A, Ell P, Soderlund T, et al. Exenatide and the treatment of patients with Parkinson's disease. *J Clin Invest.* (2013) 123:2730–6. doi: 10.1172/JCI68295
55. Moroo I, Yamada T, Makino H, Tooyama I, McGeer PL, McGeer EG, et al. Loss of insulin receptor immunoreactivity from the substantia nigra pars compacta neurons in Parkinson's disease. *Acta Neuropathol.* (1994) 87:343–8. doi: 10.1007/BF00313602
56. Morris JK, Bomhoff GL, Gorres BK, Davis VA, Kim J, Lee PP, et al. Insulin resistance impairs nigrostriatal dopamine function. *Exp Neurol.* (2011) 231:171–80. doi: 10.1016/j.expneurol.2011.06.005
57. Campbell JE, Drucker DJ. Pharmacology, physiology, and mechanisms of incretin hormone action. *Cell Metab.* (2013) 17:819–37. doi: 10.1016/j.cmet.2013.04.008
58. Holst JJ. Treatment of type 2 diabetes mellitus with agonists of the GLP-1 receptor or DPP-IV inhibitors. *Expert Opin Emerg Drugs.* (2004) 9:155–66. doi: 10.1517/14728214.9.1.155
59. Salameh TS, Rhea EM, Talbot K, Banks WA. Brain uptake pharmacokinetics of incretin receptor agonists showing promise as Alzheimer's and Parkinson's disease therapeutics. *Biochem Pharmacol.* (2020) 180:114187. doi: 10.1016/j.bcp.2020.114187
60. Hosogi S, Ohsawa M, Kato I, Kuwahara A, Inui T, Inui A, et al. Improvement of diabetes mellitus symptoms by intake of Ninjin'yoeito. *Front Nutr.* (2018) 5:112. doi: 10.3389/fnut.2018.00112
61. Gonçalves P, Martel F. Butyrate and colorectal cancer: the role of butyrate transport. *Curr Drug Metab.* (2013) 14:994–1008. doi: 10.2174/1389200211314090006
62. Gao Z, Yin J, Zhang J, Ward RE, Martin RJ, Lefevre M, et al. Butyrate improves insulin sensitivity and increases energy expenditure in mice. *Diabetes.* (2009) 58:1509–17. doi: 10.2337/db08-1637
63. Yang Y, Bec J, Zhou J, Zhang M, Judenhofer MS, Bai X, et al. A prototype high-resolution small-animal PET scanner dedicated to mouse brain imaging. *J Nucl Med.* (2016) 57:1130–5. doi: 10.2967/jnumed.115.165886
64. Magota K, Kubo N, Kuge Y, Nishijima K, Zhao S, Tamaki N. Performance characterization of the Inveon preclinical small-animal PET/SPECT/CT system for multimodality imaging. *Eur J Nucl Med Mol Imaging.* (2011) 38:742–52. doi: 10.1007/s00259-010-1683-y

Conflict of Interest: RI and YO were employed by the company Tsumura & Co.

The remaining authors declare that the research was conducted in the absence of any commercial or financial relationships that could be construed as a potential conflict of interest.

Copyright © 2021 Zhao, Imai, Ukon, Shimoyama, Tan, Maejima, Omiya, Takahashi, Nan, Zhao, Ito and Shimomura. This is an open-access article distributed under the terms of the Creative Commons Attribution License (CC BY). The use, distribution or reproduction in other forums is permitted, provided the original author(s) and the copyright owner(s) are credited and that the original publication in this journal is cited, in accordance with accepted academic practice. No use, distribution or reproduction is permitted which does not comply with these terms.

Bilateral Medial Medullary Infarction Accompanied by Cerebral Watershed Infarction: A case report

Jingmin Zhao^{1,2}, Guangxian Nan^{1*}, Guangxun Shen¹, Songji Zhao^{3,4}, Hiroshi Ito^{2,3}

1. Department of Neurology, China-Japan Union Hospital of Jilin University, Changchun, China

2. Department of Radiology and Nuclear Medicine, Fukushima Medical University, Fukushima, Japan

3. Advanced Clinical Research Center, Fukushima Global Medical Science Center, Fukushima Medical University, Fukushima, Japan

4. Basic Medical College of Jilin University, Changchun, China

* **Correspondence:** Guangxian Nan, MD, PhD, Department of Neurology, China-Japan Union Hospital of Jilin University, 126 XianTai Street, Changchun, 130031, Jilin, China
(✉ nanguangxian@hotmail.com)

Radiology Case. 2020 Apr; 14(4):1-7 :: DOI: 10.3941/jrcr.v14i4.3905

ABSTRACT

Bilateral medial medullary infarction is a rare stroke subtype, and its diagnosis has become possible by brain magnetic resonance imaging. In this report, we describe a case in which acute bilateral medial medullary infarction accompanied by cerebral watershed infarction was clearly identified by diffusion-weighted imaging, and we discuss the mechanisms of bilateral medial medullary infarction accompanied by cerebral watershed infarction.

CASE REPORT

CASE REPORT

A 50-year-old man was admitted to our hospital with sensory dysfunction and pain in the four limbs, which began 2 hours before admission. The patient's condition, however, worsened into a rapidly progressive tetraparesis with slurred speech and dysphagia within 3 hours after admission. He had a history of hypertension, cigarette smoking, and myocardial infarction. Neurologic examination revealed breathing difficulty, dysarthria, hyporeflexia, quadriplegia, diminished pain sensation, and a muscle power of grade 4 for his four limbs. His National Institutes of Health Stroke Scale score was 12/42. Brain magnetic resonance imaging (MRI) performed 11 hours after admission showed the 'heart appearance' sign detected as a hyperintense signal in the bilateral anteromedial medullae (Fig. 1A), cortical watershed infarction (CWI) (Fig. 1B), and internal watershed infarction (IWI) (Fig. 1C) of the right cerebral hemisphere shown by diffusion-weighted

imaging (DWI), respectively. He then underwent a brain digital subtraction angiography (DSA), which showed mild stenosis in the basilar artery (BA) (Fig. 2A), plaque formation in the right internal carotid artery (ICA) without obvious stenosis (Fig. 2B), mild stenosis in the right middle cerebral artery (MCA) (Fig. 2C), and a normal right vertebral artery (VA) (Fig. 2D), which appeared more dominant than the left in the extracranial portion (Fig. 2E). The left VA was occluded at the distal intracranial portion (Fig. 2F). Two days after admission, the patient required an endotracheal intubation because of respiratory distress with disorder of consciousness (Glasgow Coma Scale score, 3/15) and a tracheotomy mask on day 3 of hospitalization. On day 10 of hospitalization, his consciousness improved (Glasgow Coma Scale score, 2+2+T/15) and his respiratory distress significantly improved; however, his four limbs remained weak. The patient had a modified Rankin Scale score of 5/6 at the time of his discharge without further treatment.

DISCUSSION

Etiology & Demographics:

Medial medullary infarction (MMI) is a rare stroke subtype, accounting for only 0.5—1.5% of all strokes [1,2], and bilateral MMI is even rarer [3]. Clinicopathologic studies have demonstrated that MMI is a rare condition, and in a series of 700 patients who died of cerebrovascular disease and were autopsied, only four were found to have ischemic damage in the medial medullae [4]. Bilateral MMI is even more rarely reported, and it is speculated that it may be related to an unpaired anterior spinal artery as an anatomical variation [5,6]. The etiological classifications of infarctions are large-artery atherosclerosis (LA), small-vessel disease (SV), arterial dissection (DI), cardiac embolism (CE), and stroke of undetermined etiology. Risk factors for cerebral infarction include atrial fibrillation, hypertension, smoking habit, diabetes mellitus, ischemic heart disease, and dyslipidemia. According to previous magnetic resonance angiography findings, bilateral MMI might be related to artery stenosis or occlusion, including VA atherosclerosis (38.5%), VA occlusion (15.4%), basilar artery atherosclerosis (19.2%), dissection (7.7%), anterior spinal artery (ASA) occlusion (3.8%; an autopsy case), and no abnormalities (38.5%) [3]. In patients with normal vascular imaging findings, the stroke mechanism was likely atheromatous branch occlusion or ASA occlusion, which could not be demonstrated by DSA [3].

Clinical & Imaging Findings:

The diagnosis of bilateral MMI was previously possible only at autopsy; however, its diagnosis has recently become possible by diffusion-weighted brain MRI, which shows the characteristic “heart appearance” sign. Previous case reports of bilateral MMI described the same heart appearance sign on axial MR images [4,5]. It is considered that blood is supplied to these areas by the vertebral and anterior spinal arteries, but it is often difficult to identify the occluded blood vessel because of the vastly complex network formed by these vessels. The heart appearance sign is considered to appear when the infarct occurs in the anteromedial territory and anterolateral territory [7].

Treatment & Prognosis:

It is difficult to diagnose bilateral MMI in its early stages. However, when properly diagnosed, its treatment is the same as that of cerebral infarction, including endotracheal intubation when respiratory distress occurs. A systematic review (38 patients, from 1992 to 2011) reported that bilateral MMI was present with quadriplegia in 24% of patients, dysarthria in 18%, and hypoglossal palsy in 9% [3]. Furthermore, approximately 9—24% of patients with bilateral MMI may develop respiratory failure, which is more prevalent in bilateral MMI than in unilateral MMI [3]. In contrast to unilateral MMI, the clinical outcome of bilateral MMI is usually poor [6]. However, no comparative studies have been reported to date.

Differential Diagnoses:

Bilateral MMI with respiratory failure can be frequently misdiagnosed as Guillain-Barre syndrome (GBS), particularly when the initial symptoms develop into flaccid quadriplegia [8]. Indeed, the patient’s medical history is very important. Brain MRI and DWI are also helpful, as they can show the classical heart or V/Y appearance at the ventral medulla in patients with bilateral MMI [7,8]. Of note, the abnormal MRI or DWI signal may be a small dot or a linear shape at the midline of the medulla in the early stages of bilateral MMI [9]. GBS can also be confirmed on the basis of the cerebrospinal finding of an elevated protein level without pleocytosis at slightly later stages. A key point to differentiate between these syndromes is the evolution of clinical presentation: GBS has a subacute evolution, whereas bilateral MMI has a more acute presentation [8].

Case Discussion:

To the best of our knowledge, bilateral MMI accompanied by cerebral watershed infarction (WSI) confirmed by DWI has not yet been reported. In this report, we first described a case in which acute bilateral MMI accompanied by WSI was identified by DWI. Below we discuss the causes of MMI and the possible mechanism of WSI.

In the current case, DWI showed bilateral MMI accompanied by WSI. WSI, that is, ischemic lesions between two non-anastomosing main arterial territories, can be classified as either CWI or IWI, which can be further divided into subtypes. CWI is further divided into anterior watershed infarction (AWI, between the anterior cerebral artery and the middle cerebral artery), posterior watershed infarction (PWI, between the middle cerebral artery and the posterior cerebral artery), and mixed-type infarction (AWI plus PWI). IWI is also further divided into partial IWI (P-IWI, a single lesion or chainlike, the so-called “rosary-like” pattern in the centrum semiovale) and confluent IWI (C-IWI, large cigar-shaped infarction alongside the lateral ventricle). The simultaneous occurrence of CWI and IWI is identified as mixed-type infarction [10]. In our case, apart from MMI, the hyperintense “heart appearance” sign in the bilateral anteromedial medullae (Fig. 1A), PWI, in the right cerebral hemisphere (Fig. 1B), and P-IWI in the right cerebral hemisphere (Fig. 1C) were detected by DWI. Most IWIs are accompanied by CWIs. To the best of our knowledge, the simultaneous occurrence of bilateral MMI and WSI has yet to be reported, and the mechanism of WSI is not yet fully understood. Traditionally, HDI has been widely accepted as a cause of WSI [11]. From the clinicians’ viewpoint, each case of IWI could be linked to a hemodynamic impairment. Previous studies demonstrated an association between IWI and critical stenosis of ICA. This finding supported the theory that HDI may be the main cause of IWI [10,12]. The relationship between CWI and HDI appears more complicated, with a previous report stating that artery-to-artery embolism might play an important role in isolated CWI [13]. The susceptibility of the internal border-zone area to HDI is probably due to low perfusion pressure in the perforating medullary arteries, the most distal branches of the ICA with insufficient collateral

supply of deep perforating lenticulostriate arteries [10]. Previous studies [10,13] revealed that the rosary-like infarction in the centrum semiovale, which was identified as P-IWI in those studies, appears to be associated with HDI. However, Moustafa et al. [14] found that in addition to HDI, microemboli might also play a role in the pathogenesis of the rosary-like infarction. If there is no blood flow reduction, an embolic mechanism can be considered. Few studies have thoroughly compared the difference between C-IWI and P-IWI. One study showed that critical ICA stenosis was more common in P-IWI patients than in C-IWI patients [10]. In our case, brain MRI showed PWI in the right cerebral hemisphere (Fig. 1B) and P-IWI in the right cerebral hemisphere (Fig. 1C) on DWI images. Furthermore, brain DSA showed mild stenosis in the BA (Fig. 2A), plaque formation in the right ICA without obvious stenosis (Fig. 2B), and mild stenosis in the right MCA (Fig. 2C). Therefore, it is considered that bilateral MMI might be associated with basilar artery atherosclerosis. However, there is no evidence to conclude that bilateral MMI might be associated with HDI or microemboli, which might cause the CWI.

Maybe there is another mechanism; in the current case, brain DSA showed that the right VA was more dominant than the left VA in the extracranial portion, and the left VA was occluded at the distal intracranial portion (Figs. 2A, E, and F). The anatomic variability of the left perforator branches, which supply the bilateral anteromedial arterial or ASAs originating from the left VA, might explain the bilateral MMI with unilateral VA occlusion [15].

TEACHING POINT

MRI shows the classical heart appearance or V/Y sign at the ventral medulla in patients with bilateral medial medullary infarction. Hemodynamic impairment and microemboli are both the causes of cortical watershed infarction.

REFERENCES

1. Toyoda K, Imamura T, Saku Y, Oita J, Ibayashi S, Minematsu K, Yamaguchi T, Fujishima M. Medial medullary infarction: analyses of eleven patients. *Neurology*. 1996;47(5):1141-1147. PMID: 8909419
2. Shono Y, Koga M, Toyoda K, et al. Medial medullary infarction identified by diffusion-weighted magnetic resonance imaging. *Cerebrovasc Dis* 2010;30:519-524. PMID: 20861624
3. Pongmoragot J, Parthasarathy S, Selchen D, et al. Bilateral medial medullary infarction: a systematic review. *J Stroke Cerebrovasc Dis* 2013;22:775-780. PMID: 22541608

4. Maeda M, Shimono T, Tsukahara H, Maier SE, Takeda K. Acute bilateral medial medullary infarction: a unique "Heart Appearance" sign by diffusion-weighted imaging. *Eur Neurol*. 2004;51(4):236-237. PMID: 15159607
5. Thijs RD, Wijman CA, van Dijk GW, van Gijn J. A case of bilateral medial medullary infarction demonstrated by magnetic resonance imaging with diffusion-weighted imaging. *J Neurol*. 2001;248:339-340. PMID: 11374104
6. Kumral E, Afsar N, Kirbas D, Balkir K, Ozdemirkiran T. Spectrum of medial medullary infarction: clinical and magnetic resonance imaging findings. *J Neurol*. 2002;249:85-93. PMID: 11954873
7. Parsi K, Itgampalli RK, Suryanarayana A, et al. Bilateral medial medullary infarction: heart appearance. *Neurol India* 2013;61:84-85. PMID: 23466852
8. Ma L, Deng Y, Wang J, et al. Bilateral medial medullary infarction presenting as Guillain-Barre-like syndrome. *Clin Neurol Neurosurg* 2011;113:589-591. PMID: 21397385
9. Torabi AM. Bilateral medial medullary stroke: a challenge in early diagnosis. *Case Rep Neurol Med* 2013;2013:274373. PMID: 24198988
10. Li Y, Li M, Zhang X, et al. Clinical features and the degree of cerebrovascular stenosis in different types and subtypes of cerebral watershed infarction. *BMC Neurology*. 2017;17:166. PMID: 28851301
11. Hoffman SJ, Yee AH, Slusser JP, et al. Neuroimaging patterns of ischemic stroke after percutaneous coronary intervention. *Catheter Cardiovasc Interv*. 2015;85(6):1033-1040. PMID: 25256948
12. Del Sette M, Eliasziw M, Streifler JY, Hachinski VC, Fox AJ, Barnett HJ. Internal borderzone infarction: a marker for severe stenosis in patients with symptomatic internal carotid artery disease. For the North American Symptomatic Carotid Endarterectomy (NASCET) Group. *Stroke*. 2000;31:631-636. PMID: 10700496
13. Derdeyn CP, Khosla A, Videen TO, et al. Severe hemodynamic impairment and border zone--region infarction. *Radiology*. 2001;220:195-201. PMID: 11425997
14. Moustafa RR, Momjian-Mayor I, Jones PS, et al. Microembolism versus hemodynamic impairment in rosary-like deep watershed infarcts: a combined positron emission tomography and transcranial Doppler study. *Stroke*. 2011;42:3138-3143. PMID: 21852602
15. Gillilan LA. The correlation of the blood supply to the human brain stem with clinical brain stem lesions. *J Neuropathol Exp Neurol* 1964;23:78-108. PMID: 14105311

FIGURES

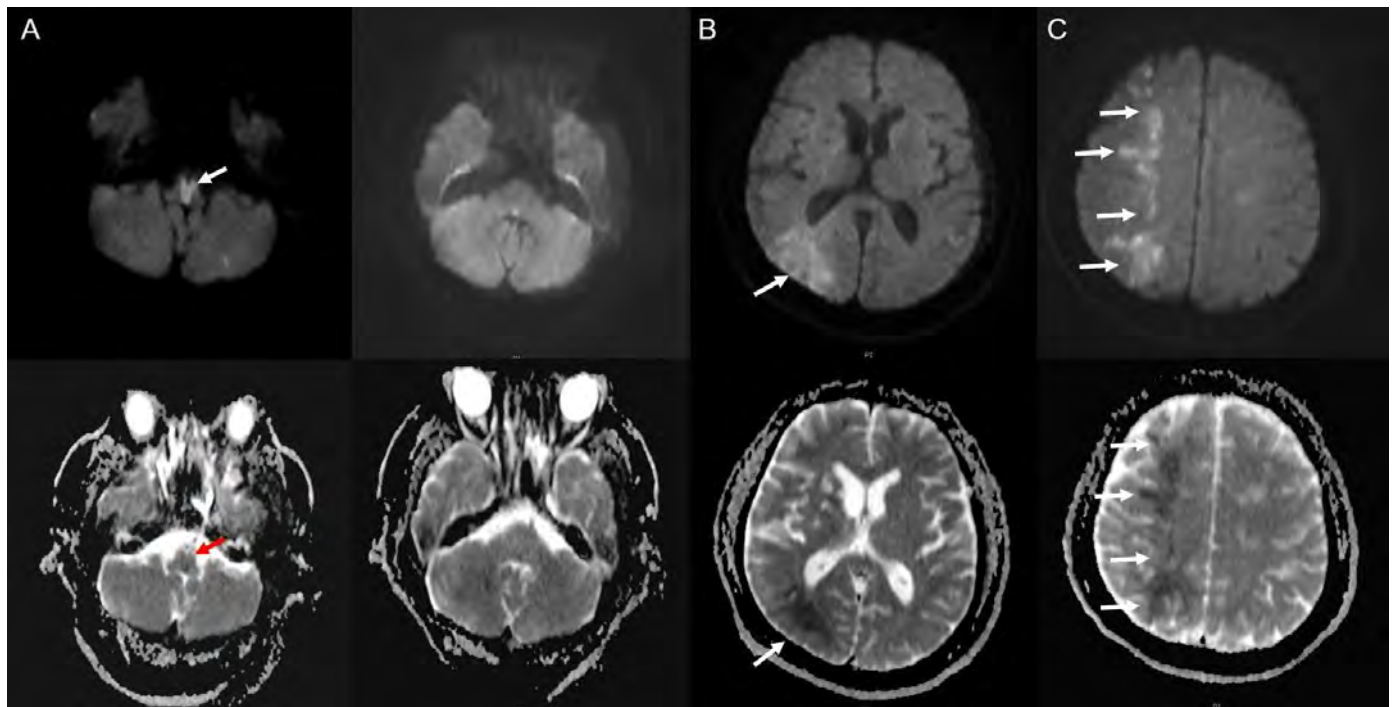


Figure 1: 50-year-old male with medial medullary infarction accompanied by cerebral watershed infarction.

Findings: MRI showed a hyperintense "heart appearance" signal in the bilateral anteromedial medullae on DWI images (top) with corresponding axial apparent diffusion coefficient (ADC) maps (bottom) (Fig. 1A), cortical watershed infarction in the right cerebral hemisphere on DWI images (top) with corresponding ADC maps (bottom) (Fig. 1B) and internal watershed infarction in the right cerebral hemisphere on DWI images (top) with corresponding ADC maps (bottom) (Fig. 1C).

TECHNIQUE: Axial diffusion-weighted 1.5T-MRI of the head.



Figure 2: 50-year-old male with medial medullary infarction accompanied by cerebral watershed infarction.

Findings: Brain digital subtraction angiography (DSA) showed mild stenosis in the basilar artery (BA) (Fig. 2A), plaque formation in the right internal carotid artery (ICA) without obvious stenosis (Fig. 2B), mild stenosis in the right middle cerebral artery (MCA) (Fig. 2C), and normal right vertebral artery (VA) (Fig. 2D), which appeared more dominant than the left in the extracranial portion (Fig. 2E). The left VA was occluded at the distal intracranial portion (Fig. 2F).

TECHNIQUE: DSA projections following vertebral (4ml/s Omnipaque 240 contrast), left SCA (8ml/s Omnipaque 240 contrast), right SCA (8ml/s Omnipaque 240 contrast), and right ICA injections (6ml/s Omnipaque 240 contrast).
Figure 2-2 (magnification of figure 2-1)

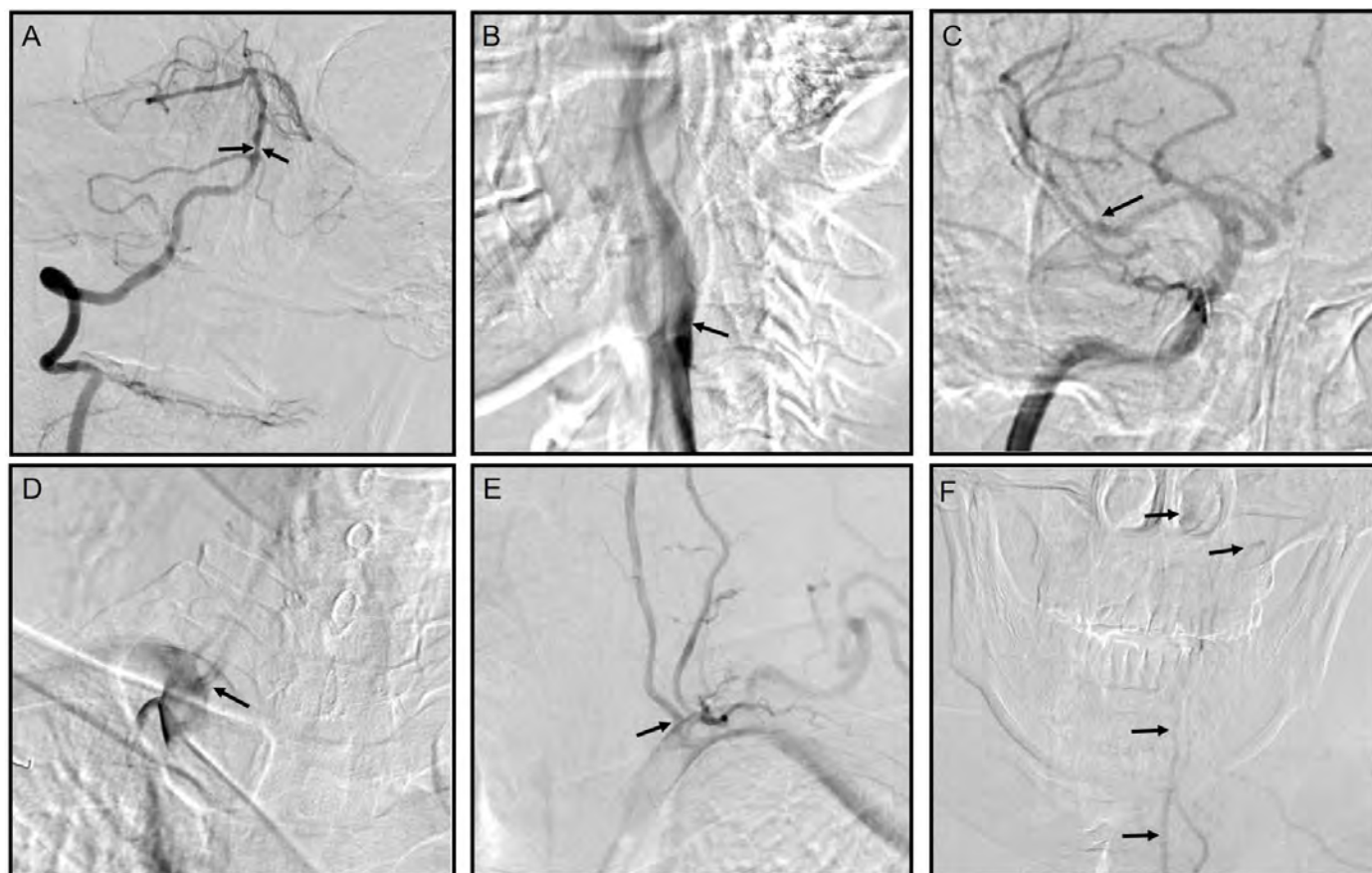


Figure 3: 50-year-old male with medial medullary infarction accompanied by cerebral watershed infarction. (magnification of figure 2)

Findings: Brain digital subtraction angiography (DSA) showed mild stenosis in the basilar artery (BA) (Fig. 2A), plaque formation in the right internal carotid artery (ICA) without obvious stenosis (Fig. 2B), mild stenosis in the right middle cerebral artery (MCA) (Fig. 2C), and normal right vertebral artery (VA) (Fig. 2D), which appeared more dominant than the left in the extracranial portion (Fig. 2E). The left VA was occluded at the distal intracranial portion (Fig. 2F).

TECHNIQUE: DSA projections following vertebral (4ml/s Omnipaque 240 contrast), left SCA (8ml/s Omnipaque 240 contrast), right SCA (8ml/s Omnipaque 240 contrast), and right ICA injections (6ml/s Omnipaque 240 contrast).

| | |
|-------------------------|--|
| Etiology | The etiological classifications of infarctions are large-artery atherosclerosis (LA), small-vessel disease (SV), arterial dissection (DI), cardiac embolism (CE), and stroke of un- determined etiology. |
| Incidence | Medial medullary infarction (MMI) is a rare stroke subtype, accounting for only 0.5—1.5% of all strokes [1,2], and bilateral MMI is even rarer [3]. |
| Risk factors | Atrial fibrillation, hypertension, smoking habits, diabetes mellitus, ischemic heart disease, and dyslipidemia |
| Treatment | The same as cerebral infarction treatment, and to perform endotracheal intubation when respiratory distress occurs. |
| Symptoms | They include quadriplegia, dysarthria, hypoglossal palsy, respiratory failure, and so on. |
| prognosis | The clinical outcome of bilateral MMI is usually poor [6]. |
| Imaging findings | Brain magnetic resonance imaging (MRI) shows a hyperintense “heart appearance” signal in the bilateral anteromedial medullae. |

Table 1: Summary table for Bilateral Medial Medullary Infarction

| Diagnosis | X-Ray | CT | MRI | Key point |
|--|---------------|---------------|--|---|
| Bilateral Medial Medullary Infarction | Not mentioned | Not mentioned | MRI shows the classical “heart” or “V/Y” appearance at the ventral medulla in patients with bilateral MMI [7, 8] | A key point to differentiate between syndromes is the evolution of the clinical presentation; BMMI has a more acute presentation [8]. |
| Guillain-Barre syndrome | Not mentioned | Not mentioned | No abnormalities found. | GBS has subacute evolution of clinical presentation [8]. |

Table 2: Differential diagnosis table for Bilateral Medial Medullary Infarction

ABBREVIATIONS

ADC = Apparent diffusion coefficient
 ASA = Anterior spinal artery
 AWI = Anterior watershed infarction
 BA = Basilar artery
 C-IWI = Confluent internal watershed infarction
 CWI = Cortical watershed infarction
 DSA = Digital subtraction angiography
 DWI = Diffusion-weighted imaging
 HDI = Hemodynamic impairment
 ICA = Internal carotid artery
 IWI = Internal watershed infarction
 MCA = Middle cerebral artery
 MMI = Medial medullary infarction
 MRI = Magnetic resonance imaging
 P-IWI = Partial internal watershed infarction
 PWI = Posterior watershed infarction
 SCA = Subclavian artery
 VA = Vertebral artery
 WSI = Watershed infarction

KEYWORDS

Bilateral medial medullary infarction; Cerebral watershed infarction; Hemodynamic impairment; Diffusion-weighted imaging; Digital subtraction angiography

ACKNOWLEDGEMENTS

We thank the patient and his family for their consent to publish the case report. We also thank Kunjun Wu who helped us during writing of this manuscript.

Online access

This publication is online available at:
www.radiologycases.com/index.php/radiologycases/article/view/3905

Peer discussion

Discuss this manuscript in our protected discussion forum at:
www.radiopolis.com/forums/JRCR

Interactivity

This publication is available as an interactive article with scroll, window/level, magnify and more features.
 Available online at www.RadiologyCases.com

Published by EduRad



www.EduRad.org

米国雑誌「Scientific Reports」掲載 (01 Apr 2021;11:7421)
(2021-05-24)

Evaluation of organ glucose metabolism by ¹⁸F-FDG accumulation with insulin loading in aged mice compared with young normal mice

高齢マウスと若齢マウスにおける臓器糖代謝の評価：インシュリン負荷による¹⁸F-FDGの取り込みの潜在力の比較



趙 景敏 (ちょう・けいびん)

医学部 放射線医学講座 大学院研究生 (日中笹川医学奨学金制度第42期研究者)

研究グループ

趙 景敏、伊藤 浩 (受入れ指導教官)：放射線医学講座
譚 成博、右近 直之、下山 彩希、高橋 和弘、趙 松吉 (責任著者)：先端臨床研究センター
前島 裕子、下村 健寿 (最終著者)：病態制御薬理医学講座
今井 亮太、大宮 雄司：株式会社ツムラ
南 光賢：吉林大学

概要

論文掲載雑誌：「Scientific Reports」 (01 Apr 2021;11:7421)

加齢に伴う臓器の機能的変化を随時予測・把握することは、高齢化社会における健康的な生活を維持する上で重要である。また生体内の糖代謝は、臓器機能の変化を評価する潜在的な指標の1つである。したがって、生体における臓器の糖代謝に関する情報の取得は、臓器の機能的変化を理解するのに役立つと考えられる。またグルコース類似体である[¹⁸F]-フルオロ-2-デオキシ-2-D-グルコース (¹⁸F-FDG) は、糖代謝の生物学的指標として、基礎医学研究、創薬や臨床診療などのさまざまな分野で広く利用されている。しかし、超高齢動物における臓器の糖代謝の変化についてはまだ完全には解明されていない。そこで本研究では、超高齢マウス (96週齢、ヒトの約70歳相当) の各臓器・組織及び局所脳組織における糖代謝の変化を¹⁸F-FDGの取り込みと¹⁸F-FDGオートラジオグラフィーの手法を用いて測定し、若齢正常マウス (9週齢、ヒトの約20歳相当) の場合と比較検討を行った。さらに加齢に伴う各臓器・組織及び局所脳組織への¹⁸F-FDG取り込みの潜在力を測定するためインシュリン負荷を実施し、非インシュリン負荷群と比較した。その結果、非インシュリン負荷群では、若齢正常マウスに比し超高齢マウスにおける血液、血漿、筋肉、肺、脾臓、膵臓、精巣、胃、小腸、腎臓、肝臓、脳及び局所脳組織 (皮質、線条体、視床と海馬) への¹⁸F-FDG取り込みは有意に高くなった。一方、超高齢マウスにおける膵臓と腎臓、また脳の局所領域の皮質、線条体、視床と海馬への¹⁸F-FDG取り込みはインシュリン負荷によって低下したのに対し、若齢マウスでは増加した。以上の結果から、超高齢マウスにおいて、一部の臓器・組織への¹⁸F-FDG取り込みはインシュリン負荷によって低下し、加齢はインシュリン抵抗性を増加させ、全身及び脳局所の糖代謝の機能低下に伴う加齢関連の疾患を引き起こすことが示唆された。

この研究の結果は、加齢による糖代謝の機能低下に伴う加齢関連疾患の予防及び治療戦略の開発につながる成果である。

本研究は、病態制御薬理医学・先端臨床研究センターと株式会社ツムラが共同で実施したものである。

Home
研究推進戦略
医療研究推進センター
業績

▶ 現在進められている研究

▶ 主な研究成果概要

2021年度
2020年度
2019年度
2018年度
2017年度
2016年度
2015年度
2014年度
2013年度
2012年度
2011年度
2010年度
2009年度
2008年度
2007年度

▶ 学会表彰

お知らせ

業績 業績 [主な研究成果概要]

福島県立医科大学

スイス雑誌「Frontiers in Nutrition, section Nutrition and Brain Health」掲載 (12 May 2021;8:657663) (2021-06-09)

Evaluation of effect of Ninjin'yoeito on regional brain glucose metabolism by ¹⁸F-FDG autoradiography with insulin loading in aged mice

高齢マウスの局所脳糖代謝に対する人参栄養湯の効果：インシュリン負荷による¹⁸F-FDG オートラジオグラフィーの画像手法を用いた評価

趙 景敏 (ちょう・けいびん)

医学部 放射線医学講座 大学院研究生 (日中笹川医学奨学金制度第42期研究者)

研究グループ

趙 景敏、伊藤 浩 (受入れ指導教官)・放射線医学講座
右近 直之、下山 彩希、譚 成博、高橋 和弘、趙 松吉 (責任著者)・先端臨床研究センター
前島 裕子、下村 健寿 (最終著者)・病態制御薬理医学講座
今井 亮太、大宮 雄司・株式会社ツムラ
南 光賢・吉林大学

概要

論文掲載雑誌：「Frontiers in Nutrition, section Nutrition and Brain Health」 (12 May 2021;8:657663)

近年の臨床研究では、人参栄養湯 (NYT) は認知機能を改善する可能性があることが明らかになりました。しかし、NYTが高齢患者におけるその効果を発揮するメカニズムは不明であります。そこで本研究では、高齢化した野生型高齢マウスにおける局所脳組織の糖代謝に及ぼすNYTの効果について、インシュリン負荷による¹⁸F-FDGのオートラジオグラフィー (ARG) の画像手法を用いて比較評価を行いました。

84週齢の雄性マウス (C57BL/6J) をNYT治療群と非治療群に分けました。NYT治療群のマウスはNYT混餌で、無治療群のマウスは普通餌で各々12週間飼育しました。マウスが96週齢になった時点で、インシュリンの感受性を評価するため、NYT混餌群と普通餌群のマウスをさらにインシュリン負荷群と生理食塩水投与群に分けました。インシュリン負荷群のマウスには単位体重 (kg) 当たりにインシュリン2単位を、無治療群のマウスには生理食塩水を、¹⁸F-FDGの投与30分前にマウスの腹腔内に投与しました。¹⁸F-FDG投与90分後、イソフルラン麻酔下で心臓より全採血し、大脳を摘出しました。摘出したマウス脳を脳スライサーに入れて、嗅球側から小脳側に向けて2mm間隔で大脳の横断面スライスを作成し、イメージングプレートに露光させ、¹⁸F-FDG ARG画像を得ました。¹⁸F-FDG ARG画像上で大脳皮質、線条体、視床及び海馬の局所に関心領域を置き、¹⁸F-FDG ARG画像の定量解析を行いました。その結果、無治療群のマウスではインシュリン負荷により大脳皮質、線条体、視床及び海馬領域への¹⁸F-FDGの取り込みは負の変化を示したのに対し、NYT治療群のマウスでは正の変化を示しました。以上の結果から人参栄養湯は高齢マウスの局所脳組織のインシュリン耐性を軽減することで、加齢による脳疾患の予防が可能であることが示唆されました。

本論文は、本学病態制御薬理医学講座、先端臨床研究センターと株式会社ツムラの共同研究の成果です。

日中笹川医学奨学金制度(学位取得コース)評価書

課程博士：指導教官用



第 42 期

研究者番号： G4202

作成日： 2022 年 2 月 7 日

| | | | | | | |
|-----------|---|-----|----|--|------|--------------|
| 氏名 | Jiao Dandan | 焦丹丹 | 性別 | F | 生年月日 | 1985. 12. 21 |
| 所属機関(役職) | 河南科技大学第一附属医院心外重症監護室(主管護師) | | | | | |
| 研究先(指導教官) | 筑波大学大学院人間総合科学研究科 国際発達ケア：エンパワメント科学研究室(安梅 勅江教授) | | | | | |
| 研究テーマ | 地域在住慢性疾患高齢者の機能維持の支援方法の解明 The role of social relationships on the functional status among community-dwelling older adults | | | | | |
| 専攻種別 | <input type="checkbox"/> 論文博士 | | | <input checked="" type="checkbox"/> 課程博士 | | |

研究者評価(指導教官記入欄)

| | | |
|------------------|---|------------------------|
| 成績状況 | <input checked="" type="checkbox"/> 優 <input type="checkbox"/> 良 <input type="checkbox"/> 可 <input type="checkbox"/> 不可 学業成績係数=3.2 | 取得単位数 38 |
| | | 取得単位数/取得すべき単位数総数 38/30 |
| 学生本人が行った研究の概要 | 焦丹丹氏は、研究室の博士課程学生の中で最も優秀な成績を収めている学生です。エンパワメントの技術を活用し、地域在住高齢者の健康増進に向けた促進因子を明らかにする研究を実施しました。健康習慣に加え社会とのかかわりが、高齢者の健康状態維持に大きく貢献する要因であることを明らかにしました。 | |
| 総合評価 | 【良かった点】 1. 多側面におよぶ高い研究技術を習得しました。 2. 学際チームワーク技術を習得しました。 3. プロジェクトマネジメントを体験し習得しました。 | |
| | 【改善すべき点】 さらに高度な統計スキルを学ぶことで解析の幅が広がります。 | |
| | 【今後の展望】 リーダーとしての資質を発揮し、国際的学際的なプロジェクトを企画し、日中の懸け橋となっていただくことを期待しています。 | |
| 学位取得見込 | 焦丹丹氏は、博士取得見込です。 | |
| 評価者(指導教官名) 安梅 勅江 | | |

日中笹川医学奨学金制度(学位取得コース)報告書 研究者用



第42期

研究者番号: G4202

作成日: 2022年3月 日

| | | | | | |
|-----------|---|--------------------------|------|-------------------------------------|-------------------|
| 氏名 | Jiao Dandan | 焦丹丹 | 性別 | F | 生年月日 1985. 12. 21 |
| 所属機関(役職) | 河南科技大学第一附属医院心外重症監護室(主管護師) | | | | |
| 研究先(指導教官) | 筑波大学大学院人間総合科学研究科 国際発達ケア: エンパワメント科学研究室(安梅 勅江教授) | | | | |
| 研究テーマ | 地域在住慢性疾患高齢者の機能維持の支援方法の解明 The role of social relationships on the functional status among community-dwelling older adults | | | | |
| 専攻種別 | 論文博士 | <input type="checkbox"/> | 課程博士 | <input checked="" type="checkbox"/> | |

1. 研究概要(1)

1) 目的(Goal)

To examine the role of social relationships on the association between chronic diseases and functional decline among community-dwelling older adults in Japan.

2) 戦略(Approach)

This three-year longitudinal study used data from a single-center cohort project, the “Community empowerment and care for well-being and healthy longevity: Evidence from a cohort study” [1], which started in 1991. This survey was conducted in a suburban area in central Japan with a population of around 5,000 with the goal of creating a health-promoting program that would maximize quantity and quality of life for residents. Questionnaires were mailed to all residents every three years, and interviews were conducted with people who needed assistance in completing the questionnaires.

3) 材料と方法(Materials and methods)

a. Participants

For the purpose of the present study, we used data collected from individuals aged 65 years and older in 2014 and 2017 as baseline and follow-up, respectively. In 2014, at baseline, 523 individuals with at least one chronic disease (hypertension, stroke, heart disease, diabetes, hyperlipidemia, lung disease, arthritis, cancer, immune disease, depression, eye disease, and ear disease) were initially included. Then, in 2017, a follow up was conducted to assess the incidence of physical function decline among participants.

b. Measurements

Functional status.

Functional status was assessed by instrumental activities of daily living (IADL) using the subscale of the Tokyo Metropolitan Institute of Gerontology Index of Competence, which was used to measure the functional competence of the community older adults [2]. The IADL subscale comprises five items, namely, using public transportation, shopping, preparing meals, paying bills, and individual banking management. For each item, a positive response was coded as 1, and a negative response was coded as 0. The total score ranges from 0 to 5. A score of 5 was considered normal IADL, while a score of 0-4 indicated low IADL [3].

Social relations.

Social relations were evaluated by the Index of Social Interaction (ISI) which was used to evaluate social relationships [4]. The ISI includes five subscales and 18 items which is comprised of 5 subscales: 1) Independence, which includes having a motivation to live an active lifestyle, taking an active approach towards one's life, being motivated to live a healthy life, and having a regular or routine lifestyle; 2) Social curiosity, which comprised reading newspapers, reading books, trying to use new equipment, having a hobby, and having a feeling of importance; 3) Interaction, composed of communication within the family, communication with non-family persons, and interactions with non-family persons; 4) Participation in society, made up of participation in social groups, participation in neighborhood affairs, watching television and having an active role in society; and 5) Feelings of safety, meaning having counsel, and having someone to give support in an emergency.

c. Statistical analysis.

Logistic regression analysis was employed to investigate the association between total changes in social relationships and physical function decline after adjusting for covariates.

1. 研究概要(2)

4) 実験結果 (Results)

Data from 422 individuals were included in the analysis after excluding participants who were lost to follow-up and had missing information in IADL. Of the participants, the majority were women, not living alone, doing exercise, no smoking and drinking. 55.7% had one chronic disease.

The logistic regression results showed that rich social relationships were significantly associated with low incidence of physical function, with the odds ratio = 0.77, 95% confidence interval = 0.64–0.93 after controlling the confounding variables.

5) 考察 (Discussion)

The present study examined the effects of social relationships on functional status and showed that rich social relationships could reduce the physical functional decline among older adults with chronic diseases. Social relationships seem to have adverse effects on functional decline in older adults with chronic disease. This result is in line with a previous study, in which Christian et al. [5] conducted research in six countries and showed that social capital was linked to increased subject well-being regardless of the chronic disease conditions. A systematic review indicated that social relationships play an important role in well-being and mental health among people with disabilities [6]. Social relations affect health outcomes through a reciprocity exchange [7] that social relations might extend resources, including transportation support and caring, which can affect health-related behavior. People with chronic diseases may gain benefits from social relationships, including a high chance of undergoing medical checkups, important health-related information, and confidence in health promotion behaviors, which can delay physical decline. Knowing the effects of social relationships on health outcomes among people with chronic conditions may provide evidence of chronic disease management.

Several limitations exist in this study. First, the disease severity and duration were not examined, which may have affected the results. Second, only one indicator was used to examine the functional status, and combining subjective and objective measurements as functional indicators might strengthen the reliability of results. Third, this study was conducted in one area, which may limit the generalizability of the results. Further studies should be conducted to address these limitations.

Despite these limitations, the present study addresses the association between social relationships and functional status among community-dwelling older adults with chronic conditions. These findings supplement evidence of the role of social relationships, indicating that social relationships contribute to health outcomes for both the general population and able-bodied people.

6) 参考文献 (References)

1. Anme, T. (2015, December 20). Community empowerment and care for well-being and healthy longevity: Evidence from cohort study (abbr. CEC). <http://plaza.umin.ac.jp/~empower/cec/en/>
2. W. Koyano, H. Shibata, K. Nakazato, H. Haga, Y. Suyama, Measurement of competence: reliability and validity of the TMIG Index of Competence, *Arch Gerontol Geriatr.* 13(2) (1991) 103–116. doi: 10.1016/0167-4943(91)90053-s
3. T. Ishizaki, I. Kai, Y. Kobayashi, Y. Imanaka, Functional transitions and active life expectancy for older Japanese living in a community, *Arch Gerontol Geriatr.* 35(2) (2002) 107–120. doi: 10.1016/s0167-4943(02)00002-x
4. T. Anme, C. Shimada, Social interaction and mortality in a five-year longitudinal study of the elderly, *Jpn. J. Public Health.* 47(2000) 127–133.
5. A.K. Christian, O.A. Sanuade, M. A. Okyere, K. Adjaye-Gbewonyo, Social capital is associated with improved subjective well-being of older adults with chronic non-communicable disease in six low- and middle-income countries, *Global Health.* 16(1) (2020) 2. doi: 10.1186/s12992-019-0538-y
6. H. Tough, J. Siegrist, C. Fekete, Social relationships, mental health and wellbeing in physical disability: a systematic review, *BMC Pub Health.* 17(1) (2017) 414. doi: 10.1186/s12889-017-4308-6
7. W.C. Cockerham, B.W. Hamby, G.R. Oates, The .Social Determinants of Chronic Disease, *Am J Prev Med.* 52(1s1) (2017) S5–s12. doi: 10.1016/j.amepre.2016.09.010
8. Jiao D, Watanabe K, Sawada Y, Tanaka E, Watanabe T, Tomisaki E, Ito S, Okumura R, Kawasaki Y, Anme T. Multimorbidity and functional limitation: the role of social relationships. *Arch Gerontol Geriatr.* 2021 Jan–Feb;92:104249. doi: 10.1016/j.archger.2020.104249. Epub 2020 Sep 7. PMID: 32980575.

2. 執筆論文 Publication of thesis ※記載した論文を添付してください。Attach all of the papers listed below.

| | | | | | | |
|---------------------------|---|------------------------|---------------|-----------------------|--------------------|---------|
| 論文名 1 Title | Multimorbidity and functional limitation: the role of social relationships | | | | | |
| 掲載誌名 Published journal | Archives of Gerontology and Geriatrics | | | | | |
| | 2021 年 1 月 | 92 巻(号) | 14049 頁 ~ | 頁 | 言語 Language | English |
| 第1著者名 First author | Dandan Jiao | 第2著者名 Second author | Kumi Watanabe | 第3著者名 Third author | Yuko Sawada | |
| その他著者名 Other authors | Emiko Tanaka, Taeko Watanabe, Etsuko Tomisaki, Sumio Ito, Rika Okumura, Yuriko Kawasaki, Tokie Anme* | | | | | |
| 論文名 2 Title | Changes in Social Relationships and Physical Function among Community-dwelling Older adults | | | | | |
| 掲載誌名 Published journal | Journal of Nursing Research (Accepted) | | | | | |
| | 年 月 | 巻(号) | 頁 ~ | 頁 | 言語 Language | |
| 第1著者名 First author | Dandan Jiao | 第2著者名 Second author | Kumi Watanabe | 第3著者名 Third author | Yuko Sawada | |
| その他著者名 Other authors | Emiko Tanaka, Taeko Watanabe, Etsuko Tomisaki, Sumio Ito, Rika Okumura, Yuriko Kawasaki, Tokie Anme* | | | | | |
| 論文名 3 Title | Home environment and social skills of Japanese preschool children pre- and post-COVID-19 | | | | | |
| 掲載誌名 Published journal | Early Child Development and Care | | | | | |
| | 2022 年 1 月 | 巻(号) | 頁 ~ | 頁 | 言語 Language | English |
| 第1著者名 First author | Xiang Li | 第2著者名 Second author | Dandan Jiao | 第3著者名 Third author | Munenori Matsumoto | |
| その他著者名 Other authors | Yantong Zhu, Jinrui Zhang, Zhu Zhu, Yang Liu, Mingyu Cui, Yanlin Wang, Meiling Qian, Ammara Ajmal, Alpona Afsari, Banua, Yolanda Graça, Emiko Tanaka, Taeko Watanabe, Yuko Sawada, Etsuko Tomisaki, Tokie Anme* | | | | | |
| 論文名 4 Title | Development of Social Skills in Kindergarten: A Latent Class Growth Modeling Approach | | | | | |
| 掲載誌名 Published journal | Children | | | | | |
| | 2021 年 9 月 | 8 巻(号) | 870 頁 ~ | 880 頁 | 言語 Language | English |
| 第1著者名 First author | Yan-Tong Zhu | 第2著者名 Second author | Xiang Li | 第3著者名 Third author | Dandan Jiao | |
| その他著者名 Other authors | Emiko Tanaka, Etsuko Tomisaki, Taeko Watanabe, Yuko Sawada, Zhu Zhu, Ammara Ajmal, Munenori Matsumoto, Tokie Anme* | | | | | |
| 論文名 5 Title | Patterns of Movement Performance Among Japanese Children and Effects of Parenting Practices: Latent class analysis | | | | | |
| 掲載誌名 Published journal | Sultan Qaboos University medical journal | | | | | |
| | 2022 年 1 月 | 巻(号) | 頁 ~ | 頁 | 言語 Language | English |
| 第1著者名 First author | Zhu Zhu | 第2著者名 Second author | Cunyoen Kim | 第3著者名 Third author | Dandan Jiao | |
| その他著者名 Other authors | Xiang Li, Ammara Ajmal, Munenori Matsumoto, Yuko Sawada, Toshiyuki Kasai, Taeko Watanabe, Etsuko Tomisaki, Emiko Tanaka, Sumio Ito, Rika Okumura, Tokie Anme* | | | | | |

3. 学会発表 Conference presentation ※筆頭演者として総会・国際学会を含む主な学会で発表したものを記載してください。

※Describe your presentation as the principal presenter in major academic meetings including general meetings or international meetings

| | | | |
|-----------------------|--|-------------|--|
| 学会名 Conference | Tsukuba Global Science Week (2020) | | |
| 演題 Topic | Multimorbidity and functional limitation: the role of social relationships | | |
| 開催日 date | 2020 年 9 月 18 日 | 開催地 venue | Tsukuba,Japan |
| 形式 method | <input checked="" type="checkbox"/> 口頭発表 Oral <input checked="" type="checkbox"/> ポスター発表 Poster | 言語 Language | <input type="checkbox"/> 日本語 <input checked="" type="checkbox"/> 英語 <input type="checkbox"/> 中国語 |
| 共同演者名 Co-presenter | Dandan Jiao, Kumi Watanabe, Yoko Sawada, Emiko Tanaka, Taeko Watanabe,Etsuko Tomisaki,Sumio Ito,Rika Okumura,Yuriko Kawasaki, Tokie Anme* | | |
| 学会名 Conference | Tsukuba Global Science Week (2021) | | |
| 演題 Topic | Social Relationships Contribute to Keep Functional Status among Older Adults | | |
| 開催日 date | 2021 年 10 月 30 日 | 開催地 venue | Tsukuba,Japan |
| 形式 method | <input checked="" type="checkbox"/> 口頭発表 Oral <input checked="" type="checkbox"/> ポスター発表 Poster | 言語 Language | <input type="checkbox"/> 日本語 <input checked="" type="checkbox"/> 英語 <input type="checkbox"/> 中国語 |
| 共同演者名 Co-presenter | Dandan Jiao, Munenori Matsumoto, Ammara Ajmal, Xiang Li, Jinrui Zhang, Zhuzhu, Zhu Yantong, Liu Yang, Cui Mingyu, Yolandan Graca, Afsari Apolna, Wang Yanlin, Qian Meiling, Yoko Sawada, Taeko Watanabe, Emiko Tanaka, Tokie Anme* | | |
| 学会名 Conference | 第34回日本保健福祉学会学術集会 | | |
| 演題 Topic | Social relationships and changes in functional status among community-dwelling older adults with chronic diseases | | |
| 開催日 date | 2021 年 11 月 3 日 | 開催地 venue | Tsukuba,Japan |
| 形式 method | <input checked="" type="checkbox"/> 口頭発表 Oral <input type="checkbox"/> ポスター発表 Poster | 言語 Language | <input type="checkbox"/> 日本語 <input checked="" type="checkbox"/> 英語 <input type="checkbox"/> 中国語 |
| 共同演者名 Co-presenter | Jiao Dandan, Ammara Ajmal, Munenori Matsumoto, Li Xiang, Zhang Jinrui, Zhuzhu, Zhu Yantong, Liuyang, Cui Mingyu, Yolandan Graca, Afsari Apolna, Wang Yanlin, Qian Mei ling,Yoko Sawada,Taeko Watanabe, Emiko Tanaka, Tokie Anme* | | |
| 学会名 Conference | | | |
| 演題 Topic | | | |
| 開催日 date | 年 月 日 | 開催地 venue | |
| 形式 method | <input type="checkbox"/> 口頭発表 Oral <input type="checkbox"/> ポスター発表 Poster | 言語 Language | <input type="checkbox"/> 日本語 <input type="checkbox"/> 英語 <input type="checkbox"/> 中国語 |
| 共同演者名 Co-presenter | | | |

4. 受賞(研究業績) Award (Research achievement)

| | | | |
|------------------|--------------------|----------------------|-----|
| 名称 Award name | 国名 Country name | 受賞年 Year of award | 年 月 |
| | | | |
| 名称 Award name | 国名 Country name | 受賞年 Year of award | 年 月 |
| | | | |

5. 本研究テーマに関わる他の研究助成金受給 Other research grants concerned with your research theme

| | |
|--------------------------|---|
| 受給実績 Receipt record | <input type="checkbox"/> 有 <input type="checkbox"/> 無 |
| 助成機関名称 Funding agency | |
| 助成金名称 Grant name | |
| 受給期間 Supported period | 年 月 ~ 年 月 |
| 受給額 Amount received | 円 |
| 受給実績 Receipt record | <input type="checkbox"/> 有 <input type="checkbox"/> 無 |
| 助成機関名称 Funding agency | |
| 助成金名称 Grant name | |
| 受給期間 Supported period | 年 月 ~ 年 月 |
| 受給額 Amount received | 円 |

6. 他の奨学金受給 Another awarded scholarship

| | |
|---------------------------|---|
| 受給実績 Receipt record | <input type="checkbox"/> 有 <input type="checkbox"/> 無 |
| 助成機関名称 Funding agency | |
| 奨学金名称 Scholarship name | |
| 受給期間 Supported period | 年 月 ~ 年 月 |
| 受給額 Amount received | 円 |

7. 研究活動に関する報道発表 Press release concerned with your research activities

※記載した記事を添付してください。Attach a copy of the article described below

| | | | |
|--------------------------|---|--------------------------|--|
| 報道発表 Press release | <input type="checkbox"/> 有 <input type="checkbox"/> 無 | 発表年月日 Date of release | |
| 発表機関 Released medium | | | |
| 発表形式 Release method | ・新聞 ・雑誌 ・Web site ・記者発表 ・その他() | | |
| 発表タイトル Released title | | | |

8. 本研究テーマに関する特許出願予定 Patent application concerned with your research theme

| | | | |
|----------------------------------|---|----------------------------|--|
| 出願予定 Scheduled | <input type="checkbox"/> 有 <input type="checkbox"/> 無 | 出願国 Application country | |
| 出願内容(概要) Application contents | | | |

9. その他 Others

| |
|--|
| |
|--|

指導責任者(記名) 安梅 勅江



Contents lists available at ScienceDirect

Archives of Gerontology and Geriatrics

journal homepage: www.elsevier.com/locate/archger

Multimorbidity and functional limitation: the role of social relationships

Dandan Jiao^a, Kumi Watanabe^a, Yuko Sawada^b, Emiko Tanaka^c, Taeko Watanabe^d, Etsuko Tomisaki^e, Sumio Ito^f, Rika Okumura^f, Yuriko Kawasaki^f, Tokie Anne^{g,*}^a Graduate School of Comprehensive Human Sciences, University of Tsukuba, Tsukuba, Ibaraki, 305-8577, Japan^b Medical Sciences, Morinomiya University of Medical Sciences, Osaka, 559-8611, Japan^c Community Nursing, Musashino University, Tokyo, 202-8585, Japan^d College of Nursing and Nutrition, Shukutoku University, Chiba, 260-8703, Japan^e Faculty of Nursing and Medical Care, Keio University, Tokyo, 160-0016, Japan^f Department of Public Welfare, Tobishima, Aichi, 490-1434, Japan^g Faculty of Medicine, University of Tsukuba, 1-1-1 Tennodai, Tsukuba, Ibaraki, 305-8577, Japan

ARTICLE INFO

Keywords:

Older adults
functioning
multimorbidity
prevention
social relationships

ABSTRACT

Objectives: To examine the relationship between multimorbidity and functional limitation, and how social relationships alter that association.**Methods:** This cross-sectional study used data collected by self-reported questionnaires from adults aged 65 years and older living in a rural area in Japan in 2017. This analysis included complete data from 570 residents. Multimorbidity status was defined as having two chronic diseases exist simultaneously in one individual, and the function status was measured by their long-term care needs. Social relationships were assessed by the Index of Social Interaction and divided into high and low levels. Multiple logistic regression analysis was used to examine the association between social relationships and functional limitation and to assess the role of social relationships in this association.**Results:** The logistic regression model indicated that the risk of functional limitation was higher in multimorbidity participants than free-of-multimorbidity participants (OR = 2.55, 95% CI = 1.56–4.16). Compared with participants with no multimorbidity and a high level of social relationships, low level of social relationships increased the risk of functional limitation among participants both with and without multimorbidity, with the OR = 7.71, 95% CI = 3.03–19.69 and OR = 3.28, 95% CI = 1.30–8.27, respectively. However, no significant result was found in participants with multimorbidity and a high level of social relationships ($P = 0.365$).**Conclusions:** Multimorbidity was associated with functional limitations. However, this association could be increased by a low level of social relationships and decreased by a high level of social relationships.

1. Introduction

Healthy Ageing is defined as ‘the process of developing and maintaining the functional ability that enables wellbeing in older age’ (WHO, 2018). Functional ability is of great concern because functional limitations would result in depression (Turvey, Schultz, Beglinger, & Klein, 2009), cognitive impairment (Zaninotto, Batty, Allerhand, & Deary, 2018), and mortality (Liu et al., 2018), posing a burden on the whole society.

Multimorbidity is defined as the co-occurrence of two chronic conditions in a person (Fortin, Bravo, Hudon, Vanasse, & Lapointe, 2005). It has increasingly gained public health attention and causes challenges for

healthcare systems because multimorbidity is linked to low quality of life (Mujica-Mota et al., 2015), impaired mental health, and a high risk of mortality (Kuzuya, 2019). Many studies have proved that multimorbidity is linked to functional limitations (Formiga et al., 2005; Storeng, Vinjerui, Sund, & Krokstad, 2020; Wensing, Vingerhoets, & Grol, 2001). However, some studies indicated that there was no significant association between multimorbidity and physical functioning (Baker & Whitfield, 2006; Parker, Moran, Roberts, Calvert, & McCahon, 2014), and a cohort study showed at least 50% of the participants were functionally independent in spite of chronic disorders among older people (Santoni et al., 2017). Although multimorbidity has gained research interest recently, many studies have been conducted in the

* Corresponding author.

E-mail address: tokieanne@gmail.com (T. Anne).<https://doi.org/10.1016/j.archger.2020.104249>

Received 23 June 2020; Received in revised form 16 August 2020; Accepted 18 August 2020

Available online 7 September 2020

0167-4943/© 2020 Elsevier B.V. All rights reserved.

United States (Baker & Whitfield, 2006) and European countries (Storeng et al., 2020; Wensing et al., 2001), but relatively few studies have been conducted in Japan. For example, Ishizaki et al. (2019) reported that both poor objective and subjective physical functioning is related to multimorbidity among people aged 60 years and older. Physiological change, however, differs with aging (Aalami, Fang, Song, & Nacamuli, 2003). Another Japanese study demonstrated that the prevalence of multimorbidity increased with age before approximately the age of 90, but decreased after 90 (Mitsutake, Ishizaki, Teramoto, Shimizu, & Ito, 2019). The effects of multimorbidity on functional status might be different according to age range. Thus, clarifying the effects of multimorbidity on functional limitation status among adults aged 65 years and over may add evidence regarding previously reported mixed results and enrich a tailored knowledge of multimorbidity management among older people in rural areas.

Social relationships positively contributed to a decrease in functional limitations. Having an active social relationship was significantly associated with higher basic activities of daily living, instrumental activities of daily living (Shinkai et al., 2003), and lower mortality (Takahashi et al., 2019). On the other hand, people with greater social relationships experienced a lower risk of multimorbidity (Cantarero-Prieto, Pascual-Saez, & Blazquez-Fernandez, 2018; Singer, Green, Rowe, Ben-Shlomo, & Morrissey, 2019). Social relationships play an important role in reducing/delaying adverse health outcomes among older adults. To date, most studies have focused separately on the association between social relationships and multimorbidity (Cantarero-Prieto et al., 2018; Singer et al., 2019), and functional status (Shinkai et al., 2003). The role of social relationships on the association between multimorbidity and functional limitation among older adults remains underexamined.

To fill in these research gaps, we aimed to investigate (1) the association of multimorbidity with functioning status, and (2) the role of social relationships in this association among older adults. Our hypothesis was that (1) multimorbidity is related to a high risk of functional limitations, and (2) high social relationships might attenuate this relationship; for e.g., rich social relationships could decrease the risk of functional limitations among people with multimorbidity. The results might provide new insights into the management of multimorbidity among older people.

2. Methods

2.1. Study design and participants

This study used data from a longitudinal cohort study, which was a survey of community-dwelling people in a rural area in the central part of Japan. The longitudinal study began in 1991, aiming to assess risk factors associated with well-being and longevity and to improve the quality of life of residents. Questionnaires were distributed to all residents every three years. For participants who needed help with answering the questionnaires, their caregivers completed them on their behalf. For the present cross-sectional study, we extracted data from people aged 65 years and older in 2017. There were 1088 people aged 65 years and older, and 842 participants with no missing data in terms of disease and functional status information were initially included. Next, we excluded participants with missing information on any of the variables, resulting in a total of 570 participants who were retained for the study.

2.2. Measurements

2.2.1. Functioning status

One question was used to assess participants' functional status: 'Do you need care/assistance in your daily life'? A 'yes' response indicated the need for long-term support and 'no' indicated otherwise. In Japan, the long-term care system is widely used and certified by the

government when people need some care support in life. People needing support suggests that their ability to perform activities of daily living is partly or totally dependent on others (Matsuda, Muramatsu, & Hayashida, 2011). Therefore, the 'yes' and 'no' responses indicate the presence or absence of functional limitations, respectively.

2.2.2. Multimorbidity

Multimorbidity was evaluated by using the simple method of counting the number of disease conditions that were self-reported by the participants. These conditions include the following ten chronic diseases: hypertension, stroke, heart disease, diabetes, lung disease, cancer, depression, dementia, Parkinson's disease, and arthritis. Respondents who answered as having any two of these conditions were classified as having multimorbidity; otherwise, they were classified as free of multimorbidity.

2.2.3. Social relationships

The Index of Social Interaction (ISI) was used to assess the social relationship status. The ISI includes 18 items which were developed for evaluating various aspects of social relationships, including independence, social curiosity, feeling of safety, interaction, and participation (Anme & Shimada, 2000). The 18 items are: 'Do you have motivation to live an active lifestyle?' 'Do you take an active approach toward your life?' 'Are you motivated to live a healthy life?' 'Do you have a regular or routine lifestyle?' 'Do you read newspapers regularly?' 'Do you read books or magazines regularly?' 'Do you try to use new equipment like a video?' 'Do you have any hobbies?' 'Do you have a feeling of importance in society?' 'Do you often communicate with your family members?' 'Do you communicate with nonfamily people regularly?' 'Do you interact with non-family people regularly?' 'Do you have a chance to participate in social groups?' 'Do you watch television?' 'Do you have a chance to participate in your neighbourhood affairs?' 'Do you have an active role in society or social affairs?' 'Do you have someone to counsel with in a difficult situation?' 'Do you have someone to support you in an emergency?' Each item was coded 1 for a positive response and 0 for a negative response. The total possible score is 18, with a higher score showing a higher level of social relationships. Due to the skewed distribution of participants, the median value (17.0) of ISI was used to divide participants into high ISI (18.0) and low ISI (≤ 17.0).

2.2.4. Covariates

Based on previous studies (Ishizaki et al., 2019; Singer et al., 2019), age, gender, physical activity, drinking, smoking, and living status were considered. Age was a continuous variable. Physical activity was dichotomized responses as activity if they answered 'usually' and 'sometimes' and inactivity for a 'no' response to the question: 'do you do physical activities?' Participants were identified as 'non-drinker' if they answered 'not drinking' and 'others' if they answered 'everyday' and 'sometimes'. The smoking status was decided based on their choices of one of three answers: 'currently smoking', 'previously smoking but now stopped', and 'never smoke'. Then smoking was trichotomously coded as 'current smoker', 'ex-smoker', and 'non-smoker'. Living status was coded as 'living alone' and 'not alone'.

2.3. Statistical analysis

Median and frequency were used to describe continuous and categorical data, respectively. Chi-square tests and the Mann-Whitney U-test were used for the bivariate analysis to examine the association between participants' characteristics and function status. Next, multiple logistic regression analysis was employed to examine the association between multimorbidity and functional status.

To examine the role of social relationships, we constructed an additional model to evaluate the risk of developing functional limitations among the different four groups: participants with no multimorbidity and low ISI (Group 1), those with multimorbidity and low ISI

(Group 2), those with multimorbidity and high ISI (Group 3), and those with no multimorbidity and high ISI (Group 4). Group 4 was considered the reference group. IBM SPSS 22.0 was used for data analysis.

2.4. Ethical considerations

This study was approved by the Ethics Committee of a University to which the authors are affiliated. The data were anonymized and provided by the municipality via written contracts.

3. Results

In total, 570 participants with completed data information were included in the analysis. For these participants, the mean (SD) for age was 74.1 (7.5) years. Of the participants, over half were women (50.2%), engaged in physical activity (58.1%), current drinkers (63.0%), non-smokers (61.6%), and not living alone (94.7%). The proportion of participants with multimorbidity was 28.6% and of participants reporting high level of social relationships was 31.2% (Table 1).

Of ten chronic diseases, hypertension has the highest prevalence (55.8%), followed by diabetes (15.8%), and arthritis (10.2%). The prevalence of stroke and lung disease is around 5%, while depression and Parkinson's disease (0.9%) has the lowest percentage (Table 2).

The bivariate analysis indicated that age, physical activity, drinking status, smoking status, and multimorbidity were significantly associated with functional status (Table 3). When these significant variables were analysed by multivariate analysis, we found that age (OR = 1.14, 95% CI = 1.10–1.17), and multimorbidity (OR = 2.55, 95% CI = 1.56–4.16) were significantly associated with functional limitation (Table 4).

Regarding the role of social relationships, the risks of functional limitation were similar in Groups 1 and 2. Compared to participants with no multimorbidity and high ISI (Group 4), the risks for functional limitation increased for individuals with no multimorbidity and low ISI

Table 1 Characteristics of participants.

| Variables | Category | n | % |
|----------------------|----------------|------------|------|
| Age (Mean ± SD) | | 74.1 ± 7.5 | |
| Sex | Men | 284 | 49.8 |
| | Women | 286 | 50.2 |
| Physical activity | Activity | 331 | 58.1 |
| | Inactivity | 239 | 41.9 |
| Drinking | Yes | 359 | 63.0 |
| | No | 211 | 37.0 |
| Smoking | Current smoker | 63 | 11.1 |
| | Ex-smoker | 156 | 27.3 |
| | Non-smoker | 351 | 61.6 |
| Living status | Alone | 30 | 5.3 |
| | Not alone | 540 | 94.7 |
| ISI | High | 178 | 31.2 |
| | Low | 392 | 68.8 |
| Multimorbidity | Yes | 163 | 28.6 |
| | No | 407 | 71.4 |
| Group 1 ^a | | 265 | 46.5 |
| Group 2 ^b | | 127 | 22.3 |
| Group 3 ^c | | 36 | 6.3 |
| Group 4 ^d | | 142 | 24.9 |

ISI = index of social interaction; SD = standard deviation.

- ^a No multimorbidity + low ISI.
- ^b Multimorbidity + low ISI.
- ^c Multimorbidity + high ISI.
- ^d No multimorbidity + high ISI.

Table 2 Percentage of each chronic disease.

| N = 570 | | |
|---------------------|-----|------|
| Disease | n | % |
| Hypertension | 252 | 55.8 |
| Diabetes | 90 | 15.8 |
| Arthritis | 58 | 10.2 |
| Heart disease | 48 | 8.4 |
| Stroke | 31 | 5.4 |
| Lung disease | 29 | 5.1 |
| Cancer | 23 | 4.0 |
| Dementia | 13 | 2.3 |
| Depression | 5 | 0.9 |
| Parkinson's disease | 5 | 0.9 |

(Groups 1) (OR = 3.28, 95% CI = 1.30–8.27), and such a relationship was greater in participants with multimorbidity and low ISI (Group 2) (OR = 7.71, 95% CI = 3.03–19.69), whereas the relationship was not observed in participants with multimorbidity and high ISI (Group 3) (P = 0.365) (Table 5).

4. Discussion

The present study identified that older persons with multimorbidity have a high risk of functional limitation if they are aged 65 years and older living in a rural area, and social relationships altered the association between multimorbidity and function status.

Our findings suggest that individuals with multimorbidity are more likely to be linked to functional limitation, which is consistent with

Table 3 Participants' characteristics and functional limitations.

| Characteristics | Category | Yes (n = 105) n (%) | No (n = 465) n (%) | χ ² /Z | P |
|----------------------|----------------|------------------------|-----------------------|-------------------|--------|
| Age | | | | -8.739 | <0.001 |
| Sex | Men | 47 (16.5) | 237 (83.5) | 1.320 | 0.251 |
| | Women | 58 (20.3) | 228 (79.7) | | |
| Physical activity | Activity | 49 (14.8) | 282 (85.2) | 6.874 | 0.009 |
| | Inactivity | 56 (23.4) | 183 (76.6) | | |
| Drinking | Yes | 52 (14.5) | 307 (85.5) | 10.000 | 0.002 |
| | No | 53 (25.1) | 158 (74.9) | | |
| Smoking | Current smoker | 4 (6.3) | 59 (93.7) | 7.395 | 0.025 |
| | Ex-smoker | 34 (21.8) | 122 (78.2) | | |
| | Non-smoker | 67 (19.1) | 284 (80.9) | | |
| Living status | Alone | 6 (20.0) | 24 (80.0) | 0.503 | 0.819 |
| | Not alone | 99 (18.3) | 441 (81.7) | | |
| ISI | High | 9 (5.1) | 169 (94.9) | 30.764 | <0.001 |
| | Low | 96 (24.5) | 296 (75.5) | | |
| Multimorbidity | Yes | 49 (30.1) | 114 (69.9) | 20.583 | <0.001 |
| | No | 56 (13.8) | 351 (86.2) | | |
| Group 1 ^a | | 50 (18.9) | 215 (81.1) | 48.289 | <0.001 |
| Group 2 ^b | | 46 (36.2) | 81 (63.8) | | |
| Group 3 ^c | | 3 (8.3) | 33 (91.7) | | |
| Group 4 ^d | | 6 (4.2) | 136 (95.8) | | |

ISI = index of social interaction.

- ^a No multimorbidity + low ISI.
- ^b Multimorbidity + low ISI.
- ^c Multimorbidity + high ISI.
- ^d No multimorbidity + high ISI.

Table 4
Association between multimorbidity and functional limitations.

| Variables | Category | Unadjusted | | | Adjusted | | | | |
|-------------------|----------------|------------|--------|------|----------|--------|------|------|--------|
| | | OR | 95% CI | P | OR | 95% CI | P | | |
| Age | | 1.14 | 1.11 | 1.18 | <0.001 | 1.14 | 1.10 | 1.17 | <0.001 |
| Physical activity | | 1.75 | 1.15 | 2.70 | 0.009 | 1.28 | 0.78 | 2.08 | 0.328 |
| Drinking | | 0.51 | 0.33 | 0.78 | 0.002 | 0.62 | 0.36 | 1.08 | 0.092 |
| Smoking | Current smoker | 0.29 | 0.10 | 0.82 | 0.020 | 0.51 | 0.16 | 1.59 | 0.245 |
| | Ex-smoker | 1.18 | 0.74 | 1.88 | 0.482 | 1.66 | 0.93 | 2.96 | 0.090 |
| | Non-smoker | ref | | | | | | | |
| Multimorbidity | | 2.69 | 1.74 | 4.17 | <0.001 | 2.55 | 1.56 | 4.16 | <0.001 |

Table 5
The role of ISI in the association between multimorbidity and functional limitations.

| Variables | Category | Unadjusted | | | Adjusted | | | | |
|--|----------------|------------|--------|-------|----------|--------|------|-------|--------|
| | | OR | 95% CI | P | OR | 95% CI | P | | |
| Age | | 1.14 | 1.11 | 1.18 | <0.001 | 1.12 | 1.08 | 1.16 | <0.001 |
| Physical activity | | 1.75 | 1.15 | 2.70 | 0.009 | 1.07 | 0.65 | 1.76 | 0.806 |
| Drinking | | 0.51 | 0.33 | 0.78 | 0.002 | 0.69 | 0.39 | 1.21 | 0.193 |
| Smoking | Current smoker | 0.29 | 0.10 | 0.82 | 0.020 | 0.49 | 0.16 | 1.57 | 0.230 |
| | Ex-smoker | 1.18 | 0.74 | 1.88 | 0.482 | 1.66 | 0.92 | 3.01 | 0.090 |
| | Non-smoker | ref | | | | | | | |
| Multimorbidity | | 2.69 | 1.74 | 4.17 | <0.001 | | | | |
| ISI | | 0.16 | 0.08 | 0.33 | <0.001 | | | | |
| Group based on multimorbidity and ISI status | | | | | | | | | |
| Group 1 ^a | | 5.27 | 2.20 | 12.63 | <0.001 | 3.28 | 1.30 | 8.27 | 0.012 |
| Group 2 ^b | | 12.87 | 5.26 | 31.46 | <0.001 | 7.71 | 3.03 | 19.69 | <0.001 |
| Group 3 ^c | | 2.06 | 0.49 | 8.67 | 0.324 | 1.99 | 0.45 | 8.88 | 0.365 |
| Group 4 ^d | | ref | | | | | | | |

ISI = index of social interaction.

^a No multimorbidity + low ISI.

^b Multimorbidity + low ISI.

^c Multimorbidity + high ISI.

^d No multimorbidity + high ISI.

previous studies. A study conducted in the United States showed participants with multimorbidity had a higher level of disability in both activities of daily living and instrumental activities of daily living compared to participants with a single disease in individuals aged 65 years or older (Quinones, Markwardt, & Botosaneanu, 2016). In a review including both cross-sectional studies and cohort studies, Ryan, Wallace, O'Hara, and Smith (2015) reported that people with multimorbidity are also more likely to have poor function status. Furthermore, even when multimorbidity was evaluated using a different counting method (three chronic conditions), the same relationship between multimorbidity and functional limitation was observed (Storeng et al., 2020). Multimorbidity appears to be an important determinant of poor physical functioning among older adults. On the other hand, functional limitation would impact multimorbidity, which will develop a 'vicious circle'. Attention should be paid and measures should be taken to reduce/delay the deterioration of function limitation among older people with multimorbidity.

Social relationships could alter the impact of multimorbidity on function limitations. Comparing with older adults with no multimorbidity and a high level of social relationships, those who experience multimorbidity and high social relationships are less likely to have function limitations. Participants with multimorbidity and low social relationships, however, have the highest risk of developing functional limitations, followed by those without multimorbidity and low social relationships. In other words, high ISI helped to decrease the likelihood of function disabilities in older people with multimorbidity, while low ISI increased the probability of functional limitation status. Similarly, a cohort study examining the moderation effects of social support on the impact of multimorbidity on mortality survival time, suggested supportive social relationships increase the survival opportunities of people

with multimorbidity (Olaya et al., 2017). Mazzella et al. (2010) found that individuals with low social support and multimorbidity presented a high rate of death. Enriching social relationships could be a protective measure against function limitation among older individuals who suffer from multimorbidity. Conversely, lacking social support may affect people's non-adherence to therapies (DiMatteo, 2004), which may accelerate the progression of diseases and cause adverse outcomes, including functional limitation.

The role of social relationships may work mainly through two pathways. First, there is the stress buffering pathway, suggesting social relationships modify personal behaviours by providing resources, including informational and emotional support, when people are experiencing stress (Cohen & Wills, 1985). Comparing participants with only one or no chronic disease, it is plausible that people with multimorbidity experience more stress. High social resources could mitigate the negative effects of stress on health outcomes and therefore modify the effects of multimorbidity on physical limitations. Second, the main direct effects model posits that social relationships have a direct benefit to health regardless of whether people are presenting as experiencing stress (Broadhead et al., 1983). Through social connection, individuals acquire signals of behavioural guidance and the feeling of meaning in life, and then these signals could regulate an individual's neuroendocrine and immunological functions to improve physical functioning (Berkman, Glass, Brissette, & Seeman, 2000).

Our findings show that participants with multimorbidity would gain benefits through rich social relationships, which may provide evidence about how to reduce the burden of their multimorbidity. Since the management of multimorbidity is costly, interventions tailored to improve social relationships such as tele-support services are cost-effective (Findlay, 2003). Promoting social relationships of

participants is likely to improve multimorbidity self-management, maintain independence, and reduce function limitation. Moreover, few studies have been conducted to examine the role of social relationships on the association between multimorbidity and function limitation. Our results conclude that developing and facilitating social relationships might be a promising strategy for multimorbidity management among adults aged 65 years and older. Furthermore, since little research on multimorbidity has been conducted in Asian countries (Kuzuya, 2019), our findings may add evidence to the research topic of multimorbidity among older people. The final strength of our study is the multidimensional evaluation of the ISI, evaluating many aspects of social relationships in the daily lives of older people.

Several limitations of this study should be considered. First, this is a cross-sectional study that cannot deduce the causation relationship between multimorbidity and function limitations. Thus, longitudinal studies are needed to examine the role of high social relationships that can attenuate the relationship between multimorbidity and functional limitations. Further longitudinal studies adjusting for more potential confounders should also be performed to confirm these findings. Second, due to the limited sample size, the confidence interval is wide after being stratified by social relationships. Moreover, the high rate of missing values might reduce the power of the results. We suggest that future studies use a larger sample size to identify the effects of social relationships on altering the association between multimorbidity and function status. Third, although social relationships were found to positively affect the impact of multimorbidity on function disability, the specific aspects of social relationships should be explored in future studies. Fourth, only one functional measure was used. Future studies can use more indicators to measure the functional status, which may strengthen the validity of the results. Fifth, the stress buffering pathway suggests social relationships could modify the effects of multimorbidity on functional limitations. However, we did not assess the specific level of stress. Future studies considering the use of stress measures are expected.

5. Conclusions

The present study supplements existing evidence that multimorbidity poses risks on function disability in older adults aged 65 years and older, and the level of social relationships may alter that association. Our study suggests that the risk of function disability among participants with multimorbidity may be reduced by increasing social relationships. These results suggest a method for health professionals to assess people's social relationship and stimulate social support for older people with multimorbidity.

Funding

This research was supported by the Grants-in-Aid for Scientific Research (JP17H02604).

CRediT authorship contribution statement

Dandan Jiao: Conceptualization, Methodology, Formal analysis, Writing - original draft. **Kumi Watanabe:** Investigation, Formal analysis. **Yuko Sawada:** Investigation. **Emiko Tanaka:** Investigation. **Taeko Watanabe:** Investigation. **Etsuko Tomisaki:** Investigation. **Sumio Ito:** Project administration. **Rika Okumura:** Project administration. **Yuriko Kawasaki:** Project administration. **Tokie Anne:** Conceptualization, Investigation, Writing - review & editing, Project administration, Funding acquisition.

Declaration of Competing Interest

The authors report no declarations of interest.

Acknowledgments

We express our deep gratitude to all study participants and investigators.

References

- Aalami, O. O., Fang, T. D., Song, H. M., & Nacamuli, R. P. (2003). Physiological features of aging persons. *Archives of Surgery*, 138(10), 1068–1076. <https://doi.org/10.1001/archsurg.138.10.1068>.
- Anne, T., & Shimada, C. (2000). Social interaction and mortality in a five year longitudinal study of the elderly. *Japanese Journal of Public Health*, 47(2), 127–133.
- Baker, T. A., & Whitfield, K. E. (2006). Physical functioning in older blacks: An exploratory study identifying psychosocial and clinical predictors. *Journal of the National Medical Association*, 98(7), 1114–1120.
- Berkman, L. F., Glass, T., Brissette, I., & Seeman, T. E. (2000). From social integration to health: Durkheim in the new millennium. *Social Science and Medicine*, 51(6), 843–857. [https://doi.org/10.1016/S0277-9536\(00\)00065-4](https://doi.org/10.1016/S0277-9536(00)00065-4).
- Broadhead, W. E., Kaplan, B. H., James, S. A., Wagner, E. H., Schoenbach, V. J., Grimson, R., & Gehlbach, S. H. (1983). The epidemiologic evidence for a relationship between social support and health. *American Journal of Epidemiology*, 117(5), 521–537. <https://doi.org/10.1093/oxfordjournals.aje.a113575>.
- Cantarero-Prieto, D., Pascual-Saez, M., & Blazquez-Fernandez, C. (2018). Social isolation and multiple chronic diseases after age 50: A European macro-regional analysis. *PLOS ONE*, 13(10), e0205062. <https://doi.org/10.1371/journal.pone.0205062>.
- DiMatteo, M. R., & MR. (2004). Social Support and Patient Adherence to Medical Treatment: A Meta-Analysis. *Health Psychology*, 23(2), 207–218. <https://doi.org/10.1037/0278-6133.23.2.207>.
- Cohen, S., & Wills, T. A. (1985). Stress, social support, and the buffering hypothesis. *Psychological Bulletin*, 98(2), 310–357. <https://doi.org/10.1037/0033-2909.98.2.310>.
- Findlay, R. A. (2003). Interventions to reduce social isolation amongst older people: Where is the evidence? *Ageing and Society*, 23(5), 647–658. <https://doi.org/10.1017/s0144686x03001296>.
- Formiga, F., Pujol, R., Perez-Castejon, J. M., Ferrer, A., Henriquez, E., & De Llobregat, S. F. (2005). Low comorbidity and male sex in nonagenarian community-dwelling people are associated with better functional and cognitive abilities: The NonaSantefeliu study. *Journal of the American Geriatrics Society*, 53(10), 1836–1837. <https://doi.org/10.1111/j.1532-5415.2005.53528.4.x>.
- Fortin, M., Bravo, G., Hudon, C., Vanasse, A., & Lapointe, L. (2005). Prevalence of multimorbidity among adults seen in family practice. *Annals of Family Medicine*, 3(3), 223–228. <https://doi.org/10.1370/afm.272>.
- Ishizaki, T., Kobayashi, E., Fukaya, T., Takahashi, Y., Shinkai, S., & Liang, J. (2019). Association of physical performance and self-rated health with multimorbidity among older adults: Results from a nationwide survey in Japan. *Archives of Gerontology and Geriatrics*, 84, Article 103904. <https://doi.org/10.1016/j.archger.2019.103904>.
- Kuzuya, M. (2019). Era of geriatric medical challenges: Multimorbidity among older patients. *Geriatrics and Gerontology International*, 19(8), 699–704. <https://doi.org/10.1111/ggi.13742>.
- Liu, Z. Y., Wei, Y. Z., Wei, L. Q., Jiang, X. Y., Wang, X. F., Shi, Y., & Hai, H. (2018). Frailty transitions and types of death in Chinese older adults: A population-based cohort study. *Clinical Interventions in Aging*, 13, 947–956. <https://doi.org/10.2147/cia.s157089>.
- Mazzella, F., Cacciatore, F., Galizia, G., Della-Morte, D., Rossetti, M., Abbruzzese, R., & Abete, P. (2010). Social support and long-term mortality in the elderly: role of comorbidity. *Archives of Gerontology and Geriatrics*, 51(3), 323–328. <https://doi.org/10.1016/j.archger.2010.01.011>.
- Matsuda, S., Muramatsu, K., & Hayashida, K. (2011). Eligibility classification logic of the Japanese long term care insurance. *Asian Pacific Journal of Disease Management*, 5(3), 65–74. <https://doi.org/10.7223/apjdm.5.65>.
- Mitsutake, S., Ishizaki, T., Teramoto, C., Shimizu, S., & Ito, H. (2019). Patterns of co-occurrence of chronic disease among older adults in Tokyo, Japan. *Preventing Chronic Disease*, 16, Article 180170. <https://doi.org/10.5888/pcd16.180170>.
- Mujica-Mota, R. E., Roberts, M., Abel, G., Elliott, M., Lyratzopoulos, G., Roland, M., & Campbell, J. (2015). Common patterns of morbidity and multi-morbidity and their impact on health-related quality of life: Evidence from a national survey. *Quality of Life Research*, 24(4), 909–918. <https://doi.org/10.1007/s11136-014-0820-7>.
- Olaya, B., Domenech-Abella, J., Moneta, M. V., Lara, E., Caballero, F. F., Rico-Uribe, L. A., & Haro, J. M. (2017). All-cause mortality and multimorbidity in older adults: The role of social support and loneliness. *Experimental Gerontology*, 99, 120–126. <https://doi.org/10.1016/j.exger.2017.10.001>.
- Parker, L., Moran, G. M., Roberts, L. M., Calvert, M., & McCahon, D. (2014). The burden of common chronic disease on health-related quality of life in an elderly community-dwelling population in the UK. *Family Practice*, 31(5), 557–563. <https://doi.org/10.1093/fampra/cmu035>.
- Quinones, A. R., Markwardt, S., & Botosaneanu, A. (2016). Multimorbidity combinations and disability in older adults. *The Journals of Gerontology: Series A*, 71(6), 823–830. <https://doi.org/10.1093/gerona/glw035>.
- Ryan, A., Wallace, E., O'Hara, P., & Smith, S. M. (2015). Multimorbidity and functional decline in community-dwelling adults: A systematic review. *Health and Quality of Life Outcomes*, 13, 168. <https://doi.org/10.1186/s12955-015-0355-9>.
- Santoni, G., Marengoni, A., Calderón-Larrañaga, A., Angleman, S., Rizzuto, D., Welmer, A. K., & Fratiglioni, L. (2017). Defining health trajectories in older adults

- with five clinical indicators. *The Journals of Gerontology. Series A*, 72(8), 1123–1129. <https://doi.org/10.1093/gerona/glw2>.
- Shinkai, S., Kumagai, S., Fujiwara, Y., Amano, H., Yoshida, Y., Watanabe, S., & Shibata, H. (2003). Predictors for the onset of functional decline among initially non-disabled older people living in a community during a 6-year follow-up. *Geriatrics and Gerontology International*, 3(1), 31–39. <https://doi.org/10.1111/j.1444-0594.2003.00094.x>.
- Singer, L., Green, M., Rowe, F., Ben-Shlomo, Y., & Morrissey, K. (2019). Social determinants of multimorbidity and multiple functional limitations among the ageing population of England, 2002–2015. *SSM Population Health*, 8, Article 100413. <https://doi.org/10.1016/j.ssmph.2019.100413>.
- Storeng, S. H., Vinjerui, K. H., Sund, E. R., & Krokstad, S. (2020). Associations between complex multimorbidity, activities of daily living and mortality among older Norwegians. A prospective cohort study: The HUNT Study, Norway. *BMC Geriatrics*, 20(1), 21. <https://doi.org/10.1186/s12877-020-1425-3>.
- Takahashi, S., Ojima, T., Kondo, K., Shimizu, S., Fukuhara, S., & Yamamoto, Y. (2019). Social participation and the combination of future needs for long-term care and mortality among older Japanese people: A prospective cohort study from the Aichi Gerontological Evaluation Study (AGES). *BMJ Open*, 9(11), e030500. <https://doi.org/10.1136/bmjopen-2019-030500>.
- Turvey, C. L., Schultz, S. K., Beglinger, L., & Klein, D. M. (2009). A longitudinal community-based study of chronic illness, cognitive and physical function, and depression. *The American Journal of Geriatric Psychiatry*, 17(8), 632–641. <https://doi.org/10.1097/JGP.0b013e31819c498c>.
- Wensing, M., Vingerhoets, E., & Grol, R. (2001). Functional status, health problems, age and comorbidity in primary care patients. *Quality of Life Research*, 10(2), 141–148. <https://doi.org/10.1023/a:1016705615207>.
- WHO. (2018). *What is healthy ageing?*. Retrieved from <https://www.who.int/ageing/healthy-ageing/en/>.
- Zaninotto, P., Batty, G. D., Allerhand, M., & Deary, I. J. (2018). Cognitive function trajectories and their determinants in older people: 8 years of follow-up in the English Longitudinal Study of Ageing. *Journal of Epidemiology and Community Health*, 72, 685–694. <https://doi.org/10.1136/jech-2017-210116>.

Nursing Research **JNR** Editorial Manager
 HOME • LOGOUT • HELP • REGISTER • UPDATE MY INFORMATION • JOURNAL OVERVIEW • Role: Author Username: TokieAnne
 NEW MENU • CONTACT US • SUBMIT A MANUSCRIPT • INSTRUCTIONS FOR AUTHORS • PRIVACY

← Submissions with an Editorial Office Decision for Author
 Page: 1 of 1 (1 total completed submissions)

| Action | Manuscript Number | Title | Initial Date Submitted | Current Status |
|--------------|-------------------|---|------------------------|----------------|
| Action Links | JNR-D-20-00705 | Changes in Social Relationships and Physical Function among Community-dwelling Older adults | 19 Nov 2020 | Accept |

Acknowledgments:

We are deeply grateful to all study participants and investigators. Dandan Jiao is grateful to receive a scholarship (Sasagawa scholarship) from the Japan-China Medical Association.

Conflict of interests: The authors report no conflicts of interest for this work.

Funding: This research was supported by the Grants-in-Aid for Scientific Research (JP17H02604).



Home environment and social skills of Japanese preschool children pre- and post-COVID-19

Xiang Li, Dandan Jiao, Munenori Matsumoto, Yantong Zhu, Jinrui Zhang, Zhu Zhu, Yang Liu, Mingyu Cui, Yanlin Wang, Meiling Qian, Ammara Ajmal, Alpona Afsari Banu, Yolanda Graça, Emiko Tanaka, Taeko Watanabe, Yuko Sawada, Etsuko Tomisaki & Tokie Anme

To cite this article: Xiang Li, Dandan Jiao, Munenori Matsumoto, Yantong Zhu, Jinrui Zhang, Zhu Zhu, Yang Liu, Mingyu Cui, Yanlin Wang, Meiling Qian, Ammara Ajmal, Alpona Afsari Banu, Yolanda Graça, Emiko Tanaka, Taeko Watanabe, Yuko Sawada, Etsuko Tomisaki & Tokie Anme (2022): Home environment and social skills of Japanese preschool children pre- and post-COVID-19, *Early Child Development and Care*, DOI: [10.1080/03004430.2021.2021896](https://doi.org/10.1080/03004430.2021.2021896)

To link to this article: <https://doi.org/10.1080/03004430.2021.2021896>



Published online: 03 Jan 2022.



Submit your article to this journal [↗](#)







View related articles [↗](#)



View Crossmark data [↗](#)



Home environment and social skills of Japanese preschool children pre- and post-COVID-19

Xiang Li ^a, Dandan Jiao^a, Munenori Matsumoto^a, Yantong Zhu^a, Jinrui Zhang^a, Zhu Zhu ^a, Yang Liu^a, Mingyu Cui^a, Yanlin Wang^a, Meiling Qian^a, Ammara Ajmal^a, Alpona Afsari Banu^a, Yolanda Graça^a, Emiko Tanaka ^b, Taeko Watanabe^c, Yuko Sawada^d, Etsuko Tomisaki ^e and Tokie Anme^f

^aSchool of Comprehensive Human Science, University of Tsukuba, Tsukuba, Japan; ^bFaculty of Nursing, Musashino University, Tokyo, Japan; ^cFaculty of Nursing, Shukutoku University, Chiba, Japan; ^dFaculty of Health Medicine, Morinomiya University Of Medical Sciences, Osaka, Japan; ^eFaculty of Nursing, Keio University, Tokyo, Japan; ^fFaculty of Medicine, University of Tsukuba, Tsukuba, Japan

ABSTRACT

The COVID-19 pandemic has impacted the daily life and social relationships of pre-school children globally. While many studies have examined the impact of the pandemic on children, few have compared the home environment and children's social skills before and after the pandemic. To address this research gap, we used data from the Japan Child Care Cohort study, which included questions on home environment answered by parents (1748 in 2019 and 1349 in 2020) of children aged 0–6 years using self-reported questionnaires and data on the social skills of children aged 1–6 years (1917 in 2019 and 1989 in 2020) that were evaluated by childcare professionals in childcare centres. Using the Chi-square test, home environments and social skills were compared. We found that frequencies of family meals, no punishment, and a positive attitude toward children's mistakes were higher in 2020. In contrast, frequencies of shopping together, visiting children's friends and relatives, and having social support from others were lower in 2020. Additionally, children's social skills in 2019 were better than in 2020. Childcare institutions can consider these differences and create a support plan to ensure quality child-rearing practices and healthy child development.

ARTICLE HISTORY



Received 24 August 2021
Accepted 18 December 2021

KEYWORDS

Home environment; social skill; children; parents; child-rearing post-pandemic; covid-19

Introduction

The COVID-19 pandemic has spread rapidly worldwide (Hiraoka & Tomoda, 2020), resulting in the closure of over 90% of schools since March 2020 (Chaabane, Doraiswamy, Chaabna, Mamtani, & Cheema, 2021). The closure of schools and public places worldwide affected approximately 1.38 billion children (Cluver et al., 2020; Roos et al., 2021). The Japanese government declared a state of emergency from April 7 to May 25, 2020 due to the COVID 19 pandemic (Ministry of Health, Labour and Welfare, 2021). The emergency did not enforce to close the childcare centres. However, the numbers of the children who were utilizing the childcare centres decreased because parents who were working remotely chose to care their children at home. During the emergency, people were encouraged to avoid going outside without legal restriction. Public healthcare services for children, such as child health check-ups, childcare consultation for families, school counselling, and social support, were also cancelled (Horiuchi et al., 2020).

CONTACT Tokie Anme  tokieanme@gmail.com  Faculty of Medicine, University of Tsukuba, 1-1-1, Tennoudai, Tsukuba, Ibaraki 305-8577, Japan

© 2022 Informa UK Limited, trading as Taylor & Francis Group

Aspects of the home environment include the degree of organisation in children's surroundings, consideration of human and physical resources, particularly parents, and the quality of close relationships around children (Anme, Shinohara, et al., 2013). COVID-19 has changed daily life, forcing parents to work from home while caring for their children; many parents attempt to keep children busy and safe at home (Cluver et al., 2020). Although parents can spend more time with their children to improve their relationship and well-being, challenges, such as financial insecurity, increasing health concerns, lack of social and physical activities, and psychological problems prevail, which are emblematic of the COVID-19 crisis (Janssen et al., 2020). Social distancing impact mental experience and daily life, and sudden changes in the environment could be stressful to both parents and children (Brown, Doom, Lechuga-Peña, Watamura, & Koppels, 2020; Chung, Lanier, & Wong, 2020; Kawaoka et al., 2021; Roos et al., 2021). The depression status of parents, caring for more than one child at home, unmet childcare needs, and relationship distress emerged as the predictors of lower-quality parenting during the COVID-19 pandemic (Roos et al., 2021).

However, the existing articles on parenting focused on the home environment during the COVID-19 pandemic and not on comparing it before and after the pandemic. Although previous studies have stated that the factors mentioned in the last paragraph—such as poor mental status of parents—were related to poor parenting, the question about whether the difference in home environment existed before and after the COVID-19 pandemic is still unclear. Besides, comparisons of relatively large cross-sectional national samples from these two years are still limited. In addition, as the home environment plays a vital role in early childhood development (Tong et al., 2015), understanding the differences in home environments before and after the COVID-19 outbreak will help social institutions provide prompt support and ensure healthy child development.

Social isolation, such as children's inability to frequently visit their friends or relatives, will decrease human and social stimulation, affecting their social and emotional behaviours (Chen et al., 2016). Previous studies state that factors leading to reduced social stimulation, such as the lack of face-to-face contact with relatives, classmates, friends, and teachers, have stressed the physical and psychological health of children during the COVID-19 pandemic (Araújo, Veloso, Souza, Azevedo, & Tarro, 2020; Shorer & Leibovich, 2020). Besides, dramatic changes resulting from the unknown duration of the pandemic, the danger of infection, frustration and boredom, inadequate information, lack of personal space at home, and family financial loss have also been problematic and affected children (Brooks et al., 2020; Liu, Bao, Huang, Shi, & Lu, 2020; Shorer & Leibovich, 2020). An increased level of stress, sadness, frustration, indiscipline, and hyperactivity among children was reported in a rapid systematic review (Chaabane et al., 2021). Compared to adults, children are more likely to experience the continuous and long-term impact of the COVID-19 pandemic (Shen et al., 2020); they are also more likely to experience a more significant impact of COVID-19 on their emotional and social development (Singh et al., 2020).

However, evidence about whether the difference in children's social skills existed before and after the COVID-19 pandemic is still unclear, especially with relatively large sample sizes. In addition, failure to build social skills in early childhood may result in problematic behaviours and later cause social and school maladaptation (Takahashi, Okada, Hoshino, & Anme, 2015). Children who do not develop basic social competence by the age of six may have trouble with social interaction when they grow older (Ladd, 2000). Studies focusing on children's social competence in the early childhood age range during the COVID-19 pandemic are still rare. Moreover, knowing the differences between children's social skill status before and after the COVID-19 outbreak is necessary for support institutions to make targeted plans for children.

Hence, considering the limitations in literature on both home environment and children's social skills, this study examines the differences in the home environment adopted by parents and pre-school children's social skills before and after the COVID-19 pandemic. We use data from a childcare cohort study across Japan, with relatively large sample size.

Method

Participants and design

Data regarding home environment and children's social skills were from a population-based nationwide longitudinal study (the Japan Child Care Cohort study), which was carried out at government-licensed childcare centres across Japan in December 2019 and December 2020.

Ethical consideration

This study was approved by the ethics committee of the University of Tsukuba, Japan.

Procedure

In this childcare cohort study, the survey was conducted in December 2019, before the outbreak of covid-19 in Japan, and again in December 2020, after the outbreak. Regarding home environment, in 2019, 1748 of 2204 parents whose children were utilising childcare centres agreed to participate in this survey (participation rate was 79.3%). In 2020, the same procedure was performed in the childcare centres with 1668 parents, where 1349 agreed to participate (participation rate was 80.9%). Home environment was evaluated using self-reported questionnaires answered by parents. Regarding children's social skills, in 2019, 1938 of 2360 children were recruited to participate in this survey (participation rate was 82.1%). After excluding children under 1 year of age ($n = 21$), we had 1917 children for the analysis. In 2020, the same procedure was performed in childcare centres, where 2007 children from 2378 children were recruited to participate (participation rate was 84.4%). After excluding children under 1 year of age ($n = 18$), we had 1989 children for the analysis. Children's social skills were evaluated by childcare professionals in the government-licensed childcare centres.

Measures

Evaluation of home environment

The home environment was evaluated based on the Index of Child Care Environment (ICCE), the Japanese questionnaire edition of the most commonly used and validated scale across countries called Home Observation for Measurement of the Environment (Anme, Tanaka, et al., 2013). The ICCE has been widely used in the national childcare cohort study in Japan and has proved to be an appropriate measurement to evaluate the home environment among families with pre-school children (Anme et al., 2012; Anme & Segal, 2004; Anme, Shinohara, et al., 2013; Mochizuki et al., 2014; Tong et al., 2009; Tong et al., 2015).

The ICCE contains 13 items categorised into four subscales:

- a) Human stimulation has five items: (1) How often do you play with your child face-to-face (except for sleep time)? (2) How often do you read to your child? (3) How often do you sing songs with your child? (4) How often does your spouse help you care for the child? (5) How often does your child eat meals with both parents?
- b) Social stimulation has three items: (1) How often do you shop with your child? (2) How often do you go to parks with your child? (3) How often do you and your child meet friends or relatives with children of a similar age?
- c) Avoidance of restriction has two items: (1) What do you do if your child spills milk on purpose? (2) How many times did you spank your child?
- d) Social support has three items: (1) Does someone help you take care of your child? (2) Do you have someone to consult about childcare? (3) How many times do you have a chance to talk with your spouse about your child?

For five items in human stimulation, three items in social stimulation, and the item of ‘talking with spouse about child’, response ranges were measured using a five-point scale (1 = rarely, 2 = 1-3 times/month, 3 = 1-2 times/week, 4 = 3-4 times/week and 5 = almost every day). For the item ‘what will you do if your child spilled milk on purpose’ (response to mistakes), response ranges were measured with a four-point scale (1 = slap or hit the child, 2 = scold the child, 3 = discipline differently, 4 = prevent the spilling of milk). For the item ‘how many times did you slap your child last week’ (punishment), response ranges were measured with a five-point scale (1 = never, 2 = 1-2 times, 3 = 3-4 times, 4 = 5-6 times, 5 = almost every day). For two items, ‘support for childcare’ and ‘have a consultation’, response ranges were measured in a binary manner (1 = no, 2 = yes).

The value assignment was modelled on a previous study (Chen et al., 2016); those who selected ‘rarely’ for each item were classified as the non-favourable group. Regarding punishment, those who selected ‘never’ were classified as the favourable group. Regarding mistakes, those who selected ‘slap’ or ‘hit the child’ or ‘scold the child’ were classified as the non-favourable group. Other selections were classified as the ‘favourable group’. Finally, the answers to each question were categorised into favourable and non-favourable groups.

Evaluation of social skills

Childcare professionals in childcare centres assessed social skills using the social skill scale (SSS), whose validity and reliability has been confirmed by Anme, Shinohara, et al. (2013). Childcare professionals have been trained several times before evaluating children’s social skills (Takahashi, Okada, Hoshino, & Anme, 2008). In Japan, SSS has been widely used in the national childcare cohort study and has proven to be an appropriate measure to evaluate children’s social skills development (Anme, Shinohara, et al., 2013; Takahashi et al., 2008, 2015).

The SSS contains 24 items clustered into three subscales: (a) assertion (8 items), (b) self-control (8 items), and (c) cooperation (8 items). Details can be seen in Table 4.

Each item was measured with a three-point scale (1 = never, 2 = sometimes, 3 = very often). The value assignment of each item was based on ‘never’, ‘sometimes’, or ‘very often’. Finally, each item was categorised as positive (sometimes or very often) or negative (never) according to evaluation results by childcare professionals.

Demographic characteristics

As for home environment, five demographic characteristic variables were considered: age (0–6 years old), gender (boy/girl), family structure (extended family/nuclear family/others), sibling (having sibling/no sibling), and main caregiver (mother/father/others). As for the children’s social skills, two demographic characteristic variables were considered: age (1–6 years old) and gender (boy/girl).

Data analysis

First, we used frequencies and percentages for sociodemographic, home environment, and social skill variables in 2019 and 2020. Second, a chi-square test was used to test the differences between sociodemographic variables in 2019 and 2020 and between home environment and social skill variables in 2019 and 2020. Statistical significance was set at $p < .05$. All statistical analyses were performed using the SPSS software (version 27.0. English).

Results

Comparing home environment between 2019 and 2020

Table 1 displays the chi-square results for demographic characteristics in the home environment survey. It shows no significant differences in demographic characteristics of the samples from 2019 and 2020.

Table 1. Chi-square results for demographic characteristics in the home environment data.

| Item | Category | 2019 | | 2020 | | χ^2 | <i>p</i> |
|--------------------|------------|------|------|------|------|----------|----------|
| | | n | % | n | % | | |
| Age of children | 0 | 46 | 2.6 | 24 | 1.8 | 11.638 | .071 |
| | 1 | 239 | 13.7 | 150 | 11.1 | | |
| | 2 | 284 | 16.2 | 205 | 15.2 | | |
| | 3 | 343 | 19.6 | 255 | 18.9 | | |
| | 4 | 340 | 19.5 | 288 | 21.3 | | |
| | 5 | 313 | 17.9 | 278 | 20.6 | | |
| Gender of children | Boy | 932 | 53.3 | 744 | 55.2 | 1.031 | .310 |
| | Girl | 816 | 46.7 | 605 | 44.8 | | |
| Family structure | Nuclear | 1517 | 86.8 | 1181 | 87.5 | 0.122 | .726 |
| | Extended | 190 | 10.9 | 154 | 11.4 | | |
| | Others | 41 | 2.3 | 14 | 1.1 | | |
| Siblings | Sibling | 1070 | 61.2 | 864 | 64.0 | 2.609 | .106 |
| | No sibling | 678 | 38.8 | 485 | 36.0 | | |
| Main caregiver | Mother | 1640 | 93.8 | 1277 | 94.6 | 0.041 | .839 |
| | Father | 89 | 5.1 | 67 | 5.0 | | |
| | Others | 19 | 1.1 | 5 | 0.4 | | |

Table 2 indicates that the 2020 sample showed a larger proportion of favourable group items, such as eating meals together, positive response to mistakes, and no punishment, and a smaller presence of group items, such as shopping together, visiting friends and relatives, and getting help from others.

Comparing children's social skills between 2019 and 2020

Table 3 presents the chi-square results for demographic characteristics in the children's social skills survey. There were no significant differences in demographic characteristics in the samples from 2019 and 2020.

Table 2. Chi-square results for home environments of 2019 and 2020.

| Item | Category | Total | Favourable | | Non-favourable | | χ^2 | <i>p</i> |
|-----------------------------|----------|-------|------------|------|----------------|------|----------|----------|
| | | | n | % | n | % | | |
| Play with child | 2019 | 1738 | 1728 | 99.4 | 10 | 0.6 | 0.111 | .739 |
| | 2020 | 1343 | 1334 | 99.3 | 9 | 0.7 | | |
| Shopping together | 2019 | 1741 | 1705 | 97.9 | 36 | 2.1 | 10.160 | .001 |
| | 2020 | 1345 | 1291 | 96.0 | 54 | 4.0 | | |
| Read for the child | 2019 | 1742 | 1475 | 84.7 | 267 | 15.3 | 0.160 | .689 |
| | 2020 | 1344 | 1145 | 85.1 | 199 | 14.9 | | |
| Sing songs together | 2019 | 1741 | 1642 | 94.3 | 99 | 5.7 | 0.091 | .763 |
| | 2020 | 1343 | 1270 | 94.4 | 73 | 5.6 | | |
| Go to the park together | 2019 | 1744 | 1561 | 89.5 | 183 | 10.5 | 0.000 | .999 |
| | 2020 | 1344 | 1203 | 89.5 | 141 | 10.5 | | |
| Visit friends and relatives | 2019 | 1743 | 1044 | 59.9 | 699 | 40.1 | 12.558 | <.001 |
| | 2020 | 1345 | 720 | 53.5 | 625 | 46.5 | | |
| Cooperate with spouse | 2019 | 1723 | 1602 | 93.0 | 121 | 7.0 | 0.868 | .351 |
| | 2020 | 1328 | 1246 | 93.8 | 82 | 6.2 | | |
| Eat meals together | 2019 | 1739 | 1676 | 96.4 | 63 | 3.6 | 4.980 | .026 |
| | 2020 | 1342 | 1312 | 97.8 | 30 | 2.2 | | |
| Respond to mistake | 2019 | 1745 | 668 | 36.3 | 1077 | 63.7 | 7.490 | .006 |
| | 2020 | 1344 | 580 | 42.1 | 764 | 57.9 | | |
| No punishment | 2019 | 1737 | 1399 | 80.5 | 338 | 19.5 | 13.257 | <.001 |
| | 2020 | 1342 | 1148 | 85.5 | 194 | 14.5 | | |
| Talk with spouse | 2019 | 1719 | 1602 | 93.2 | 117 | 6.8 | 0.041 | .840 |
| | 2020 | 1329 | 1241 | 93.4 | 88 | 6.6 | | |
| Help from others | 2019 | 1743 | 1474 | 84.6 | 269 | 15.4 | 10.455 | .001 |
| | 2020 | 1343 | 1076 | 80.1 | 267 | 19.9 | | |
| Consultation | 2019 | 1745 | 1699 | 97.3 | 46 | 2.7 | 0.107 | .743 |
| | 2020 | 1343 | 1305 | 97.2 | 38 | 2.8 | | |

Note: Some missing data in 2019 or 2020 lead to the sum of some home environment items not equal to the total sample size each year, which should be a total of 1748 in 2019 and 1349 in 2020. Significant values are in boldface.

Table 3. Chi-square results for demographic characteristics in the children's social skill data.

| Item | Category | 2019 | | 2020 | | χ^2 | <i>p</i> |
|--------------------|----------|------|------|------|------|----------|----------|
| | | n | % | n | % | | |
| Age of children | 1 | 179 | 9.3 | 208 | 10.5 | 10.138 | .071 |
| | 2 | 253 | 13.2 | 305 | 15.3 | | |
| | 3 | 371 | 19.4 | 327 | 16.4 | | |
| | 4 | 425 | 22.2 | 419 | 21.1 | | |
| | 5 | 391 | 20.4 | 427 | 21.5 | | |
| | 6 | 298 | 15.5 | 303 | 15.2 | | |
| Gender of children | Boy | 1045 | 54.5 | 1085 | 54.6 | 0.001 | .981 |
| | Girl | 872 | 45.5 | 904 | 45.4 | | |

Table 4 indicates that children's social skills from the 2019 sample were better than those in the 2020 sample. The significant results in each subscale are as follows: (1) subscale of assertion: expresses appropriate greeting to others; (2) subscale of self-control: waits for his/her turn; resist his/her demands when persuaded, and (3) subscale of cooperation: helps friends when friends get hurt; brings cheer to friends who look lonely; cheers up and comforts those who fail; happy when friends succeed, and praises friends' success. Almost all significant items belong to the cooperation subscale.

Discussion

Regarding home environment, negative changes, such as a reduced frequency of shopping together and visiting friends and relatives, were observed in the social stimulation. A report from Benesse (2020), showed that, during the state of emergency, mothers of pre-school children were worried about the lack of space for children to play outside, reduced chances for children to stay physically active, and the inability of children to meet their friends in Japan. Our results confirmed that the decrease in social stimulation existed before and after the pandemic. Not only opportunities to go outside, but also opportunities to contact relatives and friends were measured. Although the Japanese government did not enforce legal restrictions on going out during COVID-19, the social stimulation domain of the home environment shows a reduction. However, we did not find a significant result when testing the item of going to the park together. This can be explained by the fact that Japanese parks are close to every living street or residential area with a large population. Parents may choose to bring their children to these low population density parks rather than high population density shopping areas. Another negative change is the decrease in support from others. Ogita, Nishimoto, Matsui, Hamazaki, and Tsuchiya (2021) indicated that the utilisation percentage of childcare support services by families decreased during the pandemic. However, our findings implied that there was also a decrease in the help received from others, such as relatives, friends, or neighbours, which can also be explained by the difficulty in social contact, resulting from the COVID-19 pandemic.

Additionally, we also confirmed that some positive changes occurred during this period. As for the human stimulation domain, the frequency of family meals at the end of 2020 was significantly higher than in 2019. However, we did not obtain any significant results from the other items of the human stimulation domain, including playing with the child, singing songs together, reading to the child, and cooperating with the spouse. This can be explained by the fact that mealtime is relatively fixed compared to other items that can be conducted flexibly. When parents work at home, a fixed mealtime allows them to eat with their children on time, directly adding to the frequency. We also found that the proportion of positive attitude in 'response to mistake' and 'lack of punishment' was higher than in 2019. Previous studies have reported an increased risk of family violence (Campbell, 2020) and child abuse and neglect during the COVID-19 pandemic (Đapić et al., 2020). Corporal punishment is related to parental stress (Mochizuki et al., 2014), and parenting stress increased significantly during the pandemic (Hiraoka & Tomoda, 2020). Greater COVID-19-related stressors, high anxiety and depressive symptoms are associated with higher

Table 4. Chi-square results for children's social skills in 2019 and 2020.

| Item | Category | Total | Positive | | Negative | | χ^2 | <i>p</i> |
|---|----------|-------|----------|------|----------|------|----------|----------|
| | | | n | % | n | % | | |
| Makes eye contact when someone speaks to him/her | 2019 | 1917 | 1910 | 99.6 | 7 | 0.4 | 0.005 | .945 |
| | 2020 | 1989 | 1982 | 99.6 | 7 | 0.4 | | |
| Displays strong reactions when he/she is spoken to | 2019 | 1916 | 1909 | 99.6 | 7 | 0.4 | 1.141 | .285 |
| | 2020 | 1989 | 1977 | 99.4 | 12 | 0.6 | | |
| Shows happiness when someone does something for him/her | 2019 | 1916 | 1904 | 99.4 | 12 | 0.6 | 0.266 | .606 |
| | 2020 | 1989 | 1979 | 99.5 | 10 | 0.5 | | |
| Shows his/her feelings through facial expressions | 2019 | 1916 | 1904 | 99.4 | 12 | 0.6 | 0.266 | .606 |
| | 2020 | 1989 | 1979 | 99.5 | 10 | 0.5 | | |
| Expresses appropriate greeting to others | 2019 | 1915 | 1758 | 91.8 | 157 | 8.2 | 5.178 | .023 |
| | 2020 | 1988 | 1783 | 89.7 | 205 | 10.3 | | |
| Initiates talk with another person | 2019 | 1916 | 1777 | 92.7 | 139 | 7.3 | 1.087 | .297 |
| | 2020 | 1989 | 1827 | 91.9 | 162 | 8.1 | | |
| Makes eye contact when speaking with others | 2019 | 1914 | 1819 | 95.0 | 95 | 5.0 | 1.135 | .287 |
| | 2020 | 1989 | 1875 | 94.3 | 114 | 5.7 | | |
| Participates in a play group (companies) when asked | 2019 | 1915 | 1712 | 89.4 | 203 | 10.6 | 0.395 | .529 |
| | 2020 | 1986 | 1763 | 88.8 | 223 | 11.2 | | |
| Does not throw temper tantrums in public | 2019 | 1916 | 1740 | 90.8 | 176 | 9.2 | 2.574 | .109 |
| | 2020 | 1986 | 1773 | 89.3 | 213 | 10.7 | | |
| Waits patiently after asking for something | 2019 | 1916 | 1679 | 87.6 | 237 | 12.4 | 1.627 | .202 |
| | 2020 | 1986 | 1713 | 86.3 | 273 | 13.7 | | |
| Share toys or food with others | 2019 | 1917 | 1628 | 84.9 | 289 | 15.1 | 0.460 | .498 |
| | 2020 | 1986 | 1671 | 84.1 | 315 | 15.9 | | |
| Does not interrupt other's speech | 2019 | 1915 | 1603 | 83.7 | 312 | 16.3 | 2.983 | .084 |
| | 2020 | 1985 | 1620 | 81.6 | 365 | 18.4 | | |
| Waits for his/her turn | 2019 | 1914 | 1642 | 85.8 | 272 | 14.2 | 5.267 | .022 |
| | 2020 | 1985 | 1650 | 83.1 | 335 | 16.9 | | |
| Borrows toys from others | 2019 | 1915 | 1607 | 83.9 | 308 | 16.1 | 0.138 | .710 |
| | 2020 | 1985 | 1657 | 83.5 | 328 | 16.5 | | |
| Behaves well as required by the situation | 2019 | 1912 | 1559 | 81.5 | 353 | 18.5 | 2.511 | .113 |
| | 2020 | 1983 | 1577 | 79.5 | 406 | 20.5 | | |
| Resist his/her own demands when persuaded | 2019 | 1910 | 1620 | 84.8 | 290 | 15.2 | 8.346 | .004 |
| | 2020 | 1983 | 1613 | 81.3 | 370 | 18.7 | | |
| Helps friends when friends get hurt | 2019 | 1894 | 1374 | 72.5 | 520 | 27.5 | 9.438 | .002 |
| | 2020 | 1980 | 1347 | 68.0 | 633 | 32.0 | | |
| Cheers up friends who look lonely | 2019 | 1898 | 1346 | 70.9 | 552 | 29.1 | 9.391 | .002 |
| | 2020 | 1979 | 1313 | 66.3 | 666 | 33.7 | | |
| Cheers up and comforts those who fail | 2019 | 1895 | 1245 | 65.7 | 650 | 34.3 | 10.193 | .001 |
| | 2020 | 1977 | 1201 | 60.7 | 776 | 39.3 | | |
| Happy when friends succeed | 2019 | 1897 | 1459 | 76.9 | 438 | 23.1 | 18.824 | <.001 |
| | 2020 | 1978 | 1400 | 70.8 | 578 | 29.2 | | |
| Praises friend's success | 2019 | 1902 | 1348 | 70.9 | 554 | 29.1 | 9.148 | .002 |
| | 2020 | 1977 | 1312 | 66.4 | 665 | 33.6 | | |
| Applauds friend who has done something well | 2019 | 1895 | 1202 | 63.4 | 693 | 36.6 | 3.507 | .061 |
| | 2020 | 1975 | 1195 | 60.5 | 780 | 39.5 | | |
| Helps friends when asked | 2019 | 1893 | 1422 | 75.1 | 471 | 24.9 | 3.291 | .070 |
| | 2020 | 1971 | 1430 | 72.6 | 541 | 27.4 | | |
| Helps friends without having to be asked | 2019 | 1893 | 1264 | 66.8 | 629 | 33.2 | 1.773 | .183 |
| | 2020 | 1971 | 1276 | 64.7 | 695 | 35.3 | | |

Note: Some missing data in 2019 or 2020 lead to the sum of some social skill items not equal to the total sample size each year, which should be a total of 1917 samples in 2019 and 1989 samples in 2020. Significant values are in boldface.

perceived stress of parents, while high anxiety and depressive symptoms are related to more child abuse (Brown et al., 2020; Chung et al., 2020). However, our results from the two items from the avoidance of restriction domain showed that 2020 was better than 2019. This may be explained by other protective factors, such as adaptive coping strategy and a supportive family environment mitigating the impact of COVID-19 on parental stress and child abuse potential (Brown et al., 2020). However, in this study, we only examined the differences in the home environment between these two years, and hence further evidence is needed to clarify whether these changes will influence children's health-related outcomes.

In this study, we confirmed that the percentage of children belonging to the negative group in 2020 was greater than that of children in 2019 across eight items in the self-control, cooperation, and assertion domains. As for the self-control domain, previous studies have already stated that an increase in children's indiscipline and hyperactivity, with worsening capacity for inhibitory self-control of children (Di Giorgio, Di Riso, Mioni, & Cellini, 2021), and an increase in externalising and aggressive behaviour was also found among children with neurodevelopmental disorders during the COVID-19 pandemic (Kawaoka et al., 2021). In our study, decreases in waiting for his/her turn and resisting their own demands when persuaded was also observed in the self-control domain. Besides, we found that significant differences also exist in children's cooperation and assertion domains. According to our results, five items are from the cooperation domain. Free socialisation and relationships are important for the construction of a social brain, which is in contrast with people wearing masks; therefore, learning facial expressions, communication skills, and language is difficult (Araújo et al., 2020). Chen et al. (2016) stated that less social contact and a lack of social relationships are associated with poor social cooperation functioning in pre-school age, while Loades et al. (2020) stated that children might experience anxiety, depression, and trauma, resulting from prolonged social isolation and loneliness due to infectious disease outbreaks. However, limited studies have focused on finding the exact factors related to changes in social skills during the COVID-19 pandemic, which requires further study. We hope that childcare institutions can provide more support for pre-school children's social skills development during the pandemic.

The present study is significant because, to the best of our knowledge, it is the first to use a relatively large sample size to clarify the differences in the home environment and children's social skills before and after the pandemic. Second, this is a national survey with a high data utilisation rate. Thus, we believe that our results can be generalised to families using childcare centres in Japan. Third, this study chose the period before and after the COVID-19 outbreak, clarifying the differences in a longer duration and solving the bias in the change in the early stage of the outbreak. Lastly, we considered less bias in our study because the surveys were conducted in 2019 and 2020, rather than letting the participants recall the situation in 2019, which is different from many previous studies conducted during the COVID-19 pandemic.

The limitations of this study need to be considered. First, we collected the data before the outbreak of COVID-19, and again after the outbreak in December 2020 in the same childcare centres. The parents and children who participated in the 2019 data collection wave were not the same as those in the 2020 wave. We compared the demographic characteristics of these two samples to ensure they are comparable. Further, the home environment and social skills were not evaluated simultaneously; therefore, not all participants who received the social skill evaluation also received the home environment evaluation. Thus, this study could not directly examine the association between changes in home environment and children's social skills before and after the COVID-19 pandemic. We only clarified the differences in the home environment and children's social skills before and after the COVID-19 pandemic. The factors related to these differences remain unclear and require further clarification. Second, because of the large no-answer rate, some demographic information, including the parents' educational background and family's economic status, could not be considered in the analyses. Third, we could not provide evidence about aspects of child health affected by these differences; thus, this requires more longitudinal evidence in the future.

Conclusion

This study explored the potential differences in the home environment and children's social skills before and after the COVID-19 pandemic. Frequent social stimulation, such as shopping together and visiting friends and relatives, decreased in the home environment. A decrease in social support was observed. We also found positive changes, such as frequent family mealtimes, no punishment, and a positive attitude toward children's mistakes.

Moreover, the study found that children's social skills in the 2019 sample were better developed compared to the 2020 sample, especially in the cooperation domain. Childcare institutions can consider these differences in home environment and children's social skills and make a support plan to ensure quality child-rearing practices and healthy child development.

Acknowledgments

We express our deepest gratitude to all the participants and staff members for their voluntary participation in this study and the Japan society for the promotion of Science (JSPS) for the funding support [Grant Number JP21H00790]. The first author, Xiang Li, a PhD candidate of Medical Science Program at School of Comprehensive Human Science, University of Tsukuba, Japan, would like to express his very great appreciation to Japan Science and Technology Agency (JST) for the scholarship of Support for Pioneering Research Initiated by the Next Generation (SPRING) and Japan Student Service Organization (JASSO) for the AY2020 Monbukagakusho Honors scholarship.

Authors' contributions:

Xiang Li: Data Curation, Formal analysis, Writing - Original Draft

Dandan Jiao: Writing-review & Editing

Munenori Matsumoto: Writing-review & Editing

Yantong Zhu: Data Curation, Formal analysis (child care environment)

Jinrui Zhang: Data Curation, Formal analysis (social skill)

Zhu Zhu: Data Curation, Formal analysis (social skill)

Yang Liu: Data Curation, Formal analysis (child care environment)

Mingyu Cui: Data Curation, Formal analysis (child care environment)

Yanlin Wang: Data Curation, Formal analysis (social skill)

Meiling Qian: Data Curation, Formal analysis (social skill)

Ammara Ajmal: Conceptualization, Methodology (child care environment and social skill)

Alpona Afsari Banu: Conceptualization, Methodology (child care environment)

Yolanda Graça: Conceptualization, Methodology (social skill)

Emiko Tanaka: Investigation

Taeko Watanabe: Investigation

Yuko Sawada: Investigation

Etsuko Tomisaki: Investigation

Tokie Anme: Visualization, Supervision, Project administration, Funding acquisition.

Note: This study is conducted by the Japan Child Care Cohort study group. The Japan Child Care Cohort study included two surveys: child care environment and social skill. Yantong Zhu, Jinrui Zhang, Zhu Zhu, Yang Liu, Mingyu Cui, Yanlin Wang, and Meiling Qian have contributed equally to this study.

Disclosure statement

No potential conflict of interest was reported by the author(s).

Funding

This work was supported by JSPS: [Grant Number JP21H00790].

Submission Declaration

This study has not been published previously, and it is not under consideration for publication elsewhere. Its publication is approved by all authors and tacitly or explicitly by the responsible

authorities where the work was carried out. If accepted, it will not be published elsewhere in the same form, in English, or in any other language, including electronically, without the written consent of the copyright holder.

Notes on contributors

Xiang Li, is a PhD candidate of medical science program at School of Comprehensive Human Science, University of Tsukuba, Japan. His current research interest lies on public health, child development and co-creative well-being.

Dandan Jiao, is a PhD candidate of biomedical science program at School of Comprehensive Human Science, University of Tsukuba, Japan. Her current research interest lies on gerontology, nursing and public health.

Munenori Matsumoto, is a PhD candidate of nursing science program at School of Comprehensive Human Science, University of Tsukuba, Japan. His current research interest lies on subjective well-being.

Yantong Zhu, is a PhD candidate of medical science program at School of Comprehensive Human Science, University of Tsukuba, Japan. His current research interest lies on child development and childcare.

Jinrui Zhang, is a master student of public health program at School of Comprehensive Human Science, University of Tsukuba, Japan. Her current research interest lies on child development and childcare.

Zhu Zhu, is a PhD candidate of medical science program at School of Comprehensive Human Science, University of Tsukuba, Japan. Her current research interest lies on child development and childcare.

Yang Liu, is a PhD candidate of medical science program at School of Comprehensive Human Science, University of Tsukuba, Japan. His current research interest lies on gerontology.

Mingyu Cui, is a PhD candidate of medical science program at School of Comprehensive Human Science, University of Tsukuba, Japan. His current research interest lies on gerontology.

Yanlin Wang, is a master student of public health program at School of Comprehensive Human Science, University of Tsukuba, Japan. Her current research interest lies on child development and childcare.

Meiling Qian, is a master student of public health program at School of Comprehensive Human Science, University of Tsukuba, Japan. Her current research interest lies on dental health.

Ammara Ajmal, is a PhD candidate of biomedical science program at School of Comprehensive Human Science, University of Tsukuba, Japan. Her current research interest lies on work performance and hospital management.

Alpona Afsari Banu, is a master student of public health program at School of Comprehensive Human Science, University of Tsukuba, Japan. Her current research interest lies on sleep condition.

Yolanda Graça, is a PhD candidate of medical science program at School of Comprehensive Human Science, University of Tsukuba, Japan. Her current research interest lies on community health.

Emiko Tanaka, PhD, is a lecturer at Nursing Department, Musashino University, Japan. Her current research interest lies on child development and childcare.

Taeko Watanabe, PhD, is a professor at Nursing Department, Shukutoku University, Japan. Her current research interest lies on child development and childcare.

Yuko Sawada, PhD, is a professor at Health Medicine Department, Morinomiya University of Medical Science, Japan. Her current research interest lies on rehabilitation and health care.

Etsuko Tomisaki, PhD, is a lecturer at Nursing Department, Keio University, Japan. Her current research interest lies on child development and sleep problems.

Tokie Anme, PhD, is a professor at Medicine Department, University of Tsukuba, Japan. She is also the director of International Systems and Empowerment Sciences for Lifespan Development. Her current research interest lies on life sciences and public health.

ORCID

Xiang Li  <http://orcid.org/0000-0001-8875-1930>

Zhu Zhu  <http://orcid.org/0000-0001-6997-5007>

Emiko Tanaka  <http://orcid.org/0000-0002-2010-243X>

Etsuko Tomisaki  <http://orcid.org/0000-0003-0886-9467>

References

- Anme, T., & Segal, U. A. (2004). Implications for the development of children in over 11 hours of centre-based care. *Child: Care, Health and Development*, 30(4), 345–352. doi:10.1111/j.1365-2214.2004.00429.x
- Anme, T., Shinohara, R., Sugisawa, Y., Tanaka, E., Watanabe, T., & Hoshino, T. (2013). Validity and reliability of the social skill scale (SSS) as an index of social competence for preschool children. *Journal of Health Science*, 3(1), 5–11. doi:10.1111/j.1365-2214.2004.00429.x.
- Anme, T., Tanaka, E., Shinohara, R., Sugisawa, Y., Watanabe, T., Tomisaki, E., & Segal, U. A. (2012). Center-based child extended care: Implications for young children's development in a five-year follow-up. *Sociology Mind*, 2(04), 435. doi:10.4236/sm.2012.24056
- Anme, T., Tanaka, E., Watanabe, T., Tomisaki, E., Mochizuki, Y., & Tokutake, K. (2013). Validity and reliability of the index of child care environment (ICCE). *Public Health Frontier*, 2(3), 141–145. doi:10.5963/PHF0203003.
- Araújo, L. A., Veloso, C. F., Souza, M. C., Azevedo, J., & Tarro, G. (2020). The potential impact of the COVID-19 pandemic on child growth and development: A systematic review. *Jornal de Pediatria*, S0021-7557(20), 30209–6. Advance online publication. doi:10.1016/j.jpmed.2020.08.008.
- Benesse. (2020). Eighty percent of mothers with preschool children thought social relationship is important in the COVID-19 pandemic. Retrieved from Benesse website: https://blog.benesse.ne.jp/bh/ja/news/20200805_release.pdf.
- Brooks, S. K., Webster, R. K., Smith, L. E., Woodland, L., Wessely, S., Greenberg, N., ... Rubin, G. J. (2020). The psychological impact of quarantine and how to reduce it: Rapid review of the evidence. *The Lancet*, 395(10227), 912–920. doi:10.1016/S0140-6736(20)30460-8.
- Brown, S. M., Doom, J. R., Lechuga-Peña, S., Watamura, S. E., & Koppels, T. (2020). Stress and parenting during the global COVID-19 pandemic. *Child Abuse & Neglect*, 110(2), 104699. doi:10.1016/j.chiabu.2020.104699
- Campbell, A. M. (2020). An increasing risk of family violence during the COVID-19 pandemic: Strengthening community collaborations to save lives. *Forensic Science International: Reports*, 2, 100089. doi:10.1016/j.fsir.2020.100089
- Chaabane, S., Doraiswamy, S., Chaabna, K., Mamtani, R., & Cheema, S. (2021). The impact of COVID-19 school closure on child and adolescent health: A rapid systematic review. *Children (basel, Switzerland)*, 8(5), 415. doi:10.3390/children8050415.
- Chen, W., Tanaka, E., Watanabe, K., Tomisaki, E., Watanabe, T., Wu, B., & Anme, T. (2016). The influence of home-rearing environment on children's behavioral problems 3 years' later. *Psychiatry Research*, 244, 185–193. doi:10.1016/j.psychres.2016.07.043
- Chung, G., Lanier, P., & Wong, P. (2020). Mediating effects of parental stress on harsh parenting and parent-child relationship during coronavirus (COVID-19) pandemic in Singapore. *Journal of Family Violence*, 1–12. Advance online publication. doi:10.1007/s10896-020-00200-1.
- Cluver, L., Lachman, J. M., Sherr, L., Wessels, I., Rakotomalala, S., ... McDonald, K. (2020). Parenting in a time of COVID-19. *The Lancet (London, England)*, 395(10231), e64. doi:10.1016/S0140-6736(20)30736-4
- Đapić, M. R., Flander, G. B. & Prijatelj, K. (2020). Children behind closed doors due to COVID-19 isolation: Abuse, neglect and domestic violence. *Archives of Psychiatry Research*, 56, 181–192. doi:10.20471/dec.2020.56.02.06
- Di Giorgio, E., Di Riso, D., Mioni, G., & Cellini, N. (2021). The interplay between mothers' and children behavioral and psychological factors during COVID-19: An Italian study. *European Child & Adolescent Psychiatry*, 1–12. Advance online publication. doi:10.1007/s00787-020-01631-3.
- Hiraoka, D., & Tomoda, A. (2020). Relationship between parenting stress and school closures due to the COVID-19 pandemic. *Psychiatry and Clinical Neurosciences*, 74(9), 497–498. doi:10.1111/pcn.13088
- Horiuchi, S., Shinohara, R., Otawa, S., Akiyama, Y., Ooka, T., Kojima, R., ... Yamagata, Z. (2020). Caregivers' mental distress and child health during the COVID-19 outbreak in Japan. *PLoS One*, 15(12), e0243702. doi:10.1371/journal.pone.0243702
- Janssen, L., Kullberg, M. J., Verkuil, B., van Zwielen, N., Wever, M., van Houtum, L., ... Elzinga, B. M. (2020). Does the COVID-19 pandemic impact parents' and adolescents' well-being? An EMA-study on daily affect and parenting. *PLoS One*, 15(10), e0240962. doi:10.1371/journal.pone.0240962.
- Kawaoka, N., Ohashi, K., Fukuhara, S., Miyachi, T., Asai, T., Imaeda, M., & Saitoh, S. (2021). Impact of school closures due to COVID-19 on children with neurodevelopmental disorders in Japan. *Journal of Autism and Developmental Disorders*, 1–7. Advance online publication. doi:10.1007/s10803-021-05119-0.
- Ladd, G. W. (2000). The fourth R: Relationships as risks and resources following children's transition to school. *American Educational Research Association Division E-Newsletter*, 19, 9–11.
- Liu, J. J., Bao, Y., Huang, X., Shi, J., & Lu, L. (2020). Mental health considerations for children quarantined because of COVID-19. *The Lancet. Child & adolescent health*, 4(5), 347–349. doi:10.1016/S2352-4642(20)30096-1
- Loades, M. E., Chatburn, E., Higson-Sweeney, N., Reynolds, S., Shafran, R., Brigden, A., ... Crawley, E. (2020). Rapid systematic review: The impact of social isolation and loneliness on the mental health of children and adolescents in the context of COVID-19. *Journal of the American Academy of Child and Adolescent Psychiatry*, 59(11), 1218–1239.e3. doi:10.1016/j.jaac.2020.05.009
- Ministry of Health, Labour and Welfare. (2021). *Information regarding COVID-19 in child care facilities*. Children's family Bureau Care. https://www.mhlw.go.jp/stf/newpage_09762.html.

- Mochizuki, Y., Tanaka, E., Shinohara, R., Sugisawa, Y., Tomisaki, E., Watanabe, T., ... Anme, T. (2014). The influence of caregivers' anxiety and the home environment on child abuse. *A Study of Children Attending Childcare Centers. Nihon Koshu Eisei Zasshi [Japanese Journal of Public Health]*, 61(6), 263–274.
- Ogita, Y., Nishimoto, M., Matsui, N., Hamazaki, Y., & Tsuchiya, H. (2021). Effects of parental stress and child care support during national state of emergency over COVID-19 pandemic in Japan. *Journal of the Institute of Joint Participation [Osaka University of Commerce]*, 2, 17–42.
- Roos, L. E., Salisbury, M., Penner-Goeke, L., Cameron, E. E., Protudjer, J., Giuliano, R., ... Reynolds, K. (2021). Supporting families to protect child health: Parenting quality and household needs during the COVID-19 pandemic. *PLoS One*, 16(5), e0251720. doi:10.1371/journal.pone.0251720.
- Shen, K., Yang, Y., Wang, T., Zhao, D., Jiang, Y., Jin, R., ... Gao, L. (2020). Diagnosis, treatment, and prevention of 2019 novel coronavirus infection in children: Experts' consensus statement. *World Journal of Pediatrics*, 16(3), 223–231. doi:10.1007/s12519-020-00343-7
- Shorer, M., & Leibovich, L. (2020). Young children's emotional stress reactions during the COVID-19 outbreak and their associations with parental emotion regulation and parental playfulness. *Early Child Development and Care*, 1–11. doi:10.1080/03004430.2020.1806830. [AHEAD-OF-PRINT].
- Singh, S., Roy, D., Sinha, K., Parveen, S., Sharma, G., & Joshi, G. (2020). Impact of COVID-19 and lockdown on mental health of children and adolescents: A narrative review with recommendations. *Psychiatry Research*, 293, 113429. doi:10.1016/j.psychres.2020.113429
- Takahashi, Y., Okada, K., Hoshino, T., & Anme, T. (2008). Social skills of preschoolers: Stability of factor structures and predictive validity from a nationwide cohort study in Japan. *Japanese Journal of Educational Psychology*, 56(1), 81–92. doi:10.1371/journal.pone.0135357.
- Takahashi, Y., Okada, K., Hoshino, T., & Anme, T. (2015). Developmental trajectories of social skills during early childhood and links to parenting practices in a Japanese sample. *PLoS One*, 10(8), e0135357. doi:10.1111/j.1365-2648.2009.05058.x.
- Tong, L., Shinohara, R., Sugisawa, Y., Tanaka, E., Maruyama, A., Sawada, Y., ... Anme, T. (2009). Relationship of working mothers' parenting style and consistency to early childhood development: A longitudinal investigation. *Journal of Advanced Nursing*, 65(10), 2067–2076. doi:10.1111/j.1365-2648.2009.05058.x
- Tong, L., Shinohara, R., Sugisawa, Y., Tanaka, E., Watanabe, T., Koeda, T., & Anme, T. (2015). Buffering effect of parental engagement on the relationship between corporal punishment and children's emotional/behavioral problems. *Pediatrics International*, 57(3), 385–392. doi:10.1111/ped.12604

Article

Development of Social Skills in Kindergarten: A Latent Class Growth Modeling Approach

Yantong Zhu ¹, Xiang Li ¹, Dandan Jiao ¹, Emiko Tanaka ², Etsuko Tomisaki ³, Taeko Watanabe ⁴, Yuko Sawada ⁵, Zhu Zhu ¹, Ammara Ajmal ¹, Munenori Matsumoto ¹ and Tokie Anne ^{6,*}

¹ School of Comprehensive Human Science, University of Tsukuba, Tsukuba 3058577, Japan; zyt199431@gmail.com (Y.Z.); lixiangdufl@gmail.com (X.L.); jdd2013112@gmail.com (D.J.); zhuzhu881231@yahoo.co.jp (Z.Z.); ammara.ajmal6@gmail.com (A.A.); m_matsumoto@g.t-junshin.ac.jp (M.M.)

² Faculty of Nursing, Musashino University, Tokyo 2028585, Japan; warakott@gmail.com

³ Faculty of Nursing, Keio University, Tokyo 1088345, Japan; ettsukot@gmail.com

⁴ Faculty of Nursing, Shukutoku University, Chiba 2608701, Japan; taeko.watanabe@soc.shukutoku.ac.jp

⁵ Faculty of Health Medicine, Morinomiya University of Medical Sciences, Osaka 5598611, Japan; ysawa1110@yahoo.co.jp

⁶ Faculty of Medicine, University of Tsukuba, Tsukuba 3058577, Japan

* Correspondence: anmet@md.tsukuba.ac.jp

Abstract: Social skills acquired during early childhood are often the foundation for success later in life. Using a nationwide survey dataset in Japan, this study aims to explore the multiple growth trajectories of social skills among children in kindergarten by using a latent class growth modeling approach. It also examines whether, and to what extent, the home-rearing environment at early age predict trajectories of social skills development. Children in this study were assessed on social skills at three waves, four home-rearing environment dimensions (human stimulation, social stimulation, avoidance of punishment, and social support for parenting) and demographic background were measured at wave 1. The results indicated that three distinct growth trajectories of social skills existed during kindergarten: high increase levels, moderate increase levels, and decreased levels. The avoidance of punishment and children's gender significantly predicted the growth trajectories of social skills. Thus, the results suggest that more attention should be paid to the home-rearing environment and boys.

Keywords: social skills; home rearing environment; kindergarten children; latent class growth analysis



Citation: Zhu, Y.; Li, X.; Jiao, D.; Tanaka, E.; Tomisaki, E.; Watanabe, T.; Sawada, Y.; Zhu, Z.; Ajmal, A.; Matsumoto, M.; et al. Development of Social Skills in Kindergarten: A Latent Class Growth Modeling Approach. *Children* **2021**, *8*, 870. <https://doi.org/10.3390/children8100870>

Academic Editor: Michelle de Haan

Received: 23 August 2021

Accepted: 28 September 2021

Published: 29 September 2021

Publisher's Note: MDPI stays neutral with regard to jurisdictional claims in published maps and institutional affiliations.



Copyright: © 2021 by the authors. Licensee MDPI, Basel, Switzerland. This article is an open access article distributed under the terms and conditions of the Creative Commons Attribution (CC BY) license (<https://creativecommons.org/licenses/by/4.0/>).

1. Introduction

Social skills are characterized as learned, socially acceptable behaviors that allow an individual to effectively communicate with others, while avoiding socially unacceptable responses (Gresham and Elliott [1]). The development of social skills is recognized as a fundamental aspect of building successful relationships with others and has shown a positive link to children's academic achievement, intellectual and behavioral development, and school adaptation (Wentzel et al. [2]; Hukkelberg et al. [3]; McIntyre et al. [4]). Conversely, low levels of social skills at early stages are associated with maladjustment problems, low self-esteem, and poorer mental and physical health (Arnold et al. [5]; Seema and Kumar, [6]; Ke et al. [7]). Many experts believe that the preschool years are a crucial time for children to improve their social skills, since most children begin to learn how to manage themselves in order to communicate effectively with peers and teachers (Fabes et al. [8]). Therefore, it is important to clarify the development of social skills during the kindergarten period, identify children manifesting social skill deficits, provide interventions aimed at enhancing their social skills, and be diligent in taking appropriate preventative steps.

Many previous studies have outlined the characteristics of children's social skills development (Lamont and Horn, [9]; Sørliie et al. [10]; Hajovsky et al. [11]; DiDonato, [12]). Sørliie et al. [10] suggested that children from 4th grade to 7th grade have three distinct trajectories, one with steady average scores through time, and the other two with high initial and dropping scores, as well as low initial and increasing scores. Lamont and colleagues (2013) also identify the three distinct social skills growth trajectories from kindergarten to third grade: stable class, increase class and decreasing class. DiDonato [12] discovered children from kindergarten to 5th grade have two unique trajectories of social skill: a higher-level trajectory with a marginally significant curved shape and a consistent moderate-level trajectory. Hajovsky et al. [11] found that from kindergarten to sixth grade, boys' social skills showed a linear decline over time, whereas girls' social skills did not change significantly over time. However, very few studies have focused on the trajectory of social skills development during the kindergarten period, which is considered a crucial time for children to improve their social skills (Kramer et al. [13]). During this time, teachers and peers expect children to begin displaying social skills while dealing with increased environmental demands (Stright et al. [14]). According to socialization theory, preschool-aged children learn how to be good as they become older, increasing the frequency of prosocial behaviors (Eisenberg et al. [15]). Simultaneously, evidence suggests that children's social skills differentiate and show heterogeneity (Caplan, [16]). Within this context, the patterns of social skills development during the kindergarten (typical age of 3–6 years) period need to be further explored.

Previous studies have shown that home-rearing environment are the growth-promoting factors of social skills development (Anme and Segal [17]). The home-rearing environment can be defined as the degree of organization in children's surroundings in relation to human and physical resources, particularly their parents, and the quality of close relationships in their environment (Anme et al. [18]). The development of social skills initially starts at home at the interpersonal level through interactions with parents (Olcer and Aytar [19]). Research has demonstrated that high quality of home rearing environment can contribute to social skills development during early childhood (Takahashi [20]). Anme and Segal found a link between parenting quality and children's social development, particularly social skill, and communication abilities [17]. Children learn social skills via parents' interactions, parental modeling and practices, parent-children attachment and warm relations, and the experiences and opportunity to develop various social skills that parents provide and organize (Grusec and Davidov [21]; Parke et al. [22]; Reich and Vandell [23]; Denham et al. [21]). The increase in parents' involvement over time was related to concomitant improvement in children's social skills and decline in problem behaviors (Nokali et al. [24]). Previous studies also found that discipline and punishment imposed by parents significantly predicted children's future social skills based on Bandura's social learning theory (1973), When parents spank their children, they model aggressive behavior, which their youngsters replicate in disagreements with friends and siblings (Altschul et al. [25]; Tompkins and Villaruel [26]). Within this context, we hypothesis that higher quality of home-rearing environment may affect growth patterns of social skill during kindergarten.

Many studies have shown that children's social skills development was important and has individual differences during the kindergarten period (Caplan [16]; Greene [20]; Takahashi et al. [27]). Traditionally, longitudinal studies have used variable-centered methods to examine the growth curve of children's social skills development and its relationship with its predictors. However, few studies have focused on the trajectory of social skills development during kindergarten. As a person-oriented approach, the latent class growth model is an analytical method to summarize data across multiple time periods and to characterize heterogeneous patterns within distinct groups (Jung and Wickrama, [28]). Utilizing LCGA can clarify the distinct growth trajectories of children social skill development during kindergarten and help us explore the related factors. Therefore, this study used latent class growth analysis (LCGA) to identify distinct growth

trajectories of social skill during kindergarten; And further investigated how the home-rearing environment and demographic characteristic affect growth patterns.

2. Materials and Methods

2.1. Participants

This study was part of a nationwide cohort study called the 'Child Care Cohort Study' (CCC). Beginning in 1998, the CCC study sought to investigate the factors associated with child development and quality of life. The goal of this cohort study is to see if there was a link between the quality and quantity of center-based care and children's social competence and vocabulary/motor/intelligence development over time, and the childrearing environment provided by parents and children's development over time. All government authorized child day-care and night-care centers across Japan participated in it. Follow-up studies were conducted every year to investigate the factors associated with these aspects. Japanese preschools are typically three-year program for children age 3–6. As the present study was longitudinal, data from 2017 and 2019 were used. In the 2017 sample, 642 Japanese children in their first kindergarten year (typical age of 3–4) were recruited, the baseline return rate was 71.5%, giving data from 26 child-care facilities. Children with missing data on all measurement occasions was excluded in this study. Overall, all 459 children responded in the baseline were included in the analyses. The mean age of the baseline year children is 47.05 months.

2.2. Procedure

In the winter of each year, data was collected with signed informed consent. Receiving consent from children's parents, we recruited children at the beginning of the project. The home-rearing environment of children and demographic characteristics was evaluated through a self-administered survey for parents at 2017. Social skills were assessed at three time points between 2017 and 2019 in the child-care facilities by trained staffs.

2.3. Measures

2.3.1. Social Skills

Teachers' reports of children's social skills development were assessed from 2017 to 2019 using the Social Skill Scale (SSS) (Anme et al. [29]), which showed good reliability and validity (Anme et al. [29]; Hosokawa, [30]; Takahashi, [31]). The reliabilities of this study were 0.942, 0.957, 0.950 in three time points, respectively. It measures social skills through 30 items regarding "cooperation," "self-control," and "assertion," all of which influence later social adaptation (Gresham and Elliott [32]). Each item was rated on a 3-point scale ranging from 0 (not at all) to 2 (often), indicating how frequently the caregivers thought children in their classroom exhibited each social skill and/or problem behavior. A higher score indicated a higher level of social skills.

2.3.2. Home-Rearing Environment

The Index of Child Care Environment (ICCE) was used to measure the home-rearing environment (HRE) (Anme et al. [18]), that included 13 items in four dimensions: five questions regarding human stimulation (e.g., "How often do you play with your children?"), three regarding social stimulation (e.g., "How often do you go shopping with your children?"), two regarding avoidance of punishment (e.g., "How many times did you spank your child last week?"), and three regarding social support (e.g., "How many times do you have a chance to talk with your spouse/partner about your child?"). The ICCE is an established and valid screening instrument, given the positive correlations observed between it and child development in previous studies (Anme et al., 2013). The correlation coefficients for between the total score and each subscale of the ICCE and the HOME (Bradley and Bradley, 1984) "total score," "human stimulation," "social stimulation," "avoidance of punishment," and "social support," were 0.76, 0.78, 0.82, 0.82, and 1.00, respectively, and showed the high reliability ($\alpha = 0.891$) (Anme et al. [18,33]). For

two of the items, “support for childcare” and “have a consultation,” the response ranges were measured in a binary manner (1 = no, 2 = yes); the other 11 items were measured on a five-point scale (1 = rarely, 2 = 1–3/month, 3 = 1–2/week, 4 = 3–4/week, 5 = almost every day). To create scores that indicate whether home rearing environment is of higher or lower quality in each subscale, in the data analysis, parents who answered “1 = rarely,” were regarded as an unfavorable group and coded as 0, while those who answered “2 = 1–3/month, 3 = 1–2/week, 4 = 3–4/week, or 5 = almost every day” were regarded as a favorable group and coded as 1. Two items regarding avoidance of punishment were reversed-coded: parents who answered that they did not spank children in the past week or when they made a mistake, were coded 1 (Chen [34]).

2.3.3. Covariates

Based on previous studies, gender, family structure, and siblings were considered as covariates (Anderson-Butcher et al. [35]; Huang et al. [36]; Sang & Nelson [37]). All covariates were considered as categorical variables: gender (boys = 0, girls = 1), family structure (nuclear family = 0, extended family = 1), and siblings (no siblings = 0, having siblings = 1).

2.4. Ethical Considerations

This study was approved by the University of Tsukuba (1657). All participants were informed about the study’s objectives and process and made aware that they had the right to withdraw from the study at any time. All participants gave their written informed consent to participate in the study and data were kept confidential and private and all participants’ identities were kept anonymous.

2.5. Statistical Analysis

The characteristics of children in their first year of kindergarten were confirmed using descriptive statistics. Latent growth curve modeling (LGCM) and Latent class growth modeling (LCGM) was performed utilizing Mplus 8.6 (Muthén and Muthén, Los Angeles, CA, USA). This study applied LCGM model, which is a special type of Growth mixture model (GMM), that assumes all individual growth trajectories in one class are homogeneous and allows only across class (Nagin [38]). Compared with GMM, LCGM can result in a more parsimonious model, and more helpful with a small sample size (Jung and Wickrama [28]; Zhang et al. [39]). We conducted our model in the following steps: First, LGCM was performed to examine the general trajectory of social skills development (e.g., linear growth or nonlinear growth) using data from three waves. Full-information maximum likelihood (FIML) and robust standard errors (MLR in Mplus) was used to deal with missing data. Because of only three waves of social skill data, we conducted three model to explore the overall social skill trajectories: no-growth mode, linear growth model and nonlinear growth model (e.g., latent basis model). Model fitness was assessed by calculating and comparing chi-square values, comparative fit index (CFI), Tucker–Lewis index (TLI), and root mean square error of approximation (RMSEA). Second, unconditional LCGA was used to categorize distinct classes based on the social skills trajectories. We estimated trajectories of social skill without predictors in the model and determined the number of classes according to the Akaike information criterion (AIC), Bayesian information criterion (BIC), sample-adjusted Bayesian information criterion (aBIC), entropy, Lo-Mendell-Rubin likelihood ratio (LMR), and bootstrapped likelihood ratio tests (BLRT), as well as theoretical justification and interpretability. Then, optimal class membership was saved and then merged with the original data. Finally, we added covariates in the conditional LCGM and explored their relationship with the trajectories, a multinomial logistic regression analysis was performed to identify predictors of classes. Our analyses and reporting of results were guided by the Guidelines for Reporting on Latent Trajectory Studies (van de Schoot et al. [40]).

3. Results

3.1. Descriptive Statistics of the Study Sample

Descriptive statistics for the background characteristics of children, home-rearing environment, and child social skill in kindergarten are presented in Table 1. Of the total sample, 52.7% ($n = 242$) were boys and 47.3% ($n = 217$) were girls. While a total of 271 (59.0%) children lived in nuclear families, 188 lived in extended ones (41.0%). Out of the children, 64.7% ($n = 297$) had siblings, while 35.3% ($n = 162$) did not. The average scores of the four aspects of the home-rearing environment in 2017 were 4.75 ± 0.57 (human stimulation), 2.57 ± 0.59 (social stimulation), 0.92 ± 0.67 (avoid of punishment), and 2.67 ± 0.59 (social support). The mean social skills scores were 42.98 ± 10.34 in 2017, 48.14 ± 11.12 in 2018, and 51.60 ± 9.46 in 2019. Bivariate correlations among the main variables are shown in Table 2.

Table 1. Descriptive statistics of the study sample.

| Variables | Categories | n (%) or Mean \pm SD | Observed Range | Possible Range |
|----------------------------|--------------------|------------------------|----------------|----------------|
| Background characteristics | | | | |
| Gender | Boy | 242 (52.7) | | |
| | Girl | 217 (47.3) | | |
| Family structure | Nuclear family | 271 (59.0) | | |
| | Extended family | 188 (41.0) | | |
| Siblings | Have siblings | 162 (35.3) | | |
| | No siblings | 297 (64.7) | | |
| Home-rearing environment | | | | |
| Human stimulation | | 4.75 ± 0.57 | 2–5 | 0–5 |
| Social stimulation | | 2.57 ± 0.60 | 0–3 | 0–3 |
| Avoidance of punishment | | 0.92 ± 0.67 | 0–2 | 0–2 |
| Social support | | 2.67 ± 0.59 | 0–3 | 0–3 |
| Social skills score | | | | |
| Social skills | 2017 ($n = 452$) | 42.98 ± 10.34 | 7–60 | 0–60 |
| | 2018 ($n = 382$) | 48.14 ± 11.12 | 5–60 | 0–60 |
| | 2019 ($n = 337$) | 51.60 ± 9.46 | 8–60 | 0–60 |

Note: Missing rates for human stimulation, social stimulation, Avoidance of punishment, and social support were 3.3%, 0.2%, 0.2%, and 1.7%, respectively.

Table 2. Bivariate Correlations among Main Study Variables.

| No. | Variables | 1 | 2 | 3 | 4 | 5 | 6 | 7 | 8 | 9 | 10 |
|-----|---------------------|----------|----------|----------|--------|----------|--------|----------|---------|----------|----|
| 1 | T1 social skill | - | | | | | | | | | |
| 2 | T2 social skill | 0.302 ** | - | | | | | | | | |
| 3 | T3 social skill | 0.279 ** | 0.388 ** | - | | | | | | | |
| 4 | Gender | 0.201 ** | 0.163 ** | 0.196 ** | - | | | | | | |
| 5 | Family structure | -0.026 | 0.038 | 0.015 | -0.063 | - | | | | | |
| 6 | Siblings | 0.071 | 0.083 | -0.014 | 0.030 | 0.120 ** | - | | | | |
| 7 | Human stimulation | 0.091 | 0.014 | 0.117 * | 0.056 | 0.008 | -0.061 | - | | | |
| 8 | Social stimulation | 0.064 | 0.062 | 0.094 | 0.078 | 0.023 | 0.043 | 0.148 ** | - | | |
| 9 | Avoid of punishment | 0.016 | -0.013 | 0.137 * | 0.052 | -0.049 | -0.044 | 0.054 | 0.029 | - | |
| 10 | Social support | -0.002 | -0.002 | 0.021 | 0.012 | 0.047 | -0.052 | 0.320 ** | 0.103 * | 0.127 ** | - |

Note: * $p < 0.05$, ** $p < 0.01$.

3.2. Overall Trajectory of Social Skill

No-growth, linear growth, and nonlinear growth model were conducted to determine the overall trajectory patterns. The no-growth model showed the poor model fit: $\chi^2(4) = 103.48$, $p < 0.001$, CFI = 0, TLI = 0, and RMSEA = 0.233, SRMR = 0.339. The linear growth

model provided good fit to the data: $\chi^2(1) = 1.48, p = 0.22, CFI = 0.988, TLI = 0.965,$ and $RMSEA = 0.032, SRMR = 0.019$. The linear growth model was significantly better than the no-growth model in the Satorra-Bentler chi-square test, $\chi^2(3) = 90.78, p < 0.001$, and no worse than latent basis growth model, $\chi^2(1) = 1.48, p = 0.22$. Therefore, we selected the linear model in the next analysis. The intercept of 42.943 ($p < 0.001$) and average slope of 8.930 ($p < 0.001$) showed that children social skill varied in the initial levels and the rate of changes.

3.3. Heterogeneity in Social Skill Trajectories

The fit information for the unconditional latent class growth model is presented in Table 3. The 2-class, 4-class, 5-class, and 6-class models did not replicate the best LMR value, and LMR and BLRT in 3-class model were both significant ($p < 0.05, p < 0.001$), suggesting that 3-class model provided better model fit than 2-class model and 4-class, 5-class, and 6-class models. LMR shows the model fit between k and $k-1$ model, the significant LMR p value imply that current model has a better model fit than $k-1$ class model. Hence, the 3-class model were selected as the best fit model for the observed data. The proportion of individuals within each class was 74.7% ($n = 343$) in class 1, 5.3% ($n = 24$) in class 2, and 20.0% ($n = 92$) in class 3.

Table 3. Model fit information.

| Model | AIC | BIC | aBIC | Entropy | LMR | BLRT |
|----------|----------------|----------------|----------------|--------------|--------------|--------------|
| 1 | 8798.61 | 8819.26 | 8803.39 | | | |
| 2 | 8637.70 | 8670.73 | 8645.34 | 0.854 | 0.068 | 0.000 |
| 3 | 8567.24 | 8612.65 | 8577.74 | 0.790 | 0.034 | 0.000 |
| 4 | 8524.30 | 8582.11 | 8537.68 | 0.815 | 0.108 | 0.000 |
| 5 | 8506.99 | 8577.19 | 8523.23 | 0.797 | 0.217 | 0.000 |
| 6 | 8492.29 | 8492.29 | 8511.40 | 0.731 | 0.865 | 0.030 |

Abbreviations: AIC—Akaïke information criteria; BIC—Bayesian information criteria; aBIC—adjusted Bayesian information criteria; LMR—Lo-Mendell-Rubin likelihood ratio; BLRT—Bootstrapped Likelihood Ratio Tests. Note: The bold row represents the selected model.

As shown in Figure 1, Class 1 was termed “high-increase class,” that had an average initial social skills score of 45.30 ($p < 0.05$) and showed a relatively modest increase compared to the Class 2 (slope = 5.37, $p < 0.05$). Class 2 was named “decrease class,” as members began with an average social skills score of 40.48, that was significantly different from zero ($p < 0.05$), and showed total decrease across the entire time period (slope = $-8.04, p < 0.05$). Class 3 was named “moderate-increase class,” that had an average initial social skills score of 36.07 ($p < 0.05$) and subsequently increased (slope = 4.01, $p < 0.05$).

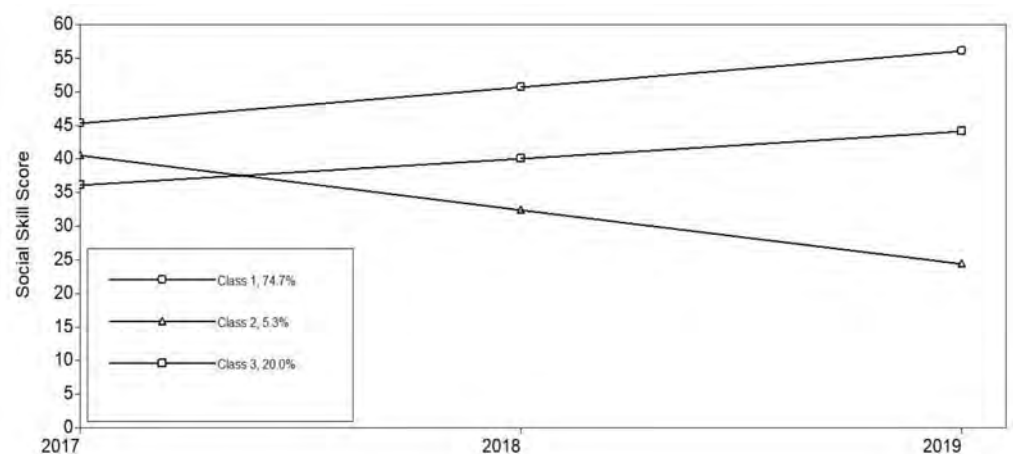


Figure 1. Class trajectories of social skills development.

3.4. Predictors of Identified Trajectories

Table 4 shows the impacts of the predictors for social skill trajectories using multinomial logistic regression. The finding indicated that gender was statistically significant in predicting the trajectories of latent class membership. Girls tended to belong to high-increase class than moderate-increase class as compared to boys ($\beta = 0.845$, $OR = 2.328$, $p < 0.01$). Children whose parents never used spanking and educated children in other ways when children make mistake were more likely to belong to high-increase class than moderate-increase class as compared to those who often did ($\beta = 0.884$, $OR = 2.421$, $p < 0.001$). However, no results were found between high-increase class and decrease class, as well as moderate-increase class and decrease class.

Table 4. Conditional latent class growth model.

| Variable | High-Increase Class vs. Decrease Class | | | Moderate-Increase Class vs. Decrease Class | | | High-Increase Class vs. Moderate-Increase Class | | |
|---------------------|--|-------|-------|--|-------|-------|---|-------|-----------|
| | Estimated | SE | OR | Estimated | SE | OR | Estimated | SE | OR |
| Girls | 0.261 | 0.549 | 1.298 | −0.091 | 0.585 | 0.913 | 0.845 | 0.312 | 2.328 ** |
| Extended family | −0.119 | 0.456 | 0.888 | 0.143 | 0.488 | 1.154 | −0.262 | 0.318 | 0.770 |
| Have siblings | −0.561 | 0.553 | 0.571 | −1.003 | 0.560 | 0.367 | 0.442 | 0.345 | 1.556 |
| Human stimulation | 0.312 | 0.406 | 1.366 | −0.261 | 0.431 | 0.770 | 0.573 | 0.337 | 1.774 |
| Social stimulation | −0.386 | 0.407 | 0.680 | −0.218 | 0.444 | 0.804 | −0.168 | 0.274 | 0.845 |
| Avoid of punishment | 0.559 | 0.381 | 1.749 | −0.325 | 0.409 | 0.723 | 0.884 | 0.247 | 2.421 *** |
| Social support | 0.355 | 0.316 | 1.426 | 0.250 | 0.351 | 1.284 | 0.105 | 0.261 | 1.111 |

Note: ** $p < 0.01$, *** $p < 0.001$.

4. Discussion

This study examined children’s social skills development during the kindergarten period and identified the predictors of this growth trajectory using a latent class growth approach. On average, children social skill in kindergarten increased linearly over time, which is a similar finding to a recent study of multicultural adolescents. In current study, the trajectory of social skill in kindergarten evaluated by latent growth curve model started at 42.943 points in the first year of kindergarten and increased by 8.930 points every year in kindergarten. Given the heterogeneity of longitudinal trajectories of children social skill over time, we found that a 3-class model best described children’s social skills development during this period. The three groups outlined were consistent with a previous study (Takahashi et al. [20]). We also found that three distinct social skills development trajectories high-increase class, moderate-increase class, and decrease class during the kindergarten period. Few studies clarified children social development in kindergarten. The three identified trajectories in this study can help parents, childcare staff and professionals have a better understand the social skill development and pay more attention to children whose social skills are decreasing.

In this study, demographic characteristics and home-rearing environment were explored to predict social skills growth trajectories. Girls were more likely to belong to the “high-increase class,” which is consistent with previous studies in the teacher-rated scale (Chan et al. [11]; Hajovsky et al. [41]). Studies have shown that girls are more likely to possess higher social skills and academic competence, boys have often more problem behaviors, which can approve the results in this study (Gresham and Elliot [32]; Abdi [42]; Mohamed [43]). Gender difference in social skill trajectories can be explained from a social perspective according to social learning theory (Bandura [44]). Once children are identified as belonging to a gender group, reinforcements from adults and peers are applied in different ways when children’s behaviors conform to gender-based expectations (Hajovsky et al. [11]). Teachers may have gendered expectations in the classroom, with girls and boys receiving differing feedback on appropriate classroom behavior (Koch, [45]), children showed different cross-gender toy choice and friends’ selection (Carter and McCloskey [46]). A study also clarified positive and healthy teacher–child relationship and

teacher-children interactions in the classroom is more advantageous for females than males (Mohamed [43]), and may naturally enhance children's classroom engagement and elicit more prosocial children behaviors (Hajovsky et al. [11]). Our study extended the literature with exploring gender difference in the longitudinal social development, and imply girl tend to be in the higher lever social skill class during kindergarten. This finding is essential, as it gave the evidence to the theory and gender difference in distinct social skill growth trajectories. And it also implied more supports, prevention and intervention methods should be provided for boys in kindergarten.

This study indicates that children whose parents avoid punishment tend to be in the "high-increase class." Tompkins and Villaruel [26] found that parental punishment is significantly related to children's social competence through parent-child exchange. This can be explained by several theoretic framework. The moral development theory established by Hoffman [47] asserts that although strong punishment can lead to compliance in young children, it can also produce fear, and obedience is often temporary because children are more concerned with their personal fear and anxiety than with internalizing the message that the behavior is unacceptable. Hence, punishment interferes with children's moral internalization of right behavior and does not foster prosocial behavior because it promotes children to focus on self-concern (Hoffman [48]). In relation to the social learning theory outlined in the introduction, punishment would be adversely or unrelated to social skills because punishment does not provide knowledge about socially competent behavior or model the behaviors we want to see children engage in (Tompkins and Villaruel [26]). According to social control theory, parents' use of harsh punishment, such as corporal punishment, is supposed to inhibit moral internalization by weakening the parent-child attachment link (Gottfredson and Hirschi [49]). Children who lack an attachment bond with their parents will struggle to identify with them and internalize their values as well as those of society, resulting in low self-control and an unwillingness to consider long-term consequences, leading to aggressive, antisocial, delinquent, or criminal behavior. Because they provide for quick and easy fulfillment of desires (Gottfredson and Hirschi, [50,51]; Sampson and Laub [52]; Gershoff [53]). Thus, parental punishment erodes parent-child relationships and reduces a child's motivation to internalize his or her parents' and society's ideals, thereby resulting in poor self-control; this process, in turn, has a negative impact on children's social development (White and Status [54]). This study is the first study that showed the longitudinal effect of parent's punishment on children's social skill growth trajectories in kindergarten, less punishment can contribute to high social skill development in kindergarten. This finding can help parent avoid to use punishment and use others parenting strategies when children make mistakes.

This study sheds new light on the growth patterns and trajectories of social skills during kindergarten, that provides new and unique perspectives for our understanding of the development of social skills with regard to factors such as demographic characteristics and home rearing environment. In addition, it highlights the utility of LCGA in elucidating the heterogeneity in social skills development among Japanese preschoolers; to our knowledge, our study is the first to examine the association between social factors and their predictors among a sample of Japanese kindergarten children using LCGA. The most significant strength of this study is that we provide an understanding for modifying the home-rearing environment, that can enhance the development of social skills during the kindergarten period.

Nevertheless, this study had several limitations. First, this study utilized teachers' reports social skill care, while some studies examine children social skill through parent-rated scale. Both measurements are a single source of information that may not capture children's social skills in other environments. In future studies, we suggest combining these methods for comprehensive measurements. Second, due to the limited sample size and missing rate, the power of the results might be reduced. We suggest that future studies use a larger sample size to identify the growth trajectories of social skills development. Third, although the current study included a number of significant demographic variables

related to social skills, other factors, such as the parents' education level, marital status, and family income, may also have a crucial effect on children's social skills development (Huang et al. [36]). Researchers may be able to learn more about how children's social skills develop in their rating settings by taking these factors into consideration.

5. Conclusions

The current study identified three latent classes with different trajectories of social skills development during the kindergarten period, as well as their associations with demographic characteristics and home-rearing environment. Although the result revealed only 5.3% children in decrease class of social skill development who are more likely to be at risk for future social problems, early identification of problematic social skills development should be paid attention from parents and practitioners. The links between predictors and social skills growth trajectories highlight the importance of observing social skills growth patterns to better perceive and improve the home-rearing environment, and pay more attention to male children. Parents and professionals should focus on improving parental practices to facilitate social skills development among kindergarten children.

Author Contributions: Conceptualization, Y.Z. and X.L.; methodology, Y.Z.; software, Y.Z.; validation, Y.Z., X.L. and D.J.; formal analysis, Y.Z.; investigation, A.A., Z.Z. and M.M.; resources, T.A.; data curation, T.A., E.T. (Emiko Tanaka), E.T. (Etsuko Tomisaki), T.W., and Y.S.; writing—original draft preparation, Y.Z.; writing—review and editing, X.L. and D.J.; visualization, T.A.; supervision, T.A.; project administration, T.A.; funding acquisition, T.A. All authors have read and agreed to the published version of the manuscript.

Funding: This research was funded by Grants-in-Aid for Scientific Research, grant number 21H00790 and 21K18449.

Institutional Review Board Statement: The study was approved by the Ethics Committee of University of Tsukuba (protocol code 1657 and date of approval 21 July 2021).

Informed Consent Statement: Informed consent was obtained from all subjects involved in the study.

Data Availability Statement: Not Applicable.

Acknowledgments: We express our deepest gratitude to the Japan Night Child Care Alliance and all the participants and staff members.

Conflicts of Interest: The authors declare no conflict of interest.

References

1. Gresham, F.M.; Elliott, S.N. Assessment and classification of children's social skills: A review of methods and issues. *Sch. Psychol. Rev.* **1984**, *13*, 292–301.
2. Wentzel, K.R.; Jablansky, S.; Scalise, N.R. Peer social acceptance and academic achievement: A meta-analytic study. *J. Educ. Psychol.* **2021**, *113*, 157–180. [[CrossRef](#)]
3. Hukkelberg, S.; Keles, S.; Ogden, T.; Hammerstrøm, K. The relation between behavioral problems and social competence: A correlational Meta-analysis. *BMC Psychiatry* **2019**, *19*, 354. [[CrossRef](#)] [[PubMed](#)]
4. McIntyre, L.L.; Blacher, J.; Baker, B.L. The transition to school: Adaptation in young children with and without intellectual disability. *J. Intellect. Disabil. Res.* **2006**, *50*, 349–361. [[CrossRef](#)]
5. Arnold, D.; Kupersmidt, J.; Voegler-Lee, M.; Marshall, N. The Association between Preschool Children's Social Functioning and Their Emergent Academic Skills. *Early Child. Res. Q.* **2012**, *27*, 376–386. [[CrossRef](#)]
6. Ali, S. Effect of Social Skills Training Program on Self- Esteem and Aggression among Children in Residential Institutions in Port Said City. *Port Said Sci. J. Nurs.* **2018**, *5*, 105–123.
7. Ke, F.; Whalon, K.; Yun, J. Social Skill Interventions for Youth and Adults With Autism Spectrum Disorder: A Systematic Review. *Rev. Educ. Res.* **2017**, *88*. [[CrossRef](#)]
8. Fabes, R.; Hanish, L.; Martin, C. Children at Play: The Role of Peers in Understanding the Effects of Child Care. *Child Dev.* **2003**, *74*, 1039–1043. [[CrossRef](#)]
9. Lamont, A.; Van Horn, M.L. Heterogeneity in Parent-reported Social Skill Development in Early Elementary School Children. *Soc. Dev.* **2013**, *22*, 384–405. [[CrossRef](#)]

10. Sørli, M.-A.; Hagen, K.; Nordahl, K. Development of social skills during middle childhood: Growth trajectories and school-related predictors. *Int. J. Sch. Educ. Psychol.* **2020**, *8*, 1–19. [[CrossRef](#)]
11. Hajovsky, D.; Caemmerer, J.; Mason, B. Gender Differences in Children’s Social Skills Growth Trajectories. *Appl. Dev. Sci.* **2021**, *25*, 1–16. [[CrossRef](#)]
12. DiDonato, A. New Directions in Social Competence Research: Examining Developmental Trajectories and Language Minority Populations. Ph.D. Thesis, Arizona State University, Tempe, AZ, USA, 2014.
13. Kramer, T.; Caldarella, P.; Christensen, L.; Shatzer, R. Social and Emotional Learning in the Kindergarten Classroom: Evaluation of the Strong Start Curriculum. *Early Child. Educ. J.* **2010**, *37*, 303–309. [[CrossRef](#)]
14. Stright, A.D.; Gallagher, K.C.; Kelley, K. Infant Temperament Moderates Relations Between Maternal Parenting in Early Childhood and Children’s Adjustment in First Grade. *Child Dev.* **2008**, *79*, 186–200. [[CrossRef](#)]
15. Eisenberg, N.; Fabes, R.A. Prosocial development. In *Handbook of Child Psychology: Social, Emotional, and Personality Development*, 5th ed.; John Wiley & Sons, Inc.: Hoboken, NJ, USA, 1998; Volume 3, pp. 701–778.
16. Flynn, E.; Ehrenreich, S.E.; Beron, K.J.; Underwood, M.K. Prosocial Behavior: Long-Term Trajectories and Psychosocial Outcomes. *Soc. Dev.* **2015**, *24*, 462–482. [[CrossRef](#)]
17. Anme, T.; Segal, U.A. Implications for the development of children in over 11 hours of centre-based care. *Child Care Health Dev.* **2004**, *30*, 345–352. [[CrossRef](#)]
18. Anme, T.; Tanaka, E.; Watanabe, T.; Tomisaki, E.; Mochizuki, Y.; Tokutake, K. Validity and Reliability of the Index of Child Care Environment (ICCE). *Public Health Front.* **2013**, *2*, 141–145. [[CrossRef](#)]
19. Ölçer, S.; Aytar, A. A Comparative Study into Social Skills of Five-six Year Old Children and Parental Behaviors. *Procedia Soc. Behav. Sci.* **2014**, *141*, 976–995. [[CrossRef](#)]
20. Takahashi, Y.; Okada, K.; Hoshino, T.; Anme, T. Developmental Trajectories of Social Skills during Early Childhood and Links to Parenting Practices in a Japanese Sample. *PLoS ONE* **2015**, *10*, e0135357. [[CrossRef](#)]
21. Denham, S.A.; Bassett, H.H.; Wyatt, T. The socialization of emotional competence. In *Handbook of Socialization: Theory and Research*, 2nd ed.; The Guilford Press: New York, NY, USA, 2015; pp. 590–613.
22. Parke, R.; Simpkins, S.; McDowell, D.; Kim, M.; Killian, C.; Dennis, J.; Flyr, M.L.; Wild, M.; Rah, Y. Relative contributions of families and peers to children’s social development. In *Handbook of Childhood Social Development*; Blackwell: London, UK, 2002; pp. 156–177.
23. Reich, S.M.; Vandell, D.L. The interplay between parents and peers as socializing influences in children’s development. In *Handbook of Childhood Social Development*, 2nd ed.; Wiley Blackwell: London, UK, 2014; pp. 263–280.
24. El Nokali, N.E.; Bachman, H.J.; Votruba-Drzal, E. Parent involvement and children’s academic and social development in elementary school. *Child Dev.* **2010**, *81*, 988–1005. [[CrossRef](#)]
25. Altschul, I.; Lee, S.J.; Gershoff, E.T. Hugs, Not Hits: Warmth and Spanking as Predictors of Child Social Competence. *J. Marriage Fam.* **2016**, *78*, 695–714. [[CrossRef](#)]
26. Tompkins, V.; Villaruel, E. Parent discipline and pre-schoolers’ social skills. *Early Child Dev. Care* **2020**, *190*. [[CrossRef](#)]
27. Greene, J.O. Models of adult communication skill acquisition: Practice and the course of performance improvement. In *Handbook of Communication and Social Interaction Skills*; Lawrence Erlbaum Associates Publishers: Mahwah, NJ, USA, 2003; pp. 51–91.
28. Jung, T.; Wickrama, K.A.S. An Introduction to Latent Class Growth Analysis and Growth Mixture Modeling. *Soc. Personal. Psychol. Compass* **2008**, *2*, 302–317. [[CrossRef](#)]
29. Anme, T.; Shinohara, R.; Sugisawa, Y.; Tanaka, E.; Watanabe, T.; Hoshino, T. Validity and Reliability of the Social Skill Scale (SSS) as an Index of Social Competence for Preschool Children. *J. Health Sci.* **2013**, *3*, 5–11.
30. Hosokawa, R.; Katsura, T. Marital relationship, parenting practices, and social skills development in preschool children. *Child Adolesc. Psychiatry Ment. Health* **2017**, *11*, 2. [[CrossRef](#)] [[PubMed](#)]
31. Takahashi, Y.; Okada, K.; Hoshino, T.; Anme, T. Social skills of preschoolers: Stability of factor structures and predictive validity from a nationwide cohort study in Japan. *Jpn. J. Educ. Psychol.* **2008**, *56*, 81–92. [[CrossRef](#)]
32. Gresham, F.M.; Elliott, S.N. *Social Skills Rating System*; American Guidance Service: Circle Pines, MI, USA, 1990.
33. Bradley, R.H.; Caldwell, B.M. The HOME Inventory and family demographics. *Dev. Psychol.* **1984**, *20*, 315–320. [[CrossRef](#)]
34. Chen, W.; Tanaka, E.; Watanabe, K.; Tomisaki, E.; Watanabe, T.; Wu, B.; Anme, T. The influence of home-rearing environment on children’s behavioral problems 3 years’ later. *Psychiatry Res.* **2016**, *244*, 185–193. [[CrossRef](#)] [[PubMed](#)]
35. Anderson-Butcher, D.; Martin, E.; Paluta, L.; Gould, D. Patterns of social skill development over-time among clusters of LiFEsports participants. *Child. Youth Serv. Rev.* **2018**, *87*, 17–25. [[CrossRef](#)]
36. Huang, C.-C.; Jin, H.; Zhang, J.; Zheng, Q.; Chen, Y.; Cheung, S.; Liu, C. The effects of an innovative e-commerce poverty alleviation platform on Chinese rural laborer skills development and family well-being. *Child. Youth Serv. Rev.* **2020**, *116*, 105189. [[CrossRef](#)]
37. Sang, S.A.; Nelson, J.A. The effect of siblings on children’s social skills and perspective taking. *Infant Child Dev.* **2017**, *26*, e2023. [[CrossRef](#)]
38. Nagin, D.S. Analyzing developmental trajectories: A semiparametric, group-based approach. *Psychol. Methods* **1999**, *4*, 139–157. [[CrossRef](#)]

39. Zhang, X.; Räsänen, P.; Koponen, T.; Aunola, K.; Lerkkanen, M.-K.; Nurmi, J.-E. Early Cognitive Precursors of Children's Mathematics Learning Disability and Persistent Low Achievement: A 5-Year Longitudinal Study. *Child Dev.* **2020**, *91*, 7–27. [[CrossRef](#)]
40. Van de Schoot, R.; Sijbrandij, M.; Winter, S.D.; Depaoli, S.; Vermunt, J.K. The GRoLTS-Checklist: Guidelines for Reporting on Latent Trajectory Studies. *Struct. Equ. Model.* **2017**, *24*, 451–467. [[CrossRef](#)]
41. Chan, D.; Ramey, S.; Ramey, C.; Schmitt, N. Modeling Intraindividual Changes in Children's Social Skills at Home and at School: A Multivariate Latent Growth Approach to Understanding Between-Settings Differences in Children's Social Skill Development. *Multivar. Behav. Res.* **2000**, *35*, 365–396. [[CrossRef](#)]
42. Abdi, B. Gender differences in social skills, problem behaviours and academic competence of Iranian kindergarten children based on their parent and teacher ratings. *Procedia Soc. Behav. Sci.* **2010**, *5*, 1175–1179. [[CrossRef](#)]
43. Mohamed, A.H.H. Gender as a moderator of the association between teacher–child relationship and social skills in preschool. *Early Child Dev. Care* **2018**, *188*, 1711–1725. [[CrossRef](#)]
44. Bandura, A. *Social Learning Theory*; Prentice-Hall: Oxford, UK, 1977; p. 247.
45. Koch, J. Gender issues in the classroom. In *Handbook of Psychology: Educational Psychology*; John Wiley & Sons Inc.: Hoboken, NJ, USA, 2003; Volume 7, pp. 259–281.
46. Carter, D.B.; Levy, G.D. Cognitive aspects of early sex-role development: The influence of gender schemas on preschoolers' memories and preferences for sex-typed toys and activities. *Child Dev.* **1988**, *59*, 782–792. [[CrossRef](#)]
47. Hoffman, M.L. *Empathy and Moral Development: Implications for Caring and Justice*; Cambridge University Press: New York, NY, USA, 2000; p. 331.
48. Hoffman, M.L. Affective and cognitive processes in moral internalization. *Soc. Cogn. Soc. Dev. A Sociocult. Perspect.* **1983**, 236–274.
49. Gottfredson, M.R.; Hirschi, T. A general theory of adolescent problem behavior: Problems and prospects. In *Adolescent Problem Behaviors: Issues and Research*; Lawrence Erlbaum Associates, Inc.: Hillsdale, NJ, USA, 1994; pp. 41–56.
50. Gottfredson, M.R.; Hirschi, T. *A General Theory of Crime*; Stanford University Press: Palo Alto, CA, USA, 1990; p. 297.
51. Hirschi, T.; Gottfredson, M.R. Control theory and the life-course perspective. *Stud. Crime Crime Prev.* **1995**, *4*, 131–142.
52. Sampson, R.J.; Laub, J.H. Urban poverty and the family context of delinquency: A new look at structure and process in a classic study. *Child Dev.* **1994**, *65*, 523–540. [[CrossRef](#)]
53. Gershoff, E.T. Corporal punishment by parents and associated child behaviors and experiences: A meta-analytic and theoretical review. *Psychol. Bull.* **2002**, *128*, 539–579. [[CrossRef](#)]
54. White, S.O.; Straus, M.A. The implications of family violence for rehabilitation strategies. In *New Directions in the Rehabilitation of Criminal Offenders*; National Academies Press: Washington, DC, USA, 1981; pp. 255–288.

1 SUBMITTED 1 SEP 21
2 REVISION REQ. 27 OCT 21; REVISION RECD. 24 NOV 21
3 ACCEPTED 28 DEC 21
4 **ONLINE-FIRST: JAN 2022**
5 **DOI: <https://doi.org/10.18295/squmj.1.2022.008>**

6
7 **Patterns of Movement Performance Among Japanese Children and Effects**
8 **of Parenting Practices**

9 *Latent class analysis*

10 **Zhu Zhu,^{1,2} Cunyoen Kim,³ Dandan Jiao,¹ Xiang Li,¹ Ammara Ajmal,¹**
11 **Munenori Matsumoto,¹ Yuko Sawada,⁴ Toshiyuki Kasai,⁵ Taeko**
12 **Watanabe,⁶ Etsuko Tomisaki,⁷ Emiko Tanaka,⁸ Sumio Ito,⁹**
13 **Rika Okumura,⁹ *Tokie Anme¹⁰**

14
15 ¹*School of Comprehensive Human Science, University of Tsukuba, Tsukuba, Japan;* ²*Faculty*
16 *of Preschool and Special Education, Xuzhou Kindergarten Teachers College, Xuzhou, China;*
17 ³*School of Education Science, Leshan Normal University, Leshan, China;* ⁴*Faculty of Health*
18 *Medicine, Morinomiya University of Medical Sciences, Osaka, Japan;* ⁵*Faculty of*
19 *Foundational Academics, Miyagi University, Miyagi, Japan;* ⁶*Faculty of Nursing, Shukutoku*
20 *University, Chiba, Japan;* ⁷*Faculty of Nursing and Medical Care, Keio University, Tokyo,*
21 *Japan;* ⁸*Faculty of Nursing, Musashino University, Tokyo, Japan;* ⁹*Department of Public*
22 *Welfare, Tobishima, Aichi, Japan;* ¹⁰*Faculty of Medicine, University of Tsukuba, Tsukuba,*
23 *Japan.*

24 **Corresponding Author's e-mail: anmet@md.tsukuba.ac.jp*

25
26 **Abstract**

27 **Objectives:** The study aimed to examine the long-term effects of parenting practice during
28 preschool years on children's movement performance in primary school. **Methods:** This
29 study involved a three-year longitudinal study including 225 children aged 3–6 years old.
30 Parents reported baseline parenting practice and evaluated children's movement performance
31 three years later. Latent class analysis was used to explore latent classes of movement
32 performance. A post hoc test was used to identify the characteristics of different patterns.

33 Finally, adjusted multinomial logistic regression models were used to test the influence of
34 parenting practice on identified patterns of movement performance. **Results:** Children in this
35 study were grouped into three movement performance patterns, labelled as ‘least difficulties’
36 (58.2%, n = 131), ‘low back pain’ (30.2%, n = 68), and ‘most difficulties’ (11.6%, n = 26).
37 After controlling for age, gender, having siblings or not, family structure, BMI SDS, sleep
38 condition and dietary habits, we found that if parents played games with children frequently,
39 the children would have a 0.287 times lower probability of being in the ‘low back pain’ class,
40 95%CI [0.105, 0.783], and if parents take children to meet peers of a similar age frequently,
41 the children would have a 0.339 times lower probability of being in ‘most difficulties’ class,
42 95%CI [0.139, 0.825]. **Conclusions:** Primary healthcare providers should pay careful
43 attention to children with movement difficulties. The study provides longitudinal evidence to
44 support the applicability of positive parenting practice in early childhood to prevent
45 children’s movement difficulties.

46 **Keywords:** Movement performance; Parenting practice; Latent class analysis; Child;
47 Longitudinal study; Japan.

48

49 **Advances in Knowledge**

- 50 • The study originally used person-centred method to explore three patterns of children’s
51 movement performance in a Japanese community context.
- 52 • This study confirmed the long-term effects of parenting practice during preschool years
53 on children’s movement performance when they enter primary school. We indicated that
54 playing games with children frequently contributed to preventing children from
55 developing low back pain, while taking children to meet peers of a similar age helped in
56 preventing children’s movement difficulties during their school age.

57

58 **Application to Patient Care**

- 59 • Primary healthcare providers should pay special attention to children with movement
60 difficulties. The study provides longitudinal evidence to support the applicability of
61 positive parenting practice in early childhood to prevent children’s movement difficulties.

62

63 **Introduction**

64 Movement performance is defined as the competence or skills related to motor coordination,
65 muscle strength and balance, which are shown in self-care, sport, and other daily activities.¹

66 School aged children need to possess motor skills, coordination, and body control in order to
67 complete daily activities.² Movement difficulties in childhood may reduce a child's
68 participation in daily activities and even impact their quality of life in adulthood.^{3,4} The
69 prevalence of movement difficulties has been rising worldwide recently.⁵ In Oman ($N = 97$;
70 $M_{\text{age}} = 12.9$, $SD = 1.6$), 55% of the total sample developed low grip strength and around 45%
71 were scored low in flexibility and sit-up tests.⁶ National reports in Japan also show a decline
72 in school-aged children's movement performance, particularly among boys, which is at a
73 historically low level.⁷ However, there is no gold standard to measure children's movement
74 performance in existing research.⁸ Therefore, person-oriented cluster analysis might be a
75 possible method to identify the characteristics of movement performance of children in a
76 community.

77

78 Movement performance is determined by complex interactions between biological
79 development and social environment.⁹ Differences are always expected for the movement
80 performance of children in terms of age, gender, body size and lifestyles.¹⁰⁻¹³ Home rearing
81 environment is one of the most important social environments, in which parenting practice
82 affects children directly.¹⁴ Parenting practice refers to the observable behaviours that parents
83 use to socialise their children in daily activities.¹⁵ A cross-sectional study demonstrated that
84 maternal permissive parenting was gender-specifically associated with better PA performance
85 in children experiencing authoritative parenting.¹⁶ However, results were not consistent with
86 the findings of Bradley et al. that indicated high parental monitoring was associated with
87 poorer PA performance for boys experiencing later puberty but increased PA performance in
88 boys experiencing early puberty using longitudinal data.¹⁷ Furthermore, only sixteen of the 30
89 quantitative studies in an integrative review showed significant positive associations between
90 supportive PA parenting and children's physical performance.¹⁸ The majority of studies to
91 date, have focused on the intensity and frequency of PA instead of using health conditions or
92 function status as the outcomes. Limited studies have explored the relationships between
93 parenting practice and movement performance.

94

95 To fill gaps in existing research, the present three-year longitudinal study examined the
96 influence of specific parenting practices for preschool children on patterns of movement
97 performance while school aged. To avoid bias of variable-centred methods, we aimed to
98 investigate (1) the patterns of children's movement performance based on person-oriented

99 cluster analysis and (2) the effects of daily parenting practice on children during the
100 preschool period. We hypothesised that (1) patterns of children's movement performance
101 could be identified using different characteristics in a typical community and (2) more
102 positive stimulations in parenting contribute to preventing children from developing
103 movement difficulties.
104

105 **Methods**

106 *Study design and participants*

107 Our three-year longitudinal research study was part of a cohort study named 'Community
108 Empowerment and Care for well-being and healthy longevity' (CEC), involving all residents
109 in T village, a typical suburban community of Japan with a population of almost 5,000 from
110 1991. The inclusion criteria were as follows: (1) being aged 3–6 years old, (2) living in T
111 village, and (3) having at least one parent living together. The exclusion criteria were as
112 follows: (1) having a disability, serious disease, or developmental delay and (2) not living in
113 T village for the next three years. In the baseline survey, 289 parents with children aged 3–6
114 years provided the information on demographics and parenting practice. After 3 years,
115 children's movement performance was evaluated by parents. As 27 families dropped out of
116 the project and 37 were excluded due to incomplete evaluation of movement performance,
117 the final sample size was 225. All research procedures were reviewed and approved by the
118 institutional review board and ethics committee of [blinded for review]. All participants
119 provided written consent before participation.
120

121 *Measures*

122 *Parenting practice*

123 Parenting practice was measured using the Index of Child Care Environment (ICCE), which
124 has been used in Japanese child cohort study for over 20.^{19,20} ICCE is Japanese questionnaire
125 edition of the globally-used scale called the Home Observation for Measurement of the
126 Environment (HOME) and shows high reliability ($\alpha = 0.891$).²¹
127

128 The ICCE is a self-reported questionnaire for parents, consisting of 13 items regarding
129 parenting practice, which are used independently in the present study. Questions for the 13
130 parenting practices are as follows: (1) How often do you play games with your child? (2)
131 How often do you go shopping with your child? (3) How often do you read to your child? (4)

132 How often do you sing songs with your child? (5) How often do you go to the park with your
133 child? (6) How often do you and your child meet with friends or relatives with children of a
134 similar age? (7) How often do you talk with your spouse about child care? (8) How often
135 does your spouse or other caregiver help you with the child? (9) How often do you and your
136 spouse eat meals together with the child? (10) What do you do if your child spills milk on
137 purpose? (11) How many times did you spank your child last week? (12) Do you have
138 anyone else that helps you with daily home-rearing? (13) Do you have anyone to consult with
139 about child care? Items 1–9 were measured using five-point Likert scale (1 = *rarely*, 2 = *1–3*
140 *times per month*, 3 = *1–2 times per week*, 4 = *3–4 times per week*, 5 = *almost every day*). As
141 the responses were not normally distributed, binary-category classification was used in the
142 analysis based on ICCE manual (Unfavourable group = *the bottom 25% of the total sample*,
143 favourable group = *the rest*). Item 10 had five options (1 = *hit the child*, 2 = *scold the child*, 3
144 = *discipline in another way*, 4 = *determine how to prevent it in the future*, 5 = *in other ways*).
145 Item 11 had five different options (1 = *never*, 2 = *1-2 times*, 3 = *3-4 times*, 4 = *5-6 times*, 5 =
146 *almost every day*). For items 10 and 11, responses were categorised into two groups
147 (unfavourable = *spank children* and favourable = *no spank*). For items 12 and 13, responses
148 were originally measured in a binary manner (i.e., *yes* or *no*), in which the answer ‘*yes*’ was
149 evaluated as favourable and ‘*no*’ was evaluated as unfavourable.

150

151 *Movement performance*

152 Movement performance of children in the present study was investigated using a nine-item
153 parent-reported movement performance questionnaire, which have been used by community
154 government in large scale population-based surveys of the general population in Japan for
155 over 20 years.²² Parents were required to compare their children’s coordination with other
156 children of the same age based on their daily observations after the community government
157 explained evaluation points in detail. The nine items included the following: (1) Does your
158 child always appear energetic before and after school? (Keep active) (2) Are there any
159 difficulties for your child to keep running? (Keep running) (3) Does your child have
160 difficulties maintaining correct sitting posture? (Good sitting posture) (4) Does your child
161 have any arm pain? (Arm strength) (5) Does your child have any lower low back pains? (Low
162 back strength) (6) Does your child have any leg pain? (Leg strength) (7) Are there any
163 difficulties for your child in moving agilely to avoid obstacles? (Agility) (8) Dose your child
164 have any difficulties balancing? (Balance) (9) Does your child have any difficulties moving

165 their body flexibly? (Flexibility). Participants could respond to each item with 'no' (without
166 any difficulties) or 'yes' (having some difficulties).

167

168 *Covariates*

169 Demographics, children's sleep condition, and their dietary habits were considered covariates
170 in the analysis models. Demographics included children's age, gender, BMI (standardised
171 BMI, BMI SDS, was used in the analysis), having siblings or not, and family structure (e.g.,
172 nuclear family type and extended family type). Children's sleep condition was reported by
173 parents as 'sufficient' or 'not sufficient'. Dietary habits were also reported by parents as 'no
174 fussy eating' or 'having fussy eating behaviours'.

175

176 ***Statistical analysis***

177 First, we used descriptive statistics to confirm demographics, baseline condition of parenting
178 practice and follow-up year's movement performance. Second, latent class analysis (LCA)
179 was used to explore patterns of movement performance.²³ Third, A post hoc test for the chi-
180 square test (Bonferroni) and ANOVA analysis (LSD and S-N-K) was used to clarify
181 differences in demographics among the patterns of movement performance and identify the
182 characteristics of the patterns. Finally, adjusted multinomial logistic regression analysis was
183 applied to confirm the associations between parenting practice and movement performance
184 patterns.

185

186 All statistical analyses were performed using SPSS (Version 26.0; SPSS Inc., Chicago, IL)
187 and Mplus (Version 8.0; Muthén and Muthén, Los Angeles, CA, USA).

188 **Results**

189 Table 1 shows descriptive statistic results of demographic background. A total of 225 children
190 (Age: M = 4.13, SD = 0.87; BMI SDS: M = 0.12, SD = 0.98) was even distributed in gender
191 and family structure (boys: n = 119, 52.9%; girls: n = 106, 47.1%; Nuclear family: n = 107,
192 47.6%; Extended family: n = 118, 52.4%), while 83.6% children (n = 188) had siblings.
193 85.8% children (n = 193) had sufficient sleep while 68.9% children (n = 155) had fussy
194 eating behaviours.

195

196 Table 2 shows baseline parenting practice conditions and follow-up year's movement

197 performance of children. In baseline year, the item with most negative evaluations was ‘How
198 many times did you spank your child last week?’, in which 37.8% parents ($n = 85$) reported
199 they had spanked their child in the last week. The item with least negative evaluations was
200 ‘Do you have anyone else help you in daily home-rearing?’, in which only 2.2% parents ($n =$
201 5) reported they took care of children without any help from others. As for the movement
202 performance of children three years’ later, our study showed that more than half of the
203 children were reported to have some difficulties on (1) maintaining right sitting posture ($n =$
204 139, 61.8%), (2) arm strength ($n = 127$, 56.4%), (3) agility ($n = 114$, 50.7%), and (4)
205 flexibility ($n = 163$, 72.4%).

206

207 Table 3 shows the model fit information for five LCA models with two to six latent classes.
208 Akaike information criterion (AIC), Bayesian information criterion (BIC) and sample-
209 adjusted Bayesian information criterion (aBIC) in three-class model decreased sharply than
210 two-class model and the decline scope was the biggest among all the models ($\Delta AIC = -$
211 71.126, $\Delta BIC = -36.965$, $\Delta aBIC = -68.657$). Entropy in three-class model was the highest in
212 all the models (0.935). The smallest sample size of the latent class is just over 25 ($n = 26$).
213 And the three-class model was significantly better than two-class model ($p < 0.01$). Based on
214 model selection recommendations for LCA model, we considered three-class model as the
215 best identified class.

216

217 Table 4 presents the results of the chi-square test and one-way ANOVA analysis, showing
218 demographics and movement performance characteristics of the three latent patterns. There
219 was no significant difference between the demographics of the three movement performance
220 patterns ($p > 0.1$). All the nine items, except flexibility, showed significant differences among
221 three movement performance patterns ($p < 0.05$). The results of post hoc test indicated the
222 number of responses of movement with difficulties in class 3 was significantly greater than
223 that in class 1 among all the nine items, except flexibility ($p < 0.05$). No significant difference
224 between class 2 and class 1 was found in the following categories: keep active, keep running,
225 arm strength, agility, and flexibility. No significant difference between class 2 and class 3 was
226 shown in the following categories: good sitting posture, arm strength, leg strength, and
227 balanced ($p > 0.05$). The number of responses indicating having low back pain in class 2 was
228 significantly greater than that in class 1, but less than that in class 3 ($p < 0.05$). Class 1 was
229 labelled as having the least difficulties (LD), class 2 was labelled as having low back pain

7

230 (LBP), and class 3 was labelled as having the most difficulties (MD). Figure 1 shows the item
231 probability of movement performance without difficulties in LD, LBP, and MD classes. The
232 LD class contained 58.2% ($n = 131$) of the sample and had high probabilities of movement
233 performance without difficulties. The LBP class contained 11.6% ($n = 26$) of the sample, and
234 all samples showed low back pain in the group. The MD class contained 30.2% ($n = 68$) of the
235 sample and had low probabilities of movement performance without difficulties.

236
237 Table 5 show the associations between parenting practice and children's movement
238 performance. In the multinomial logistic regression models, each parenting practice was
239 considered as independent variable respectively, while age, gender, having siblings or not,
240 family structure, BMI SDS, sleep condition and dietary habits were included in the models as
241 covariates. The LD class was used as the reference class to show the effect of positive
242 parenting practice on preventing movement difficulties. Model 1 indicated that if parents
243 played games with children frequently, the children would have a 0.287 times lower
244 probability of being in the LBP class, 95%CI [0.105, 0.783]. Model 2 indicated that if parents
245 take their children to meet peers of a similar age frequently, the children would have a 0.339
246 times lower probability of being in the MD class, 95%CI [0.139, 0.825].

247 248 **Discussion**

249 To the best of the authors' knowledge, this study is the first in Japan to examine the long-term
250 effects of parenting practice in children's preschool period on their movement performance
251 outcomes when they are school age. We originally explored three patterns of children's
252 movement performance and identified their characteristics in a sample of children from a
253 suburban area in central Japan. Based on our longitudinal results, we indicated that more
254 positive stimulations in parenting practice, such as playing games with children frequently
255 and frequently taking children to meet peers of a similar age, contribute to preventing
256 children from developing movement difficulties three years later.

257
258 Several studies have used person-oriented method to explore patterns of movement
259 performance, however, got inconsistent results. Jaakkola et al. investigated PA, sedentary
260 time, perceived competence, motor competence, cardiorespiratory fitness, and muscular
261 fitness in a Finnish elementary school student sample ($N = 491$; $M_{age} = 11.27$, $SD = 0.32$) and
262 labelled three movement profiles as 'at-risk' (37.7%, $n = 185$), 'intermediate' (49.3%, $n =$

242), and 'desirable' (13.0%, $n = 64$).²⁴ Four movement profiles, which were 'poor movers' (27.9%, $n = 129$), 'average movers' (38.4%, $n = 177$), 'skilled movers' (18.9%, $n = 87$), and 'expert movers' (14.8%, $n = 68$), were identified when the performance of leap, throw-catch, jump, push-up, sit-up tests were focused on.²⁵ Our study explored three patterns of children's movement performance and originally identified the characteristics associated with different types of movement difficulties. The biggest cluster, LD (58.2%, $n = 131$), received significantly higher probability of 'no difficulties' than the MD cluster (30.2%, $n = 68$) for all nine items except flexibility. All samples in the LBP cluster (11.6%, $n = 26$) reported having pains in their low back, which was significantly different from the other two clusters. Previous studies highlighted the prevalence of low back pain in school-aged children was 24% in a British sample ($N = 1376$) while it was 22% in an American sample ($N = 1241$) and 51% in a Danish sample ($N = 1395$). This suggests low back pain is an important and relatively common problem in school children.²⁶ Our results are consistent with the existing research and additionally suggested low back pains should also be given attention in Japan.

Many previous studies have indicated parent-related factors, such as parents' attitude towards children's PA, parents' exercise habits, and parenting practice, are associated with children's daily physical activities, and therefore, influence children's motor competence and physical performance.²⁷ A systematic review indicated supporting children to do PA or enrol in PA classes, doing PA together significantly contributed to improving children's physical performance.²⁸ Davison originally created the Activity Support Scale (ACTS) to measure parental support for children's PA and confirmed that providing children with the chance or places to be active, and playing sports with children is beneficial for children to improve their physical activity levels.²⁹ In addition, previous studies also highlighted the important role of peer interactions on children's motor performance.³⁰ One systematic review reported positive influence of peers' support on PA and health outcomes.³¹ Our results are consistent with previous studies and further clarified long-term effects of parenting practice during preschool years on children's movement performance when they entered primary school. We indicated that playing games with preschool children frequently contributes to preventing children from developing back pain three years later; while taking children to meet peers of a similar age is beneficial to the prevention of children's movement difficulties when reaching school age.

On the other hand, children's age, gender, BMI, sleep condition, and dietary habits were not

296 significantly associated with children's movement performance in the current study, which
297 are not consistent with existing research. Boys performed better in 'walking', while girls
298 performed better in 'ball control', and no gender difference were observed in 'running' and
299 'kicking' in a meta-analysis for Japanese preschool children.³² Cardio-respiratory fitness
300 (CRF) and flexibility decreased with increasing age in a sample of 4,903 European children
301 aged 6–11 years.³³ Sleep duration did not have a consistent significant effect on physical
302 fitness while fruit and vegetable intake positively related to physical performance with small
303 effects.³⁴ Inconsistent results suggested influence factors and their effects of movement
304 performance are complex and different across culture.

305
306 Several limitations should be considered when interpreting our results and designing future
307 studies. First, children's movement performance was only measured by parent-reported
308 questionnaires in the present study. Objective tests should be performed to verify the
309 consistency of the results in the future. Second, although we have controlled several
310 covariates, more related factors, such as SES and baseline movement performance, should
311 also be included in the final analysis model. Finally, the sample size was small because of the
312 loss of follow-up.

313 **Conclusions**

314 In conclusion, children in this study were grouped into three movement performance patterns
315 labelled 'least difficulties (LD)', 'low back pain (LBP)', and 'most difficulties (MD)', based
316 on a person-oriented perspective and cluster analysis. The LD group was characterised as
317 having highest probability of having no difficulties for all items, while the MD group was
318 characterised as having lowest probability of having no difficulties. The LBP group was
319 characterised by having all samples in the group develop low back pain. More positive
320 stimulations in parenting practice during preschool years, such as frequently playing games
321 with children and taking children to meet peers of a similar age, contributed to preventing
322 children's movement difficulties when they entered primary school. Children with movement
323 difficulties should be carefully monitored by healthcare providers. Parents' support is
324 beneficial for children to prevent developing movement difficulties. Nevertheless, there is
325 still a great need for more diverse samples and sufficient sample sizes to confirm the results
326 across cultures.

327

328 **Conflict of Interest**

329 The authors declare no conflicts of interest.

330

331 **Funding**

332 Japan Society for the Promotion of Science under Grants-in-Aid for Scientific Research
333 17H02604.

334

335 **Acknowledgement**

336 We express our deepest gratitude to all the participants and staff members of Tobishima for
337 their voluntary participation in this study. The work was also supported by Japan society for
338 the promotion of Science (JSPS) to provide the funding [Grant nos. JP21H00790 and
339 JP21K18449].

340

341 **Authors' Contribution**

342 Conceptualization, Zhu Zhu and Cunyoen Kim; methodology, Zhu Zhu, Dandan Jiao, and
343 Toshiyuki Kasai; software, Yantong Zhu and Xiang Li; validation, Zhu Zhu, Dandan Jiao,
344 Ammara Ajmal, and Munenori Matsumoto; formal analysis, Zhu Zhu; investigation, Dandan
345 Jiao, Xiang Li, Ammara Ajmal, Munenori Matsumoto, Yuko Sawada, Sumio Ito, and Rika
346 Okumura; resources, Tokie Anme; data curation, Dandan, Jiao, Yuko Sawada, Taeko
347 Watanabe, Etsuko Tomisaki, Emiko Tanaka, and Tokie Anme; writing original draft
348 preparation, Zhu Zhu; writing—review and editing, Cunyoen Kim, Dandan Jiao, and Xiang
349 Li; visualization, Tokie Anme; supervision, Tokie Anme; project administration, Tokie Anme;
350 funding acquisition, Tokie Anme. All authors have read and agreed to the published version
351 of the manuscript.

352

353 **References**

- 354 1. Missiuna C, Moll S, King S, King G, Law M. A trajectory of troubles: parents'
355 impressions of the impact of developmental coordination disorder. *Phys Occup Ther*
356 *Pediatr.* 2007; 27(1):81-101.
- 357 2. Holm I, Tveter AT, Aulie VS, Stuge B. High intra- and inter-rater chance variation of the
358 movement assessment battery for children 2, ageband 2. *Res Dev Disabil.* 2013;
359 34(2):795-800.

- 360 3. Kwan MY, Cairney J, Hay JA, Faught BE. Understanding physical activity and
361 motivations for children with developmental coordination disorder: an investigation using
362 the theory of planned behavior. *Res Dev Disabil.* 2013; 34(11):3691-8.
- 363 4. Canto EG, Guillamon AR, Lopez LN. Relationship between overall physical condition,
364 211 motor coordination and perceived quality of life in Spanish adolescents. *Acta Colomb
365 de 212 Psicol* 2021; 24:96–106. <https://doi.org/10.14718/acp.2021.24.1.9>
- 366 5. World Health Organization. Guidelines on physical activity, sedentary behaviour and
367 sleep for children under 5 years of age. From:
368 <https://apps.who.int/iris/handle/10665/311664>. Accessed: Aug 2021.
- 369 6. Kilani H, Alyaarubi S, Zayed K, Alzakwani I, Bererhi H, Shukri R, Alrasadi K. Physical
370 Fitness Attributes, Vitamin D, Depression, and BMD in Omani's Children. *Eur. Sci. J.*
371 2013; 9(30): 156-173.
- 372 7. Japan Sports Agency. The national survey of children's physical fitness, motor 221
373 competence, and physical activity. From: 222
374 https://www.mext.go.jp/sports/content/20191225-spt_sseisaku02-000003330_1.pdf.
375 Accessed: 223 Aug 2021.
- 376 8. Cools W, Martelaer KD, Samaey C, Andries C. Movement skill assessment of typically
377 developing preschool children: a review of seven movement skill assessment tools. *J*
378 *Sports Sci Med.* 2009; 8(2):154-68.
- 379 9. Davids K, Baker J. Genes, environment, and sport performance: why the nature-nurture
380 dualism is no longer relevant. *Sports Med.* 2007; 37(11):961-80.
- 381 10. Johnston LM, Burns YR, Brauer SG, Richardson CA. Differences in postural control and
382 movement performance during goal directed reaching in children with developmental
383 coordination disorder. *Hum Mov Sci.* 2002; 21(5-6):583-601.
- 384 11. Ikeda T, Aoyagi O. Relationships between gender difference in motor performance and
385 age, movement skills and physical fitness among 3- to 6-year-old Japanese children based
386 on effect size calculated by meta-analysis. *School Health* 2009; 5:9-23. doi:
387 10.20812/jash.SH-2009_031
- 388 12. Jaric S. Role of body size in the relation between muscle strength and movement
389 performance. *Exerc. Sport Sci. Rev.* 2003; 31(1): 8-12.
- 390 13. Tyler RPO. Health, Fitness, Lifestyle and Physical Competency of School Children in
391 Wales. Swansea University. 2018; <https://doi.org/10.23889/Suthesis.50798>

- 392 14. Newland LA. Family well-being, parenting, and child well-being: Pathways to healthy
393 adjustment. *Clinical Psychologist*. 2020; 19(1):3-14.
- 394 15. Kahraman H, Yilmaz Irmak T, Basokcu TO. Parenting Practices Scale: Its Validity and
395 Reliability for Parents of School-Aged Children. *Educ. Sci.: Theory Pract*. 2017;
396 17:745–769. doi:10.12738/estp.2017.3.0312
- 397 16. Jago R, Davison KK, Brockman R, Page AS, Thompson JL, Fox KR. Parenting styles,
398 parenting practices, and physical activity in 10- to 11-year olds. *Prev Med*. 2011;
399 52(1):44-7.
- 400 17. Bradley RH, McRitchie S, Houts RM, Nader P, O'brien M. Parenting and the decline of
401 physical activity from age 9 to 15. *Int. J. Behav. Nutr. Phys. Act*. 2011; 8(1): 1-10.
- 402 18. Hutchens A, Lee RE. Parenting Practices and Children's Physical Activity: An Integrative
403 Review. *J Sch Nurs*. 2018;34(1):68-85.
- 404 19. Anme T, Tanaka E, Watanabe T, Tomisaki E, Mochizuki Y, Tokutake K. Validity and
405 reliability of the Index of Child Care Environment (ICCE). *Public Health Front* 2013; 2:
406 141–5 <https://doi.org/10.5963/PHF0203003>
- 407 20. Chen W, Tanaka E, Watanabe K, Tomisaki E, Watanabe T, Wu B, Anme T. The influence
408 of home-rearing environment on children's behavioral problems 3 years' later.
409 *Psychiatry Res*. 2016; 244:185–193.
- 410 21. Bradley RH, Caldwell BM. The HOME Inventory and family demographics. *Dev*.
411 *Psychol*. 1984; 20:315–320.
- 412 22. Anme T. Empowerment for Healthy Longevity–Effective Utilization as Skills for Care
413 Prevention and Health Promotion (in Japanese). Tokyo, Japan: Ishiyaku Publishers, Inc.,
414 2007. P. 42-55.
- 415 23. Lanza ST, Cooper BR. Latent class analysis for developmental research. *Child Dev*
416 *Perspect* 2016; 10: 59–64. <https://doi.org/10.1111/cdep.12163>
- 417 24. Jaakkola T, Yli-Piipari S, Stodden DF, Huhtiniemi M, Salin K, Seppälä S, et al.
418 Identifying childhood movement profiles and tracking physical activity and sedentary
419 time across 1 year. *Transl. Sports Med*. 2020;3(5):480-7.
- 420 25. Jaakkola T, Hakkarainen A, Grasten A, Sipinen E, Vanhala A, Huhtiniemi M, et al.
421 Identifying childhood movement profiles and comparing differences in mathematical
422 skills between clusters: A latent profile analysis. *J Sports Sci*. 2021;39(21): 2503-2508.
- 423 26. Watson KD, Papageorgiou AC, Jones GT, Taylor S, Symmons DP, Silman AJ,
424 Macfarlane, GJ. Low back pain in schoolchildren: occurrence and characteristics. *Pain*

- 425 2002; 97(1-2): 87-92.
- 426 27. Newland LA. Family well-being, parenting, and child well-being: Pathways to healthy
427 adjustment. *Clinical Psychologist*. 2020;19(1):3-14.
- 428 28. Sleddens EF, Kremers SP, Hughes SO, Cross MB, Thijs C, De Vries NK, et al. Physical
429 activity parenting: a systematic review of questionnaires and their associations with
430 child activity levels. *Obes Rev*. 2012; 13(11):1015-33.
- 431 29. Davison, K. Activity-related support from parents, peers and siblings and adolescents'
432 physical activity: are there gender differences? *J. Phys. Activ. Health* 2004; 1: 363–376.
- 433 30. Herrmann C, Bretz K, Khnis J, Seelig H, Keller R, Ferrari I. Connection between social
434 relationships and basic motor competencies in early childhood. *Children* 2021; 8:10.
435 <https://doi.org/10.3390/children8010053>
- 436 31. Jenkinson KA, Naughton G, Benson AC. Peer-assisted learning in school physical
437 education, sport and physical activity programmes: A systematic review. *Phys Educ
438 Sport Pedagogy* 2014; 19: 253–77. <https://doi.org/10.1080/17408989.2012.754004>
- 439 32. Ikeda T, Aoyagi O. Relationships between gender difference in motor performance and
440 age, movement skills and physical fitness among 3-to 6-year-old Japanese children
441 based on effect size calculated by meta-analysis[J]. *School Health*, 2009, 5: 9-23.
- 442 33. Zaqout M, Vyncke K, Moreno LA, De Miguel-Etayo P, Lauria F, Molnar D, et al.
443 Determinant factors of physical fitness in European children. *Int J Public Health*.
444 2016;61(5):573-82.
- 445 34. Jaikaew R, Satiansukpong N. Movement performance and movement difficulties in
446 typical school-aged children. *PLoS One*. 2021; 16(4): e0249401.

Table 1: Demographic background in the baseline year

| | | N = 225 | |
|---------------------------------|-----------------|------------------------|------|
| Variables | Categories | N | % |
| Age of child (years) | | 4.13±0.87 ^a | |
| Gender of child | Boy | 119 | 52.9 |
| | Girl | 106 | 47.1 |
| Siblings | Only child | 37 | 16.4 |
| | Having siblings | 188 | 83.6 |
| Family structure | Nuclear family | 107 | 47.6 |
| | Extended family | 118 | 52.4 |
| BMI SDS of child | | 0.12±0.98 ^a | |
| Sleep condition of child | Sufficient | 193 | 85.8 |
| | Not sufficient | 32 | 14.2 |
| Fussy eating behaviour of child | No | 70 | 31.1 |
| | Yes | 155 | 68.9 |

Note: ^a Mean and SD were shown for continuous variables.

Table 2: Parenting practice in baseline year and movement performance of children three years' later

| | | N = 225 | |
|---|------------|---------|------|
| Items | Categories | n | % |
| Parenting practice | | | |
| Play games with child | Few | 44 | 19.6 |
| | Frequently | 181 | 80.4 |
| Shopping with child | Few | 21 | 9.3 |
| | Frequently | 204 | 90.7 |
| Read books to child | Few | 56 | 24.9 |
| | Frequently | 169 | 75.1 |
| Sing songs with child | Few | 45 | 20.0 |
| | Frequently | 179 | 79.6 |
| | NA | 1 | 0.4 |
| Take child to play outside | Few | 27 | 12.0 |
| | Frequently | 197 | 87.6 |
| | NA | 1 | 0.4 |
| Take child to meet peers of similar age | Few | 46 | 20.5 |
| | Frequently | 178 | 79.1 |
| | NA | 1 | 0.4 |
| Eat meals together with child | Few | 48 | 21.4 |
| | Frequently | 176 | 78.2 |
| | NA | 1 | 0.4 |
| Spank child for mistakes | Spank | 14 | 6.3 |
| | Not spank | 210 | 93.3 |
| | NA | 1 | 0.4 |
| Spank child last week | Spank | 85 | 37.8 |
| | Not spank | 138 | 61.3 |
| | NA | 2 | 0.9 |
| Take care of child with others | Few | 18 | 8.0 |
| | Frequently | 204 | 90.7 |
| | NA | 3 | 1.3 |
| Talk with spouse about child | Few | 50 | 22.3 |
| | Frequently | 174 | 77.3 |
| | NA | 1 | 0.4 |
| Have helpers | No | 5 | 2.2 |
| | Yes | 218 | 96.9 |
| | NA | 2 | 0.9 |
| Have someone to consult with | No | 7 | 3.1 |
| | Yes | 216 | 96.0 |
| | NA | 2 | 0.9 |
| Movement performance | | | |

| | | | |
|----------------------|----------------------|-----|------|
| Keep active | With difficulties | 69 | 30.7 |
| | Without difficulties | 156 | 69.3 |
| Keep running | With difficulties | 62 | 27.6 |
| | Without difficulties | 163 | 72.4 |
| Good sitting posture | With difficulties | 139 | 61.8 |
| | Without difficulties | 86 | 38.2 |
| Arm strength | With difficulties | 127 | 56.4 |
| | Without difficulties | 98 | 43.6 |
| Low back strength | With difficulties | 59 | 26.2 |
| | Without difficulties | 166 | 73.8 |
| Leg strength | With difficulties | 54 | 24.0 |
| | Without difficulties | 171 | 76.0 |
| Agility | With difficulties | 114 | 50.7 |
| | Without difficulties | 111 | 49.3 |
| Balanced | With difficulties | 94 | 41.8 |
| | Without difficulties | 131 | 58.2 |
| Flexibility | With difficulties | 163 | 72.4 |
| | Without difficulties | 62 | 27.6 |

447 *Note: NA = No answer*

Accepted

Table 3: Model fit information for the LCA models

| | Log-likelihood | df | G-squared | AIC | BIC | aBIC | Entropy | BLRT |
|-------------------|----------------|-----|-----------|----------|----------|----------|---------|-------|
| Two-class model | -1112.676 | 492 | 381.606 | 2263.352 | 2328.258 | 2268.043 | 0.827 | <0.01 |
| Three-class model | -1067.113 | 481 | 278.509 | 2192.226 | 2291.293 | 2199.386 | 0.935 | <0.01 |
| Four-class model | -1036.648 | 471 | 217.222 | 2151.296 | 2284.524 | 2160.925 | 0.903 | <0.01 |
| Five-class model | -1018.885 | 462 | 194.023 | 2135.769 | 2303.158 | 2147.867 | 0.921 | <0.01 |
| Six-class model | -1009.066 | 452 | 174.386 | 2136.133 | 2337.683 | 2150.700 | 0.935 | 0.122 |

Note: *df*=degrees of freedom; *AIC*=Akaike information criteria; *BIC*=Bayesian information criteria; *aBIC*=adjusted Bayesian information criteria; *BLRT*= Bootstrapped Likelihood Ratio Test

Table 4: Demographics and movement performance characteristics of three patterns

| Variables | Categories | Movement performance | | | | | | F/c ² | p |
|----------------------|----------------------|----------------------|------|-------------------|------|-----------------|------|------------------|-------|
| | | Class1 | | Class 2 | | Class 3 | | | |
| | | n | % | n | % | n | % | | |
| Age | | 4.13±0.87 | | | | | | 2.112 | 0.123 |
| Gender | Boy | 65 | 54.6 | 14 | 11.8 | 40 | 33.6 | 1.533 | 0.465 |
| | Girl | 66 | 62.3 | 12 | 11.3 | 28 | 26.4 | | |
| Siblings | Single child | 23 | 62.2 | 4 | 10.8 | 10 | 27.0 | 0.289 | 0.865 |
| | Having siblings | 108 | 57.4 | 22 | 11.7 | 58 | 30.9 | | |
| Family structure | Nuclear family | 61 | 57.0 | 11 | 10.3 | 35 | 32.7 | 0.757 | 0.685 |
| | Extended family | 70 | 59.3 | 15 | 12.7 | 33 | 28.0 | | |
| BMISDS | | 0.12±0.98 | | | | | | 0.389 | 0.678 |
| Sleep | Sufficient | 19 | 59.4 | 3 | 9.4 | 10 | 31.3 | 0.175 | 0.916 |
| | Not sufficient | 112 | 58.0 | 23 | 11.9 | 58 | 30.1 | | |
| Fussy eating | No | 93 | 60.0 | 17 | 11.0 | 45 | 29.0 | 0.653 | 0.721 |
| | Yes | 38 | 54.3 | 9 | 12.9 | 23 | 32.9 | | |
| Keep active | With difficulties | 21 _a | 30.4 | 5 _a | 7.2 | 43 _b | 62.3 | 48.721 | 0.000 |
| | Without difficulties | 110 | 70.5 | 21 | 13.5 | 25 | 16.0 | | |
| Keep running | With difficulties | 15 _a | 24.2 | 4 _a | 6.5 | 43 _b | 69.4 | 62.315 | 0.000 |
| | Without difficulties | 116 | 71.2 | 22 | 13.5 | 25 | 15.3 | | |
| Good sitting posture | With difficulties | 66 _a | 47.5 | 20 _b | 14.4 | 53 _b | 38.1 | 17.254 | 0.000 |
| | Without difficulties | 65 | 75.6 | 6 | 7.0 | 15 | 17.4 | | |
| Arm strength | With difficulties | 59 _a | 46.5 | 16 _{a,b} | 12.6 | 52 _b | 40.9 | 18.300 | 0.000 |
| | Without difficulties | 72 | 73.5 | 10 | 10.2 | 16 | 16.3 | | |
| Low back strength | With difficulties | 12 _a | 20.3 | 20 _b | 33.9 | 27 _c | 45.8 | 60.649 | 0.000 |
| | Without difficulties | 119 | 71.7 | 6 | 3.6 | 41 | 24.7 | | |

| | | | | | | | | | |
|--------------|----------------------|-----------------|------|-------------------|------|-----------------|------|--------|-------|
| Leg strength | With difficulties | 15 _a | 27.8 | 14 _b | 25.9 | 25 _b | 46.3 | 30.083 | 0.000 |
| | Without difficulties | 116 | 67.8 | 12 | 7.0 | 43 | 25.1 | | |
| Agility | With difficulties | 47 _a | 41.2 | 15 _{a,b} | 13.2 | 52 _b | 45.6 | 30.090 | 0.000 |
| | Without difficulties | 84 | 75.7 | 11 | 9.9 | 16 | 14.4 | | |
| Balanced | With difficulties | 42 _a | 44.7 | 16 _b | 17.0 | 36 _b | 38.3 | 12.743 | 0.002 |
| | Without difficulties | 89 | 67.9 | 10 | 7.6 | 32 | 24.4 | | |
| Flexibility | With difficulties | 95 _a | 58.3 | 18 _a | 11.0 | 50 _a | 30.7 | 0.175 | 0.916 |
| | Without difficulties | 36 | 58.1 | 8 | 12.9 | 18 | 29.0 | | |

450 *Note: a, b refers different groups based on the results of Post hoc test using Bonferroni method.*

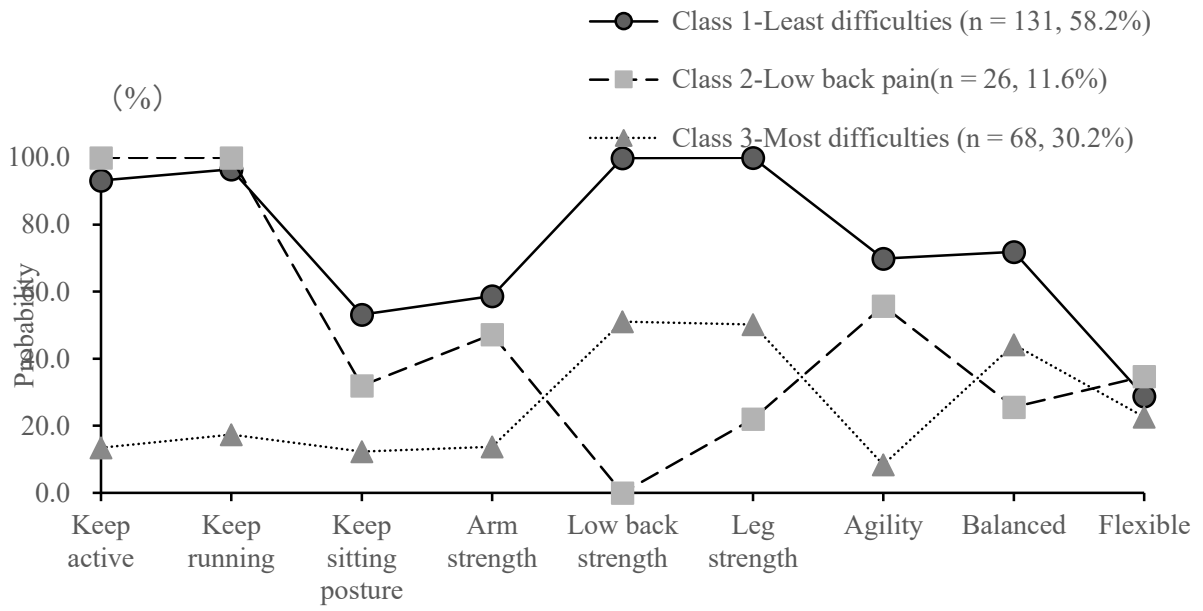
451 **Table 5:** Significant results of multinomial logistic regression model showing associations
 452 between parenting practice and movement performance

| Variables | LBP class vs. LD class | | | | MD class vs. LD class | | | | |
|---|------------------------|---------------|--|----------|-----------------------|---------------|--|----------|--|
| | OR | 95%CI | | <i>p</i> | OR | 95%CI | | <i>p</i> | |
| | Model 1 | | | | | | | | |
| Play games with child | 0.287 | 0.105 - 0.783 | | 0.015 | 0.834 | 0.371 - 1.873 | | 0.660 | |
| Age | 0.860 | 0.499 - 1.480 | | 0.585 | 1.389 | 0.965 - 1.998 | | 0.077 | |
| Gender | 1.101 | 0.453 - 2.674 | | 0.833 | 1.491 | 0.804 - 2.764 | | 0.205 | |
| Having siblings or not | 0.543 | 0.141 - 2.092 | | 0.375 | 0.847 | 0.362 - 1.984 | | 0.702 | |
| Family structure | 0.773 | 0.315 - 1.901 | | 0.575 | 1.166 | 0.634 - 2.147 | | 0.621 | |
| BMI SDS | 0.997 | 0.616 - 1.612 | | 0.989 | 0.957 | 0.695 - 1.316 | | 0.785 | |
| Sleep condition | 0.961 | 0.245 - 3.777 | | 0.955 | 1.144 | 0.475 - 2.759 | | 0.764 | |
| Fussy eating | 0.914 | 0.349 - 2.393 | | 0.855 | 0.843 | 0.436 - 1.631 | | 0.613 | |
| | Model 2 | | | | | | | | |
| Take child to meet peers of a similar age | 1.175 | 0.443 - 3.115 | | 0.746 | 0.339 | 0.139 - 0.825 | | 0.017 | |
| Age | 0.936 | 0.552 - 1.586 | | 0.806 | 1.401 | 0.973 - 2.019 | | 0.070 | |
| Gender | 1.006 | 0.419 - 2.413 | | 0.990 | 1.399 | 0.745 - 2.627 | | 0.296 | |
| Having siblings or not | 0.634 | 0.169 - 2.378 | | 0.499 | 0.837 | 0.357 - 1.964 | | 0.682 | |
| Family structure | 0.880 | 0.367 - 2.110 | | 0.774 | 1.155 | 0.626 - 2.134 | | 0.645 | |
| BMI SDS | 1.085 | 0.681 - 1.728 | | 0.732 | 0.941 | 0.685 - 1.294 | | 0.710 | |
| Sleep condition | 0.853 | 0.220 - 3.300 | | 0.818 | 1.117 | 0.459 - 2.718 | | 0.807 | |
| Fussy eating | 0.921 | 0.356 - 2.385 | | 0.865 | 0.878 | 0.450 - 1.712 | | 0.703 | |

453 *Note: 1. Reference group: play games with child = few, encourage child to play with peers of*
 454 *a similar age = few, gender = boy, having siblings or not = only child, family structure =*
 455 *nuclear family, sleep = sufficient, fussy eating = no fussy eating behaviours, age, BMI SDS =*
 456 *continuous variables.*

457 *2. LD = least difficulties, LBP = low back pain, MD = most difficulties*

458 **Figure 1:** Item probability of movement performance without difficulties in three classes.



459

Accepted A

日中笹川医学奨学金制度(学位取得コース)評価書

課程博士：指導教官用



第 42 期

研究者番号： G4203

作成日 □ 2022 年 3 月 11 日

| | | | | | | |
|-----------|--|------|----|--|------|--------------|
| 氏名 | Zhang Bihang | 張 碧航 | 性別 | F | 生年月日 | 1994. 03. 19 |
| 所属機関(役職) | 中南大学湘雅医院整形重建外科(大学院生) | | | | | |
| 研究先(指導教官) | 自治医科大学外科学講座(吉村 浩太郎教授) | | | | | |
| 研究テーマ | 幹細胞培養上清成分を用いた再生医療の開発 The Role of Adipose-derived Stem/Stromal Cell Concentrated Conditioned Medium (ASC-CCM) in Regenerative Medicine | | | | | |
| 専攻種別 | <input type="checkbox"/> 論文博士 | | | <input checked="" type="checkbox"/> 課程博士 | | |

研究者評価(指導教官記入欄)

| 成績状況 | (優) 良 可 不可 学業成績係数= | 取得単位数 |
|---------------|--|--------------------------|
| | | 取得単位数 23 / 取得すべき単位数総数 23 |
| 学生本人が行った研究の概要 | 1) 毛包由来幹細胞を用いた上皮化再生医療の開発 2) 放射線障害に対する脂肪幹細胞浄化濃縮培養上清の効能 | |
| 総合評価 | 【良かった点】 1) 着実に研究を進めている 2) 自ら情報や論文を検索することができる | |
| | 【改善すべき点】 1) 日本語能力 | |
| | 【今後の展望】 1) おおむね予定通りに進めることができる | |
| 学位取得見込 | 2024 年 3 月 | |
| 評価者(指導教官名) | | 吉村浩太郎 |

日中笹川医学奨学金制度(学位取得コース)報告書 研究者用



第42期

研究者番号: G4203

作成日: 2022年3月1日

| | | | | | |
|-----------|--|--------------------------|------|-------------------------------------|-------------------|
| 氏名 | Zhang Bihang | 張 碧航 | 性別 | F | 生年月日 1994. 03. 19 |
| 所属機関(役職) | 中南大学湘雅医院整形重建外科(大学院生) | | | | |
| 研究先(指導教官) | 自治医科大学外科学講座(吉村 浩太郎教授) | | | | |
| 研究テーマ | 幹細胞培養上清成分を用いた再生医療の開発 - 放射線皮膚障害マウスの創傷治癒に対する幹細胞培養上清の効果に関する研究 The Role of Adipose-derived Stem/Stromal Cell Conditioned Medium (ASC-CM) in Regenerative Medicine: Irradiated Chronic Wound Healing with ASC-CM Application | | | | |
| 専攻種別 | 論文博士 | <input type="checkbox"/> | 課程博士 | <input checked="" type="checkbox"/> | |

1. 研究概要(1)

1) 目的(Goal)

1. To investigate an optimum and effective ASCs' culture medium without xenogeneic serum in lower cost. It is expected that the usage of culture medium without xenogeneic serum, which is widely used in ASCs culture but not biosafe for clinical use due to its potential risks of disease transmission and immune reaction, would be more biosafe for clinical use. However, the commercial medium without xenogeneic serum nowadays is sold at a high price, which would cost a lot if the mass production of CM is applied. Thus, an optimum and effective ASCs' culture medium without serum in lower cost is needed.

2. Radiation therapy has been important treatment for treating and preventing cancer growth and recurrence for many years. However, the clinical use of therapy with irradiation always resulted in devitalized tissue and impaired wound healing, such as ischemia, fibrosis, and atrophy, which puzzles both patients and doctors. Thus, it is necessary to investigate a novel and effective therapy for irradiated and impaired wound healing.

3. To investigate the effect of ASC-CM *in vitro* and its effects on irradiated chronic wound healing animal models *in vivo*, compared with basic culture medium, ASCs and healthy control group.

4. To characterize the exact contents and concentrations of the effective factors in the ASC-CM, and try to explain their underlying mechanism in wound healing and tissue regeneration.

5. The amount of culture supernatant that is discarded daily around the world is enormous. What if the discarded media can be reused and applied into regenerative medicine, the benefits will be numerous. Besides, it can be applied into allograft for no cell substances. Since the production and storage are simple with no need to maintain cell viability, it can be administrated directly when emergency needs arise. Thus, this is an epoch-making research plan from the viewpoint of ecology and reusing waste.

2) 戦略(Approach)

1. To investigate an optimum and effective ASCs' culture medium without serum in lower cost. The basic culture media of DMEM/F12 of ASCs are supplemented with different effective factors, such as human platelet lysate (hPL), IGF, bFGF and PDGF. And the function of supplemented medium is compared with commercial culture medium by the proliferation assay of ASCs, ELISA of growth factors, and so on.

2. To evaluate the effects of ASC-CM *in vitro*.

The *in vitro* effects of purified and concentrated CM on wound healing are investigated by the proliferation assay of fibroblasts and keratinocytes.

3. To investigate the effects of ASC-CM on irradiated chronic would healing animal models *in vivo*.

3) 材料と方法(Materials and methods)

1. Isolation and culture of hASCs, fibroblasts and keratinocytes:

Cells were primary isolated from fat tissue or skin tissue harvested from surgery and cultured as described previously.

2. The ELISA testing:

The ASC-CM are collected and the concentrations of growth factors and cytokines are measured using sandwich ELISA kits according to the manufacturer's instructions.

3. The proliferation assay of fibroblasts and keratinocytes:

The fibroblasts and keratinocytes are seeded in plates respectively and cultured with correspondingly appropriate culture medium. After overnight attachment, the cells are incubated in the medium containing the ASC-CM for 72 hours. The cell number is measured by the CCK-8 assay kit.

1. 研究概要(2)

Absorbance is measured at 450nm using a microplate reader to represent the proliferation of fibroblasts and keratinocytes. All the experiments need to be performed in triplicate.

4. In vivo wound healing models:

Only mice's full-thickness dorsal skin (with whole-body protection) was exposed to radiation as described previously and waited for 6 months before wounding to simulate chronic radiation tissue damage. Five mice (healthy control group) did not receive radiation and waited 6 months too.

Then mice were wounded with cutaneous defects and treated with ASC-CM, ASCs, basic culture medium to investigate its effects in wound healing, tissue regeneration and angiogenesis.

5. Histological examinations:

28 days after wounding, these mice are sacrificed and the skin around the wounds are harvested. Skin samples are fixed in 4% formalin, embedded in paraffin, and sectioned. The sections are subjected to Hematoxylin and Eosin (H&E) staining and immunohistochemistry staining for the analysis of the epithelialization, collagenization, and angiogenesis of wounds.

4) 実験結果 (Results)

1. The ASCs can be cultured well in DMEM/F12 with hPL and growth factor supplements.
2. The ASC-CM collected from above culture medium contains high concentrations of growth factors and cytokines like HGF, KGF, VEGF and so on.
3. The ASC-CM can improve the proliferations of fibroblasts and keratinocytes.
4. The ASC-CM can improve irradiated chronic wound healing significantly.
5. The vWF and CD-34 expression are higher in ASC-CM application group.

5) 考察 (Discussion)

The ASCs can be cultured well in DMEM/F12 with hPL and growth factor supplements, which do not contain xenogeneic serum with relatively lower cost when applied to mass production of CM. And the harvested CM contained high concentrations of growth factors and cytokines like HGF, KGF, VEGF, which were proved to enhance wound healing and tissue regeneration.

The in vitro assays showed that ASC-CM can improve wound healing via fibroblasts and keratinocytes proliferations. And the in vivo experiments proved that it can improved irradiation impaired chronic wound healing. And it can be concluded that the ASC-CM can improve irradiated impaired wound healing via the epithelialization, collagenization, and angiogenesis of wounds.

6) 参考文献 (References)

1. Weller CD, Team V, Sussman G. First-Line Interactive Wound Dressing Update: A Comprehensive Review of the Evidence. *Frontiers in pharmacology*. 2020;11:155.
2. Las Heras K, Igartua M, Santos-Vizcaino E, Hernandez RM. Chronic wounds: Current status, available strategies and emerging therapeutic solutions. *Journal of controlled release : official journal of the Controlled Release Society*. 2020;328:532-550.
3. Lombardi F, Palumbo P, Augello FR, Cifone MG, Cinque B, Giuliani M. Secretome of Adipose Tissue-Derived Stem Cells (ASCs) as a Novel Trend in Chronic Non-Healing Wounds: An Overview of Experimental In Vitro and In Vivo Studies and Methodological Variables. *Int J Mol Sci*. 2019;20(15).
4. L PK, Kandoi S, Misra R, S V, K R, Verma RS. The mesenchymal stem cell secretome: A new paradigm towards cell-free therapeutic mode in regenerative medicine. *Cytokine & growth factor reviews*. 2019;46:1-9.
5. Park SR, Kim JW, Jun HS, Roh JY, Lee HY, Hong IS. Stem Cell Secretome and Its Effect on Cellular Mechanisms Relevant to Wound Healing. *Molecular therapy : the journal of the American Society of Gene Therapy*. 2018;26(2):606-617.
6. Vizoso FJ, Eiro N, Cid S, Schneider J, Perez-Fernandez R. Mesenchymal Stem Cell Secretome: Toward Cell-Free Therapeutic Strategies in Regenerative Medicine. *Int J Mol Sci*. 2017;18(9).
7. Kichenbrand C, Velot E, Menu P, Moby V. Dental Pulp Stem Cell-Derived Conditioned Medium: An Attractive Alternative for Regenerative Therapy. *Tissue engineering Part B, Reviews*. 2019;25(1):78-88.
8. Sagaradze G, Grigorieva O, Nimiritsky P, et al. Conditioned Medium from Human Mesenchymal Stromal Cells: Towards the Clinical Translation. *Int J Mol Sci*. 2019;20(7).

2. 執筆論文 Publication of thesis ※記載した論文を添付してください。Attach all of the papers listed below.

| | | | | | | |
|---------------------------|--|---|------------------------|-----------|---|-----------------------|
| 論文名 1 Title | Adipose-Derived Stem Cell Conditioned Medium and Wound Healing: A Systematic Review. | | | | | |
| 掲載誌名 Published journal | Tissue Engineering Part B Review (Ahead of Print) | | | | | |
| | 年 | 月 | 巻(号) | 頁 ~ | 頁 | 言語 Language |
| 第1著者名 First author | Zhang Bihang | | 第2著者名 Second author | Wu Yunyan | | 第3著者名 Third author |
| その他著者名 Other authors | Yoshimura Kotaro (Corresponding Author) | | | | | |
| 論文名 2 Title | | | | | | |
| 掲載誌名 Published journal | | | | | | |
| | 年 | 月 | 巻(号) | 頁 ~ | 頁 | 言語 Language |
| 第1著者名 First author | | | 第2著者名 Second author | | | 第3著者名 Third author |
| その他著者名 Other authors | | | | | | |
| 論文名 3 Title | | | | | | |
| 掲載誌名 Published journal | | | | | | |
| | 年 | 月 | 巻(号) | 頁 ~ | 頁 | 言語 Language |
| 第1著者名 First author | | | 第2著者名 Second author | | | 第3著者名 Third author |
| その他著者名 Other authors | | | | | | |
| 論文名 4 Title | | | | | | |
| 掲載誌名 Published journal | | | | | | |
| | 年 | 月 | 巻(号) | 頁 ~ | 頁 | 言語 Language |
| 第1著者名 First author | | | 第2著者名 Second author | | | 第3著者名 Third author |
| その他著者名 Other authors | | | | | | |
| 論文名 5 Title | | | | | | |
| 掲載誌名 Published journal | | | | | | |
| | 年 | 月 | 巻(号) | 頁 ~ | 頁 | 言語 Language |
| 第1著者名 First author | | | 第2著者名 Second author | | | 第3著者名 Third author |
| その他著者名 Other authors | | | | | | |

3. 学会発表 Conference presentation ※筆頭演者として総会・国際学会を含む主な学会で発表したものを記載してください。

※Describe your presentation as the principal presenter in major academic meetings including general meetings or international meetings

| | | | | | |
|-----------------------|------------------------------------|--|-------------|------------------------------|--|
| 学会名 Conference | | | | | |
| 演題 Topic | | | | | |
| 開催日 date | 年 | 月 | 日 | 開催地 venue | |
| 形式 method | <input type="checkbox"/> 口頭発表 Oral | <input type="checkbox"/> ポスター発表 Poster | 言語 Language | <input type="checkbox"/> 日本語 | <input type="checkbox"/> 英語 <input type="checkbox"/> 中国語 |
| 共同演者名 Co-presenter | | | | | |
| 学会名 Conference | | | | | |
| 演題 Topic | | | | | |
| 開催日 date | 年 | 月 | 日 | 開催地 venue | |
| 形式 method | <input type="checkbox"/> 口頭発表 Oral | <input type="checkbox"/> ポスター発表 Poster | 言語 Language | <input type="checkbox"/> 日本語 | <input type="checkbox"/> 英語 <input type="checkbox"/> 中国語 |
| 共同演者名 Co-presenter | | | | | |
| 学会名 Conference | | | | | |
| 演題 Topic | | | | | |
| 開催日 date | 年 | 月 | 日 | 開催地 venue | |
| 形式 method | <input type="checkbox"/> 口頭発表 Oral | <input type="checkbox"/> ポスター発表 Poster | 言語 Language | <input type="checkbox"/> 日本語 | <input type="checkbox"/> 英語 <input type="checkbox"/> 中国語 |
| 共同演者名 Co-presenter | | | | | |
| 学会名 Conference | | | | | |
| 演題 Topic | | | | | |
| 開催日 date | 年 | 月 | 日 | 開催地 venue | |
| 形式 method | <input type="checkbox"/> 口頭発表 Oral | <input type="checkbox"/> ポスター発表 Poster | 言語 Language | <input type="checkbox"/> 日本語 | <input type="checkbox"/> 英語 <input type="checkbox"/> 中国語 |
| 共同演者名 Co-presenter | | | | | |

4. 受賞(研究業績) Award (Research achievement)

| | | | | |
|------------------|--------------|---------------|---|---|
| 名称 Award name | 国名 | 受賞年 | 年 | 月 |
| | Country name | Year of award | | |
| 名称 Award name | 国名 | 受賞年 | 年 | 月 |
| | Country name | Year of award | | |

5. 本研究テーマに関わる他の研究助成金受給 Other research grants concerned with your research theme

| | |
|--------------------------|---|
| 受給実績 Receipt record | <input type="checkbox"/> 有 <input type="checkbox"/> 無 |
| 助成機関名称 Funding agency | |
| 助成金名称 Grant name | |
| 受給期間 Supported period | 年 月 ~ 年 月 |
| 受給額 Amount received | 円 |
| 受給実績 Receipt record | <input type="checkbox"/> 有 <input type="checkbox"/> 無 |
| 助成機関名称 Funding agency | |
| 助成金名称 Grant name | |
| 受給期間 Supported period | 年 月 ~ 年 月 |
| 受給額 Amount received | 円 |

6. 他の奨学金受給 Another awarded scholarship

| | |
|---------------------------|---|
| 受給実績 Receipt record | <input type="checkbox"/> 有 <input type="checkbox"/> 無 |
| 助成機関名称 Funding agency | |
| 奨学金名称 Scholarship name | |
| 受給期間 Supported period | 年 月 ~ 年 月 |
| 受給額 Amount received | 円 |

7. 研究活動に関する報道発表 Press release concerned with your research activities

※記載した記事を添付してください。Attach a copy of the article described below

| | | | |
|--------------------------|---|--------------------------|--|
| 報道発表 Press release | <input type="checkbox"/> 有 <input type="checkbox"/> 無 | 発表年月日 Date of release | |
| 発表機関 Released medium | | | |
| 発表形式 Release method | ・新聞 ・雑誌 ・Web site ・記者発表 ・その他() | | |
| 発表タイトル Released title | | | |

8. 本研究テーマに関する特許出願予定 Patent application concerned with your research theme

| | | | |
|----------------------------------|---|----------------------------|--|
| 出願予定 Scheduled | <input type="checkbox"/> 有 <input type="checkbox"/> 無 | 出願国 Application country | |
| 出願内容(概要) Application contents | | | |

9. その他 Others

| |
|--|
| |
|--|

指導責任者(記名) 吉村 浩太郎

日中笹川医学奨学金制度(学位取得コース)評価書

課程博士:指導教官用




第 42 期 研究者番号: G4205

作成日 : 2022 年 3 月 日

| | | | | | | |
|-----------|--|-----|----|--|------|--------------|
| 氏名 | Liu Xiao | 劉 霄 | 性別 | F | 生年月日 | 1989. 10. 09 |
| 所属機関(役職) | 慶應義塾大学医学部眼科(大学院生) | | | | | |
| 研究先(指導教官) | 慶應義塾大学医学部・医学研究科眼科学教室(根岸 一乃教授) | | | | | |
| 研究テーマ | 東アジア人における ABCA4 関連網膜症の臨床的・分子遺伝学的調査 Clinical and genetic Investigation of ABCA4-associated Retinal Disorder in East Asian population | | | | | |
| 専攻種別 | <input type="checkbox"/> 論文博士 | | | <input checked="" type="checkbox"/> 課程博士 | | |

研究者評価(指導教官記入欄)

| 成績状況 | (優) 良 可 不可 学業成績係数=優 | 取得単位数 |
|--|--|-------|
| | | |
| 学生本人が行った研究の概要 | 東アジア人における ABCA4 関連網膜症の臨床的・分子遺伝学的調査研究において、中国人・日本人コホートを構築し、臨床情報の解析・分子遺伝学的情報の解析を行った。さらに、視力、視野、網膜画像、電気生理学的検査を含む臨床情報と病源性・遺伝型などの遺伝情報についての関連解析、並びに他民族との比較検討解析を行い、ABCA4 バリエントの世界的な分布を解明した。 | |
| 総合評価 | 【良かった点】 眼科臨床情報、遺伝情報の基礎から臨床情報についての解析を主体的に取り組み、他施設の眼科臨床医、遺伝学者、遺伝情報学者と密に連携をとりながら、研究業務を遂行した。在学期間中に第一著者として5報の英文論文をインパクトの高い国際雑誌にて発表しており、研究成果を世界へむけて発信できている。 | |
| | 【改善すべき点】 今回東アジア人データの集積を行う中で、東アジア内での疾患分布や原因バリエントが地域的に異なる事が明らかになった。民族の小分類や移動の経緯を含め、「遺伝的浮動」を検討・考慮する事が、更なる遺伝背景の理解、同一疾患内の遺伝的異質性(allelic heterogeneity)の解明につながると考える。 | |
| | 【今後の展望】 中東アジア人全体でのコホート研究の成果を、RNA 治療やコンパウンド治療等のバリエント毎の個別化医療に活かす事で、地球規模での治療導入の実現が望まれる。 | |
| 学位取得見込 | 2022年3月 学位取得見込 | |
| 評価者(指導教官名) 根岸 一乃 (印)  | | |

日中笹川医学奨学金制度(学位取得コース)中間報告書 研究者用



第42期

研究者番号: G4205

作成日: 2022年02月08日

| | | | | | | |
|-----------|--|--------------------------|------|-------------------------------------|------|--------------|
| 氏名 | Liu Xiao | 劉 霄 | 性別 | F | 生年月日 | 1989. 10. 09 |
| 所属機関(役職) | 慶應義塾大学医学部眼科(大学院生) | | | | | |
| 研究先(指導教官) | 慶應義塾大学医学部・医学研究科眼科学教室(根岸 一乃教授) | | | | | |
| 研究テーマ | 東アジア人におけるABCA4関連網膜症の臨床的・分子遺伝学的調査 Clinical and Genetic Investigation of <i>ABCA4</i> -associated Retinal Disorder in East Asian population | | | | | |
| 専攻種別 | 論文博士 | <input type="checkbox"/> | 課程博士 | <input checked="" type="checkbox"/> | | |

1. 研究概要(1)

1) 目的(Goal)

Inherited Retinal Disease (IRD) have become one of the leading causes of blindness in advanced countries and the *ABCA4*-retinopathy (*ABCA4*-RD) is thought to be the most common inherited macular dystrophy while the available effective treatments are limited(1-4). The purpose of this study is to intensively investigate the clinical and genetic features in East Asian patients with *ABCA4*-RD.

2) 戦略(Approach)

- Collect the clinical and genetic data of the patients with *ABCA4*-RD from China and Japan.
- Analyse the phenotype and genotype of the patients with *ABCA4*-RD.
- Investigate an association between the phenotype and genotype.
- Compare the East Asian features to the Europeans to figure out the similarities/differences.

3) 材料と方法(Materials and methods)

The patients with multiple pathogenic *ABCA4* variants or with one *ABCA4* variant and classical phenotype were recruited. Advanced technologies in retinal imaging capabilities, including fundus autofluorescence (FAF) and spectral-domain optical coherence tomography (SD-OCT), as well as psychophysical testing methods such as microperimetry, electrophysiological examination, etc. were applied, offering new possibilities to identify biomarkers for severity/progression.

For the genetic data, genetic screening in the *ABCA4* gene was performed by utilising whole exome sequencing with target analysis, target enrichment-based exome sequencing, and direct sequencing. Molecular genetic analysis was performed for the detected variants with prediction software and public databases.

Comparison analysis of prevalent *ABCA4* variants was performed among ethnicities utilising the resources of thousands of patients from the other continents, to identify the geographical distribution of pathogenic variants.

4) 実験結果(Results)

Forty-two unrelated patients with *ABCA4*-RD mostly originating from Western China were recruited. Comprehensive ophthalmological examinations, including visual acuity measurements, fundus photography, FAF imaging, and full-field electroretinography, were performed. Next-generation sequencing (target/whole exome) and direct sequencing were conducted. Genotype grouping was performed based on the presence of deleterious variants. The median age of onset/age was 10.0 (5-52)/29.5 (12-72) years, and the median visual acuity in the right/left eye was 1.30 (0.15-2.28)/1.30 (0.15-2.28) in the logarithm of the minimum angle of resolution unit. Ten patients (10/38, 27.0%) showed confined macular dysfunction, and 27 (27/37, 73.7%) had generalized retinal dysfunction. Fifty-eight pathogenic/likely pathogenic *ABCA4* variants, including 14 novel variants, were identified. Eight patients (8/35, 22.8%) harbored multiple deleterious variants, and 17 (17/35, 48.6%) had a single deleterious variant. Prevalent variants in total were c.101_106del (p.Ser34_Leu35del) (allele frequency of 6%); c.2894A>G (p.Asn965Ser) (allele frequency of 4%); c.6563T>G (p.Phe2188Ser) (allele frequency of 4%); and c.2424C>G (p.Tyr808Ter) (allele frequency of 3%). Significant associations were revealed between subjective functional, retinal imaging, and objective functional groups, identifying a significant genotype-phenotype association.

Thirty-three affected subjects from 29 Japanese families with *ABCA4*-RD were recruited. The median age/age of onset was 29.0/9.0 years (range, 7.0-85.0/2.0-70.0). The best corrected median visual acuity in the logarithm of the minimum angle of resolution unit in the right/left eye was 0.7(0.0-2.28)/ 0.76 (-0.18-2.28). There were 23 patients with available ffERG; 11 (11/23, 47.8%) in ERG group 1, 4 (4/23, 17.4%) in ERG group 2, and 8(8/23, 34.8%) in ERG group 3. 34 disease causing/associated variants were identified, including 7 novel variants. The three most prevalent variants are c.1760+2T>G (16.7%), c.6445C>T, p.Arg2149Ter (5.0%), and c.869G>A, p.Arg290Gln (5.0%). 24 probands with multiple pathogenic *ABCA4* variants were identified; 9 (9/24, 37.5%) in Genotype group A, 9 (9/24, 37.5%) in Genotype group B, and 6 (6/24, 25.0%) in Genotype group C. The distribution of Genotype Groups A/B/C of the European dominated and Chinese cohorts was 5.7%/44.4%/49.8% and 22.2%/47.2%/30.6%, which revealed a significant difference of genotype based on each ethnic group (P<0.001).

1. 研究概要(2)

5) 考察(Discussion)

a) This study is the first to comprehensively reveal the demographic, morphological, and functional features of patients with STGD1 in a large molecularly confirmed cohort, which enabled an elucidation of the genotype–phenotype association in the East Asian population.

b) The median onset in Chinese cohort (10.0 years) and Japanese cohort (9.0 years) was earlier than that in the large prospective international *ABCA4*–RD (STGD1) cohort (21.8 years for the retrospective cohort and 22.3 years for the prospective cohort in the ProgStar studies) or the other reports from Europe(5–8).

c) The three most prevalent variants detected in the two East Asian cohorts were completely different from the three most prevalent variants (c.5882G>A (p.Gly1961Glu); c.2588G>C (p.Gly863Ala); and c.5461–10T>C) in the ProgStar study(9).

d) There are several limitations in this study. First, selection bias at recruitment related to disease severity should be inherent since it is difficult to collect data from genetically affected subjects with good vision who do not visit clinics/hospitals. Second, this cross–sectional retrospective case series study did not include longitudinal data; thus, prospective natural history studies in a larger cohort could provide more accurate information on the disease severity and progression of *ABCA4*–RD. Third, the molecular mechanisms of disease causation for most variants have been unclear, and the clinical effects of variants are not perfectly understood. Further functional analysis is required to conclude the disease causation of each variant. Fourth, due to the limited number of subjects, statistical analysis to investigate correlations between the clinical parameters and the particular variants (or genotype groups) were not available in the current study. Last, the number of our patients was too small to draw conclusions about the genotype–phenotype associations in such a heterogeneous disease.

6) 参考文献(References)

1. Stargardt K. Über familiäre, progressive Degeneration in der Maculagegend des Auges. Graefe's Archive for Clinical and Experimental Ophthalmology. 1909;71(3):534–50.
2. Allikmets R, Singh N, Sun H, Shroyer NF, Hutchinson A, Chidambaram A, Gerrard B, Baird L, Stauffer D, Peiffer A. A photoreceptor cell–specific ATP–binding transporter gene (ABCR) is mutated in recessive Stargardt macular dystrophy. Nature genetics. 1997;15(3):236.
3. Anna P, Strauss RW, Fujinami K, Michaelides M. Stargardt disease: clinical features, molecular genetics, animal models and therapeutic options. Br J Ophthalmol. 2017;101(1):25–30.
4. Fujinami–Yokokawa Y, Pontikos N, Yang L, Tsunoda K, Yoshitake K, Iwata T, Miyata H, Fujinami K, Japan Eye Genetics Consortium obo. Prediction of Causative Genes in Inherited Retinal Disorders from Spectral–Domain Optical Coherence Tomography Utilizing Deep Learning Techniques. Journal of Ophthalmology. 2019;2019:1691064.
5. Fujinami K, Zernant J, Chana RK, Wright GA, Tsunoda K, Ozawa Y, Tsubota K, Webster AR, Moore AT, Allikmets R. *ABCA4* gene screening by next–generation sequencing in a British cohort. Investigative ophthalmology & visual science. 2013;54(10):6662–74.
6. Zahid S, Jayasundera T, Rhoades W, Branham K, Khan N, Niziol LM, Musch DC, Heckenlively JR. Clinical phenotypes and prognostic full–field electroretinographic findings in Stargardt disease. Am J Ophthalmol. 2013;155(3):465–73 e3.
7. Fujinami K, Singh R, Carroll J, Zernant J, Allikmets R, Michaelides M, Moore AT. Fine central macular dots associated with childhood–onset Stargardt Disease. Acta ophthalmologica. 2014;92(2):e157.
8. Strauss RW, Ho A, Munoz B, Cideciyan AV, Sahel JA, Sunness JS, Birch DG, Bernstein PS, Michaelides M, Traboulsi EI, et al. The Natural History of the Progression of Atrophy Secondary to Stargardt Disease (ProgStar) Studies: Design and Baseline Characteristics: ProgStar Report No. 1. Ophthalmology. 2016;123(4):817–28.
9. Fujinami K, Strauss RW, Chiang JP, Audo IS, Bernstein PS, Birch DG, Bomotti SM, Cideciyan AV, Ervin AM, Marino MJ, et al. Detailed genetic characteristics of an international large cohort of patients with Stargardt disease: ProgStar study report 8. Br J Ophthalmol. 2019;103(3):390–7.

2. 執筆論文 Publication of thesis ※記載した論文を添付してください。Attach all of the papers listed below.

| | | | | | | |
|---------------------------|--|------------------------|------------------|-----------------------|----------------|--|
| 論文名 1 Title | Oguchi disease caused by a homozygous novel <i>SAG</i> splicing alteration associated with the multiple evanescent white dot syndrome: A 15-month follow-up | | | | | |
| 掲載誌名 Published journal | Documenta Ophthalmologica | | | | | |
| | 2020 年 4 月 | 141(3) 巻(号) | 217 頁 ~ 226 頁 | 言語 Language | English | |
| 第1著者名 First author | Xiao Liu,Lixia Gao | 第2著者名 Second author | Gang Wang | 第3著者名 Third author | Yanling Long | |
| その他著者名 Other authors | Jiayun Ren, Kaoru Fujinami, Xiaohong Meng, Shiyong Li | | | | | |
| 論文名 2 Title | Clinical and Genetic Characteristics of 15 Affected Patients From 12 Japanese Families with <i>GUCY2D</i> -Associated Retinal Disorder | | | | | |
| 掲載誌名 Published journal | Translational Vision Science & Technology | | | | | |
| | 2020 年 5 月 | 9(6) 巻(号) | 2:01 頁 ~ 2:19 頁 | 言語 Language | English | |
| 第1著者名 First author | Xiao Liu, Kaoru Fujinami | 第2著者名 Second author | Kazuki Kuniyoshi | 第3著者名 Third author | Mineo Kondo | |
| その他著者名 Other authors | Shinji Ueno, Takaaki Hayashi, Kiyofumi Mochizuki, Shuhei Kameya, Lizhu Yang, Yu Fujinami-Yokokawa, Gavin Arno, Nikolas Pontikos, Hiroyuki Sakuramoto, Taro Kominami, Hiroko Terasaki, Satoshi Katagiri, Kei Mizobuchi, Natsuko Nakamura, Kazutoshi Yoshitake, Yozo Miyake1, Shiyong Li, Toshihide Kurihara, Kazuo Tsubota, Takeshi Iwata, Kazushige Tsunoda, Japan Eye Genetics Consortium Study Group | | | | | |
| 論文名 3 Title | Clinical and genetic characteristics of Stargardt disease in a large Western China cohort: Report 1 | | | | | |
| 掲載誌名 Published journal | American Journal of Medical Genetics Part C Seminars in Medical Genetics | | | | | |
| | 2020 年 8 月 | 184(3) 巻(号) | 694 頁 ~ 707 頁 | 言語 Language | English | |
| 第1著者名 First author | Xiao Liu | 第2著者名 Second author | Xiaohong Meng | 第3著者名 Third author | Lizhu Yang | |
| その他著者名 Other authors | Yanling Long, Yu Fujinami-Yokokawa, Jiayun Ren, Toshihide Kurihara, Kazuo Tsubota, Kazushige Tsunoda, Kaoru Fujinami, Shiyong Li | | | | | |
| 論文名 4 Title | RP2-associated retinal disorder in a Japanese cohort: report of novel variants and a literature review, identifying a genotype-phenotype association | | | | | |
| 掲載誌名 Published journal | American Journal of Medical Genetics Part C Seminars in Medical Genetics | | | | | |
| | 2020 年 8 月 | 184(3) 巻(号) | 675 頁 ~ 693 頁 | 言語 Language | English | |
| 第1著者名 First author | Kaoru Fujinami, Xiao Liu | 第2著者名 Second author | Shinji Ueno | 第3著者名 Third author | Atsushi Mizota | |
| その他著者名 Other authors | Kei Shinoda, Kazuki Kuniyoshi, Yu Fujinami-Yokokawa, Lizhu Yang, Gavin Arno, Nikolas Pontikos, Shuhei Kameya, Taro Kominami, Hiroko Terasaki, Hiroyuki Sakuramoto, Natsuko Nakamura, Toshihide Kurihara, Kazuo Tsubota, Yozo Miyake, Kazutoshi Yoshiake, Takeshi Iwata, Kazushige Tsunoda, Japan Eye Genetics Consortium Study Group | | | | | |
| 論文名 5 Title | Long-term follow-up of a Chinese patient with <i>KCNV2</i> -retinopathy | | | | | |
| 掲載誌名 Published journal | OPHTHALMIC GENETICS | | | | | |
| | 2021 年 4 月 | 42(2) 巻(号) | 144 頁 ~ 149 頁 | 言語 Language | English | |
| 第1著者名 First author | Hongxuan Lie, Gang Wang, Xiao Liu | 第2著者名 Second author | Xiaohong Meng | 第3著者名 Third author | Yanling Long | |
| その他著者名 Other authors | Yanling Long, Jiayun Ren, Lizhu Yang, Yu Fujinami-Yokokawa, Toshihide Kurihara, Kazuo Tsubota, Kaoru Fujinami, Shiyong Li | | | | | |

3. 学会発表 Conference presentation ※筆頭演者として総会・国際学会を含む主な学会で発表したものを記載してください。

※Describe your presentation as the principal presenter in major academic meetings including general meetings or international meetings.

| | | | |
|-----------------------|---|-------------|--|
| 学会名 Conference | The 58th Annual Symposium of the International Society for Clinical Electrophysiology of Vision (ISCEV) | | |
| 演題 Topic | Oguchi disease Licaused by a homozygous novel <i>SAG</i> splicing alteration associated with the multiple evanescent white dot syndrome: A 15-month follow-up | | |
| 開催日 date | 2020 年 9 月 14 日 | 開催地 venue | Virtual. Les Iles-de-la-Madeleine, Québec, Canada |
| 形式 method | <input type="checkbox"/> 口頭発表 Oral <input checked="" type="checkbox"/> ポスター発表 Poster | 言語 Language | <input type="checkbox"/> 日本語 <input checked="" type="checkbox"/> 英語 <input type="checkbox"/> 中国語 |
| 共同演者名 Co-presenter | Lixia, Gao, Jiayun Ren, Xiaohong Meng, Yu Fujinami-Yokokawa, Lizhu Yang, Kaoru Fujinami, Shiyong Li | | |
| 学会名 Conference | 第68回日本臨床視覚電気生理学会 | | |
| 演題 Topic | Electrophysiological characteristics of Stargardt disease in a large Western China cohort | | |
| 開催日 date | 2020 年 9 月 20 日 | 開催地 venue | Virtual, Tokyo, Japan |
| 形式 method | <input checked="" type="checkbox"/> 口頭発表 Oral <input type="checkbox"/> ポスター発表 Poster | 言語 Language | <input type="checkbox"/> 日本語 <input checked="" type="checkbox"/> 英語 <input type="checkbox"/> 中国語 |
| 共同演者名 Co-presenter | Xiaohong Meng, Lizhu Yang, Yanling Long, Yu Fujinami-Yokokawa, Jiayun Ren, Toshihide Kurihara, Kazuo Tsubota, Kazushige Tsunoda, Kaoru Fujinami, Shiyong Li | | |
| 学会名 Conference | The 2nd Symposium of East Asia Inherited Retinal Disease Society (EAIRDs) | | |
| 演題 Topic | Clinical and genetic characteristics of Stargardt disease in a large Western China cohort: report 1 | | |
| 開催日 date | 2020 年 11 月 14 日 | 開催地 venue | Virtual, Tokyo, Japan |
| 形式 method | <input checked="" type="checkbox"/> 口頭発表 Oral <input type="checkbox"/> ポスター発表 Poster | 言語 Language | <input type="checkbox"/> 日本語 <input checked="" type="checkbox"/> 英語 <input type="checkbox"/> 中国語 |
| 共同演者名 Co-presenter | Xiaohong Meng, Lizhu Yang, Yanling Long, Yu Fujinami-Yokokawa, Jiayun Ren, Toshihide Kurihara, Kazuo Tsubota, Kazushige Tsunoda, Kaoru Fujinami, Shiyong Li | | |
| 学会名 Conference | The 14th Joint Meeting of Japan-China-Korea Ophthalmologists | | |
| 演題 Topic | Clinical and genetic characteristics of Stargardt disease in a large Western China cohort: report 1 | | |
| 開催日 date | 2021 年 11 月 27 日 | 開催地 venue | Virtual, Japan |
| 形式 method | <input type="checkbox"/> 口頭発表 Oral <input checked="" type="checkbox"/> ポスター発表 Poster | 言語 Language | <input type="checkbox"/> 日本語 <input checked="" type="checkbox"/> 英語 <input type="checkbox"/> 中国語 |
| 共同演者名 Co-presenter | Xiaohong Meng, Lizhu Yang, Yanling Long, Yu Fujinami-Yokokawa, Jiayun Ren, Toshihide Kurihara, Kazuo Tsubota, Kazushige Tsunoda, Kaoru Fujinami, Shiyong Li | | |

4. 受賞(研究業績) Award (Research achievement)

| | | | |
|------------------|---|-------|----------------------|
| 名称 Award name | Best Yong Investigator Award (2nd East Asia Inherited Retinal Disease Society symposium) | | |
| | 国名 Country name | Japan | 受賞年 Year of award |
| 名称 Award name | 2020 Keio Ophthalmology best graduate student | | |
| | 国名 Country name | Japan | 受賞年 Year of award |
| 名称 Award name | Youth Science Investigator Award (3rd Chinese Eye Genetics Consortium) | | |
| | 国名 Country name | China | 受賞年 Year of award |

5. 本研究テーマに関わる他の研究助成金受給 Other research grants concerned with your research theme

| | |
|--------------------------|--|
| 受給実績 Receipt record | <input type="checkbox"/> 有 <input checked="" type="checkbox"/> 無 |
| 助成機関名称 Funding agency | |
| 助成金名称 Grant name | |
| 受給期間 Supported period | 年 月 ~ 年 月 |
| 受給額 Amount received | 円 |
| 受給実績 Receipt record | <input type="checkbox"/> 有 <input checked="" type="checkbox"/> 無 |
| 助成機関名称 Funding agency | |
| 助成金名称 Grant name | |
| 受給期間 Supported period | 年 月 ~ 年 月 |
| 受給額 Amount received | 円 |

6. 他の奨学金受給 Another awarded scholarship

| | |
|---------------------------|--|
| 受給実績 Receipt record | <input checked="" type="checkbox"/> 有 <input type="checkbox"/> 無 |
| 助成機関名称 Funding agency | 慶應義塾大学 |
| 奨学金名称 Scholarship name | 慶應義塾大学院医学研究科博士課程奨学金 |
| 受給期間 Supported period | 2019 年 6 月 ~ 2020 年 6 月 |
| 受給額 Amount received | 1,000,000 円 |

7. 研究活動に関する報道発表 Press release concerned with your research activities

※記載した記事を添付してください。Attach a copy of the article described below

| | | | |
|--------------------------|--|--------------------------|--|
| 報道発表 Press release | <input type="checkbox"/> 有 <input checked="" type="checkbox"/> 無 | 発表年月日 Date of release | |
| 発表機関 Released medium | | | |
| 発表形式 Release method | ・新聞 ・雑誌 ・Web site ・記者発表 ・その他() | | |
| 発表タイトル Released title | | | |

8. 本研究テーマに関する特許出願予定 Patent application concerned with your research theme

| | | | |
|----------------------------------|--|--------------------|--|
| 出願予定 Scheduled application | <input type="checkbox"/> 有 <input checked="" type="checkbox"/> 無 | 出願国 Application | |
| 出願内容(概要) Application contents | | | |

9. その他 Others

| |
|--|
| |
|--|

指導責任者(署名) 根岸 一乃





Oguchi disease caused by a homozygous novel *SAG* splicing alteration associated with the multiple evanescent white dot syndrome: A 15-month follow-up

Xiao Liu · Lixia Gao · Gang Wang · Yanling Long · Jiayun Ren ·
Kaoru Fujinami · Xiaohong Meng · Shiyong Li

Received: 8 December 2019 / Accepted: 31 March 2020
© Springer-Verlag GmbH Germany, part of Springer Nature 2020

Abstract

Purpose We report a 15-month follow-up case on a Chinese patient with Oguchi disease associated with the multiple evanescent white dot syndrome (MEWDS).

Methods The patient's clinical presentation and follow-up visits were documented via decimal best-corrected visual acuity, fundus photography, fundus autofluorescence (FAF) imaging, near-infrared FAF, spectral domain optical coherence tomography,

Humphrey's visual fields, microperimetry, and multi-focal electroretinography. We also performed whole exome sequencing for screening variation in the patient and her relatives.

Results The patient had typical clinical characteristic of Oguchi disease, including night blindness, the Mizuo–Nakamura phenomenon (a golden yellow discoloration of the fundus that disappears in the prolonged dark adaptation [DA]) and typical full-field electroretinogram changes (nearly undetected b-wave in 0.01 and 0.03 ERGs that can partially recover only after prolonged DA). Aside from Oguchi disease, the

Co-first authors: Xiao Liu and Lixia Gao

X. Liu · L. Gao · G. Wang · Y. Long · J. Ren ·
X. Meng (✉) · S. Li (✉)
Southwest Hospital/Southwest Eye Hospital, Third
Military Medical University (Army Medical University),
No. 30 Gaotanyan Street Shapingba District, Chongqing,
China
e-mail: cqwmwm@163.com

S. Li
e-mail: shiyong_li@126.com

X. Liu · L. Gao · G. Wang · Y. Long · J. Ren ·
X. Meng · S. Li
Key Lab of Visual Damage and Regeneration &
Restoration of Chongqing, Chongqing, China

X. Liu
Laboratory of Visual Physiology, Division for Vision
Research, National Institute of Sensory Organs, National
Hospital Organization, Tokyo Medical Center, Tokyo,
Japan

X. Liu · K. Fujinami
Department of Ophthalmology, Keio University School of
Medicine, Tokyo, Japan

K. Fujinami
Department of Genetics, UCL Institute of Ophthalmology,
London, UK

K. Fujinami
Division of Inherited Eye Diseases, Moorfields Eye
Hospital, London, UK

patient was also diagnosed with the MEWDS based on clinical detections, including suddenly reduced visual acuity, appeared white dots, blurred ellipsoid zone and disrupted interdigitation zone, enlarged blind spot, and reduced macular sensitivity. A series of investigations revealed that along with the 15-month follow-up after onset, the visual acuity enhanced, the numerous white dots disappeared, and the macular structure returned to normal. Moreover, the novel homozygous splicing alteration c.181 + 1G > A was identified in the *SAG* gene.

Conclusions This work is the first long-term case study of a patient with Oguchi disease associated with the MEWDS. The recovery period of symptoms caused by the MEWDS was much longer than that in typical patients with MEWDS. Molecular genetics demonstrate that this is the first case of Oguchi disease caused by splicing alterations in the *SAG* gene.

Keywords Oguchi disease · MEWDS · Longitudinal follow-up · Electroretinogram · Optical coherence tomography

Introduction

Oguchi disease (MIM # 258100) is a rare autosomal recessive form of congenital stationary night blindness, first described in 1907 [1]. It is characterized by a tapetal-like fundus discoloration after dark adaptation (DA), called the Mizuo–Nakamura phenomenon, along with characteristic electroretinographic (ERG) abnormalities [2, 3]. Two genes, namely *SAG* (s-antigen; OMIM: 181031) and *GRK1* (G protein-coupled receptor kinase 1; OMIM: 180381), have been reported to be associated with Oguchi disease. *SAG* encodes arrestin, which forms a complex with phosphorylated rhodopsin, preventing the further interaction of the activated rhodopsin during transduction. *GRK1* encodes rhodopsin kinase that recognizes photoactivated rhodopsin and desensitizes rhodopsin to receive new light stimuli [4]. The multiple evanescent white dot syndrome (MEWDS) is a unilateral chorioretinitis that affects young women in the third and fourth decades of life; it is characterized with multiple small subretinal white dots, extending from the posterior pole to the midperiphery and associated with a self-healing capacity in a few

weeks or months [5, 6]. In this study, we report a 15-month follow-up case of Oguchi disease caused by novel *SAG* splicing alterations (novel variant) associated with MEWDS.

Methods

Patient recruitment

The patient and her relatives, who were also studied upon, gave informed consent for all procedures described here and the publication of this case study. The procedures used were approved by the local ethics committee of Southwest Eye Hospital, Third Military Medical University (Army Medical University), Chongqing, China (reference number: 73981486-2), and all procedures were performed in accordance with the Declaration of Helsinki.

Clinical investigation

Detailed history and comprehensive ophthalmological examinations were conducted, including decimal best-corrected visual acuity (BCVA), dilated ophthalmoscopy, color fundus photography, spectral domain optical coherence tomography (SD-OCT, Heidelberg and Zeiss), fundus autofluorescence imaging (FAF; excitation: 488 nm, Spectralis HRA + OCT; Heidelberg Engineering, Dossenheim, Germany), near-infrared fundus autofluorescence (NIR-FAF; excitation: 787 nm), Humphrey's visual fields (HVF, 30-2), and microperimetry (MP, MAIA, 4-2). We recorded full-field ERGs (ffERGs, Diagnosys LLC, Lowell, MA) in accordance with the standards of the International Society for Clinical Electrophysiology of Vision (ISCEV) [7]. We also recorded ffERGs after 3, 4, and 12 h DA. Multifocal ERGs (mf-ERGs) were recorded with a VERIS Science 6.3.2 imaging system (EDI, San Mateo, CA) in accordance with the ISCEV standard protocol [8]. We selected mf-ERGs with a stable fixation for further analysis.

Pathogenic variant detection

After obtaining informed consent, we collected blood samples in EDTA tubes from the proband and the unaffected father, mother, and son of the proband. The genomic DNA was subjected to whole exome

sequencing (WES) with an Illumina Genome Analyzer II platform in accordance with the manufacturer's (Illumina's) instructions. It covered 20,794 genes and 201,121 exons in the Consensus Coding Sequence (CCDS) Region database, and approximately 97.0% of CCDS exons or 96.5% of Reference Sequence (RefSeq) exons were captured, all called SNVs and INDELs of the 790 genes registered as retinal disease-causing genes on the RetNet database (<https://sph.uth.edu/retnet/home.htm>) were selected for further analysis in the public domain. The identified variants were filtered with allele frequency (less than 1%) of 1000 Genomes Project Database (1000 genome; <https://www.internationalgenome.org>). WES and annotation were done by Genesky Biotechnologies (Shanghai, China). Polyphen2, SIFT, and MutationTaster were used to predict the pathogenicity of candidate variants. PCR amplification and bidirectional sequencing were performed to confirm the variant.

Case description

Baseline

A 28-year-old female with a complaint of photopsia with periphery visual field loss of the right eye for 10 days was presented. The patient reported no flu-like symptoms, such as fever and headache. She denied allergies to medicine and foods. She declared a history of measles 7 years ago and additionally remarked night blindness since her childhood and did not see a doctor before. Comprehensive antibodies of autoimmune diseases and inflammation revealed negative responses. She reported no family history, and her parents were not consanguineous (Fig. 1). On the first examination, slit-lamp examination showed that the pupil, intraocular pressure, and motility were normal and had no evidence of intraocular inflammation. Her best-corrected LogMAR visual acuity was 0.05 OD and – 0.08 OS with a myopic refractive error of – 5.75 and – 5.00 diopters in her right and left eyes, respectively.

The fundus of both eyes revealed a widespread golden yellow discoloration throughout the posterior pole (Fig. 2a) and showed the normal appearance of the retina after 4 h DA (Fig. 2b). ffERGs were recorded after 30 min, 3 h, 4 h, and 12 h DA. The DA with 30 min was recorded at the first visit time,

and DA with 3 h, 4 h, and 12 h was recorded at the 2-day interval following the first time. The results showed that rod photoreceptor ERG amplitudes were nonrecordable under 30 min, 3 h, and 4 h DA, and the a-wave and b-wave responses partly recovered in the initial single flash after 12 h DA of both eyes. The combined cone-rod ERGs of the right eye were absent after 12 h DA, and her left eye showed a slight recovery. The mixed cone-rod ERGs were severely reduced due to the second combined flash, which is compatible with previous reports [9]. The cone responses were normal at all recordings (Fig. 2c).

FAF images of the right eye showed the presence of several hyperfluorescent dots in the posterior pole, which fuse in a flake-like manner in the area surrounding the optic disc (Fig. 3a). The hypofluorescent areas showed in the NIF were associated with the demarcated dark region without golden yellow reflexes of both eyes in the fundus images (Fig. 3a).

The SD-OCT showed that the hyperreflective bands corresponding to the outer segments were densely packed in the temporal and nasal sides of the left eye and the temporal side of the right eye outside the fovea. This packed structure of the parafovea is thought to be a specific feature in patients with Oguchi disease. The fovea area and nasal side of the right eye showed a blurred ellipsoid zone (EZ) and disrupted outer segments. Hyperreflective materials accumulated over the retinal pigment epithelium (RPE) to the interdigitation zone (IZ) and EZ. The fovea structure of the left eye was perfectly preserved (Fig. 3a).

The HFV demonstrated a blind spot enlargement breaking out to the temporal periphery in the right eye at the first examination (Fig. 4a). The MP examinations demonstrated the abnormality of the macular integrity of the right eye (Fig. 4a). The average of the macular sensitivity dropped to 25.6 dB at the presentation compared with the normal reference (27–36 dB).

The mfERGs revealed lower amplitudes of N1- and P1- in rings 1–2 compared with the normal. Moreover, the right eye showed severer reduction than the left eye and severely attenuated responses along the nasal region of the fovea (Fig. 5a).

Pathogenic variants screening

WES was performed in the patient and three relatives (parents and son). After processing the annotation, a

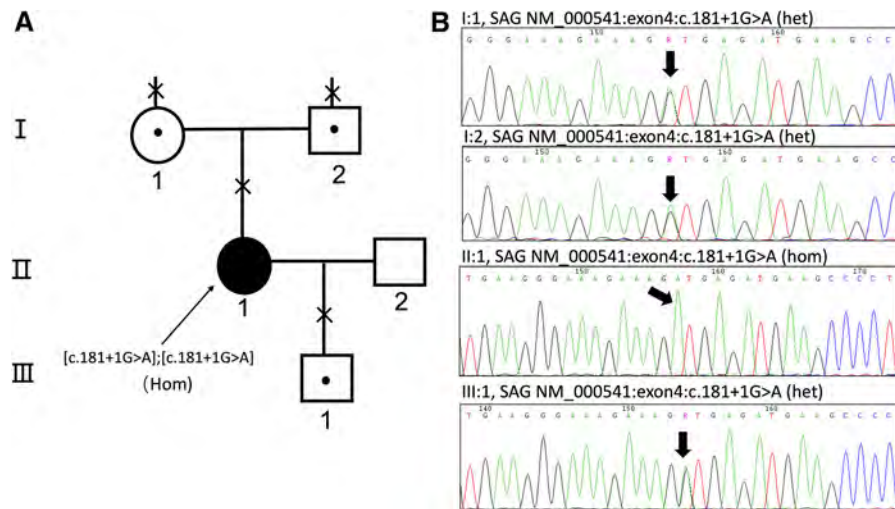


Fig. 1 Family pedigree of the patient. **a** Filled shape with an arrow indicates the affected proband with a homozygous c.181 + 1G > A splicing alteration. (●) indicates a heterozygous state in her parents and her son. (×) indicates the family members who got whole exome sequencing detection.

b Sequence chromatogram of SAG c.181 + 1G > A variant. Sequence trace of part of exon 4 of SAG in proband and relatives carrying the homozygous and heterozygous c.181 + 1G > A pathogenic variant which are indicated by black arrows, respectively

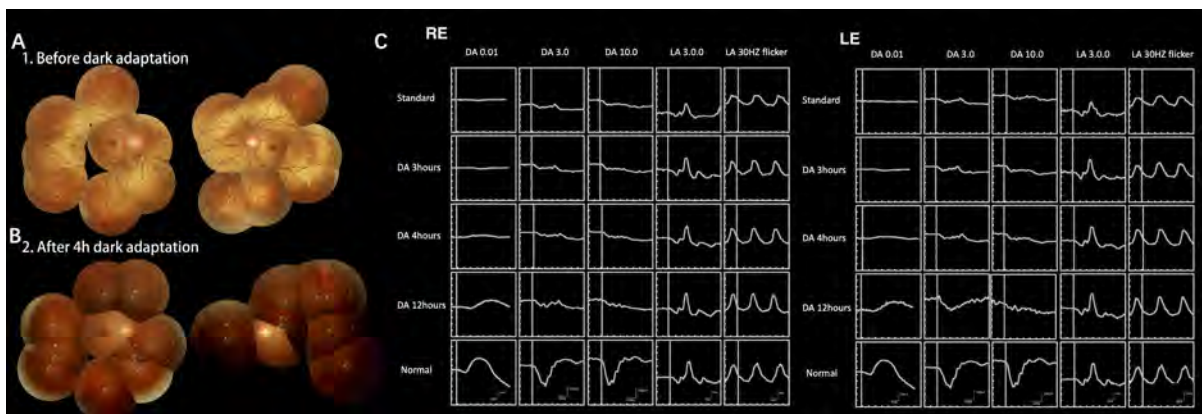


Fig. 2 Fundus photographs and full-field ERG before and after DA of the patient. **a** Fundus images before and after 4 h dark adaptation (DA). The golden discoloration of fundus appearance disappeared after 4 h DA. **b** ffERGs of both eyes after DA at different time points and the normal reference for comparison.

Rod ERGs were undetectable after 30 min, 3 h, and 4 h DA. Rod response had a partial recovery after the DA time prolonged to 12 h. Light-adapted ERGs reveal the normal function of a generalized cone system of both eyes

total 143,052 coding and splice sites variants, including 4114 variants with $MAF \leq 1\%$ in genes unrelated to retinopathies and 16 variants with $MAF \leq 1\%$ in genes related to retinopathies, were identified. The average sequencing coverage of the targeted exons was 86.53%. The coverage of targeted exons for > 10 reads was 96.57% and > 20 reads was 85.19%. A splicing alteration of c.181 + 1G > A was identified in the SAG gene (NM_000541) with a homozygous status in this patient. All other three relatives had a

heterozygous status (Fig. 1). No variants in *GRK1* were found. The splicing alteration of the SAG gene is first reported in this study.

Overall, we diagnosed the patient with Oguchi disease associated with the MEWDS in accordance with her characteristic clinical appearance and genetic molecular test results.

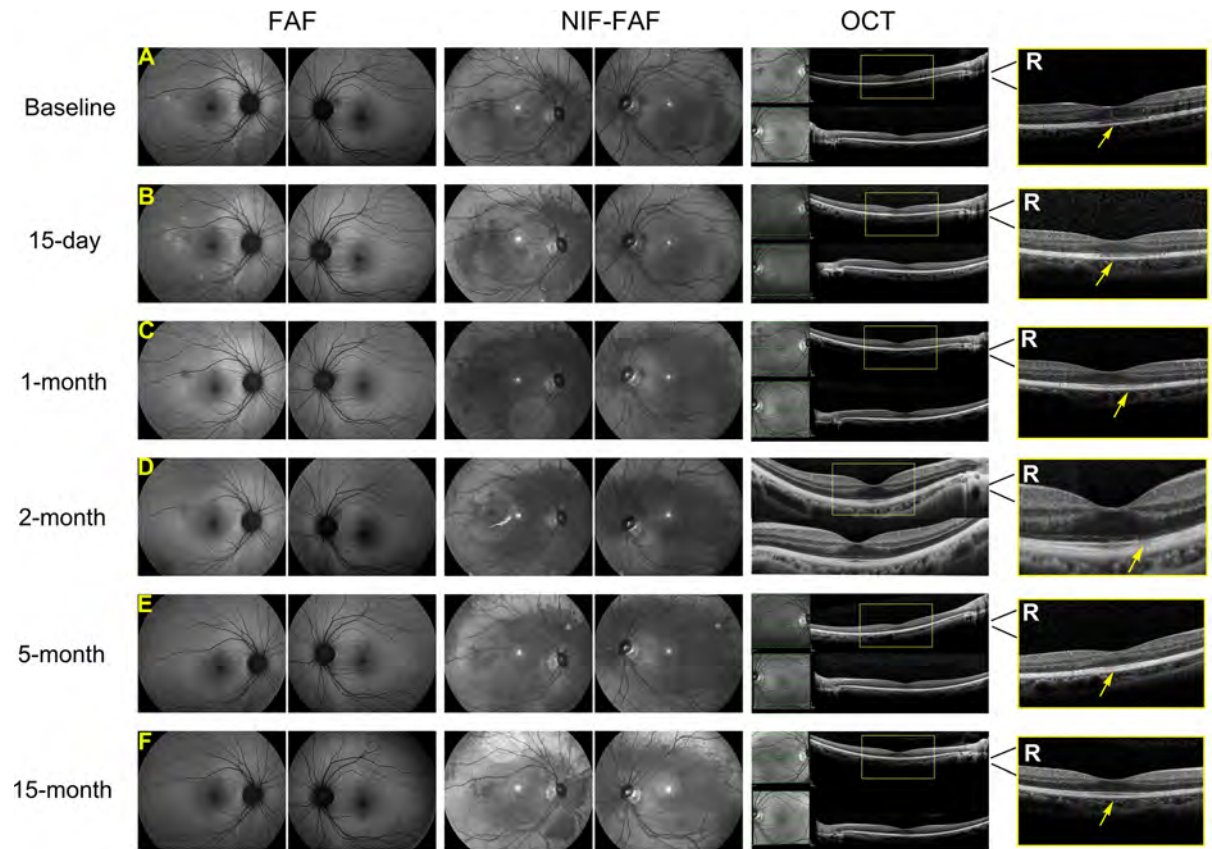


Fig. 3 Serial changes of autofluorescence, near-infrared, and SD-OCT with 15-month follow-up. FAF, NIR, and SD-OCT images of both eyes at baseline (a), 15-day (b), 1-month (c), 2-month (d), 5-month (e), and 15-month (f) follow-up. FAF detected several hyperfluorescent lesions at posterior at the initial presentation of the right eye, which showed consecutive disappearance during follow-up. NIR images showed a

corresponding golden discoloration area with fundus images. SD-OCT demonstrated the recovery of disrupted EZ and IZ at the macula with a maintained RPE over the followings. The fovea of the right eye is framed by a yellow rectangular box and enlarged (right). Atrophic fovea area marked by single-head yellow arrow is given

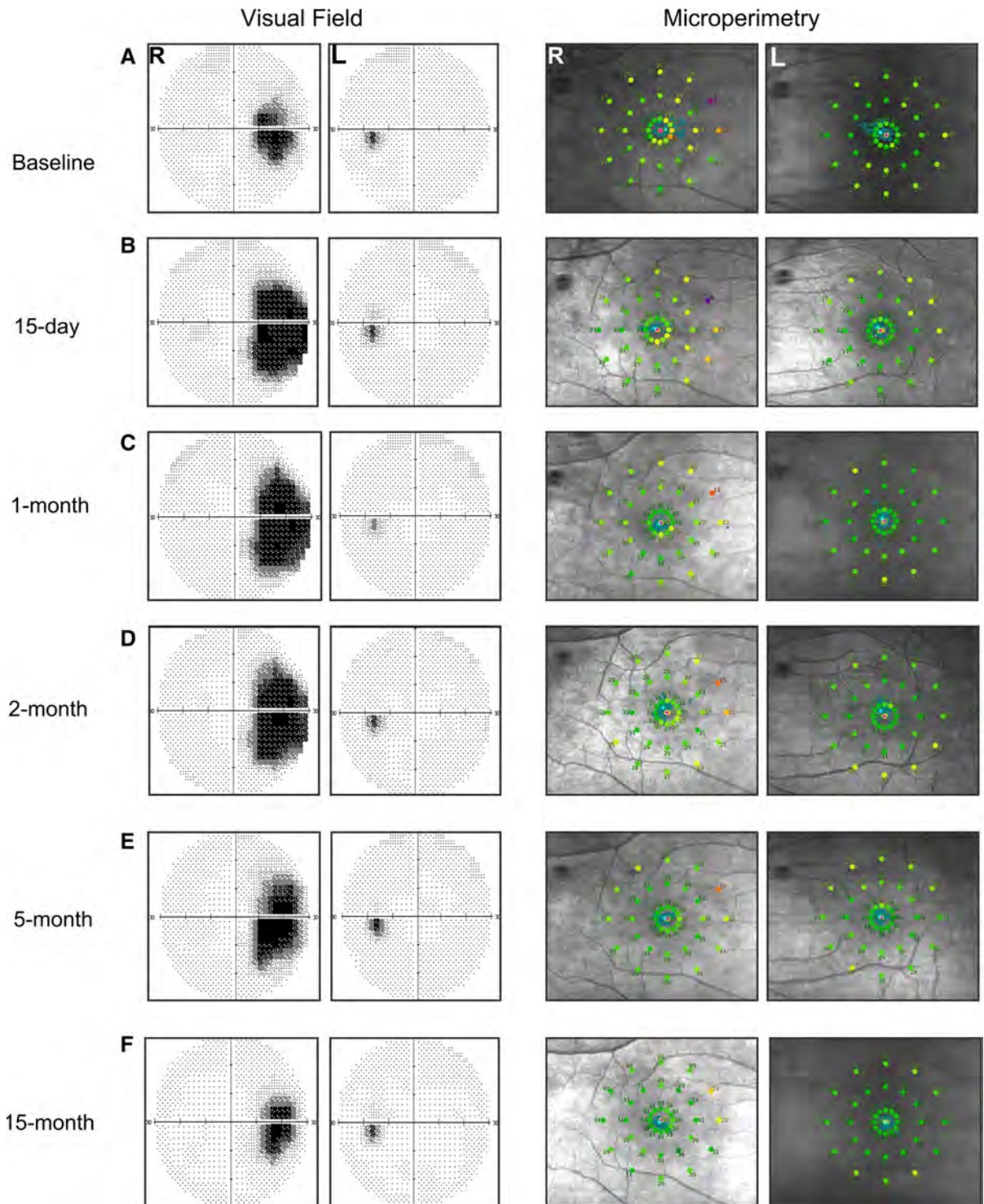
Follow-up

We observed the patient through a 15-month follow-up. The LogMAR BCVA of the right eye dropped to 0.4 in a 1-month time, which lasted until the 5-month follow-up time. The BCVA improved to 0.22 at the 15-month follow-up time, which was still lower than the first time she came to see a doctor.

Numerous hyperfluorescent white dots in the posterior pole were increased to the peak, and the hyperfluorescent area surrounding the optic disc became larger at the 15-day follow-up. Then, all the symptoms gradually reduced starting from the 1-month follow-up, with a 1/4 PD hypofluorescent

area showing at the vessel arcade and kept almost stable until the 2-month follow-up. These phenomena almost disappeared from the 5-month and 15-month follow-up (Fig. 3b–e). Only a tiny hyperfluorescent area was found at the temporal side of the optic disc border at the last examination (Fig. 3f).

The fovea region of the blurred EZ and disrupted IS/OS junction line obviously spreads, and the granularity deposit increased at the 15-day follow-up (Fig. 3b). Over time, these changes tended to disappear with a partial restoration from the 1-month to 2-month follow-up time (Fig. 3c, d). A slight patchy change of the IS/OS junction line can be observed at



◀ **Fig. 4** Serial changes of visual field and MP with a 15-month follow-up. Visual field and MP images at baseline (a), 15-day (b), 1-month (c), 2-month (d), 5-month (e), and 15-month (f) follow-up. Visual field images note the progress of an enlarged blind spot (black color) of the right eye that started to get smaller at the 2-month follow-up. The improvement is evidenced by the average intensity of macular measured by MP from 25.6, 26.4, 27.7, 27.5, 28.8, and 30 dB at presentation, 15-day, 1-month, 2-month, 5-month, and 15-month follow-up

the 5-month follow-up (Fig. 3e), with a normal retinal appearance at the 15-month follow-up (Fig. 3f).

The blind spot enlarged to the summit at the 15-day follow-up time and kept almost the same size when detected at the 2-month follow-up (Fig. 4b–d). The enlarged blind spot area had partial recovery at the 5-month follow-up and reverted to a similar size to baseline at the 15-month follow-up (Fig. 4e, f). In terms of the MP results, the average intensity consequently had an increment from 26.4 dB at the 15-day follow-up to 30 dB at the 15-month follow-up. The average intensity was 27.7, 27.5, and 28.8 at the 1-month, 2-month, and 5-month follow-up, respectively (Fig. 4b–f).

The mfERG records in the central and nasal regions of the fovea eventually enhanced from the 1-month to the 5-month follow-up but were still smaller than the control (Fig. 5b–d). The left eye served as a control.

Discussion

Oguchi disease is characterized by nyctalopia with the Mizuo–Nakamura phenomenon, golden retinal exhibition, abnormal rod responses in electroretinography,

and no obvious subjective changes in other symptoms, such as visual acuity reduction, achromatopsia, or visual field loss [1]. It is an unusual form of congenital stationary night blindness. However, Nishiguchi et al. [10] recently reported Oguchi disease shows a progressive degeneration to retinitis pigmentosa after a long-term follow-up. Our patient was suffering night blindness since her childhood and presented with a golden discoloration of the fundus; the SD-OCT findings of the well-structured fovea accompany complex packed highly reflective bands at parafovea, which are compatible to reported Oguchi cases [9, 11–17]. Hayashi et al. reported mfERG findings in one Oguchi case with homozygous 1147delA in the *SAG* gene. The patient showed preserved central (ring 1) and paracentral (ring 2) responses with normal latencies but attenuated and prolonged responses in the periphery macular (rings 3–5) [18]. On the contrary, our patient showed a severe response reduction in the central and paracentral macular along with the relatively preserved responses at the outer macular of both eyes.

For the DA 3.0 ERG, after 12 h of dark adaptation, the amplitude of the right eye was smaller than that of the left eye. The right eye was at the inflammatory stage of MEWDS which temporarily influenced the function of photoreceptors. Most reports revealed that a longer DA time can produce the b-wave of rods. The DA time varies from “longer than 30 min” to “overnight” [2, 9, 19]. No exact DA time was available for reference. We first conducted a series of DA time points to determine the optimal time. We found a single flash and combined cone-rod responses, which can be recorded after 12 h (overnight) DA, which is compatible with previous papers [9]. Our

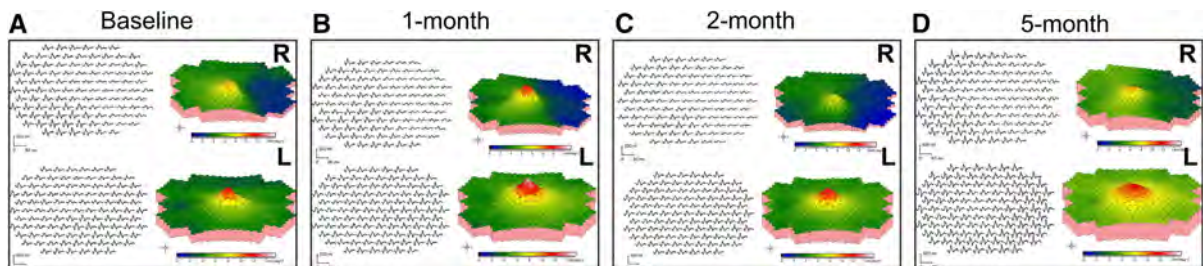


Fig. 5 Serial recordings of multifocal electroretinography with the 5-month follow-up. Trace and 3D-plot waveform of mfERGs at baseline (a), 1-month (b), 2-month (c), and 5-month (d) follow-up shows the reductive central region of both eyes and severely attenuated responses along the nasal region of the

fovea of the right eye. Responses of the right eye eventually recovered from the 1-month to 5-month follow-up: Responses of the central and nasal regions of the fovea enhanced along the time but were still smaller than the control. The left eye served as a control

results also indicate that although the Mizuo–Nakamura phenomenon can occur after 4 h DA through fundus images, the occurrence of b-wave in ffERGs needs longer DA.

The typical characteristics of the MEWDS have been known since its first description by Jampol et al. in 1984 [20]. The condition predominantly affects young women with myopia. The symptoms usually start with vaccination, allergy, and flulike episode complaints, followed by photopsia, enlarged blind spot, and unilateral blurred vision, which can totally recover within 10 weeks. The multimodal ophthalmology examinations are crucial to distinct MEWDS cases from other white dot syndromes: Fundus images show white patches scattered over the posterior macular area to the optic. The AF and fluorescein angiography (FA) show hyperfluorescent wreath-like dots corresponding to the hypofluorescent spots on the indocyanine green angiography (ICGA) images; the NIR reveals small areas of hypo-NIR-AF; the EZ and IZ disruptions can be seen in majority of patients and some cases showed focal choroidal excavation via OCT; and the VF test shows the enlarged blind spot [6, 21–23]. The expressions of this case were mostly consistent with the typical MEWDS, except that no lesions can be observed in the fundus images. It may be due to the dots that overlapped with tapetal-like fundus changes caused by Oguchi disease. The clinical course of typical MEWDS patients is short, the period of completed visual acuity recovery can be within three to 10 weeks, and the period of recovery of enlarged blind spots may last longer than 1 year [24–27]. In prospective studies, Marcela et al. reported 34 MEWDS patients experienced visual acuity recovery in 10 weeks [28]. Li et al. reported visual acuity, OCT, and FAF findings of seven MEWDS patients, which show full recovery within 3 months, and the visual field returned to normal in five patients within 6 months [29]. In the present patient, the visual acuity, OCT structure, FAF images, and visual field were still abnormal at the 5-month follow-up. These parameters returned to normal at the 15-month follow-up. The extension of the recovery time of her Oguchi disease was mainly caused by the photoreceptor dysfunction. The precise pathogenesis of MEWDS was unknown although it has been reckoned as an immune-mediated process [30].

This patient suffered Oguchi disease caused by *SAG* gene which is critical for recovery to normal

vision by deactivating phosphorylated opsins. Autoimmune affections or viral infections are thought to be the main causes of MEWDS, and the presence of antibodies could be detected in certain patients in the process of the infections as reported [31]. Although our patient had negative results for the antibody test, the time point of the presence of inflammatory antibodies is variable. We cannot exclude the possibility that this patient is susceptible to be affected by the MEWDS caused by inflammation antibodies.

SAG variations are mostly discovered in the Japanese population, and one specific homozygous frameshift alteration (c.924delA, previously named 1147delA) has been reported in majority of Japanese patients [10, 18, 32–34]. To date, in total 17 different pathogenic variants have been reported in the *SAG* gene (HGMD database) including eight missense, four nonsense, and five frameshift alterations [9, 16, 35]. A Chinese patient with a compound heterozygosity of a nonsense pathogenic variants and a heterozygous deletion of 3224 bp encompassing exon 2 has been reported by Huang et al. in 2012 [14]. Our patient's screening results showed a novel homozygous splicing alteration in the *SAG* gene (c.181 + 1G > A). It is the first time to report a splicing variant associated with Oguchi disease.

Conclusion

We first determine the exact time point of DA to induce b-wave in the rod response in ffERGs. This is the first case of Oguchi disease associated with the MEWDS and the first case of Oguchi disease caused by a *SAG* homozygous splicing alteration.

Acknowledgements Kaoru Fujinami is a paid consultant of Astellas Pharma Inc, Kubota Pharmaceutical Holdings Co., Ltd, and Acucela Inc. Kaoru Fujinami reports personal fees from Astellas Pharma Inc, personal fees from Kubota Pharmaceutical Holdings Co., Ltd., personal fees from Acucela Inc., personal fees from SANTEN Company Limited, personal fees from Foundation Fighting Blindness, personal fees from Foundation Fighting Blindness Clinical Research Institute, personal fees from Japanese Ophthalmology Society, personal fees from Japan Retinitis Pigmentosa Society. Kaoru Fujinami reports grants from Astellas Pharma Inc (NCT03281005), outside the submitted work.

Funding Shiyong Li is supported by grants from the National Nature Science Foundation of China (81974138), Third Military Medical University (Army Medical University) research grant

(2017XYY02), and National Basic Research Program of China (2018YFA0107301). Gang Wang is supported by grants from the Third Military Medical University, Southwest Hospital Innovation Grant (SWH2015LC15). Kaoru Fujinami is supported by grants from Grant-in-Aid for Young Scientists (A) of the Ministry of Education, Culture, Sports, Science and Technology, Japan (16H06269), grants from Grant-in-Aid for Scientists to support international collaborative studies of the Ministry of Education, Culture, Sports, Science and Technology, Japan (16KK01930002), grants from National Hospital Organization Network Research Fund (H30-NHO-2-12), grants from the Foundation for Fighting Blindness–Alan Lattes Career Development Program (CF-CL-0416-0696-UCL), grants from Health Labor Sciences Research Grant, The Ministry of Health, Labor and Welfare (201711107A), and grants from the Great Britain Sasakawa Foundation Butterfly Awards.

Compliance with ethical standards

Conflict of interest All authors have completed the COI Form for Disclosure of Potential Conflicts of Interest. Individual investigators who participate in the sponsored project(s) are not directly compensated by the sponsor but may receive a salary or other support from the institution to support their effort on the project(s).

Statements of human rights The procedures used were approved by the local ethics committee of Southwest Eye Hospital, Third Military Medical University (Army Medical University), Chongqing, China (reference number: 73981486-2), and all procedures were performed in accordance with the Declaration of Helsinki.

Informed consent The patient and her relatives, who were also studied upon, gave informed consent for all procedures described involved in the study.

Statement on the welfare of animals All the experimental procedures were performed in accordance with institutional animal welfare guidelines, were approved by the Third Military Medical University Animal Care and Use Committee

References

- Fuchs S, Nakazawa M, Maw M, Tamai M, Oguchi Y, Gal A (1995) A homozygous 1-base pair deletion in the arrestin gene is a frequent cause of Oguchi disease in Japanese. *Nat Genet* 10(3):360
- Miyake Y, Horiguchi M, Suzuki S, Kondo M, Tanikawa A (1996) Electrophysiological findings in patients with Oguchi's disease. *Jpn J Ophthalmol* 40(4):511–519
- Godara P, Cooper RF, Sergouniotis PI, Diederichs MA, Streb MR, Genead MA et al (2012) Assessing retinal structure in complete congenital stationary night blindness and Oguchi disease. *Am J Ophthalmol* 154(6):987–1001.e1
- Yamamoto S, Sippel KC, Berson EL, Dryja TP (1997) Defects in the rhodopsin kinase gene in the Oguchi form of stationary night blindness. *Nat Genet* 15(2):175
- dell'Omo R, Pavesio CE (2012) Multiple evanescent white dot syndrome (MEWDS). *Int Ophthalmol Clin* 52(4):221–228
- Brydak-Godowska J, Golebiewska J, Turczynska M, Moneta-Wielgos J, Samsel A, Borkowski PK et al (2017) Observation and clinical pattern in patients with white dot syndromes: the role of color photography in monitoring ocular changes in long-term observation. *Med Sci Monit: Int Med J Exp Clin Res* 23:1106–1115
- McCulloch DL, Marmor MF, Brigell MG, Hamilton R, Holder GE, Tzekov R et al (2015) ISCEV Standard for full-field clinical electroretinography (2015 update). *Doc Ophthalmol* 130(1):1–12
- Hood DC, Bach M, Brigell M, Keating D, Kondo M, Lyons JS et al (2012) ISCEV standard for clinical multifocal electroretinography (mfERG) (2011 edition). *Doc Ophthalmol* 124(1):1–13
- Sergouniotis PI, Davidson AE, Sehmi K, Webster AR, Robson AG, Moore AT (2011) Mizuo–Nakamura phenomenon in Oguchi disease due to a homozygous nonsense mutation in the SAG gene. *Eye (London, England)*. 25(8):1098–1101
- Nishiguchi KM, Ikeda Y, Fujita K, Kunikata H, Akiho M, Hashimoto K et al (2019) Phenotypic features of Oguchi disease and retinitis pigmentosa in patients with S-antigen mutations: a long-term follow-up study. *Ophthalmology* 126:1557–1566
- Yuan A, Nusinowitz S, Sarraf D (2011) Mizuo–Nakamura phenomenon with a negative waveform ERG. *Br J Ophthalmol* 95(1):147–148
- Agarwal R, Tripathy K, Bandyopadhyay G, Basu K (2019) Mizuo–Nakamura phenomenon in an Indian male. *Clin Case Rep* 7(2):401–403
- Colombo L, Abeshi A, Maltese PE, Frecer V, Miertus J, Cerra D et al (2018) Oguchi type I caused by a homozygous missense variation in the SAG gene. *Eur J Med Genet* 62:103548
- Huang L, Li W, Tang W, Zhu X, Ou-Yang P, Lu G (2012) A Chinese family with Oguchi's disease due to compound heterozygosity including a novel deletion in the arrestin gene. *Mol Vis* 18:528–536
- Kuroda M, Hirami Y, Nishida A, Jin ZB, Ishigami C, Takahashi M et al (2011) A case of Oguchi disease with disappearance of golden tapetal-like fundus reflex after vitreous resection. *Nippon Ganka Gakkai Zasshi* 115(10):916–923
- Fujinami K, Tsunoda K, Nakamura M, Oguchi Y, Miyake Y (2011) Oguchi disease with unusual findings associated with a heterozygous mutation in the SAG gene. *Arch Ophthalmol (Chicago, IL: 1960)* 129(10):1375–1376
- Maw M, Kumaramanickavel G, Kar B, John S, Bridges R, Denton M (1998) Two Indian siblings with Oguchi disease are homozygous for an arrestin mutation encoding premature termination. *Hum Mutat* 50(Suppl 1):S317–S319
- Hayashi T, Tsuzuranuki S, Kozaki K, Urashima M, Tsuneoka H (2011) Macular dysfunction in Oguchi disease with the frequent mutation 1147delA in the SAG gene. *Ophthalmic Res* 46(4):175–180

19. Zhang Q, Zulfiqar F, Riazuddin SA, Xiao X, Yasmeen A, Rogan PK et al (2005) A variant form of Oguchi disease mapped to 13q34 associated with partial deletion of GRK1 gene. *Mol Vis* 11:977–985
20. Jampol LM, Sieving PA, Pugh D, Fishman GA, Gilbert H (1984) Multiple evanescent white dot syndrome: I. Clinical findings. *Arch Ophthalmol* 102(5):671–674
21. Cahuzac A, Wolff B, Mathis T, Errera MH, Sahel JA, Mauget-Faysse M (2017) Multimodal imaging findings in ‘hyper-early’ stage MEWDS. *Br J Ophthalmol* 101(10):1381–1385
22. Furino C, Boscia F, Cardascia N, Alessio G, Sborgia C (2009) Fundus autofluorescence and multiple evanescent white dot syndrome. *Retina* 29(1):60–63
23. Margolis R, Mukkamala SK, Jampol LM, Spaide RF, Ober MD, Sorenson JA et al (2011) The expanded spectrum of focal choroidal excavation. *Arch Ophthalmol* 129(10):1320–1325
24. Mantovani A, Invernizzi A, Staurengi G, Herbort CP Jr (2019) Multiple evanescent white dot syndrome: a multimodal imaging study of foveal granularity. *Ocular Immunol Inflamm* 27(1):141–147
25. Hashimoto Y, Saito W, Hasegawa Y, Noda K, Ishida S (2019) Involvement of inner choroidal layer in choroidal thinning during regression of multiple evanescent white dot syndrome. *J Ophthalmol* 2019:6816925
26. Yang JS, Chen CL, Hu YZ, Zeng R (2018) Multiple evanescent white dot syndrome following rabies vaccination: a case report. *BMC Ophthalmol* 18(1):312
27. Yang CS, Wang AG, Lin YH, Huang YM, Lee FL, Lee SM (2012) Optical coherence tomography in resolution of photoreceptor damage in multiple evanescent white dot syndrome. *J Chin Med Assoc: JCMS* 75(12):663–666
28. Marsiglia M, Gallego-Pinazo R, De Souza EC, Munk MR, Yu S, Mrejen S et al (2016) Expanded clinical spectrum of multiple evanescent white dot syndrome with multimodal imaging. *Retina* 36(1):64–74
29. Li D, Kishi S (2009) Restored photoreceptor outer segment damage in multiple evanescent white dot syndrome. *Ophthalmology* 116(4):762–770
30. Jampol LM, Becker KG (2003) White spot syndromes of the retina: a hypothesis based on the common genetic hypothesis of autoimmune/inflammatory disease. *Am J Ophthalmol* 135(3):376–379
31. Gass JD (2003) Are acute zonal occult outer retinopathy and the white spot syndromes (AZOOR complex) specific autoimmune diseases? *Am J Ophthalmol* 135:380–381
32. Yamada T, Matsumoto M, Kadoi C, Nagaki Y, Hayasaka Y, Hayasaka S, Hayasaka S (1999) 1147 del A mutation in the arrestin gene in Japanese patients with Oguchi disease. *Ophthalmic Genet* 20(2):117–120
33. Nakamachi Y, Nakamura M, Fujii S, Yamamoto M, Okubo K (1998) Oguchi disease with sectoral retinitis pigmentosa harboring adenine deletion at position 1147 in the arrestin gene. *Am J Ophthalmol* 125(2):249–251
34. Nakazawa M, Wada Y, Fuchs S, Gal A, Tamai M (1997) Oguchi disease: phenotypic characteristics of patients with the frequent 1147delA mutation in the arrestin gene. *Retina (Philadelphia, PA)* 17(1):17–22
35. Waheed NK, Qavi AH, Malik SN, Maria M, Riaz M, Cremers FP et al (2012) A nonsense mutation in S-antigen (p.Glu306*) causes Oguchi disease. *Mol Vis* 18:1253–1259

Publisher’s Note Springer Nature remains neutral with regard to jurisdictional claims in published maps and institutional affiliations.

Clinical and Genetic Characteristics of 15 Affected Patients From 12 Japanese Families with *GUCY2D*-Associated Retinal Disorder

Xiao Liu^{1-3,*}, Kaoru Fujinami^{1,2,4,5,*}, Kazuki Kuniyoshi⁶, Mineo Kondo⁷, Shinji Ueno⁸, Takaaki Hayashi⁹, Kiyofumi Mochizuki¹⁰, Shuhei Kameya¹¹, Lizhu Yang^{1,2}, Yu Fujinami-Yokokawa^{1,12,13}, Gavin Arno^{1,4,5,14}, Nikolas Pontikos^{4,5}, Hiroyuki Sakuramoto⁶, Taro Kominami⁸, Hiroko Terasaki⁸, Satoshi Katagiri⁹, Kei Mizobuchi⁹, Natsuko Nakamura^{1,15}, Kazutoshi Yoshitake¹⁶, Yoza Miyake^{1,17}, Shiyong Li³, Toshihide Kurihara², Kazuo Tsubota², Takeshi Iwata¹⁶, and Kazushige Tsunoda¹, Japan Eye Genetics Consortium

¹ Laboratory of Visual Physiology, Division of Vision Research, National Institute of Sensory Organs, National Hospital Organization Tokyo Medical Center, Meguro-ku, Tokyo, Japan

² Department of Ophthalmology, Keio University School of Medicine, Shinjuku-ku, Tokyo, Japan

³ Southwest Hospital/Southwest Eye Hospital, Third Military Medical University (Army Medical University), Chongqing, China

⁴ UCL Institute of Ophthalmology, London, UK

⁵ Moorfields Eye Hospital, London, UK

⁶ Department of Ophthalmology, Kindai University Faculty of Medicine, Osakasayama, Osaka, Japan

⁷ Department of Ophthalmology, Mie University Graduate School of Medicine, Tsu, Mie, Japan

⁸ Department of Ophthalmology, Nagoya University Graduate School of Medicine, Showa-ku, Nagoya, Japan

⁹ Department of Ophthalmology, The Jikei University School of Medicine, Minato-ku, Tokyo, Japan

¹⁰ Department of Ophthalmology, Gifu University Graduate School of Medicine, Gifu-shi, Gifu, Japan

¹¹ Department of Ophthalmology, Nippon Medical School Chiba Hokusoh Hospital, Inzai, Chiba, Japan

¹² Graduate School of Health Management, Keio University, Shinjuku-ku, Tokyo, Japan

¹³ Division of Public Health, Yokokawa Clinic, Suita, Osaka, Japan

¹⁴ North East Thames Regional Genetics Service, UCL Great Ormond Street Institute of Child Health, Great Ormond Street NHS Foundation Trust, London, UK

¹⁵ Department of Ophthalmology, The University of Tokyo, Bunkyo-ku, Tokyo, Japan

¹⁶ Division of Molecular and Cellular Biology, National Institute of Sensory Organs, National Hospital Organization National Tokyo Medical Center, Meguro-ku, Tokyo, Japan

¹⁷ Aichi Medical University, Nagakute, Aichi, Japan

Correspondence: Kaoru Fujinami, Laboratory of Visual Physiology, Division of Vision Research, National Institute of Sensory Organs, National Hospital Organization, Tokyo Medical Center, 2-5-1 Higashigaoka, Meguro-ku, Tokyo 152-8902, Japan. e-mail: k.fujinami@ucl.ac.uk

Received: March 21, 2019

Accepted: January 9, 2020

Published: May 11, 2020

Keywords: macular dystrophy; cone rod dystrophy; *GUCY2D*; autosomal dominant; Leber congenital amaurosis

Purpose: To determine the clinical and genetic characteristics of patients with *GUCY2D*-associated retinal disorder (*GUCY2D*-RD).

Methods: Fifteen patients from 12 families with inherited retinal disorder (IRD) and harboring *GUCY2D* variants were ascertained from 730 Japanese families with IRD. Comprehensive ophthalmological examinations, including visual acuity (VA) measurement, retinal imaging, and electrophysiological assessment were performed to classify patients into three phenotype subgroups; macular dystrophy (MD), cone-rod dystrophy (CORD), and Leber congenital amaurosis (LCA). In silico analysis was performed for the detected variants, and the molecularly confirmed inheritance pattern was determined (autosomal dominant/recessive [AD/AR]).

Results: The median age of onset/examination was 22.0/38.0 years (ranges, 0-55 and 1-73) with a median VA of 0.80/0.70 LogMAR units (ranges, 0.00-1.52 and 0.10-1.52) in the right/left eye, respectively. Macular atrophy was identified in seven patients (46.7%), and two had diffuse fundus disturbance (13.3%), and six had an essentially normal

Citation: Liu X, Fujinami K, Kuniyoshi K, Kondo M, Ueno S, Hayashi T, Mochizuki K, Kameya S, Yang L, Fujinami-Yokokawa Y, Arno G, Pontikos N, Sakuramoto H, Kominami T, Terasaki H, Katagiri S, Mizobuchi K, Nakamura N, Yoshitake K, Miyake Y, Li S, Kurihara T, Tsubota K, Iwata T, Tsunoda K, Japan Eye Genetics Consortium. Clinical and genetic characteristics of 15 affected patients from 12 Japanese families with *GUCY2D*-associated retinal disorder. *Trans Vis Sci Tech.* 2020;9(6):2. <https://doi.org/10.1167/tvst.9.6.2>

fundus (40.0%). There were 11 patients with generalized cone-rod dysfunction (78.6%), two with entire functional loss (14.3%), and one with confined macular dysfunction (7.1%). There were nine families with ADCORD, one with ARCORD, one with ADMD, and one with ARLCA. Ten *GUCY2D* variants were identified, including four novel variants (p.Val56GlyfsTer262, p.Met246Ile, p.Arg761Trp, p.Glu874Lys).

Conclusions: This large cohort study delineates the disease spectrum of *GUCY2D*-RD. Diverse clinical presentations with various severities of ADCORD and the early-onset severe phenotype of ARLCA are illustrated. A relatively lower prevalence of *GUCY2D*-RD for ADCORD and ARLCA in the Japanese population was revealed.

Translational Relevance: The obtained data help to monitor and counsel patients, especially in East Asia, as well as to design future therapeutic approaches.

Introduction

Inherited retinal disorder (IRD) is a leading cause of blindness,¹ and includes disorders such as retinitis pigmentosa (RP), cone/cone-rod dystrophy (CORD), macular dystrophy (MD), Stargardt disease (STGD), Leber congenital amaurosis (LCA) and others.^{1–6} IRD is characterized by heterogeneity both in the clinical and genetic aspects, with different inheritance patterns, including autosomal dominant (AD), autosomal recessive (AR), X-linked, and mitochondrial inheritance.^{7–9} Significant clinical and genetic overlap is well-known in the spectrum of IRD, and diverse clinical phenotypes, including CORD, MD, STGD, RP, and LCA, can manifest as a result of pathogenic variants in a single gene (e.g., *ABCA4*, *BEST1*, *PRPH2*, *RPGR*, *CRX*, *GUCY2D*, *RS1*, *POC1B*, *PROM1*, *CNGA3*, *CNGB3*).^{2,3,7,8,10–18}

GUCY2D, denoted as guanylate cyclase 2D (OMIM: 600179), is located on 17p13.1 and contains 20 exons and encodes one of the two retinal membrane guanylyl cyclase isozymes expressed in photoreceptors.^{19,20} Retinal membrane guanylyl cyclase isozymes synthesize the intracellular messenger of photoreceptor excitation, cyclic guanosine monophosphate, which is regulated by the intracellular Ca²⁺-sensor proteins of guanylate cyclase-activating proteins.^{19–26} RetGCs and guanylate cyclase-activating proteins are responsible for the Ca²⁺-sensitive restoration of cyclic guanosine monophosphate levels after the light activation of the phototransduction cascade.²⁶

A locus and gene for LCA was first mapped and identified as *GUCY2D* (LCA1) in 1995 and 1996.^{19,27} Since then, more than 200 variants in the

GUCY2D gene have been associated with a wide range of different phenotypes of IRDs.^{9,19,20,28–39} Sharon et al. reported that 88% of *GUCY2D*-associated retinal disorder (*GUCY2D*-RD) is AR-LCA, whereas pathogenic heterozygous missense *GUCY2D* variants cause AD-CORD.²⁰ In that, pathogenic *GUCY2D* variants are one of the major causes of LCA, as well as a major cause of AD-CORD.²⁰ Recently, Stunkel et al. identified five patients with AR congenital night blindness caused by biallelic *GUCY2D* variants, which may slowly progress to mild retinitis pigmentosa.⁴⁰ Thus, AR-LCA, AD-CORD, and AR congenital night blindness are the main clinical presentations of *GUCY2D*-RD.

Studies of *GUCY2D*-RD have been conducted separately for each phenotype, such as CORD or RP/LCA; thus, it has been hard to comprehensively understand the disorder with diverse clinical manifestations and different modes of inheritance. To grasp the whole picture of *GUCY2D*-RD, large cohort studies with standardized clinical and genetic investigations for IRD in total are required.

The purpose of this study was to characterize the clinical and molecular genetic features of *GUCY2D*-RD in a large nationwide cohort of Japanese subjects diagnosed with IRD.

Methods

The protocol of this study followed the tenets of the Declaration of Helsinki. Informed consent was obtained from all affected subjects and unaffected subjects after explanation of the nature and possible consequences of the study. This research was

approved by the Institutional Review Board of the National Institute of Sensory Organs, National Hospital Organization Tokyo Medical Center (Reference R18-029).

Participants from the Japan Eye Genetics Consortium Study

Participants with a clinical diagnosis of IRD and available genetic data by whole-exome sequencing (WES) were studied between 2008 and 2018 as part of the Japan Eye Genetics Consortium Study (JEGC studies; <http://www.jegc.org/>) conducted in collaboration of 38 institutes all over Japan.⁴¹ A total of 1294 subjects from 730 families were reviewed, including 30 families with AD-CORD/MD/STGD (defined as families with clear AD family history) and 41 families with AR or sporadic LCA.

Clinical Examinations

A detailed history was obtained in all affected subjects and unaffected family members (where available). The onset of disease was defined as the age when any visual symptom was first noted by patients or parents or when the subject was first diagnosed. The duration of disease was defined as the time between the onset of disease and the latest examination.

Comprehensive ophthalmological investigations were performed, including measurements of the best-corrected decimal visual acuity (BCVA) converted to the logarithm of the minimum angle of resolution (LogMAR) units, ophthalmoscopy, fundus photography, fundus autofluorescence (FAF) imaging, spectral-domain optical coherence tomography (SD-OCT), visual field testing, and electrophysiological assessments mainly according to the international standards of the International Society for Clinical Electrophysiology of Vision.^{42–45}

Phenotype Subgroup

For the purpose of this study, the phenotype subgroup was defined based on clinical findings such as disease onset, symptoms, natural course, affected part on retinal imaging, the pattern of retinal dysfunction, and the history and phenotype of affected family members, partially according to the previous report¹³: LCA (including early-onset RP), a severe retinal dystrophy with early onset (<10 years) and complete loss of retinal function; RP (including rod-cone dystro-

phy), a progressive retinal dystrophy initially often affecting the peripheral retina with generalized rod dysfunction; CORD, a progressive retinal dystrophy initially often affecting the macula with generalized cone dysfunction; MD, a progressive retinal dystrophy presenting macular atrophy with confined macular dysfunction despite no abnormal generalized retinal function; and SNB, a stationary night blindness presenting congenital or early-onset night blindness, often affecting generalized rod function despite essentially normal visual acuity (VA) and no atrophy.

GUCY2D Variant Detection

Genomic DNA was extracted from affected subjects and unaffected family members (where available for cosegregation analysis). WES with target analysis of 301 retinal disease-associated genes (RetNET) was performed based on the previously published method and through the Phenopolis platform.^{41,46} The identified variants were filtered with the allele frequency (less than 1%) of the Human Genetic Variation Database (HGVD), which provides the allele frequency of the general Japanese population. Depth and coverage for the target exons were examined with the integrative Genomics Viewer.

Disease-causing variants were determined from the detected variants in the 301 retinal-disease-associated genes, considering the clinical findings of the affected subjects, the pattern of inheritance in the pedigree, and the results of cosegregation analysis.

In Silico Molecular Genetic Analysis

Sequence variant nomenclature was performed according to the guidelines of the Human Genome Variation Society (HGVS). The allele frequency of all detected *GUCY2D* variants in the HGVD, Integrative Japanese Genome Variation (iJGVD 2k), the 1000 Genomes Project, and the genome Aggregation Database (gnomAD) was established according to the previous method.⁴¹

All detected *GUCY2D* variants were analyzed with the following prediction programs; MutationTaster, FATHMM, SIFT, PROVEAN, and PolyPhen-2. Evolutional conservation scores were calculated for all detected *GUCY2D* variants by the UCSC database. Pathogenicity classification of all detected *GUCY2D* variants was performed based on the guidelines of the American College of Medical Genetics and Genomics.⁴⁷

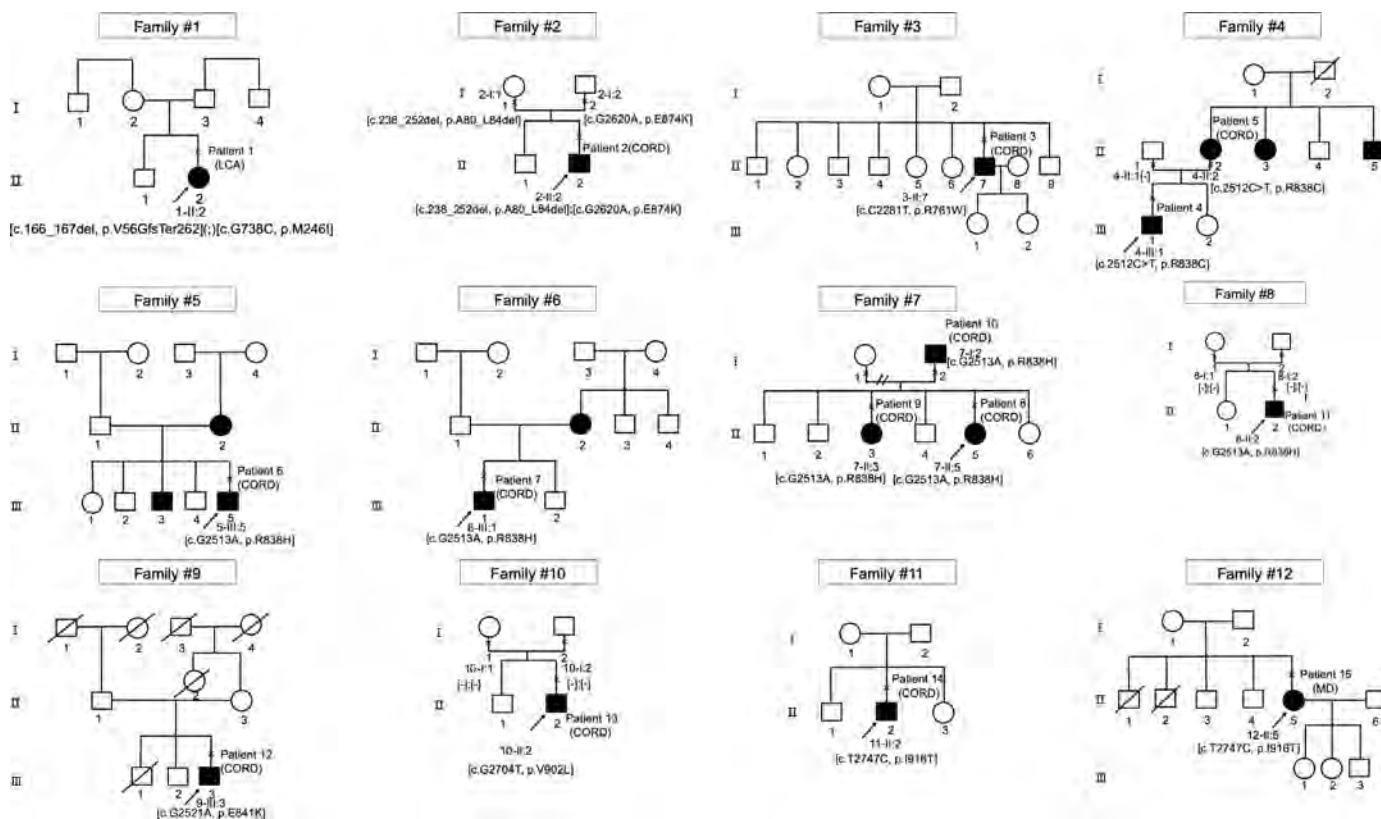


Figure 1. Pedigrees of 12 Japanese families with inherited retinal disorder harboring *GUCY2D* variants. The solid squares and circles (men and women, respectively) represent the affected subjects and the white icons represent the unaffected family members. The slash symbol indicates deceased individuals. The generation number is noted on the left. The proband is marked by an arrow; the clinically investigated individuals are indicated by a cross.

Results

Participants

Fifteen affected subjects from 12 families with a clinical diagnosis of IRD and harboring *GUCY2D* variants were ascertained. The detailed demographic features and summarized genetic results are provided in Table 1, and the pedigrees of 12 families are shown in Figure 1.

All affected and unaffected subjects were Japanese, and any mixture with other ethnicity was not reported. There were four families with clear AD family history (4/12, 33.3%; families 4–7), and eight sporadic families with no affected family members than the proband (8/12, 66.7%; families 1–3, 8–12). There were four families with unknown familial information (families 3, 9, 11, 12). Consanguineous marriage was not reported in any of the 12 families.

There were five affected females (5/15, 33.3%) and 10 affected males (10/15, 66.7%). The median age at

the latest examination of the 15 affected subjects was 38.0 years (range, 1–73).

Onset, Chief Complaint, and Visual Acuity

The median age of onset and duration of disease of the 12 affected subjects with available records was 22.0 years (range, 0–55), and 11.5 years (range, 1–40), respectively.

Four subjects had childhood-onset of 15 years or earlier (4/12, 33.3%; patients 1, 2, 7, 13). Later onset of disease (45 years or later) was reported in one subject (1/12, 8.3%; patient 15).

Reduced visual acuity/poor visual acuity was reported as a chief complaint at the initial visit in 12 of 14 affected subjects with available records (12/14, 85.7%; patients 1, 2, 4–9, 12–14, 15), one with photophobia (1/14, 7.1%; patient 11), and one with night blindness (1/14, 7.1%; patient 3).

The median BCVA in the right and left eyes of the 12 affected subjects with available records was 0.80 (range, 0.00–1.52) and 0.70 (range, 0.10–1.52) LogMAR units,

Table 1. Demographic Features of 15 Japanese Patients with GUCY2D-Associated Retinal Disorder (GUCY2D-RD)

| Family No. | Patient No. | Inheritance | Sex | Age (at Latest Examination) | Onset | Chief Complaint | Other ocular symptoms | Refraction | | | | LogMAR VA | | Phenotype Subgroup | Inheritance Suggested by Molecular genetic diagnosis | Genotype |
|------------|----------------------|-------------|-----|-----------------------------|-------|--|---------------------------|------------|-------|------|------|-----------|-----------------|--------------------|---|----------|
| | | | | | | | | RE | LE | NA | NA | RE | LE | | | |
| 1 (MU01) | 1-II:2 (Patient 1) | Sporadic | F | 1 | 0 | Reduced visual acuity/poor visual acuity | Nystagmus | NA | NA | NA | NA | NA | LCA | AR | c.167_168delTG, p.Val56GlyfsTer262; c.738G>C, p.Met246Ile | |
| 2 (TMC01) | 2-II:2 (Patient 2) | Sporadic | M | 12 | 3 | Reduced visual acuity/poor visual acuity | Night blindness | -1 | -1 | 0.22 | 0.22 | 0.22 | CORD (moderate) | AR | c.238_252del, p.Ala80_Leu84del; c.2620G>A, p.Glu874Lys | |
| 3 (NU01) | 3-II:7 (Patient 3) | Sporadic | M | 73 | NA | Night blindness | NA | +1.5 | +3.5 | 1 | 1.52 | 1.52 | CORD (severe) | AD | c.2281C>T, p.Arg761Trp | |
| 4 (KDU01) | 4-III:1 (Patient 4) | AD | M | 30 | 23 | Reduced visual acuity/poor visual acuity | NA | -2.5 | 2.5 | 0.82 | 0.82 | 0.82 | CORD (moderate) | AD | c.2512C>T, p.Arg838Cys | |
| 4 (KDU01) | 4-II:2 (Patient 5) | AD | F | 61 | 21 | Reduced visual acuity/poor visual acuity | Photophobia | -1.5 | -1.5 | 1.05 | 1.05 | 1.05 | CORD (moderate) | AD | c.2512C>T, p.Arg838Cys | |
| 5 (GU01) | 5-III:5 (Patient 6) | AD | F | 31 | 18 | Reduced visual acuity/poor visual acuity | Photophobia | -7 | -7 | 0 | 0.1 | 0.1 | CORD (mild) | AD | c.2513G>A, p.Arg838His | |
| 6 (TMC02) | 6-III:1 (Patient 7) | AD | M | 38 | 7 | Reduced visual acuity/poor visual acuity | Photophobia | -5 | -5 | 1.52 | 1.52 | 1.52 | CORD (severe) | AD | c.2513G>A, p.Arg838His | |
| 7 (JU01) | 7-II:5 (Patient 8) | AD | F | 36 | 35 | Reduced visual acuity/poor visual acuity | NA | -6 | -6.5 | 0.22 | 0.52 | 0.52 | CORD (mild) | AD | c.2513G>A, p.Arg838His | |
| 7 (JU01) | 7-II:3 (Patient 9) | AD | F | 43 | 30 | Reduced visual acuity/poor visual acuity | NA | -6 | -6.5 | 0.7 | 0.7 | 0.7 | CORD (moderate) | AD | c.2513G>A, p.Arg838His | |
| 7 (JU01) | 7-I:2 (Patient 10) | AD | M | 68 | NA | NA | NA | +1 | -2 | 0.82 | 1 | 1 | CORD (NA) | AD | c.2513G>A, p.Arg838His | |
| 8 (JU02) | 8-II:2 (Patient 11) | Sporadic | M | 23 | 23 | Photophobia | Color vision abnormality | -11.5 | -11.5 | 0.15 | 0.15 | 0.15 | CORD (mild) | AD (de novo) | c.2513G>A, p.Arg838His | |
| 9 (KDU02) | 9-III:3 (Patient 12) | Sporadic | M | 64 | 41 | Reduced visual acuity/poor visual acuity | NA | NA | NA | NA | NA | NA | CORD (NA) | AD | c.2521G>A, p.Glu841Lys | |
| 10 (TMC03) | 10-II:2 (Patient 13) | Sporadic | M | 10 | 0 | Reduced visual acuity/poor visual acuity | Photophobia | +1.5 | +1.5 | 1 | 1 | 1 | CORD (moderate) | AD (de novo) | c.2704G>T, p.Val902Leu | |
| 11 (NU02) | 11-II:2 (Patient 14) | Sporadic | M | 43 | NA | Reduced visual acuity/poor visual acuity | Central visual field loss | -10 | -12 | 0.8 | 0.6 | 0.6 | CORD (moderate) | AD | c.2747T>C, p.Ile916Thr | |
| 12 (MU02) | 12-II:5 (Patient 15) | Sporadic | F | 71 | 55 | Reduced visual acuity/poor visual acuity | Photophobia | 0 | 0 | 0.52 | 0.52 | 0.52 | MD | AD | c.2747T>C, p.Ile916Thr | |

AD, autosomal dominant; AR, autosomal recessive; CORD, cone rod dystrophy; F, female; LCA, Leber congenital amaurosis; LE, left eye; M, male; NA, not available; RE, right eye; LogMAR VA, best corrected logarithm of the minimum angle of resolution visual acuity; MD, macular dystrophy.

Autosomal dominant family history (at least having two affected subjects in two consecutive generations) was clearly reported in four families. Age described in the column was defined as the age when the latest examination was performed. The age of onset was defined as either the age at which visual loss was first noted by the patient or, in the 'asymptomatic' patients, when an abnormal retinal finding was first detected. Patients 10 and 14 had cataract. The phenotype subgroup was defined based on clinical findings, such as disease onset, symptoms, natural course, affected part on retinal imaging, the pattern of retinal dysfunction, and the history and phenotype of affected family members, partially according to the previous report: LCA (including early-onset RP), a severe retinal dystrophy with early-onset (<10 years) and complete loss of retinal function; RP (including rod-cone dystrophy), a progressive retinal dystrophy initially often affecting the peripheral retina with generalized rod dysfunction; CORD, a progressive retinal dystrophy initially often affecting the macula with generalized cone dysfunction; MD, a progressive retinal dystrophy presenting macular atrophy with confined macular dysfunction despite no abnormal generalized retinal function; and SNB, a stationary night blindness presenting congenital or early-onset night blindness often affecting generalized rod function despite essentially normal visual acuity and no atrophy.

There were two severe CORD subjects with poor VA and severe retinal dysfunction (patients 3, 7), six moderate CORD subjects with intermediate severity of VA or retinal function (patients 2, 4, 5, 9, 13, 14), and three mild CORD subjects with relatively favorable VA and relatively preserved generalized rod function (patients 6, 8, 11). Two subjects with CORD were unavailable for severity assessment due to unavailable VA or electrophysiological data. Sequence variant nomenclature was performed according to the guidelines of the Human Genome Variation Society.

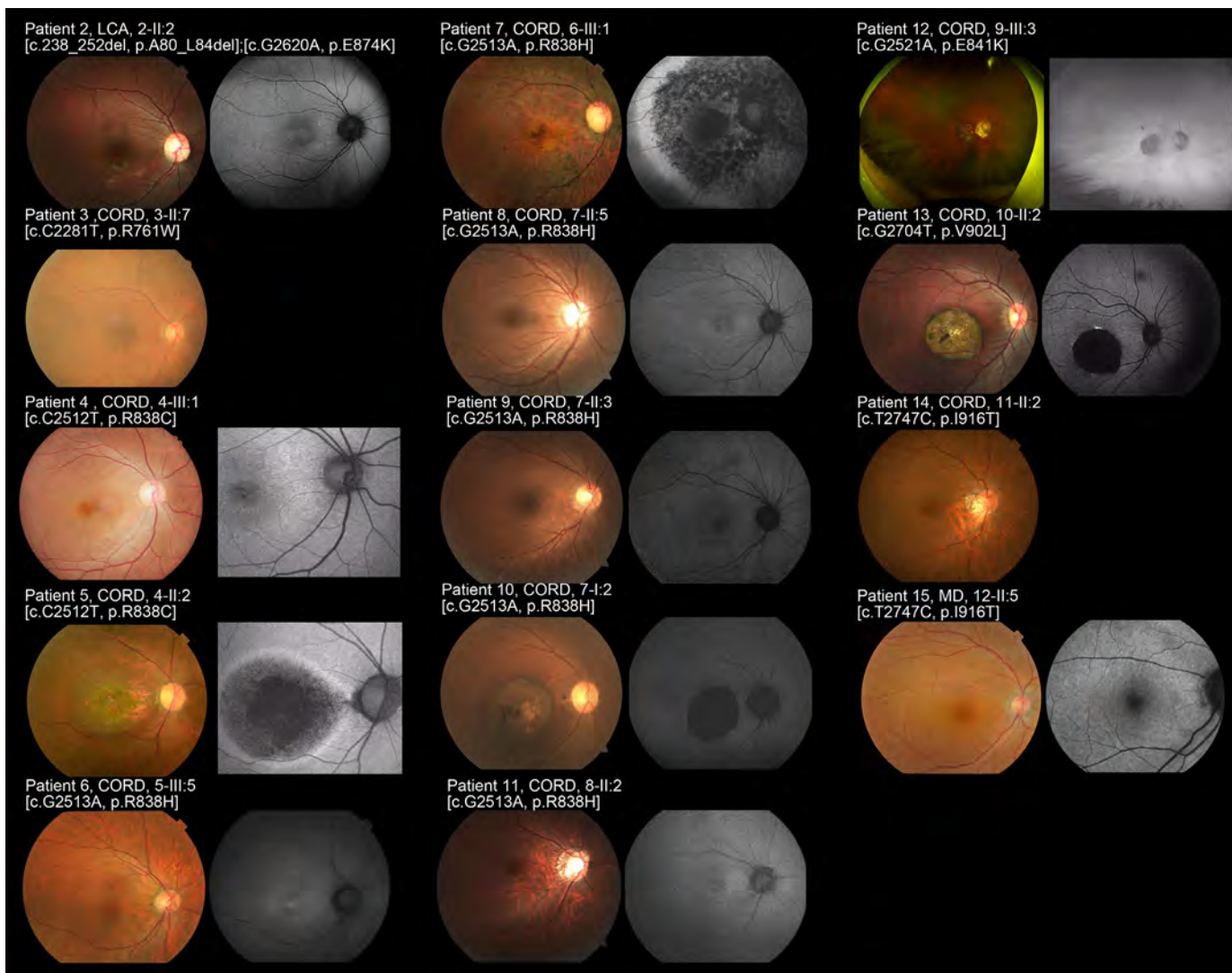


Figure 2. Fundus photographs and fundus autofluorescence images of 14 patients with *GUCY2D*-associated retinal disorder (*GUCY2D*-RD; patients 2–15). Fundus photographs and fundus autofluorescence (FAF) images of the right eyes demonstrated macular atrophy in seven affected subjects (patients 4, 5, 7, 9, 10, 12, 13) with intrachoroidal cavitation in three subjects (patients 5, left; 10, left; 13) and slight fine dots at the macula in two subjects (patients 4, 9). Atrophic change at the posterior pole extending to the periphery was observed in patient 7 and subtle diffuse disturbance at the posterior pole with vessel attenuation was found in patient 7. Normal fundus appearance was noted in five subjects (patients 1, 2, 6, 8, 14). Patient 11 had essentially normal retinal appearance except for optic disk cupping. The atrophic changes were more evident on FAF images. A loss of AF signal at the macula was identified in five subjects (patients 5, 7, 10, 12, 13). Increased AF signal at the macula was observed in five subjects (patients 2, 4, 6, 8, 11). A patchy area of decreased AF signal at the posterior pole extending to the periphery surrounded by a ring of increased AF signal was found in patient 7.

respectively. One of the two subjects with unavailable LogMAR VA testing had nystagmus (patient 1). Four subjects of 13 with available records had relatively favorable VA (4/13, 30.8%, patients 2, 6, 8, 11; 0.22 or better LogMAR units in the better eye), five subjects had intermediate VA (5/13, 38.5%, patients 4, 9, 10, 14, 15; between 0.22 and 1.0 LogMAR units in the better eye), and four subjects had poor VA (4/13, 30.8%; patients 3, 5, 7, 13; 1.0 or worse LogMAR units in the better eye).

Retinal Imaging and Morphological Findings

Fundus photographs were obtained in 14 affected subjects (patients 2–15), and FAF images were available in 12 affected subjects (patients 2, 4–13, 15). A description of funduscopy was available in one subject (patient 1). The representative images are presented in [Figure 2](#), and the detailed findings are described in [Table 2](#).

Macular atrophy was identified in seven affected subjects (7/15, 46.7%; patients 4, 5, 7, 9, 10, 12, 13), with

Table 2. Retinal Imaging and Morphological Findings of 15 Patients with *GUCY2D*-RD

| Patient No. | Phenotype Subgroup | Fundus | | | | FAF | | | | SD-OCT | | | | | | | | | | | |
|--------------|--------------------|-----------------------------------|--------------------|--------------------|--------------|---|---|---|---------------------------|------------------------------------|--|---------------------------|---|------------------------------|---------------------------------------|---|---------------------------------|----------------------|-----------------------------------|----------|--|
| | | Macular Atrophy Along the Arcades | Peripheral Atrophy | Vessel Attenuation | Pigmentation | Comments | Area of Decreased Density at the Central Retina | Area of Increased Density at the Macula | Ring of Increased Density | Abnormal Density Along the Arcades | Areas of Abnormal Density in the Periphery | Areas of Abnormal Density | Decreased Density at the Parafovea | Foveal Sparing Surrounded by | Outer Retinal Disruption at the Fovea | Outer Retinal Disruption at the Parafovea | Increased Signal of the Choroid | EZ Preservation (RE) | EZ Preservation at the fovea (LE) | Comments | |
| 1 (MU01-01) | LCA | No | No | No | No | Funduscopy, normal | NA | NA | NA | NA | NA | NA | NA | NA | NA | NA | NA | NA | NA | NA | NA |
| 2 (TMC01-01) | CORD | No | No | No | No | Normal | No | Yes | No | No | No | No | Slightly increased AF at the fovea | No | No | No | No | Yes | Yes | Yes | Loss of IZ at the macula |
| 3 (NU01-01) | CORD | No | No | Yes | No | Subtle diffuse disturbance at the posterior pole | NA | NA | NA | NA | NA | NA | NA | No | Yes | Yes | No | Yes | Yes | Yes | Loss of IZ at the macula with ERM in the right eye |
| 4 (KDU01-01) | CORD | Yes | No | No | No | Subtle fine dots at the macula | No | Yes | No | No | No | No | No | No | No | No | No | No | No | No | Loss of EZ/IZ at the fovea |
| 5 (KDU01-02) | CORD | Yes | No | No | No | Intrachoroidal cavitation in the left eye | Yes | No | Yes | No | No | No | No | Yes | Yes | Yes | Yes | No | No | No | Loss of EZ/IZ at the fovea Thinned sensory retina and loss of EZ/IZ at the macula; Intra-choroidal cavitation at the left macula |
| 6 (GU01-01) | CORD | No | No | No | No | Normal | No | Yes | No | No | No | No | Slightly increased AF at the fovea | No | No | No | No | Yes | Yes | Yes | Loss of IZ at the macula |
| 7 (TMC02-01) | CORD | Yes | Yes | Yes | Yes | Atrophic changes with at the posterior pole extended to the periphery | Yes | No | Yes | Yes | Yes | Yes | No | Yes | Yes | Yes | Yes | No | No | No | Loss of IZ at the macula |
| 8 (JU01-01) | CORD | No | No | No | No | Normal | No | Yes | No | No | No | No | Slightly increased AF at the fovea of the right eye | No | No | No | No | Yes | Yes | Yes | Loss of IZ at the macula |
| 9 (JU01-02) | CORD | Yes | No | No | No | Subtle fine dots at the macula | No | No | No | No | No | No | Slightly abnormal background | Yes | No | No | No | No | No | No | No |

Table 2. Continued

| Patient No. | Fundus | | | FAF | | | SD-OCT | | | Comments | | | | | | | | |
|---------------|--------------------|----------------------------------|--------------------|--------------------|--------------|---|---|---|--|----------|--|---|----------------|---------------------------------------|---|---------------------------------|-----------------------------------|--|
| | Phenotype Subgroup | Macular Atrophy Along the Arcade | Peripheral Atrophy | Vessel Attenuation | Pigmentation | Comments | Area of Decreased Density at the Central Retina | Area of Increased Density at the Macula | Ring of Increased Density Along the Arcade | | Areas of Abnormal Density in the Periphery | Areas of Abnormal Density Surrounding the Parafovea | Foveal Sparing | Outer Retinal Disruption at the Fovea | Outer Retinal Disruption at the Parafovea | Increased Signal of the Choroid | EZ Preservation at the fovea (RE) | EZ Preservation at the fovea (LE) |
| 10 (JU01-03) | CORD | Yes | No | No | Yes | Pigmentation at the macula in both eyes, intra-choroidal cavitation in the left eye | Yes | No | No | No | No | No | Yes | Yes | Yes | No | No | Intrachoroidal cavitation at the left macula. |
| 11 (JU02-01) | CORD | No | No | No | No | Essential normal except for optic disc cupping | No | Yes | No | No | No | Yes | No | No | No | Yes | Yes | Loss of IZ at the macula |
| 12 (KDU02-01) | CORD | Yes | No | No | Yes | | Yes | No | No | No | No | Artifact due to the medial condition | Yes | Yes | Yes | No | No | Thinned sensory retina and loss of EZ/IZ at the macula |
| 13 (TMC03-01) | CORD | Yes | No | No | No | Intrachoroidal cavitation | Yes | No | No | No | No | Loss of AF signal at the macula | Yes | Yes | Yes | No | No | Thinned sensory retina/intrachoroidal cavitation at the macula |
| 14 (NU02-01) | CORD | No | No | No | No | Normal | NA | NA | NA | NA | NA | NA | No | No | No | No | No | Loss of EZ/IZ at the macula |
| 15 (MU02-01) | MD | No | No | No | No | Subtle diffuse disturbance at the posterior pole | No | No | No | No | No | Slightly abnormal background | No | No | No | Yes | Yes | Loss of IZ at the macula |

BE, both eyes; EZ, ellipsoid zone; FAF, fundus autofluorescence; F5, foveal sparing; LE, left eye; M, male; NA, not available; RE, right eye; SD-OCT, spectral domain optical coherence tomography. Foveal sparing was defined as remaining foveal AF signal surrounded by the area of decreased AF.

intrachoroidal cavitation in three subjects (patients 5, 10, 13) and slight fine dots at the macula in two subjects (patients 4, 9). Atrophic change at the posterior pole extending to the periphery was observed in one subject (1/15, 6.7%; patient 7). Subtle diffuse disturbance at the posterior pole with vessel attenuation was found in two subjects (2/15, 13.3%; patients 3, 15). Normal fundus appearance was noted in five subjects (5/15, 33.3%; patients 1, 2, 6, 8, 14). One subject had a normal retinal appearance except for optic disk cupping (1/15, 6.7%, patient 11).

The retinal atrophy at the macula was more evident on FAF images, and the loss of AF signal at the macula was identified in five subjects (5/12, 41.7%, patients 5, 7, 10, 12, 13). Increased AF signal at the macula was observed in five subjects (5/12, 41.7%; patients 2, 4, 6, 8, 11), one of whom showed subtle fine dots at the macula and the other four subjects had no abnormal findings at the macula on fundus photography. One subject showed patchy areas of decreased AF signal at the posterior pole extending to the periphery (1/12, 8.3%; patient 7).

SD-OCT images were obtained in 14 affected subjects (patients 2–15), and the representative images are presented in [Figure 3](#). One subject had an epiretinal membrane (patient 3, right). Outer retinal disruption at the fovea and/or parafovea was identified in six subjects (6/14, 42.9%; patients 5, 7, 9, 10, 12, 13), three of whom showed intrachoroidal cavitation (patients 5, left; 10, left; 13). A relatively preserved photoreceptor ellipsoid zone (EZ) line at the fovea was found in six subjects (6/14, 42.9%; patients 2, 3, 6, 8, 11, 15), one of whom showed outer retinal disruption at the parafovea (patient 3).

Visual Fields and Electrophysiological Findings

The detailed findings of visual fields and electrophysiological assessments are described in [Table 3](#). Visual field testing was performed in nine affected subjects (patients 2, 4–9, 12, 13), with Goldmann perimetry (seven subjects) and Humphrey visual field analyzer (four subjects). Central scotoma was detected in eight subjects (8/9, 88.9%; patients 4–9, 12, 13) and paracentral scotoma was observed in all nine subjects (9/9; 100%). Peripheral visual loss was found in four subjects (4/9, 44.4%; patients 2, 5–7).

Full-field electroretinograms were recorded in 14 affected subjects (patients 2–9, 11–15). Multifocal ERGs (mfERGs) were recorded in three subjects (patients 4, 6, 11), and focal macular ERGs (FMERGs) were obtained in one subject (patient 15).

Undetectable light-adapted (LA) responses were demonstrated in seven subjects (7/14, 50.0%; patients 1–3, 5, 7, 11, 13), with undetectable dark-adapted (DA) responses in two subjects (patients 1, 3), severely decreased DA responses in two subjects (patients 2, 7), moderately decreased DA responses in one subject (patient 13), and mildly decreased DA responses in two subjects (patients 5, 11). Severely decreased LA responses were identified in four subjects (4/14, 28.6%; patients 6, 8, 12, 14), with moderately decreased DA responses in one subject (patient 12) and mildly decreased DA responses in three subjects (patients 6, 8, 14). Moderately decreased LA responses with mildly decreased DA responses were shown in one subject (1/14, 7.1%; patient 9). Mildly decreased LA responses with normal DA responses were found in one subject (1/14, 7.1%; patient 4). Normal responses both in LA and DA conditions were noted in one subject (1/14, 7.1%; patient 15). A lower b-to-a ratio (ratio of b wave to a wave for dark-adapted bright flash responses was less than 0.9) was observed in three subjects (3/14, 21.4%; patients 5, 11, 14). Reduced central responses were detected by mfERG in three subjects (patients 4, 6, 11), and reduced central focal responses were demonstrated by FMERGs in one subject (patient 15).

Generalized entire loss of function was identified in two subjects (2/14, 14.3%; patients 1, 3), generalized cone rod dysfunction was found in 11 subjects (11/14, 78.6%; patients 2, 4, 5–9, 11–14), and confined macular dysfunction was noted in one subject (1/14, 7.1%; patient 15).

Phenotype Subgroups

Phenotype subgroup classification was performed in all 15 affected subjects. There were 13 subjects with CORD (13/15, 86.7%; patients 2–14), one with MD (1/15, 6.7%; patient 15), and one with LCA (1/15, 6.7%; patient 1). There were no subjects with RP or SNB.

The mean age of onset of the 13 subjects with CORD/one with MD/one with LCA was 20.0 (range, 0–41)/55/0 years, with the mean duration of disease of 14.7 (range, 0–40)/1.0/16.0 years, respectively. The mean VA for eyes with CORD/MD was 0.73 (range, 0.00–1.52)/0.52 in LogMAR units.

There were two severe CORD subjects with poor VA and severe retinal dysfunction (patients 3, 7), six moderate CORD subjects with intermediate severity of VA or retinal function (patients 2, 4, 5, 9, 13, 14), and three mild CORD subjects with relatively favorable VA and relatively preserved generalized rod function (patients 6, 8, 11). Two subjects with CORD were unavailable for severity assessment because of unavailable VA or electrophysiological data.

Table 3. Visual fields, and Electrophysiological Assessments of 15 Patients with GUCY2D-RD

| Patient No. | Phenotype Subgroup | Method | Visual Fields | | | Comments | Responses in Dark-adapted Condition | Responses in Light-adapted Condition | Electrophysiological Assessment | |
|---------------|--------------------|--------|-----------------|---------------------|------------------------------|--|-------------------------------------|--------------------------------------|---|-------------------------------------|
| | | | Central Scotoma | Paracentral Scotoma | Peripheral Visual Field Loss | | | | Lower b to a Ratio in Dark-adapted Bright Flash Responses | Comments |
| 1 (MU01-01) | LCA | NA | NA | NA | NA | Undetectable | Undetectable | Undetectable | No | Skin electrodes |
| 2 (TMC01-01) | CORD | GP | No | Yes | Yes | Severely decreased | Undetectable | Undetectable | No | |
| 3 (NU01-01) | CORD | NA | NA | NA | NA | Undetectable | Undetectable | Undetectable | No | Recorded in the right eye |
| 4 (KDU01-01) | CORD | GP/HFA | Yes | Yes | No | WNL | WNL | Mildly decreased | NA | Reduced central responses in mfERGs |
| 5 (KDU01-02) | CORD | GP/HFA | Yes | Yes | Yes | Mildly decreased | Mildly decreased | Undetectable | Yes | |
| 6 (GU01-01) | CORD | HFA | Yes | Yes | Yes | Central and paracentral relative scotoma | Mildly decreased | Severely decreased | No | Reduced central responses in mfERGs |
| 7 (TMC02-01) | CORD | GP | Yes | Yes | Yes | Central and paracentral relative scotoma | Severely decreased | Undetectable | No | |
| 8 (JU01-01) | CORD | GP | Yes | Yes | No | | Mildly decreased | Severely decreased | No | |
| 9 (JU01-02) | CORD | GP/HFA | Yes | Yes | No | | Mildly decreased | Moderately decreased | No | |
| 10 (JU01-03) | CORD | NA | NA | NA | NA | NA | NA | NA | NA | |
| 11 (JU02-01) | CORD | NA | NA | NA | NA | Mildly decreased | Undetectable | Undetectable | Yes | Reduced central responses in mfERGs |
| 12 (KDU02-01) | CORD | GP | Yes | Yes | Yes | | Moderately decreased | Severely decreased | No | |
| 13 (TMC03-01) | CORD | GP | Yes | Yes | No | | Moderately decreased | Undetectable | No | |
| 14 (NU02-01) | CORD | NA | NA | NA | NA | Mildly decreased | Severely decreased | Severely decreased | Yes | |
| 15 (MU02-01) | MD | NA | NA | NA | NA | WNL | WNL | WNL | No | Reduced central responses in FMERG |

FMERG, focal macular electroretinogram; GP, Goldmann kinetic perimetry; HFA, Humphry field analyzer; mfERG, multifocal electroretinogram; WNL, within normal limit.

Lower b to a ratio in dark-adapted bright flash responses was defined as less than 0.9.

Severity of electrophysiological responses were defined as follows; undetectable, more than 90% amplitude reduction compared to the normal reference; severely decreased response, between 90% and 75% amplitude reduction; moderately decreased response, between 75% and 50% amplitude reduction; mildly decreased responses, less than 50% amplitude reduction.

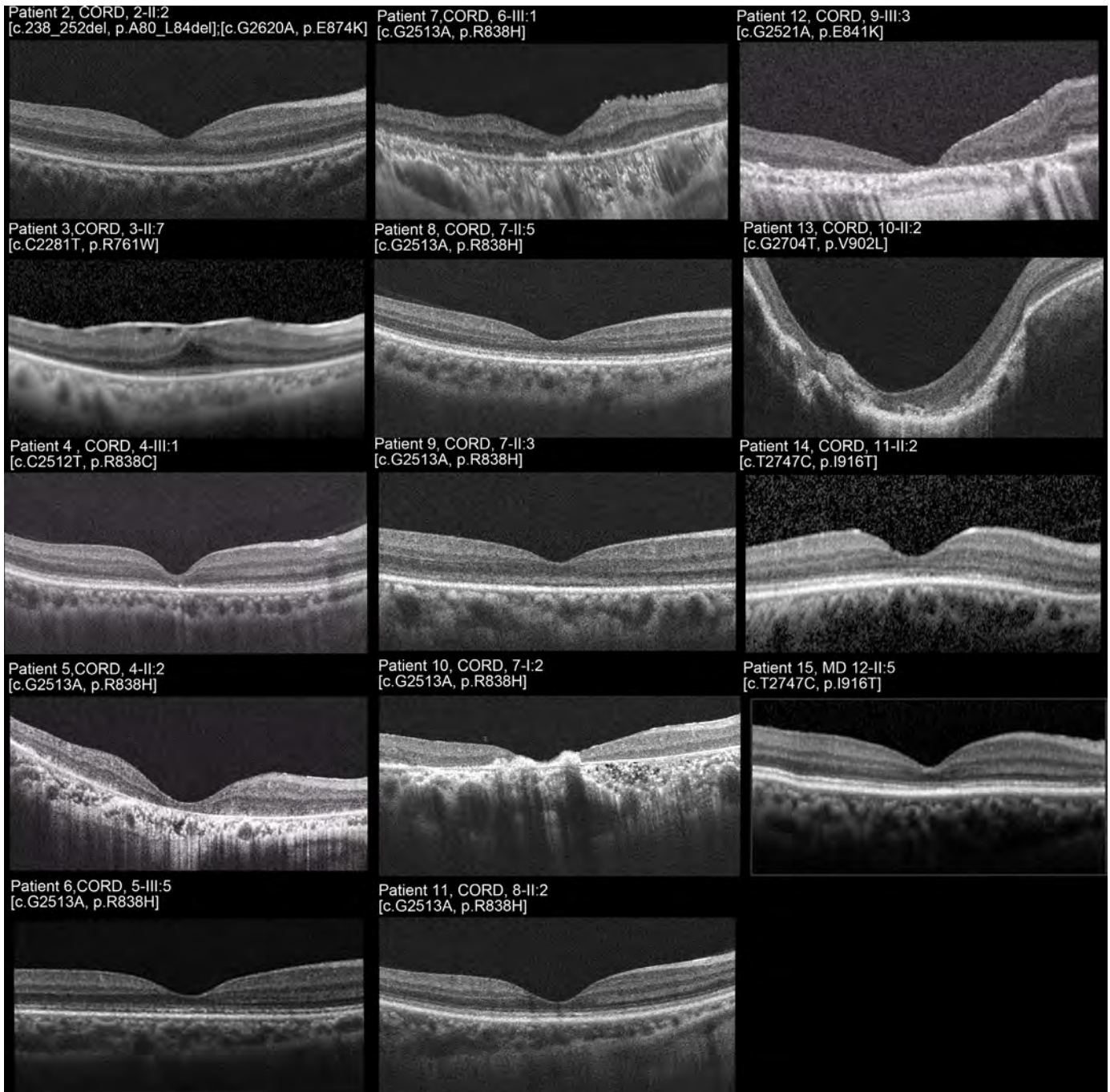


Figure 3. Spectral-domain optical coherence tomographic images of 11 patients with *GUCY2D*-RD (patients 2, 3, 6–11, 13–15). Spectral-domain optical coherence tomography of the right eye demonstrated outer retinal disruption at the fovea in six subjects (patients 5, 7, 9, 10, 12, 13) and at the parafovea in six subjects (patients 3, 5, 7, 10, 12, 13) with intrachoroidal cavitation in one subject (patient 13, right). A relatively preserved photoreceptor ellipsoid zone (EZ) line at the fovea was found in six subjects (patients 2, 3, 6, 8, 11, 15), one of whom showed outer retinal disruption at the parafovea (patient 3). One subject had an epiretinal membrane (patient 3).

GUCY2D Variants

The variant data of 15 affected and seven unaffected subjects from 12 families are summarized in [Table 4](#). Ten *GUCY2D* variants were identi-

fied in the heterozygous state: c.167_168delTG, p.Val56GlyfsTer262; c.238_252del, p.Ala80_Leu84del; c.738G>C, p.Met246Ile; c.2281C>T, p.Arg761Trp; c.2513G>A, p.Arg838His; c.2512C>T, p.Arg838Cys; c.2521G>A, p.Glu841Lys; c.2620G>A, p.Glu874Lys;

Table 4. Summary of Detected Variants of 15 Affected and 7 Unaffected Subjects from 12 Families with *GUCY2D*-RD

| Family ID | Subject ID | Affected/ Unaffected | Exon | Nucleotide and Amino Acid Changes | State | | |
|------------|----------------------|-------------------------|--------------------|---|---------------------------|----------------------------------|--------------|
| 1 (MU01) | 1-II:2 (patient 1) | Affected | 2 | <i>c.167_168delTG, p.Val56GlyfsTer262</i> | Heterozygous | | |
| | | | 3 | <i>c.738G>C, p.Met246Ile</i> | Heterozygous | | |
| 2 (TMC01) | 2-II:2 (patient 2) | Affected | 2 | <i>c.238_252del, p.Ala80_Leu84del</i> | Compound heterozygous | | |
| | | | 14 | <i>c.2620G>A, p.Glu874Lys</i> | Heterozygous | | |
| 3 (NU01) | 2-I:1 | Unaffected | 14 | <i>c.2620G>A, p.Glu874Lys</i> | Heterozygous | | |
| | | | 2 | <i>c.226_240del, p.Ala76_Ala80del</i> | Heterozygous | | |
| 4 (KDU01) | 3-II:7 (patient 3) | Affected | 12 | <i>c.2281C>T, p.Arg761Trp</i> | Heterozygous | | |
| 4 (KDU01) | 4-III:1 (patient 4) | Affected | 13 | <i>c.2512C>T, p.Arg838Cys</i> | Heterozygous | | |
| | | | 4-II:2 (patient 5) | Affected | 13 | <i>c.2512C>T, p.Arg838Cys</i> | Heterozygous |
| | | | 4-II:1 | Unaffected | 13 | <i>c.2512C>T, p.Arg838Cys</i> | ND |
| 5 (GU01) | 5-III:5 (patient 6) | Affected | 13 | <i>c.2513G>A, p.Arg838His</i> | Heterozygous | | |
| 6 (TMC02) | 6-III:1 (patient 7) | Affected | 13 | <i>c.2513G>A, p.Arg838His</i> | Heterozygous | | |
| 7 (JU01) | 7-II:5 (patient 8) | Affected | 13 | <i>c.2513G>A, p.Arg838His</i> | Heterozygous | | |
| | | | 7-II:3 (patient 9) | Affected | 13 | <i>c.2513G>A, p.Arg838His</i> | Heterozygous |
| | | | 7-I:2 (patient 10) | Affected | 13 | <i>c.2513G>A, p.Arg838His</i> | Heterozygous |
| 8 (JU02) | 8-II:2 (patient 11) | Affected | 13 | <i>c.2513G>A, p.Arg838His</i> | Heterozygous (de novo) | | |
| | | | 8-I:2 | Unaffected | 13 | <i>c.2513G>A, p.Arg838His</i> | ND |
| | | | 8-I:1 | Unaffected | 13 | <i>c.2513G>A, p.Arg838His</i> | ND |
| 9 (KDU02) | 9-III:3 (patient 12) | Affected | 13 | <i>c.2521G>A, p.Glu841Lys</i> | Heterozygous | | |
| 10 (TMC03) | 10-II:2 (patient 13) | Affected | 14 | <i>c.2704G>T, p.Val902Leu</i> | Heterozygous (de novo) | | |
| | | | 10-I:2 | Unaffected | 14 | <i>c.2704G>T, p.Val902Leu</i> | ND |
| | | | 10-I:1 | Unaffected | 14 | <i>c.2704G>T, p.Val902Leu</i> | ND |
| 11 (NU02) | 11-II:2 (patient 14) | Affected | 14 | <i>c.2747T>C, p.Ile916Thr</i> | Heterozygous | | |
| 12 (MU02) | 12-II:5 (patient 15) | Affected | 14 | <i>c.2747T>C, p.Ile916Thr</i> | Heterozygous | | |

GUCY2D transcript ID: NM_000180.3

ND, not detected

Novel variants are shown in italic.

Whole-exome sequencing with targeted analysis for retinal disease-causing genes on RetNET (<https://sph.uth.edu/retnet/>) was performed in 15 affected and 7 unaffected subjects from 12 families.

c.2704G>T, p.Val902Leu; and *c.2747T>C, p.Ile916Thr* (NM_000180.3).

There were eight missense variants, one with a 2-bp deletion leading to a frame shift, and one with an in-frame deletion. Three variants were identified in multiple families: *p.Arg838Cys* (families 4, 5), *p.Arg838His* (families 6–8), and *p.Ile916Thr* (families 11, 12). Intrafamilial cosegregation analysis was performed in five families (families 2, 4, 7, 8, 10), and the de novo (patient 11, *p.Arg838His*; patient 10, *p.Val902Leu*), compound heterozygous (patient 2; *p.Ala80_Leu84del, p.Glu874Lys*), and heterozygous (patient 4, *p.Arg838Cys*; patient 8, *p.Arg838His*; patient 11, *p.Arg838His*) states were confirmed.

GUCY2D-RD caused by six detected variants has been reported before: CORD for *p.Ala80_Leu84del*⁹; ADCORD for *p.Arg838His*;^{34,38} ADCORD for *p.Arg838Cys*;^{29,34} ADCORD for *p.Glu841Lys*;³⁰ ADCORD for *p.Val902Leu*;³¹ ADCORD for *p.Ile916Thr*.³² Four variants have never been reported; *p.Val56GlyfsTer262, p.Met246Ile, p.Arg761Trp,* and *p.Glu874Lys*.

In Silico Molecular Genetic Analysis

The detailed results of in silico molecular genetic analyses for the 10 detected *GUCY2D* variants are

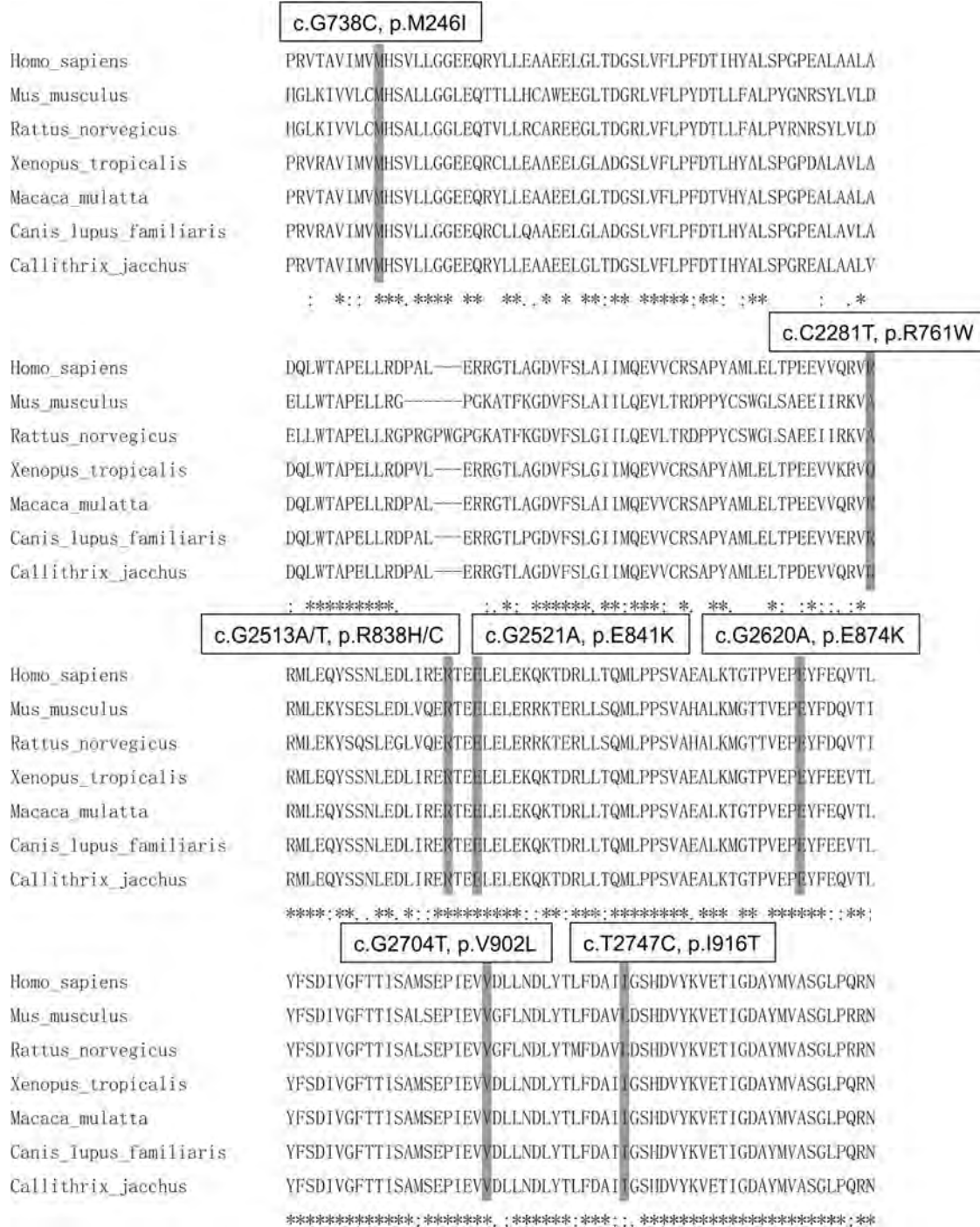


Figure 4. Multiple alignment of eight species of *GUCY2D*. The alignment was performed with the Clustal Omega program (<https://www.ebi.ac.uk/Tools/msa/clustalo/>) and the amino-acid-sequence alignment was numbered in accordance with the Homo sapiens *GUCY2D* sequence (ENST00000254854.4). *Complete conservation across the eight species. The positions of eight missense variant residues are highlighted with gray background: p.Met246Ile, p.Arg761Trp, p.Arg838His, p.Arg838Cys, p.Glu841Lys, p.Glu874Lys, p.Val902Leu, and p.Ile916.

presented in Supplementary Tables S1 and S2. A schematic genetic and protein structure of *GUCY2D* and multiple alignments of eight species of *GUCY2D* are shown in Figures 4 and 5.

Seven variants are located in exons 12-14 (p.Arg761Trp, p.Arg838His, p.Arg838Cys, p.Glu841Lys, p.Glu874Lys, p.Val902Leu, p.Ile916Thr), which are presumably associated

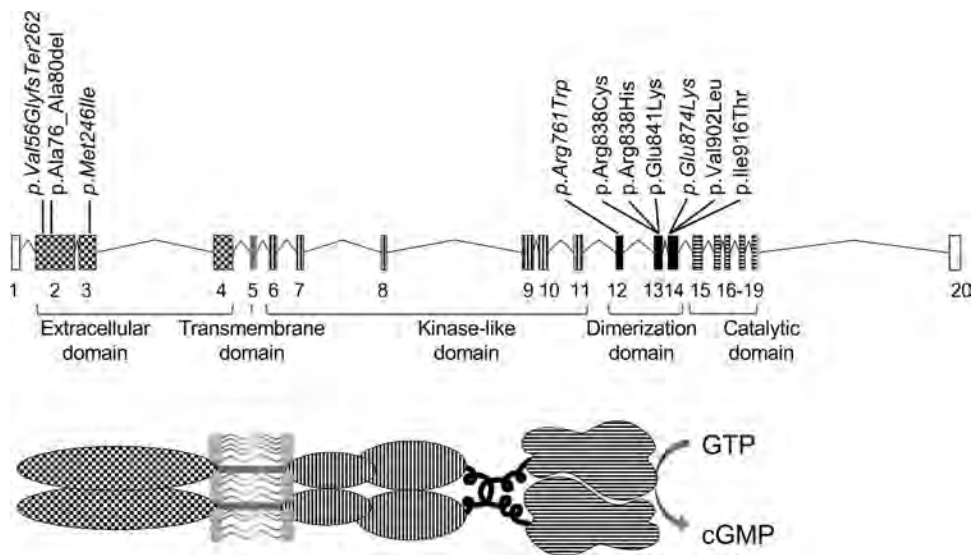


Figure 5. A schematic genetic and protein structure of *GUCY2D* and the location of the detected variants. The *GUCY2D* gene (ENST00000254854.4) contains 20 exons that encode a protein containing an extracellular domain, transmembrane domain, kinase-like domain, dimerization domain, catalytic domain, and others (Lazar et al., 2014). The 10 variants detected in this study are presented. The four novel variants are shown: p.Val56GlyfsTer262, p.Met246Ile, p.Arg761Trp, and p.Glu874Lys.

with the dimerization domain in the *GUCY2D* protein, and the other missense variant was in exon 3, which is associated with the extracellular domain (Fig. 4). Complete evolutionary conservation was confirmed in six missense variants (p.Met246Ile, p.Arg838His, p.Arg838Cys, p.Glu841Lys, p.Glu874Lys, p.Val902Leu) and relatively high conservation was found in two variants (p.Arg761Trp, p.Ile916Thr) (Fig. 5).

The allele frequency available for three *GUCY2D* variants (p.Ala80_Leu84del, p.Arg761Trp, and p.Arg838Cys) in the East Asian/South Asian/African/European (non-Finnish) general population was 0.0%/0.000055%/0.00085%/0.0%, 0.0%/0.0%/0.0%/0.000045%, and 0.0%/0.0%/0.0%/0.0%, respectively. All detected *GUCY2D* variants were not found in the general Japanese population according to the HGVD and iJGVD databases.

General prediction, functional prediction, and conservation were assessed for the 10 *GUCY2D* variants, and the pathogenicity classification according to the American College of Medical Genetics and Genomics guidelines was pathogenic for the four missense variants (p.Arg838His, p.Arg838Cys, p.Glu841Lys, p.Val902Leu); likely pathogenic for the truncating variant, the in-frame deletion variant, and the missense variant (p.Val56GlyfsTer262, p.Ala80_Leu84del, p.Ile916Thr, respectively); and

uncertain significance for the three missense variants (p.Met246Ile, p.Arg761Trp, p.Glu874Lys).

Overall, 10 disease-causing variants in the *GUCY2D* gene were ascertained in nine families with ADCORD, one family with ARCORD, one family with MD, and one family with ARLCA. Together with the clinical features of the affected subjects and the models of inheritance in the pedigree, 10 disease-causing variants in the *GUCY2D* gene were determined.

Discussion

The detailed clinical and genetic characteristics of a cohort of 15 affected subjects from 12 families with *GUCY2D*-RD are illustrated in a nationwide cohort with IRD in Japan. Different clinical presentations were identified with different inheritance patterns, including ADCORD with various severities, severe ARLCA, severe ARCORD, and mild ADMD.

To our knowledge, this large cohort of *GUCY2D*-RD patients includes the highest number of ADCORD patients to date. Four of 30 families (13.3%) with ADCORD/MD/STGD in the JEGC IRD cohort were associated with AD*GUCY2D*-CORD. The proportion of *GUCY2D*-RD in molecularly confirmed ADCORD/MD/STGD in the JEGC cohort was 27.2% (6/22 families). In a previous report of a Chinese cohort, Jiang et al. reported nine unrelated probands

with *GUCY2D*-RD ascertained from 74 probands with COD (9/74, 12.2%) and seven of 15 ADCORD families had *GUCY2D*-RD (7/15, 46.7%).³⁷ The proportion of *GUCY2D*-RD in molecularly confirmed ADCORD was 34.6% in a UK cohort and 29.4% in a French cohort.^{5,48} Given these results, the prevalence of *GUCY2D*-RD for COD in Japan was not as high as that in other populations in Asia or Europe; however, *GUCY2D*-RD is a major cause of the ADCORD.

One family with ARLCA was ascertained from 41 families with AR or sporadic LCA in the JEGC cohort (1/41 families, 2.4%). The proportion of *GUCY2D*-RD for molecularly confirmed LCA in the JEGC cohort was 5.3% (1/19 families). Hosono et al. reported two families with ARLCA in 34 Japanese families with LCA (2/34, 5.9%).³⁶ In previous reports of Chinese cohorts, Wang et al. reported the prevalence of *GUCY2D*-RD as 10.7% (14/131 LCA families), and Xu et al. reported the prevalence as 10.7% (17/159 LCA families).^{49,50} In European cohorts, *GUCY2D*-RD accounts for approximately 10% to 20% of LCA.⁴ These findings imply the low prevalence of ARLCA in the Japanese population, although data from a larger cohort of *ARGUCY2D*-LCA patients are still to draw conclusions.

In the present study of Japanese *GUCY2D*-RD, there were no patients with SNB. There was one 12-year-old subject with night blindness, favorable VA, normal fundus, and compound heterozygous *GUCY2D* variants (patient 2). These findings were consistent with the spectrum of SNB; however, this subject demonstrated undetectable generalized cone function with severely decreased rod function, which is not compatible with the striking ERG features of SNB (undetectable rod responses with identical traces for a single cone and DA bright flash ERGs).⁴⁰

Thirteen affected subjects from nine families with molecularly confirmed *GUCY2D*-associated ADCORD demonstrated various findings, in terms of onset (0-41 years), the duration of disease (0-40 years), VA (0.0-1.52) in LogMAR units, fundus appearance (normal to extended atrophy, without/with intrachoroidal cavitation), and morphological finding (EZ preservation at the fovea to outer retinal disruption at the macula and paramacula); however, ocular symptoms such as reduced VA/poor VA, photophobia, and the pattern of dysfunction in electrophysiology with early involvement of generalized cone function were commonly shared.

Several reports have described patients with COD/CORD showing a coloboma-like macular atrophy caused by pathogenic variants in several genes, such as *NMNAT1*,^{51,52} *ADAM9*,⁵³ *GUCAIA*,⁵⁴ and

GUCY2D.⁵⁵ In the present study, an intrachoroidal cavitation resembling coloboma-like macular atrophy was presented in three subjects bilaterally or unilaterally. Poor visual acuity was observed in the eyes with intrachoroidal cavitation; thus, this striking finding implies severe central visual loss. The mechanism that causes the coloboma-like macular atrophy/intrachoroidal cavitation remains uncertain.

All eight subjects with normal or subtle changes demonstrated generalized retinal dysfunction (patients 2-4, 6, 8, 9, 11, 14), which is crucial to make a clinical diagnosis of *GUCY2D*-RD. Interestingly, a lower b-to-a ratio in dark-adapted bright flash responses was identified in three subjects (3/14, 21.4%). This electronegative finding is also observed in the early stage of other COD and may not be specific for *GUCY2D*-RD.^{11-13,16,56} These findings are consistent with previous reports of *ADGUCY2D*-CORD.^{20,34,37,38} Therefore, comprehensive clinical investigations, including electrophysiological assessments, are essential for the diagnosis and monitoring of *GUCY2D*-RD.

Ten *GUCY2D* variants were identified in our cohort, including six previously reported and four novel variants. Six pathogenic and three likely pathogenic variants have been previously reported, and the phenotype subgroups determined in our cohort were compatible with those of the previous reports, whereas the phenotype subgroup for p.Ile916Thr in our cohort was MD, and the phenotype subgroup for this variant in the previous report was COD. Two variants (p.Arg838His, p.Val902Leu) were found in the de novo state in our cohort (patients 11, 13), and these variants were also identified as de novo in the previous report.^{31,39} Because haplotype analysis around these variants was not performed, the possibility of the nonpaternity cannot be formally excluded in these families (families 8, 10). Therefore, it is more precise to describe these variants not found in parents as “most likely de novo.” A different inheritance pattern of ADCORD was described for p.Ala80_Leu84del in the previous report⁹; however, the detailed information of the parents of the proband was not shown. Thus, the disease causation by this variant, in our case with AR inheritance (patient 2), is still unclear.

Four novel *GUCY2D* variants were found in our cohort: one variant with likely pathogenic frameshift (p.Val56GlyfsTer262) and three variants of uncertain significance (p.Met246Ile, p.Arg761Trp, p.Glu874Lys). Two variants in the compound heterozygous state (p.Val56GlyfsTer262, p.Met246Ile) were found in a subject with ARLCA (Patient 1). Because there are no candidate variants for the other ARLCA-associated genes, the putative causation of these

two *GUCY2D* variants is predicted. One missense variant (p.Arg761Trp) was found in a subject with night blindness, normal fundus, relatively preserved foveal structure, and a loss of generalized retinal function. Although there were no candidate variants causative for *ARRP*, *ARCORD*, and *ARLCA*, further detailed analyses with more samples/information of the other family members are required to decide the conclusive genetic diagnosis. Another missense variant (p.Glu874Lys) was identified with the aforementioned in-frame deletion variant (p.Ala80_Leu84del) in a subject with *ARCORD* (patient 2). Given the clinically examined unaffected mother harboring this variant (p.Glu874Lys), the possibility that the disease was caused by this variant in an AR manner cannot be excluded.

This study has several limitations. The selection bias related to disease severity is inherent because it is uncommon for genetically affected subjects with good vision to visit clinics or hospitals. The resources of clinical information or genomic DNA from unaffected family members are limited in our cohort, and it was hard to conclusively determine the inheritance pattern in most families. Further information on clinical and genetic assessment both in affected and unaffected subjects could improve the accuracy of clinical inheritance, as well as molecularly confirmed inheritance.

The data of the current study were obtained from the JEGC IRD database. The clinical data from patients registered from multiple institutions were uploaded into the database and shared among the JEGC study group. However, the examination devices used at the different institutions could have been different because the diagnostic criteria and monitoring methods were shared. It is of note that the information was collected retrospectively, and that some of the interpatient variability may be due to differences in methods of testing patients in different institutions. Therefore, a detailed quantitative analysis could not be performed.

WES with targeted analysis applied in the current study could miss the disease-causing variants in the genes outside of the target (301 retinal disease-associated genes) and structural variants, including large deletions in the target region. More comprehensive gene screening and analysis by methods such as long-read whole-genome sequencing could help to determine the genetic aberrations, including structural and noncoding variants, in our cohort. The molecular mechanisms of some AD missense, AR missense, and AR in-frame deletion variants have not yet been clarified, and further functional investigation for each variant is required to draw conclusions on the disease causation.

In conclusion, this nationwide large cohort study delineates the clinical and genetic characteristics of *GUCY2D*-RD, including nine *ADCORD* families, one *ARCORD* family, one MD family, and one *ARLCA* family. Diverse clinical presentations with various severities were demonstrated in *ADCORD*, and an early-onset severe phenotype was shown in *ARLCA*. A relatively low prevalence of *GUCY2D*-RD for *ADCORD* and *ARLCA* in the Japanese population was identified compared to the other populations. This information helps to monitor and counsel patients, especially in East Asia, as well as to design future therapeutic approaches.

Acknowledgments

We thank Kazuki Yamazawa and Satomi Inoue, National Institute of Sensory Organs, National Tokyo Medical Center, Japan, for their help in the clinical genetic data analysis.

The laboratory of Visual Physiology, Division for Vision Research, National Institute of Sensory Organs, National Hospital Organization, Tokyo Medical Center, Tokyo, Japan is supported by grants from Astellas Pharma Inc. (NCT03281005), outside the submitted work. Supported by grants from Grant-in-Aid for Young Scientists (A) of the Ministry of Education, Culture, Sports, Science and Technology, Japan (16H06269); grants from Grant-in-Aid for Scientists to support international collaborative studies of the Ministry of Education, Culture, Sports, Science and Technology, Japan (16KK01930002); grants from the National Hospital Organization Network Research Fund (H30-NHO-Sensory Organs-03); grants from FOUNDATION FIGHTING BLINDNESS ALAN LATIES CAREER DEVELOPMENT PROGRAM (CF-CL-0416-0696-UCL); grants from Health Labour Sciences Research Grant, the Ministry of Health, Labour and Welfare (201711107A); and grants from the Great Britain Sasakawa Foundation Butterfield Awards (KF). Supported by grants from Grant-in-Aid for Young Scientists of the Ministry of Education, Culture, Sports, Science and Technology, Japan (18K16943) (YF-Y). Supported by a Fight for Sight (UK) early career investigator award, NIHR-BRC at Moorfields Eye Hospital and the UCL Institute of Ophthalmology, NIHR-BRC at Great Ormond Street Hospital and UCL Institute of Child Health, and Great Britain Sasakawa Foundation Butterfield Award, UK (GA). Funded by the NIHR-BRC at Moorfields Eye Hospital and the UCL Institute of Ophthalmology (NP). Supported by Tsubota Laboratory, Inc, Fuji

Xerox Co., Ltd, Kirin Company, Ltd, Kowa Company, Ltd, Novartis Pharmaceuticals, Santen Pharmaceutical Co. Ltd, and ROHTO Pharmaceutical Co.,Ltd. (TK). Supported by the Japan Agency for Medical Research and Development (AMED) (18ek0109282h0002) (TI). Supported by AMED; the Ministry of Health, Labor and Welfare, Japan (18ek0109282h0002); Grants-in-Aid for Scientific Research, Japan Society for the Promotion of Science, Japan (H26-26462674); grants from the National Hospital Organization Network Research Fund, Japan (H30-NHO-Sensory Organs-03) and Novartis Research Grant (2018) (KT). The funding sources had no role in the design and conduct of the study; the collection, management, analysis, and interpretation of the data; the preparation, review, and approval of the manuscript; or the decision to submit the manuscript for publication.

Kaoru Fujinami has full access to all the data in the study and takes responsibility for the integrity of the data and the accuracy of the data analysis. Research design: Xiao Liu, Kaoru Fujinami, Lizhu Yang, Yu Fujinami-Yokokawa, Kazushige Tsunoda. Data acquisition and/or research execution: All authors. Data analysis and/or interpretation: All authors. Manuscript preparation: Xiao Liu, Kaoru Fujinami, Lizhu Yang, Yu Fujinami-Yokokawa, Gavin Arno, Nikolas Pontikos, Kazushige Tsunoda.

Disclosure: **X. Liu**, None; **K. Fujinami**, Astellas Pharma Inc. (C, F), Kubota Pharmaceutical Holdings Co. Ltd (C, F), Acucela Inc. (C, F), Novartis AG (C), Janssen Pharmaceutical K.K. (C), NightStar (C, F), SANTEN Company Limited (F), Foundation Fighting Blindness (F), Foundation Fighting Blindness Clinical Research Institute (F), Japanese Ophthalmology Society (F), Japan Retinitis Pigmentosa Society (F); **K. Kuniyoshi**, None; **M. Kondo**, None; **S. Ueno**, None; **T. Hayashi**, None; **K. Mochizuki**, None; **S. Kameya**, None; **L. Yang**, None; **Y. Fujinami-Yokokawa**, None; **G. Arno**, None; **N. Pontikos**, None; **H. Sakuramoto**, None; **T. Kominami**, None; **H. Terasaki**, None; **S. Katagiri**, None; **K. Mizobuchi**, None; **N. Nakamura**, None; **K. Yoshitake**, None; **Y. Miyake**, None; **S. Li**, None; **T. Kurihara**, Tsubota Laboratory, Inc. (F), Fuji Xerox Co., Ltd. (F), Kirin Company, Ltd. (F), Kowa Company, Ltd. (F), Novartis Pharmaceuticals (F), Santen Pharmaceutical Co., Ltd. (F), ROHTO Pharmaceutical Co., Ltd. (F); **K. Tsubota**, None; **T. Iwata**, None; **K. Tsunoda**, None

* XL and KF are joint first authors.

References

1. Liew G, Michaelides M, Bunce C. A comparison of the causes of blindness certifications in England and Wales in working age adults (16-64 years), 1999-2000 with 2009-2010. *BMJ Open*. 2014;4:e004015.
2. Tee JJ, Smith AJ, Hardcastle AJ, Michaelides M. RPGR-associated retinopathy: clinical features, molecular genetics, animal models and therapeutic options. *Br J Ophthalmol*. 2016;100:1022-1027.
3. Hirji N, Aboshiha J, Georgiou M, Bainbridge J, Michaelides M. Achromatopsia: clinical features, molecular genetics, animal models and therapeutic options. *Ophthalmic Genet*. 2018;39:149-157.
4. Kumaran N, Pennesi ME, Yang P, et al. Leber congenital amaurosis/early-onset severe retinal dystrophy overview. In: Adam MP, Ardinger HH, Pagon RA, et al. (eds), *GeneReviews*(*(R)*). Seattle (WA); 2018.
5. Gill JS, Georgiou M, Kalitzeos A, Moore AT, Michaelides M. Progressive cone and cone-rod dystrophies: clinical features, molecular genetics and prospects for therapy. *Br J Ophthalmol*. 2019;103:711-720.
6. Tanna P, Strauss RW, Fujinami K, Michaelides M. Stargardt disease: clinical features, molecular genetics, animal models and therapeutic options. *Br J Ophthalmol*. 2017;101:25-30.
7. Neveling K, Collin RW, Gilissen C, et al. Next-generation genetic testing for retinitis pigmentosa. *Hum Mutat*. 2012;33:963-972.
8. Stone EM, Andorf JL, Whitmore SS, et al. Clinically focused molecular investigation of 1000 consecutive families with inherited retinal disease. *Ophthalmology*. 2017;124:1314-1331.
9. Carss KJ, Arno G, Erwood M, et al. Comprehensive rare variant analysis via whole-genome sequencing to determine the molecular pathology of inherited retinal disease. *Am J Hum Genet*. 2017;100:75-90.
10. Michaelides M, Hardcastle AJ, Hunt DM, Moore AT. Progressive cone and cone-rod dystrophies: phenotypes and underlying molecular genetic basis. *Surv Ophthalmol*. 2006;51:232-258.
11. Fujinami K, Lois N, Davidson AE, et al. A longitudinal study of Stargardt disease: clinical and electrophysiologic assessment, progression, and genotype correlations. *Am J Ophthalmol*. 2013;155:1075-1088 e1013.

12. Fujinami K, Sergouniotis PI, Davidson AE, et al. The clinical effect of homozygous ABCA4 alleles in 18 patients. *Ophthalmology*. 2013;120:2324–2331.
13. Hull S, Arno G, Plagnol V, et al. The phenotypic variability of retinal dystrophies associated with mutations in *CRX*, with report of a novel macular dystrophy phenotype. *Invest Ophthalmol Vis Sci*. 2014;55:6934–6944.
14. Oishi M, Oishi A, Gotoh N, et al. Comprehensive molecular diagnosis of a large cohort of Japanese retinitis pigmentosa and Usher syndrome patients by next-generation sequencing. *Invest Ophthalmol Vis Sci*. 2014;55:7369–7375.
15. Arai Y, Maeda A, Hirami Y, et al. Retinitis pigmentosa with *EYS* mutations is the most prevalent inherited retinal dystrophy in Japanese populations. *J Ophthalmol*. 2015;2015:819760.
16. Fujinami K, Zernant J, Chana RK, et al. Clinical and molecular characteristics of childhood-onset Stargardt disease. *Ophthalmology*. 2015;122:326–334.
17. Nakanishi A, Ueno S, Hayashi T, et al. Clinical and genetic findings of autosomal recessive bestrophinopathy in Japanese cohort. *Am J Ophthalmol*. 2016;168:86–94.
18. Oishi M, Oishi A, Gotoh N, et al. Next-generation sequencing-based comprehensive molecular analysis of 43 Japanese patients with cone and cone-rod dystrophies. *Mol Vis*. 2016;22:150–160.
19. Perrault I, Rozet JM, Calvas P, et al. Retinal-specific guanylate cyclase gene mutations in Leber's congenital amaurosis. *Nat Genet*. 1996;14:461–464.
20. Sharon D, Wimberg H, Kinarty Y, Koch KW. Genotype-functional-phenotype correlations in photoreceptor guanylate cyclase (GC-E) encoded by *GUCY2D*. *Prog Retin Eye Res*. 2018;63:69–91.
21. Goraczniak RM, Duda T, Sitaramayya A, Sharma RK. Structural and functional characterization of the rod outer segment membrane guanylate cyclase. *Biochem J*. 1994;302(Pt 2):455–461.
22. Yang RB, Foster DC, Garbers DL, Fulle HJ. Two membrane forms of guanylyl cyclase found in the eye. *Proc Natl Acad Sci USA*. 1995;92:602–606.
23. Goraczniak R, Duda T, Sharma RK. Structural and functional characterization of a second subfamily member of the calcium-modulated bovine rod outer segment membrane guanylate cyclase, ROS-GC2. *Biochem Biophys Res Commun*. 1997;234:666–670.
24. Pugh EN, Jr., Duda T, Sitaramayya A, Sharma RK. Photoreceptor guanylate cyclases: a review. *Biosci Rep*. 1997;17:429–473.
25. Dizhoor AM, Hurley JB. Regulation of photoreceptor membrane guanylyl cyclases by guanylyl cyclase activator proteins. *Methods*. 1999;19:521–531.
26. Hunt DM, Buch P, Michaelides M. Guanylate cyclases and associated activator proteins in retinal disease. *Mol Cell Biochem*. 2010;334:157–168.
27. Camuzat A, Dollfus H, Rozet JM, et al. A gene for Leber's congenital amaurosis maps to chromosome 17p. *Hum Mol Genet*. 1995;4:1447–1452.
28. Downes SM, Payne AM, Kelsell RE, et al. Autosomal dominant cone-rod dystrophy with mutations in the guanylate cyclase 2D gene encoding retinal guanylate cyclase-1. *Arch Ophthalmol*. 2001;119:1667–1673.
29. Kelsell RE, Gregory-Evans K, Payne AM, et al. Mutations in the retinal guanylate cyclase (*RETGC-1*) gene in dominant cone-rod dystrophy. *Hum Mol Genet*. 1998;7:1179–1184.
30. Lazar CH, Mutsuddi M, Kimchi A, et al. Whole exome sequencing reveals *GUCY2D* as a major gene associated with cone and cone-rod dystrophy in Israel. *Invest Ophthalmol Vis Sci*. 2014;56:420–430.
31. Wimberg H, Lev D, Yosovich K, et al. Photoreceptor guanylate cyclase (*GUCY2D*) mutations cause retinal dystrophies by severe malfunction of Ca(2+)-dependent cyclic GMP synthesis. *Front Mol Neurosci*. 2018;11:348.
32. de Castro-Miro M, Pomares E, Lores-Motta L, et al. Combined genetic and high-throughput strategies for molecular diagnosis of inherited retinal dystrophies. *PLoS One*. 2014;9:e88410.
33. Ito S, Nakamura M, Nuno Y, Ohnishi Y, Nishida T, Miyake Y. Novel complex *GUCY2D* mutation in Japanese family with cone-rod dystrophy. *Invest Ophthalmol Vis Sci*. 2004;45:1480–1485.
34. Ito S, Nakamura M, Ohnishi Y, Miyake Y. Autosomal dominant cone-rod dystrophy with R838H and R838C mutations in the *GUCY2D* gene in Japanese patients. *Jpn J Ophthalmol*. 2004;48:228–235.
35. Hosono K, Harada Y, Kurata K, et al. Novel *GUCY2D* gene mutations in Japanese male twins with Leber congenital amaurosis. *J Ophthalmol*. 2015;2015:693468.
36. Hosono K, Nishina S, Yokoi T, et al. Molecular diagnosis of 34 Japanese families with Leber congenital amaurosis using targeted next generation sequencing. *Sci Rep*. 2018;8:8279.
37. Jiang F, Xu K, Zhang X, Xie Y, Bai F, Li Y. *GUCY2D* mutations in a Chinese cohort with autosomal dominant cone or cone-rod dystrophies. *Doc Ophthalmol*. 2015;131:105–114.
38. Payne AM, Morris AG, Downes SM, et al. Clustering and frequency of mutations in the retinal

- guanylate cyclase (*GUCY2D*) gene in patients with dominant cone-rod dystrophies. *J Med Genet.* 2001;38:611–614.
39. Mukherjee R, Robson AG, Holder GE, et al. A detailed phenotypic description of autosomal dominant cone dystrophy due to a de novo mutation in the *GUCY2D* gene. *Eye (Lond).* 2014;28:481–487.
 40. Stunkel ML, Brodie SE, Cideciyan AV, et al. Expanded retinal disease spectrum associated with autosomal recessive mutations in *GUCY2D*. *Am J Ophthalmol.* 2018;190:58–68.
 41. Fujinami K, Kameya S, Kikuchi S, et al. Novel *RP1L1* variants and genotype-photoreceptor microstructural phenotype associations in cohort of Japanese patients with occult macular dystrophy. *Invest Ophthalmol Vis Sci.* 2016;57:4837–4846.
 42. Hood DC, Bach M, Brigell M, et al. ISCEV standard for clinical multifocal electroretinography (mfERG) (2011 edition). *Doc Ophthalmol.* 2012;124:1–13.
 43. McCulloch DL, Marmor MF, Brigell MG, et al. Erratum to: ISCEV Standard for full-field clinical electroretinography (2015 update). *Doc Ophthalmol.* 2015;131:81–83.
 44. McCulloch DL, Marmor MF, Brigell MG, et al. ISCEV Standard for full-field clinical electroretinography (2015 update). *Doc Ophthalmol.* 2015;130:1–12.
 45. Terasaki H, Miyake Y, Nomura R, et al. Focal macular ERGs in eyes after removal of macular ILM during macular hole surgery. *Invest Ophthalmol Vis Sci.* 2001;42:229–234.
 46. Pontikos N, Yu J, Moghul I, et al. Phenopolis: an open platform for harmonization and analysis of genetic and phenotypic data. *Bioinformatics.* 2017;33:2421–2423.
 47. Richards S, Aziz N, Bale S, et al. Standards and guidelines for the interpretation of sequence variants: a joint consensus recommendation of the American College of Medical Genetics and Genomics and the Association for Molecular Pathology. *Genet Med.* 2015;17:405–424.
 48. Boulanger-Scemama E, El Shamieh S, Demontant V, et al. Next-generation sequencing applied to a large French cone and cone-rod dystrophy cohort: mutation spectrum and new genotype-phenotype correlation. *Orphanet J Rare Dis.* 2015;10:85.
 49. Wang H, Wang X, Zou X, et al. Comprehensive molecular diagnosis of a large Chinese Leber congenital amaurosis cohort. *Invest Ophthalmol Vis Sci.* 2015;56:3642–3655.
 50. Xu Y, Xiao X, Li S, et al. Molecular genetics of Leber congenital amaurosis in Chinese: new data from 66 probands and mutation overview of 159 probands. *Exp Eye Res.* 2016;149:93–99.
 51. Falk MJ, Zhang Q, Nakamaru-Ogiso E, et al. *NMNAT1* mutations cause Leber congenital amaurosis. *Nat Genet.* 2012;44:1040–1045.
 52. Nash BM, Symes R, Goel H, et al. *NMNAT1* variants cause cone and cone-rod dystrophy. *Eur J Hum Genet.* 2018;26:428–433.
 53. El-Haig WM, Jakobsson C, Favez T, Schorderet DF, Abouzeid H. Novel *ADAM9* homozygous mutation in a consanguineous Egyptian family with severe cone-rod dystrophy and cataract. *Br J Ophthalmol.* 2014;98:1718–1723.
 54. Kamenarova K, Corton M, Garcia-Sandoval B, et al. Novel *GUCA1A* mutations suggesting possible mechanisms of pathogenesis in cone, cone-rod, and macular dystrophy patients. *Biomed Res Int.* 2013;2013:517570.
 55. Xu F, Dong F, Li H, Li X, Jiang R, Sui R. Phenotypic characterization of a Chinese family with autosomal dominant cone-rod dystrophy related to *GUCY2D*. *Doc Ophthalmol.* 2013;126:233–240.
 56. Khan KN, Kasilian M, Mahroo OAR, et al. Early patterns of macular degeneration in *ABCA4*-associated retinopathy. *Ophthalmology.* 2018;125:735–746.



RESEARCH ARTICLE

Clinical and genetic characteristics of Stargardt disease in a large Western China cohort: Report 1

Xiao Liu^{1,2,3} | Xiaohong Meng¹ | Lizhu Yang^{2,3} | Yanling Long¹ |
Yu Fujinami-Yokokawa^{2,4,5} | Jiayun Ren¹ | Toshihide Kurihara³ | Kazuo Tsubota³ |
Kazushige Tsunoda² | Kaoru Fujinami^{2,3,6,7} | Shiyong Li¹ | East Asia Inherited
Retinal Disease Society Study Group

¹Southwest Hospital/Southwest Eye Hospital, Third Military Medical University (Army Medical University), Chongqing, China

²Laboratory of Visual Physiology, Division of Vision Research, National Institute of Sensory Organs, National Hospital Organization Tokyo Medical Center, Tokyo, Japan

³Department of Ophthalmology, Keio University School of Medicine, Tokyo, Japan

⁴Department of Health Policy and Management, Keio University School of Medicine, Tokyo, Japan

⁵Department of Public Health Research, Yokokawa Clinic, Osaka, Japan

⁶UCL Institute of Ophthalmology, London, UK

⁷Moorfields Eye Hospital, London, UK

Correspondence

Kaoru Fujinami, 2-5-1, Higashigaoka, Meguro-ku, Laboratory of Visual Physiology, Division for Vision Research, National Institute of Sensory Organs, National Hospital Organization, Tokyo Medical Center, Tokyo 152-8902 Japan.
Email: k.fujinami@ucl.ac.uk

Shiyong Li, Southwest Hospital/Southwest Eye Hospital, Third Military Medical University (Army Medical University), No. 30 Gaotanyan Street, Shapingba District, Chongqing 400038, P.R. China.
Email: shiyong_li@126.com

Funding information

Chongqing Social and Livelihood Science Innovation grant, Grant/Award Number: cstc2017shmsA130100; Foundation for Fighting Blindness - Alan Lattes Career Development Program, Grant/Award Number: CF-CL-0416-0696-UCL; Grant-in-Aid for Scientists to support international collaborative studies of the Ministry of Education, Culture, Sports, Science and Technology, Japan, Grant/Award Number: 16KK01930002; Grant-in-Aid for Young Scientists (A) of the Ministry of Education, Culture, Sports, Science and

Abstract

Stargardt disease 1 (STGD1) is the most prevalent retinal dystrophy caused by pathogenic biallelic *ABCA4* variants. Forty-two unrelated patients mostly originating from Western China were recruited. Comprehensive ophthalmological examinations, including visual acuity measurements (subjective function), fundus autofluorescence (retinal imaging), and full-field electroretinography (objective function), were performed. Next-generation sequencing (target/whole exome) and direct sequencing were conducted. Genotype grouping was performed based on the presence of deleterious variants. The median age of onset/age was 10.0 (5–52)/29.5 (12–72) years, and the median visual acuity in the right/left eye was 1.30 (0.15–2.28)/1.30 (0.15–2.28) in the logarithm of the minimum angle of resolution unit. Ten patients (10/38, 27.0%) showed confined macular dysfunction, and 27 (27/37, 73.7%) had generalized retinal dysfunction. Fifty-eight pathogenic/likely pathogenic *ABCA4* variants, including 14 novel variants, were identified. Eight patients (8/35, 22.8%) harbored multiple deleterious variants, and 17 (17/35, 48.6%) had a single deleterious variant. Significant associations were revealed between subjective functional, retinal imaging, and objective functional groups, identifying a significant genotype–phenotype association. This study illustrates a large phenotypic/genotypic spectrum in a large well-characterized STGD1 cohort. A

This is an open access article under the terms of the Creative Commons Attribution-NonCommercial-NoDerivs License, which permits use and distribution in any medium, provided the original work is properly cited, the use is non-commercial and no modifications or adaptations are made.

© 2020 The Authors. *American Journal of Medical Genetics Part C: Seminars in Medical Genetics* published by Wiley Periodicals LLC.

Technology, Japan, Grant/Award Numbers: 16H06269, 18K16943; Health Labor Sciences Research Grant, The Ministry of Health, Labor and Welfare, Grant/Award Number: 201711107A; National Basic Research Program of China, Grant/Award Number: 2018YFA0107301; National Hospital Organization Network Research Fund, Grant/Award Number: H30-NHO-2-12; National Nature Science Foundation of China, Grant/Award Number: 81974138; The Great Britain Sasakawa Foundation Butterfield Awards

distinct genetic background of the Chinese population from the Caucasian population was identified; meanwhile, a genotype–phenotype association was similarly represented.

KEYWORDS

ABCA4, electroretinogram, multifocal electroretinogram, Stargardt disease

1 | INTRODUCTION

Stargardt disease (STGD1; MIM 248200), first described by Karl Stargardt, is an autosomal recessive retinal dystrophy caused by biallelic pathogenic variants in the *ABCA4* gene (ATP-binding cassette subfamily A member 4; MIM 601691) (Allikmets et al., 1997; K S, 1909). The *ABCA4* gene encodes a transmembrane rim protein (a member of the ABCA subfamily of ATP-binding cassette [ABC] transporters) in the outer segment discs of photoreceptors, which is involved in the active transport of retinoids from photoreceptors to retinal pigment epithelium (RPE) (Molday, 2015; Molday, Zhong, & Quazi, 2009; Quazi, Lenevich, & Molday, 2012). Failure of the transport results in accelerated deposition of a major lipofuscin fluorophore (N-retinylidene-N-retinylethanolamine; A2E) in the RPE, and A2E-associated cytotoxicity is believed to cause RPE dysfunction with subsequent photoreceptor cell loss over time (Chen et al., 2012; Maeda, Maeda, Golczak, & Palczewski, 2008; Molday, Rabin, & Molday, 2000; Tsybovsky, Molday, & Palczewski, 2010).

STGD1, with a prevalence of 1 in 8,000–10,000, is one of the most common inherited macular dystrophies with characteristic features, including macular atrophy and yellow–white flecks at the level of the RPE at the posterior pole (Gill, Georgiou, Kalitzeos, Moore, & Michaelides, 2019; Liu, Fujinami, Yang, Arno, & Fujinami, 2019; Rahman, Georgiou, Khan, & Michaelides, 2020; Tanna, Strauss, Fujinami, & Michaelides, 2017). Onset is most common in teens but variable, and a severe and progressive phenotype has been associated with childhood-onset and a mild phenotype with late-onset (Fujinami et al., 2011; Fujinami, Lois, Davidson, et al., 2013; Fujinami, Lois, Mukherjee, et al., 2013; Fujinami, Sergouniotis, Davidson, Mackay, et al., 2013; Fujinami, Sergouniotis, Davidson, Wright, et al., 2013; Fujinami et al., 2014; Fujinami et al., 2015; Fujinami-Yokokawa et al., 2019; Georgiou et al., 2020; Gill et al., 2019; Khan et al., 2018; Liu et al., 2019; Rahman et al., 2020; Singh, Fujinami, Chen, Michaelides, & Moore, 2014; Tanna et al., 2017, 2019). The vast phenotypic heterogeneity and variable severity of *ABCA4*-associated retinopathy are well-known and encompass macular atrophy without flecks, bull's-eye maculopathy, fundus flavimaculatus (retinal flecks without macular atrophy), a foveal sparing phenotype, cone-rod dystrophy, and “retinitis pigmentosa”; genotype–phenotype associations have been reported based on clinical severity and the presence of deleterious variants (Fujinami et al., 2011, 2014, 2015; Fujinami, Lois, Davidson, et al., 2013; Fujinami, Lois, Mukherjee, et al., 2013;

Fujinami, Sergouniotis, Davidson, Mackay, et al., 2013; Fujinami, Sergouniotis, Davidson, Wright, et al., 2013; Georgiou et al., 2020; McBain, Townend, & Lois, 2012; Singh et al., 2014; Strauss et al., 2019; Tanna et al., 2017, 2019; Testa et al., 2014).

Cross-sectional and longitudinal studies in large cohorts focusing mainly on the European population have been widely performed (Fujinami, Zernant, et al., 2013; Fujinami et al., 2019; Kong et al., 2016, 2018; Schonbach et al., 2017; Schulz et al., 2017; Strauss et al., 2016; Strauss, Munoz, Ho, Jha, Michaelides, Cideciyan, et al., 2017; Strauss, Munoz, Ho, Jha, Michaelides, Mohand-Said, et al., 2017; Strauss et al., 2019). Clinical trials of treatments including visual cycle modification (ClinicalTrials.gov Identifier: NCT02402660), gene augmentation therapy (ClinicalTrials.gov Identifier: NCT01367444), and stem cell therapy (ClinicalTrials.gov Identifier: NCT01469832) are ongoing mainly in Europe/North America (Charbel Issa, Barnard, Herrmann, Washington, & MacLaren, 2015; Hussain, Ciulla, et al., 2018; Hussain, Gregori, Ciulla, & Lam, 2018; Kubota et al., 2012; Kubota, Calkins, Henry, & Linsenmeier, 2019; Mehat et al., 2018; Rosenfeld et al., 2018; Schwartz et al., 2012, 2015). However, large cohort studies based on standardized clinical and genetic diagnostic criteria in the Asian population are very limited.

Therefore, the purpose of this study was to characterize the comprehensive phenotypic and genotypic features of Chinese patients with STGD1 in a large cohort in preparation for therapeutic trials. A systematic review of *ABCA4* variants was performed to delineate the genetic spectrum in the Chinese population.

2 | METHODS

The procedures applied in this study were approved by the local ethics committee of Southwest Eye Hospital, Third Military Medical University (Army Medical University), Chongqing, China (reference number: 73981486-2), and all procedures were performed in accordance with the Declaration of Helsinki.

2.1 | Participants

Patients were recruited at the Southwest Eye Hospital, Third Military Medical University (Army Medical University), Chongqing, China, from 2013 to 2019 according to the following criteria mainly described in a

previous publication: (Strauss et al., 2016) patients with multiple disease-causing variants in the *ABCA4* gene or patients with one disease-causing variant and typical clinical findings (i.e., macular atrophy with flecks) for STGD1. Clinical and molecular genetic diagnoses were confirmed by three senior doctors (XM, KF, SL). Patients who had other ocular diseases, such as choroidal neovascularization, glaucoma, and diabetic retinopathy, or were undergoing treatments/therapeutic trials were excluded.

2.2 | Clinical investigations

Detailed history and comprehensive ophthalmological examinations were conducted, including best-corrected decimal visual acuity (BCVA), dilated ophthalmoscopy, color fundus photography (non-myd WX 3D, Kowa, Tokyo, Japan), fundus autofluorescence imaging (FAF; excitation light: 488 nm, barrier filter: 500 nm, field of view: 30° × 30°, 55° × 55°; Spectralis, Heidelberg Engineering, Heidelberg, Germany), optical coherence tomography (OCT; Spectralis, Heidelberg Engineering; and ZEISS CIRRUS, Carl Zeiss Meditec AG, Oberkochen, Germany), and microperimetry (MP, MAIA, Padoba, Italy). BCVA was converted to the equivalent value in the logarithm of the minimum angle of resolution (LogMAR) unit, and low visual categories, including counting finger (CF) and hand movement (HM), were valued at 1.98 and 2.28, as reported previously (Fujinami, Lois, Mukherjee, et al., 2013; Lange, Feltgen, Junker, Schulze-Bonsel, & Bach, 2009).

Full-field electroretinograms (ffERGs; Diagnosys LLC, Lowell, MA) were recorded in accordance with the international standards of the International Society for Clinical Electrophysiology of Vision (ISCEV) (McCulloch et al., 2015a; McCulloch et al., 2015b) Multifocal ERGs (mfERGs) were recorded with a VERIS imaging system (EDI, San Mateo, CA) in accordance with the ISCEV standard protocol, and eyes with stable fixation during the mfERG recording were selected for further analyses (Hood et al., 2012).

Fundus appearance, FAF findings, OCT findings, and ffERG findings were classified based on specific features according to previous publications (Table 1) (Fujinami, Lois, Davidson, et al., 2013; Fujinami, Lois, Mukherjee, et al., 2013; Lois, Holder, Bunce, Fitzke, & Bird, 2001; Testa et al., 2014).

Fundus appearance was classified into four grades (grade 3 has three subgroups) based on the presence and location of central (macular), RPE atrophy and yellowish-white flecks. Grade 1: normal fundus; grade 2: macular and/or peripheral flecks without central atrophy; grade 3a: central atrophy without flecks; grade 3b: central atrophy with macular and/or peripheral flecks; grade 3c: paracentral atrophy with macular and/or peripheral flecks, without central atrophy; grade 4: multiple extensive atrophic changes of the RPE, extending beyond the vascular arcades.

Patterns of AF signal of the central retina and background was classified into three types. Type 1: localized low AF signal at the fovea surrounded by a homogeneous background, with/without perifoveal foci of high or low AF signal; Type 2: localized low AF signal at the

TABLE 1 Classification for fundus appearance, fundus autofluorescence images, optical coherence tomographic images, and full-field electroretinograms in Stargardt disease (STGD1)

| Grade | Fundus grade | AF pattern | OCT category | FFERG group |
|----------|---|---|--|--|
| Grade 1 | Normal fundus | Pattern 1 Localized low AF signal at the fovea surrounded by a homogeneous background with/without perifoveal foci of high or low signal | Category I EZ preservation in the fovea | Group 1 Macular dysfunction (normal full-field ERG) |
| Grade 2 | Macular and/or peripheral flecks without central atrophy | Pattern 2 Localized low AF signal at the macula surrounded by a heterogeneous background and widespread foci of high or low AF signal extending anterior to the vascular arcades | Category II EZ loss in the foveal area | Group 2 Macular dysfunction with generalized cone dysfunction |
| Grade 3a | Central atrophy without flecks | Pattern 3 Multiple areas of low AF signal at posterior pole with a heterogeneous background and/or foci of high or low signal | Category III Extensive loss of EZ line | Group 3 Macular dysfunction with generalized cone and rod dysfunction |
| Grade 3b | Central atrophy with macular and/or peripheral flecks | | | |
| Grade 3c | Para-central atrophy with macular and/or peripheral flecks, without a central atrophy | | | |

Abbreviations: AF, autofluorescence; ERG, electroretinogram; EZ, photoreceptor ellipsoid zone; RPE, retinal pigment epithelium.

macula surrounded by a heterogeneous background, and widespread foci of high or low AF signal extending anterior to the vascular arcades; Type 3: multiple areas of low AF signal at the posterior pole with a heterogeneous background, with/without foci of high or low AF signal.

Morphological changes of photoreceptor ellipsoid zone (EZ) in the central retina detected by OCT were classified into three categories. Category I: preserved EZ in the fovea; category II: loss of EZ in the fovea; category III: extensive loss of EZ.

Based on the ffERGs findings, patients were assigned to three ffERG groups. Group 1: normal ffERG responses; group 2: generalized cone ERG abnormality with normal rod responses; group 3: generalized cone and rod ERG abnormality.

The median P1 amplitude decline rates [(medical value of normative range – P1 value)/medical value of normative range] of mfERG rings 1 and 2, rings 3 and 4, and rings 5 and 6 were calculated for the analyses.

One eye was randomly selected using random.org software (<https://www.random.org/>) for the classification and analysis of fundus appearance, FAF images, OCT images, and ffERGs.

2.3 | Classification of phenotypic severity

The overall classification of phenotypic severity was performed based on the following clinical parameters mainly according to a previous publication: (Fujinami, Sergouniotis, Davidson, Mackay, et al., 2013) age of onset, BCVA (LogMAR), fundus grade, AF pattern, OCT category, and ffERG grouping (group 1: mild phenotype; group 2: moderate phenotype; and group 3: severe phenotype) (Table 2).

2.4 | Variant detection

After obtaining informed consent, peripheral venous blood samples were collected from all subjects and unaffected family members (if available) for co-segregation analysis. Genomic DNA was isolated by a standard procedure. Either eye gene-enriched (from 36 to

450 target genes) panel-based next-generation sequencing (NGS) or whole exome sequencing (WES) was performed. Sanger bi-directional sequencing was conducted to confirm the rare candidate variants (allele frequency: less than 1.0% of the general population) and to perform the co-segregation analysis. Disease-causing variants were determined from the detected variants while considering the clinical findings of the affected subjects, the pattern of inheritance in the pedigree, and the results of the co-segregation analysis.

2.5 | *In silico* molecular genetic analyses

Sequence variant nomenclature was performed according to the guidelines of the Human Genome Variation Society (HGVS; <https://varnomen.hgvs.org>) with Mutalyzer (<https://mutalyzer.nl/>). All variants were analyzed using the following databases and prediction software: GnomAD (<http://gnomad.broadinstitute.org/>), 1,000 Genome (<https://www.internationalgenome.org/>), MutationTaster (<http://www.mutationtaster.org/>), FATHMM (<http://fathmm.biocompute.org.uk/9>), SIFT (<https://www.sift.co.uk/>), PROVEAN (<http://provean.jcvi.org/index.php>), Polyphen2 (<http://genetics.bwh.harvard.edu/pph2/>) PhyloP and Phastcons from the University of California Santa Cruz database (<https://genome.ucsc.edu/index.html>), Human Splicing Finder (HSF, <http://www.umd.be/HSF3/>), Database Splicing Consensus Single Nucleotide Variant (dbSNV, <http://sites.google.com/site/jpopgen/dbSNV>), and Ensembl Variant Effect Predictor (VEP, <http://grch37.ensembl.org/info/docs/tools/vep/index.html>). Missense variants with predicted splice site alterations were treated as deleterious variants.

In accordance with the American College of Medical Genetics (ACMG) guidelines, variants were classified as pathogenic, likely pathogenic, uncertain significance (VUS), likely benign, or benign (Richards et al., 2015).

2.6 | Genotype group classification

The patients harboring multiple pathogenic or likely pathogenic variants were classified into three genotype groups based on the

TABLE 2 Classification of phenotypic severity

| | Onset of disease (years) | BCVA (logMAR) in the better eye | Fundus grade | AF type | OCT category | FfERG group |
|------------------------------|--|---------------------------------|--------------|---------|--------------|-------------|
| Mild phenotype (group 1) | Later onset (≥ 40) | < 0.78 | 1 | 1 | 1 | 1 |
| Moderate phenotype (group 2) | Patients who did not meet at least two criteria of either mild phenotype or severe phenotype were classified into the moderate phenotype subgroup. | | | | | |
| Severe phenotype (group 3) | Early onset (< 10) | > 1.0 | 4 | 3 | 3 | 3 |

Note: For the purpose of this study, patients who met at least three criteria of mild phenotype were classified into the mild phenotype subgroup and those who had at least three features of severe phenotype were classified into the severe phenotype subgroup. Patients who met both at least three features of mild phenotype and at least three features of severe phenotype were classified into group 2 (moderate phenotype).

Abbreviation: BCVA, best-corrected visual acuity in the LogMAR VA in the logarithm of the minimum angle of resolution (logMAR) unit.

number/presence of deleterious variants according to previous reports: (Fujinami et al., 2015; Fujinami et al., 2019; Fujinami, Lois, Mukherjee, et al., 2013; Kong et al., 2018) Sequence variants which presumably lead loss-of-function (frameshift, stop-gained, splice site alteration) are defined as null variants. Variants that are not likely to have null-effects such as missense variants or in-frame alteration were defined as non-null variants. Group A: patients with multiple definite or likely null variants; group B: patients with one null variant and one or more non-null variant(s); and group C: patients with multiple non-null variants.

2.7 | A systematic review of ABCA4 variants

A literature review of ABCA4-associated retinal disease in the Chinese population was performed. Peer-reviewed published papers were searched with the terms Chinese, ABCA4, and Stargardt disease; articles reporting at least 10 patients were surveyed.

In silico molecular genetic analyses were performed, and assessment of pathogenicity was performed with the same method applied in the current study cohort. Prevalent variants based on allele frequency in the affected group cohort were calculated for each study and the total study.

2.8 | Statistical analysis

Data analyses were performed using SPSS version 23.0 (IBM Corp, Armonk, NY). The age at baseline examination, age of onset, BCVA (in the LogMAR unit), MP threshold (4-2), and amplitude of P1 of mfERG were compared between fundus, FAF, OCT, fERG, and genotype groups with Mann-Whitney *U* tests. An association between phenotypic severity classification and genotype group classification was investigated by Fisher's exact test. *p* values <.05 were considered statistically significant.

3 | RESULTS

3.1 | Demographics

A total of 42 unrelated patients (28 men and 14 women) were included in this study. Two patients (A002 and A035) were from consanguineous families (Figure 1). The detailed clinical findings are presented in Data S1.

The patients mostly originated from the western part of China (32/42, 76.2%). The median age at baseline examination was 29.5 years (range, 12-72), and the median age of onset was 10 years (range, 5-52). The median BCVA, available in 40 patients, was 1.30 (range, 0.15-2.28) for the right eye and 1.30 (range, 0.15-2.28) for the left eye.

3.2 | Retinal images

The fundus photographs, autofluorescence images, and OCT images for three representative patients are shown in Figure 2.

Fundus photographs were obtained in 41 patients (Data S1). All these patients were classified into grades 3b and 4 according to their fundus appearance. No asymmetric grades were observed. There were 22 patients (22/41, 53.7%) in grade 3b and 19 (19/31, 61.3%) in grade 4 (Figure S1). There was a significant difference in BCVA between grades 3b and 4 ($p = .0004$; Data S1 and Figure S2). FAF images were obtained in 41 patients (Data S1). There were 10 patients (10/41, 24.4%) with a type 1 AF pattern, 18 (18/41, 43.9%) with a type 2 AF pattern, and 13 (13/41, 31.7%) with a type 1 AF pattern (Figure S1). No asymmetric types were observed. There were significant differences in age and BCVA between patients with AF type 1 and type 3 patterns ($p = .0111$, $p = .0167$; Data S1, Figure S2). OCT images were obtained in 39 patients (Data S1). There were eight patients (8/39, 20.5%) with category II OCT findings and 31 (31/39, 79.5%) with category III OCT findings (Figure S1). One patient (A013) showed an asymmetric classification with category II of the right eye and category III of the left eye. There was a significant difference in BCVA between patients with OCT category II and category III ($p = .000086$; Data S1, Figure S2).

3.3 | Retinal function and microperimetry

The traces of fFERGs and mfERGs and MP results for three representative patients are presented in Figure 3.

fFERGs were recorded in 37 patients (Data S1). There were 10 patients (10/37, 27.0%) in fFERG group 1, four patients (4/37, 10.8%) in group 2, and 23 patients (23/37, 62.2%) in group 3 (Figure S1). No asymmetric fFERG groups were observed. There were significant differences in age between patients in group 1 and group 2 as well as in BCVA between patients in fFERG group 1 and group 3 ($p = .034$, $p = .002$; Data S1 and Figure S2).

MfERGs were obtained in 30 patients, and 40 eyes from 24 patients with stable fixation were analyzed (Data S1). There were 15 eyes in fFERG group 1, seven eyes in fFERG group 2, and 18 eyes in fFERG group 3. The median P1 amplitude decline rates of mfERG rings 1 and 2, 3 and 4, and 5 and 6 in the fFERG groups are summarized in Table S2. There were significant differences in terms of the P1 amplitude decline rate of rings 1 and 2, rings 3 and 4, and rings 5 and 6 between fFERG group 1 and group 3 ($p = .0033$, $p = .000005$, $p = .0000009$). Significant differences were found in terms of the P1 amplitude decline rate for rings 3 and 4 and rings 5 and 6 between fFERG group 2 and group 3 ($p = .0012$, $p = .0004$). Significant differences in terms of the P1 amplitude decline rate of rings 5 and 6 were observed between fFERG group 1 and group 2 as well ($p = .059$, Figure S3).

MP was performed in 23 patients. All 23 patients showed preferred retinal locus (PRL)-fixation changes. There were 12 eyes in fFERG group 1, eight eyes in fFERG group 2, and 25 eyes in fFERG

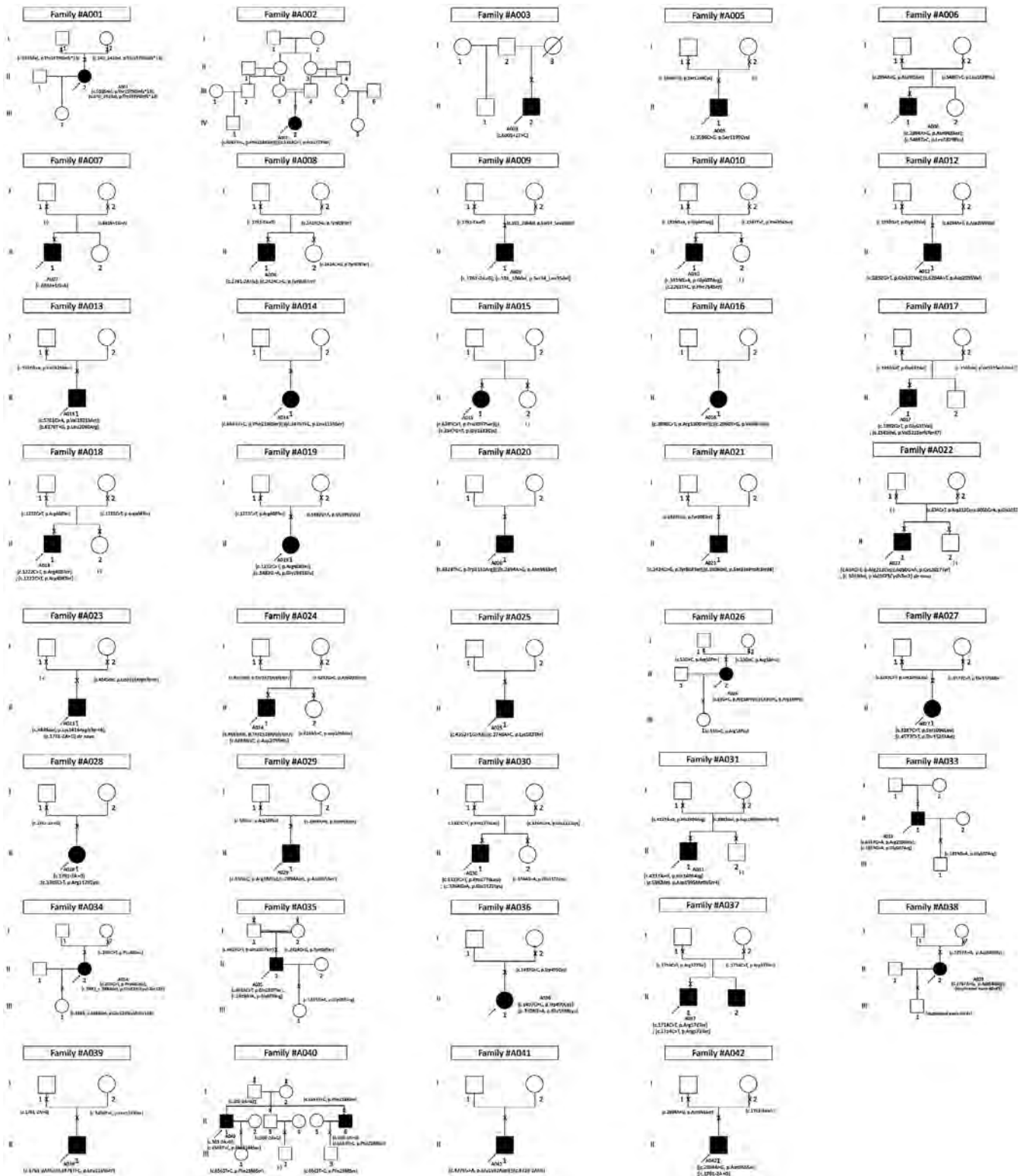


FIGURE 1 Pedigree charts of 42 families with Stargardt disease. An arrow (→) indicates the proband. A filled shape indicates the affected individual, and a cross (x) indicates the family members who underwent genetic testing. Square, male; circle, female. The generation number is shown on the left

group 3. The median average sensitivity threshold of the macula was 19.8 dB (range, 0.0–29.2), 15.1 dB (range, 0.0–25.8), and 0.0 dB (range, 0.0–18.9) in ffERG group 1, group 2, and group 3, respectively.

There was a significant difference between ffERG group 1 and group 3 as well as between ffERG group 2 and group 3 ($p = .000003$, $p = .076$; Figure S4).

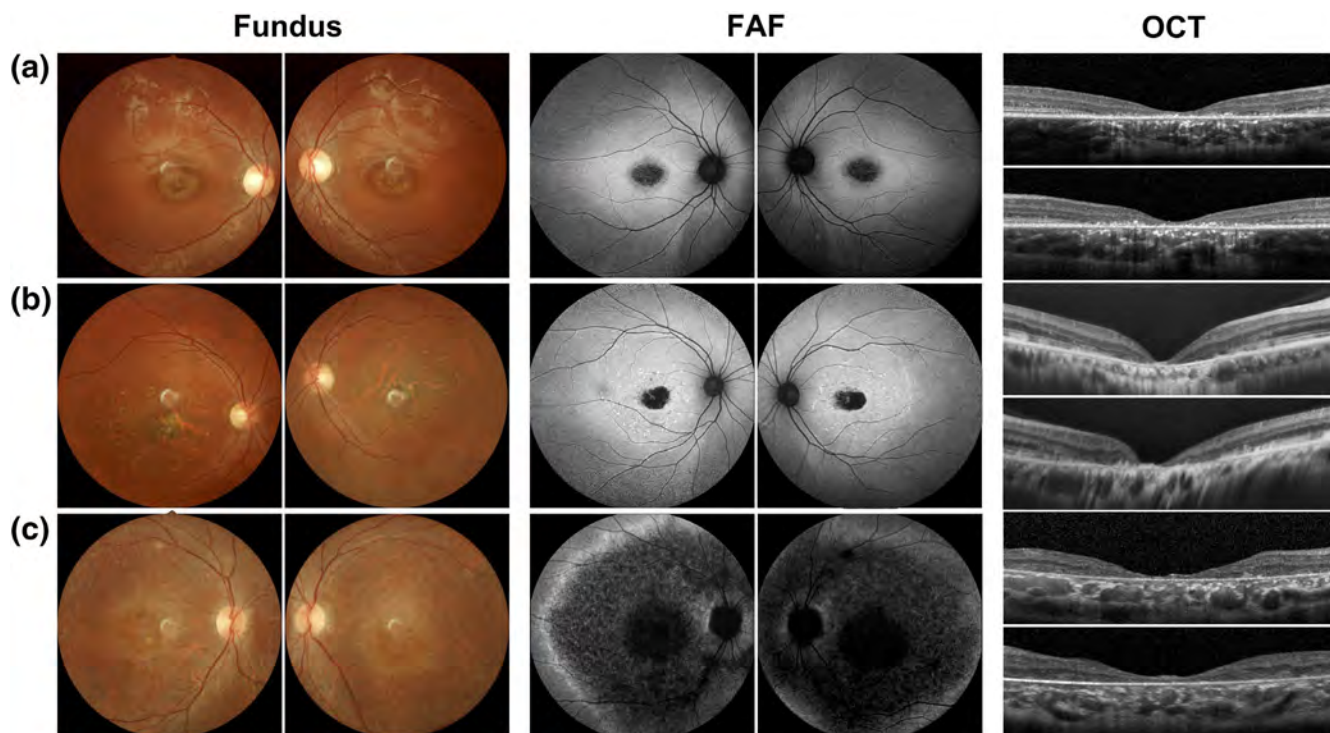


FIGURE 2 Color fundus photographs, fundus autofluorescence images, and optical coherence tomographic images from three representative patients with Stargardt disease (STGD1). (a) A002 (15-year-old female; onset at 9 years; best-corrected visual acuity of 0.82/0.82 in the logMAR unit for the right/left eye; [c.6563T>C (p.Phe2188Ser) and c.5318C>T (p.Ala1773Val)]; genotype group C). Fundus photographs show a central atrophy without flecks at the posterior. Fundus autofluorescence (FAF) images identify an area of low AF signal located at the fovea with homogenous background. Optical coherence tomographic (OCT) images demonstrate outer retinal disruption at the macula. (b) A040 (34-year-old male; onset at 10 years; best-corrected visual acuity of 1.00/1.00 in the logMAR unit for the right/left eye; [c.6563T>C (p.Phe2188Ser)] and [c.303-2A>G]; genotype group B). Fundus photographs show a central atrophy surrounded by flecks at the posterior pole; FAF images identify an area of low AF signal located at the macula with numerous foci of high AF density at the posterior pole; OCT images demonstrate outer retinal disruption at the macula. (c) A008 (22-year-old male; onset at 10 years; best-corrected visual acuity of 2.28/1.98 in the logMAR unit for the right/left eye; [c.1761-2A>G] and [c.2424C>G (p.Tyr808ter)]; genotype group A). Fundus photographs show multiple extensive atrophic changes in the retinal pigment epithelium (RPE), extending beyond the vascular arcades. FAF images identify multiple areas of low AF signal at posterior pole with a heterogeneous background. OCT images demonstrate widespread outer retinal disruption

3.4 | Phenotypic severity

Phenotype severity classification was available in 42 patients (Data S1). There was no patient (0/42, 0.0%) with a mild phenotype, 16 patients (16/42, 38.1%) with a moderate phenotype and 26 (26/42, 61.9%) with a severe phenotype.

3.5 | ABCA4 variants

Genetic results were obtained in all 42 unrelated patients: 34 patients underwent panel-based NGS, and eight patients underwent WES. Two ABCA4 variants were detected in 39 patients, while two patients (A003 and A005) had a single variant and one (A022) had three variants. Co-segregation analyses were available in 32 families: 26 probands with confirmed biallelic variants with genetic results of parents or certain family members; six probands with partially segregated results of a single parent or relatives; and 10 probands with no available data (Data S1 and Figure 1).

The detailed molecular genetic results are provided in Table S3. In total, 60 ABCA4 variants were identified in this study, including 36 missense variants (36/60, 60.0%), nine frameshift alterations (9/60, 15.0%), eight splice site alterations (13.3%), five nonsense variants (5/60, 8.3%), one in-frame deletion (1/60, 1.7%) and one duplication of exons 40–41 (1/60, 1.7%) (Figure 4). Two missense variants (c.6284A>T (p.Asp2095Val) and c.6283G>C (p.Asp2095His)) located around the end of exon 46 was predicted to cause splice site alterations. Fourteen novel ABCA4 variants were first reported in this study (Table S3). Two de novo ABCA4 variants were identified in two families: c.5019del (p.Val1673CysfsTer2) (A022) and c.1761-2A>G (A023) (Figure 1). There are three variants identified in the homozygous status: c.1222C>T (p.Arg408Ter) (A020); c.53G>C (p.Arg18Pro) (A030); and c.1714C>T (p.Arg572Ter) (A045).

The most prevalent six variants were c.1761-2A>G (6/80 alleles, 8%); c.2894A>G (p.Asn965Ser) (5/80 alleles, 6%); c.1222C>T (p.Arg408Ter) (4/80 alleles, 5%); c.2424C>G (p.Tyr808Ter) (3/80 alleles, 4%); c.53G>C (p.Arg18Pro) (3/80 alleles, 4%); and c.6563T>C (p.Phe2188Ser) (3/80 alleles, 4%) (Figure 4).

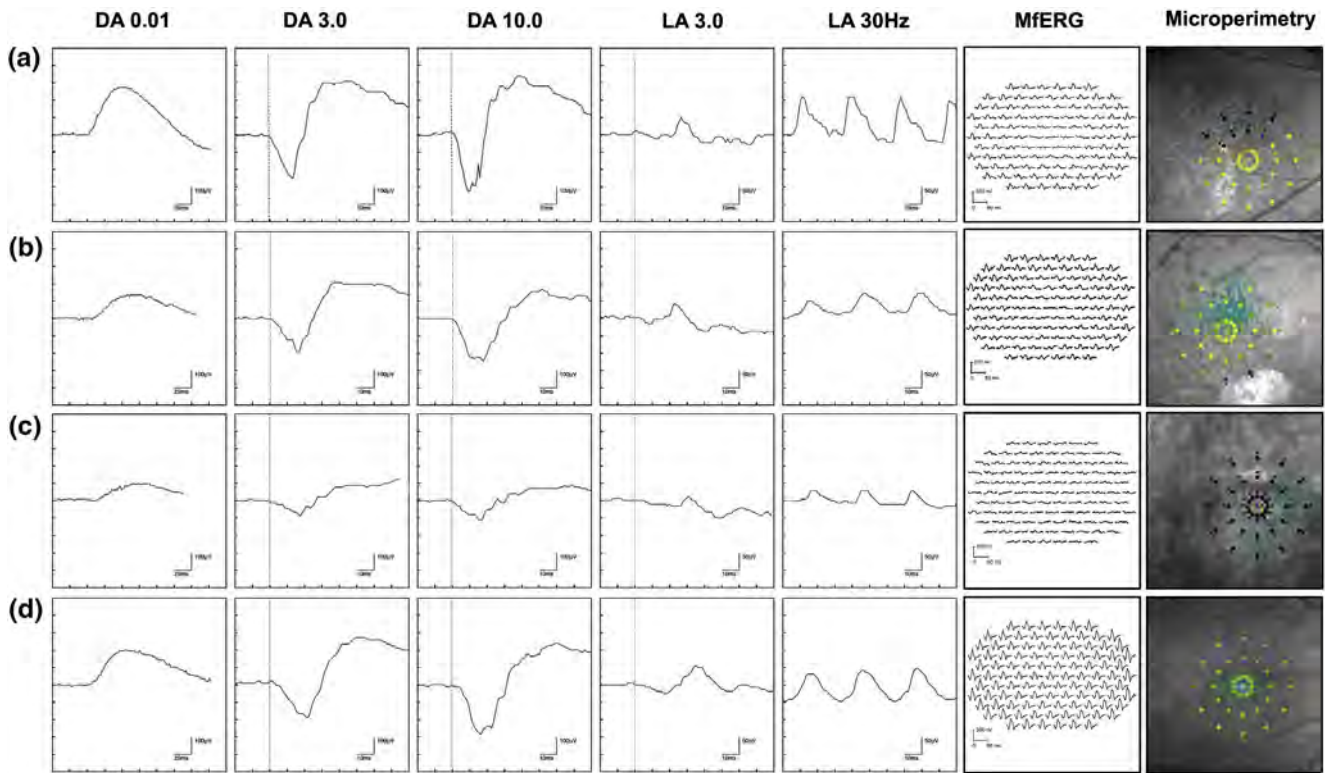


FIGURE 3 Full-field electroretinograms (ffERGs), multifocal ERGs (mfERGs), and microperimetry from three representative patients with STGD1. (a) A002 (full-field electroretinogram group 1; ffERG group 1). FfERGs demonstrate normal dark-adapted (DA) responses (DA 0.01, DA 3.0, DA 10.0) and normal light-adapted (LA) responses (LA 3.0, LA 3.0 30 Hz flicker). Multifocal ERGs (mfERGs) detect severely decreased responses in the central area (rings 1–2) and mildly decreased responses in rings 3–6. Microperimetry (MP) presents a preferred retinal locus (PRL) located at the nasal fovea, and the average threshold at the macula is 26.4 dB. (b) A040 (ffERG group 2). FfERGs demonstrate normal DA responses and mildly decreased LA responses. MfERGs detect severely decreased responses in rings 1–4 and mildly decreased responses in rings 5–6. MP present a PRL located at the superior fovea, and the average threshold at the macula is 25.8 dB. (c) A008 (ffERG group 3). FfERGs demonstrate moderately decreased DA responses and moderately decreased LA responses. MfERGs detect severely decreased responses over the recorded area. MP presents the average threshold of 0 dB. (d) Normal reference. Data from a normal subject are shown for reference

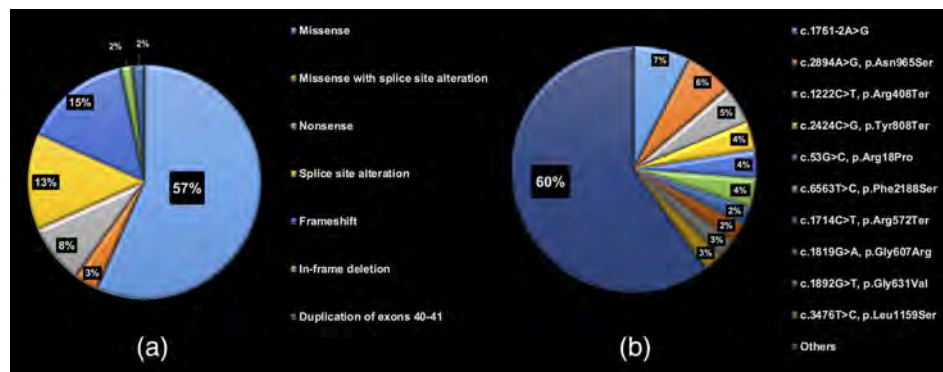


FIGURE 4 Distribution of detected *ABCA4* variants in a Western China cohort. (a) Type of detected variants. There were 36 missense variants (36/60, 60.0%), nine frameshift alterations (9/60, 15.0%), eight splice site alterations (13.3%), five nonsense variants (5/60, 8.3%), one in-frame deletion (1/60, 1.7%), and one duplication of exons 40–41 (1/60, 1.7%) identified in this study. Two missense variants (c.6284A>T (p.Asp2095Val) and c.6283G>C (p.Asp2095His)) are predicted to cause splice site alterations. (b) Allele frequency of detected variants. The distribution of 10 relatively prevalent variants identified in at least two families is demonstrated. The variants with allele frequencies less than 2% are summarized into others

The allele frequency provided by gnomAD in the total/East Asian general population for these six prevalent variants was 0.0004092%/0% for c.1761-2A>G; 0.013%/0% for p.Asn965Ser;

0.001625%/0.005% for p.Arg408Ter; 0%/0% for p.Tyr808Ter; 0%/0% for p.Arg18Pro; and 0.0008122%/0.005% for p.Phe2188Ser. The allele frequency provided by gnomAD in the total/East Asian

general population and this study for each variant was performed (Table S4).

Pathogenicity classification based on the ACMG guidelines was available for 60 detected variants. There were 24 variants classified as pathogenic, 34 as likely pathogenic, one as a variant of uncertain significance (VUS) (c.4577C>T (p.Thr152Met); A027), and one as a likely benign variant (c.3547G>T (p.Gly1183Cys); A015) (Table S3).

3.6 | Genotype classification

Genotype group classification was performed in 36 patients harboring multiple pathogenic or likely pathogenic variants. There were eight patients (8/36, 22.2%) with genotype A, 17 patients (47.2%) with genotype B, and 11 patients (30.5%) with genotype C (Figure S1).

The median age, age of onset, and BCVA in genotype A was 29.0 years (range, 18–52), 10.0 years (range, 8–14), and 1.64 in the LogMAR unit (range, 1.00–2.28), respectively. The median age, age of onset, and BCVA in genotype B was 34.0 years (range, 12–72), 10.0 years (range, 5–49), and 1.30 in the LogMAR unit (range, 0.15–1.98), respectively. The median age, age of onset, and BCVA in genotype C was 28.0 years (range, 15–46), 10.0 years (range, 8–20), and 1.00 in the LogMAR unit (range, 0.40–1.30), respectively. There was a significant difference in BCVA between genotype group A and genotype group C ($p = .0052$, Table S5).

3.7 | Genotype–phenotype association

An association between phenotypic severity and genotype group was investigated in 36 patients. The number of phenotypically moderate patients in genotype groups A, B, and C was zero, five, and seven, respectively (0%, 29.4%, 63.6%). The number of phenotypically severe patients in genotype groups A, B, and C was eight, twelve, and four, respectively (100%, 70.6%, 36.4%). A statistically significant association between phenotypic severity and genotype group was revealed ($p < .05$) ($p = .01$, Table 3 and Figure 5).

3.8 | A systematic review of ABCA4 variants

Four articles were selected for the analysis of Chinese ABCA4 variants (Table S6). A total of 212 ABCA4 variants were identified in these four

studies, including 114 missense, 36 splice site alterations, 31 nonsense variants, 25 frameshift variants, 3 synonymous variants, and 3 others (Table S7). Out of 212 ABCA4 variants, 150 were classified as pathogenic or likely pathogenic according to the ACMG guidelines. Prevalent variants in total were c.101_106del (p.Ser34_Leu35del) (allele frequency of 6%); c.2894A>G (p.Asn965Ser) (allele frequency of 4%); c.6563T>G (p.Phe2188Ser) (allele frequency of 4%); and c.2424C>G (p.Tyr808Ter) (allele frequency of 3%) (Figure S5).

Prevalent variants in each study were c.101_106del (p.Ser34_Leu35del); c.4773+1G>T; c.5646G>A (p.Met1882Ile); and c.1804C>T (p.Arg602Trp) in study 1 (Xin et al., 2015; $N = 33$). c.2424C>G (p.Tyr808Ter); c.6563T>G (p.Phe2188Ser); c.101_106del (p.Ser34_Leu35del); and c.2894A>G (p.Asn965Ser) in study 2 (Jiang, Pan, Xu, Tian, & Li, 2016; $N = 161$). c.101_106del (p.Ser34_Leu35del); c.2894A>G (p.Asn965Ser); c.6563T>G (p.Phe2188Ser); and c.1819G > A (p.Gly607Arg) in study 3 (Hu, J-k, Gao, Qi, & Wu, 2019; $N = 153$) and c.2894A>G (p.Asn965Ser); and c.101_106del (p.Ser34_Leu35del) in study 4 (Dan, Huang, Xing, & Shen, 2019; $N = 12$) (Table S6). Basically, those articles mainly focused on genotype analysis. There were little phenotypic data such as retinal image and electrophysiology was available and the correlation between phenotype and genotype was not analyzed.

4 | DISCUSSION

Detailed clinical and genetic characteristics are illustrated in a Western China cohort of 42 probands with STGD1. A wide disease spectrum both in phenotype and genotype was determined in a large Chinese cohort, identifying no patient with a mild phenotype, 38.1% with a moderate phenotype, and 61.9% with a severe phenotype associated with genetic severity.

To the best of the authors' knowledge, this study is the first to comprehensively reveal the demographic, morphological, and functional features of patients with STGD1 in a large molecularly confirmed cohort, which enabled an elucidation of the genotype–phenotype association in the Chinese population.

The median onset in our cohort (10.0 years) was earlier than that in the large prospective international STGD1 cohort (21.8 years for the retrospective cohort and 22.3 years for the prospective cohort in the ProgStar studies) or other reports from Europe (approximately 20 years) (Fujinami, Lois, Davidson, et al., 2013; Fujinami, Lois,

TABLE 3 Association between genotype group and phenotypic severity

| | | Phenotypic severity | | |
|----------------|--------------------------------|---------------------|--------------------|------------------|
| | | Group 1 (mild) | Group 2 (moderate) | Group 3 (severe) |
| Genotype group | Group A (multiple deleterious) | 0 | 0 | 8 |
| | Group B (one deleterious) | 0 | 5 | 12 |
| | Group C (multiple missense) | 0 | 7 | 4 |

Note: A statistically significant association was revealed between genotype group classification and phenotypic severity classification ($p = .014$; $p < .05$, Fisher exact test).

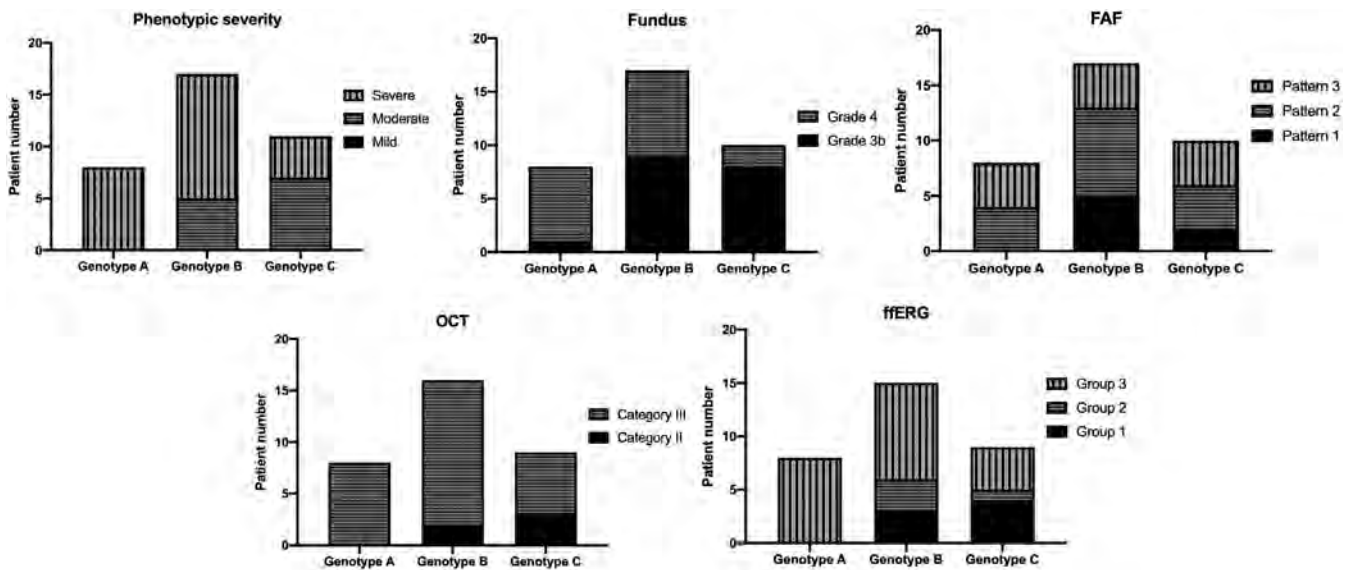


FIGURE 5 Clinical classification for each genotype group. Clinical classifications of phenotypic severity, fundus grades, FAF types, ffERG groups, and OCT categories for each genotype group are shown in bar graphs. There was a significant association between phenotypic severity and genotype group classification

Mukherjee, et al., 2013; Fujinami, Zernant, et al., 2013; Strauss et al., 2016). These findings were associated with a high proportion of severe phenotype in our cohort. The higher proportion of genotype group A with multiple deleterious variants (22%) in our cohort than in the other cohort (ProgStar cohort; 6%) supports this important fact (Fujinami et al., 2019; Kong et al., 2018). A similar proportion of genotype group A to our cohort was also found in the childhood-onset Stargardt disease cohort in the United Kingdom (Fujinami et al., 2015; Georgiou et al., 2020; Tanna et al., 2019).

Functional assessment is crucial in STGD1, since it provides not only distribution of the affected retinal area and affected systems (cone or rod) but also a prognostic value (Fujinami, Lois, Davidson, et al., 2013; Lois et al., 2001). The most severe functional phenotype (ffERG group 3: generalized cone and rod dysfunction) showed significant progression (over 50% loss of function) during the 10-year follow-up; (Fujinami, Lois, Davidson, et al., 2013) thus, careful observation and constructive intervention (if possible) are needed during the course in approximately 60% of our cohort. Spatial functional assessment with mfERGs detected a trend of an extended reduction in P1 amplitude according to the severity of ffERGs. This new approach could provide more detailed assessment/monitoring of retinal function in patients with STGD1 in natural history studies and therapeutic trials.

The combination of subjective and objective functional assessments provided useful information in our study. MP, a procedure to assess retinal sensitivity by monitoring the fundus, detected a lack of fixation stability with lower sensitivity thresholds, in keeping with previous reports (Sasso et al., 2017; Schonbach et al., 2017, 2020; Tanna et al., 2018, 2019). In addition, the severity of retinal sensitivity loss was associated with the severity of generalized retinal functional loss detected by ffERG, which suggests that the combination of subjective

and objective functional assessments could explain the key symptom of poor fixation and blurred central vision often associated with peripheral functional impairment.

Fourteen detected *ABCA4* variants (14/60, 23.3%) identified in our cohort have never been reported. This fact implies that the genetic background of the Chinese population was distinct from that of other populations. In addition, the three most prevalent variants (c.1761-2A>G; c.2894A>G (p.Asn965Ser); and c.1222C>T (p.Arg408Ter)) detected in our cohort were completely different from the three most prevalent variants (c.5882G>A (p.Gly1961Glu); c.2588G>C (p.Gly863Ala); and c.5461-10T>C) in the ProgStar study (Fujinami et al., 2019). In contrast to this regional/ethnic variation, genotype–phenotype associations were similarly identified in our cohort compared with cohorts from other populations, which supports the fact that the same approach to interpret/assess disease severity and the same concept of therapeutic window of opportunity can be applicable to the Chinese population.

There are four major reports describing *ABCA4*-associated retinal disease. The four prevalent variants (c.101_106del (p.Ser34-Leu35del); c.2894A>G (p.Asn965Ser); c.6563T>C (p.Phe2188Ser); and c.2424C>G (p.Tyr808Ter)) were different from those of the European population. In addition, the proportions of the types of detected variants were also different; a higher proportion of deleterious variants (43.4%; 92/212) was identified in the Chinese population compared to the ProgStar cohort (29.0%; 71/245), although the recruitment criteria can differ. In our study, three null variants: c.1761-2A>G (6/80 alleles, 8%), c.1222C>T (p.Arg408Ter) (4/80 alleles, 5%), and c.2424C>G (p.Tyr808Ter) (3/80 alleles, 4%) account for 16.3% (13/80 alleles) in total, and the association between genotype and phenotype has been revealed. The prevalence of null variants in this cohort is much higher than the European population, which can be considered as founder

alleles; although further genetic analysis utilizing haplotype data is required to conclude this hypothesis. Interestingly, four previous Chinese studies showed some regional differences, although similar features were observed. Three prevalent variants (c.2894A>G (p. Asn965Ser); c.6563T>G (p.Phe2188Ser); and c.101_106del (p. Ser34_Leu35del)) are shared among three out of the four Chinese cohorts, and the first two variants were prevalent in our cohort. On the other hand, the most prevalent variant (c.1761-2A>G) associated with a severe phenotype in our cohort was not listed as a frequently found variant in the other four Chinese cohorts. In most large Chinese cohort studies, patients were recruited without providing any clinical and genetic criteria of STGD1. This recruitment bias should include or exclude severe phenotypes, such as “retinitis pigmentosa.”

Three out of the most prevalent six variants in this study were only reported in the Chinese population: c.1761-2A>G; c.2424C>G (p.Tyr808Ter); and c.53G>C (p.Arg18Pro). Founder effects of these three variants can be considered. It is still difficult to conclude the enriched variants in Western China because the allele frequency data of the general population is only available as a cohort of the Western Chinese population.

In the current study, panel-based NGS targeting 36–450 genes have been applied that enables to detect 3–29% in patients with inherited retinal diseases. The advanced screening methods specifically designed for ABCA4 have been developed with a detection rate of 80% or more elsewhere (Cremers, Lee, Collin, & Allikmets, 2020; Jana et al., 2014). However, it is still not perfect for diagnosing patients only by genetic results. The vast phenotypic heterogeneity confounds the phenotypic diagnosis, especially in patients with generalized retinal dysfunction, thus the phenotypic criterion is focusing on the patients with macular atrophy that misses patients with generalized retinal dysfunction. The ProgStar criteria can miss patients with generalized retinal dysfunction with one pathogenic ABCA4 variant; however, we believe the present criteria are most suitable at this moment for a comprehensive diagnosis aiming for treatment.

There are several limitations in this study. First, selection bias at recruitment related to disease severity should be inherent since it is difficult to collect data from genetically affected subjects with good vision who do not visit clinics/hospitals. Second, this cross-sectional retrospective case series study did not include longitudinal data; thus, prospective natural history studies in a larger cohort could provide more accurate information on the disease severity and progression of STGD1. Third, the molecular mechanisms of disease causation for most variants have been unclear, and the clinical effects of variants are not perfectly understood. Further functional analysis is required to conclude the disease causation of each variant. Forth, due to the limited number of subjects, statistical analysis to investigate correlations between the clinical parameters and the particular variants (or genotype groups) were not available in the current study. Fifth, in our cohort, two patients harbor a VUS or likely benign variants for whom genotype grouping was unavailable. The further genetic analysis would help to determine their genotypes with identifying/excluding other candidate variants. Last, the number of our patients was too

small to draw conclusions about the genotype–phenotype associations/correlations in such a heterogeneous disease; therefore, larger cohort studies are required for further detailed analyses.

In conclusion, this study, for the first time, illustrated a spectrum of morphological and functional phenotypes and genotypes in a molecularly confirmed large STGD1 cohort in the Chinese population. A different genetic background underlying STGD1 from the Caucasian population was revealed in this study; meanwhile, shared features based on genotype–phenotype associations were determined. These findings delineate the clinical and genetic characteristics of STGD1.

ACKNOWLEDGEMENTS

The East Asia Inherited Retinal Disease Society (EAIRDs) Study Group: The East Asia Stargardt disease (EASTAR) study is supported by a contract from the EAIRDs. The EAIRDs Study Group members are as follows: Chair's Office: National Institute of Sensory Organs, Kaoru Fujinami, Se Joon Woo, Ruifang Sui, Shiyong Li, Hyeong Gon Yu, Bo Lei, Qingjiong Zhang, Chan Choi Mun, Fred Chen, Mineo Kondo, Takeshi Iwata, Kazushige Tsunoda, Yozo Miyake, Kunihiko Akiyama, Gen Hanazono, Masaki Fukui, Yu Fujinami-Yokokawa, Tatsuo Matsunaga, Satomi Inoue, Kazuki Yamazawa, Takayuki Kinoshita, Yasuhiro Yamada, Michel Michaelides, Gavin Arno, Nikolas Pontikos, Alice Davidson, Yasutaka Suzuki, Asako Ihama, Reina Akita, Jun Ohashi, Izumi Naka, Kazutoshi Yoshitake, Daisuke Mori, Toshihide Kurihara, Kazuo Tsubota, Hiroaki Miyata, Kei Shinoda, Atsushi Mizota, Natsuko Nakamura, Takaaki Hayashi, Kazuki Kuniyoshi, Shuhei Kameya, Kwangsic Joo, Min Seok Kim, Kyu Hyung Park, Seong Joon Ahn, Dae Joong Ma, Baek-Lok Oh, Joo Yong Lee, Sang Jin Kim, Christopher Seungkyu Lee, Jinu Han, Hyewon Chung, Jeeyun Ahn, Min Sagong, Young-Hoon-Ohn, Dong Ho Park, You Na Kim, Jong Suk Lee, Sang Jun Park, Jun Young Park, Won Kyung Song, Tae Kwan Park, Lizhu Yang, Xuan Zou, Hui Li, Zhengqin Yin, Yong Liu, Xiaohong Meng, Xiao Liu, Yanling Long, Jiayun Ren, Hongxuan Lie, Gang Wang, Anthony G. Robson, Xuemin Jin, Kunpeng Xie, Ya Li, Chonglin Chen, Qingge Guo, Lin Yang, Ya You, Tin Aung, Graham E. Holder, John N De Roach.

CONFLICT OF INTEREST

All authors have completed and submitted the ICMJE Form for Disclosure of Potential Conflicts of Interest. Individual investigators who participate in the sponsored project(s) are not directly compensated by the sponsor but may receive salary or other support from the institution to support their effort on the project(s).

Toshihide Kurihara is an investor in Tsubota Laboratory, Inc and RestoreVision, Inc. Toshihide Kurihara reports grants and personal fees from ROHTO Pharmaceutical Co., Ltd, Tsubota Laboratory, Inc, Fuji Xerox Co., Ltd, Kowa Company, Ltd, Santen Pharmaceutical Co. Ltd., outside the submitted work.

Kazuo Tsubota reports grants and personal fees from Santen Pharmaceutical Co., Ltd., grants and personal fees from Otsuka Pharmaceutical Co., Ltd., grants and personal fees from Wakamoto Pharmaceutical Co., Ltd., grants from Rohto Pharmaceutical Co., Ltd., grants from R-Tech Ueno, personal fees from Laboratoires Thea,

grants from Alcon Japan, investor of Tear Solutions, grants and investor of Tsubota Laboratory, Inc., outside the submitted work.

Kaoru Fujinami: Paid consultant—Astellas Pharma Inc., Kubota Pharmaceutical Holdings Co., Ltd, Acucela Inc., Novartis AG, Janssen Pharmaceutica, Sanofi Genzyme, NightstaRx Limited; Personal fees—Astellas Pharma Inc., Kubota Pharmaceutical Holdings Co., Ltd., Acucela Inc., Novartis AG, Santen Company Limited, Foundation Fighting Blindness, Foundation Fighting Blindness Clinical Research Institute, Japanese Ophthalmology Society, Japan Retinitis Pigmentosa Society; Grants—Astellas Pharma Inc. (NCT03281005), outside the submitted work.

DATA AVAILABILITY STATEMENT

Data available on request from the authors.

ORCID

Kaoru Fujinami  <https://orcid.org/0000-0003-4248-0033>

Shiyang Li  <https://orcid.org/0000-0001-9783-9520>

REFERENCES

- Allikmets, R., Singh, N., Sun, H., Shroyer, N. F., Hutchinson, A., Chidambaram, A., ... Lupski, J. R. (1997). A photoreceptor cell-specific ATP-binding transporter gene (ABCR) is mutated in recessive Stargardt macular dystrophy. *Nature Genetics*, *15*(3), 236–246.
- Charbel Issa, P., Barnard, A. R., Herrmann, P., Washington, I., & MacLaren, R. E. (2015). Rescue of the Stargardt phenotype in Abca4 knockout mice through inhibition of vitamin A dimerization. *Proceedings of the National Academy of Sciences of the United States of America*, *112*(27), 8415–8420.
- Chen, Y., Okano, K., Maeda, T., Chauhan, V., Golczak, M., Maeda, A., & Palczewski, K. (2012). Mechanism of all-trans-retinal toxicity with implications for stargardt disease and age-related macular degeneration. *The Journal of Biological Chemistry*, *287*(7), 5059–5069.
- Cremers, F. P. M., Lee, W., Collin, R. W. J., & Allikmets, R. (2020). Clinical spectrum, genetic complexity and therapeutic approaches for retinal disease caused by ABCA4 mutations. *Progress in Retinal and Eye Research*, 100861. <https://doi.org/10.1016/j.preteyeres.2020.100861>.
- Dan, H., Huang, X., Xing, Y., & Shen, Y. (2019). Application of targeted exome and whole-exome sequencing for Chinese families with Stargardt disease. *Annals of Human Genetics*, *84*(2), 177–184.
- Fujinami, K., Akahori, M., Fukui, M., Tsunoda, K., Iwata, T., & Miyake, Y. (2011). Stargardt disease with preserved central vision: Identification of a putative novel mutation in ATP-binding cassette transporter gene. *Acta Ophthalmologica*, *89*(3), e297–e298.
- Fujinami, K., Lois, N., Davidson, A. E., Mackay, D. S., Hogg, C. R., Stone, E. M., ... Michaelides, M. (2013). A longitudinal study of stargardt disease: Clinical and electrophysiologic assessment, progression, and genotype correlations. *American Journal of Ophthalmology*, *155*(6), 1075–1088 e1013.
- Fujinami, K., Lois, N., Mukherjee, R., McBain, V. A., Tsunoda, K., Tsubota, K., ... Michaelides, M. (2013). A longitudinal study of Stargardt disease: Quantitative assessment of fundus autofluorescence, progression, and genotype correlations. *Investigative Ophthalmology & Visual Science*, *54*(13), 8181–8190.
- Fujinami, K., Sergouniotis, P. I., Davidson, A. E., Mackay, D. S., Tsunoda, K., Tsubota, K., ... Webster, A. R. (2013). The clinical effect of homozygous ABCA4 alleles in 18 patients. *Ophthalmology*, *120*(11), 2324–2331.
- Fujinami, K., Sergouniotis, P. I., Davidson, A. E., Wright, G., Chana, R. K., Tsunoda, K., ... Webster, A. R. (2013). Clinical and molecular analysis of Stargardt disease with preserved foveal structure and function. *American Journal of Ophthalmology*, *156*(3), 487–501 e481.
- Fujinami, K., Singh, R., Carroll, J., Zernant, J., Allikmets, R., Michaelides, M., & Moore, A. T. (2014). Fine central macular dots associated with childhood-onset Stargardt disease. *Acta Ophthalmologica*, *92*(2), e157–e159.
- Fujinami, K., Strauss, R. W., Chiang, J. P., Audo, I. S., Bernstein, P. S., Birch, D. G., ... ProgStar Study, G. (2019). Detailed genetic characteristics of an international large cohort of patients with Stargardt disease: ProgStar study report 8. *The British Journal of Ophthalmology*, *103*(3), 390–397.
- Fujinami, K., Zernant, J., Chana, R. K., Wright, G. A., Tsunoda, K., Ozawa, Y., ... Moore, A. T. (2015). Clinical and molecular characteristics of childhood-onset Stargardt disease. *Ophthalmology*, *122*(2), 326–334.
- Fujinami, K., Zernant, J., Chana, R. K., Wright, G. A., Tsunoda, K., Ozawa, Y., ... Michaelides, M. (2013). ABCA4 gene screening by next-generation sequencing in a British cohort. *Investigative Ophthalmology & Visual Science*, *54*(10), 6662–6674.
- Fujinami-Yokokawa, Y., Pontikos, N., Yang, L., Tsunoda, K., Yoshitake, K., Iwata, T., ... Fujinami, K. (2019). Japan eye genetics consortium OBO. 2019. Prediction of causative genes in inherited retinal disorders from spectral-domain optical coherence tomography utilizing deep learning techniques. *Journal of Ophthalmology*, 2019, 1691064.
- Georgiou, M., Kane, T., Tanna, P., Bouzia, Z., Singh, N., Kalitzeos, A., ... Michaelides, M. (2020). Prospective cohort Study of childhood-onset Stargardt disease: Fundus autofluorescence imaging, progression, comparison with adult-onset disease, and disease symmetry. *American Journal of Ophthalmology*, *211*, 159–175.
- Gill, J. S., Georgiou, M., Kalitzeos, A., Moore, A. T., & Michaelides, M. (2019). Progressive cone and cone-rod dystrophies: Clinical features, molecular genetics and prospects for therapy. *The British Journal of Ophthalmology*, *103*, 711–720.
- Hood, D. C., Bach, M., Brigell, M., Keating, D., Kondo, M., Lyons, J. S., ... International Society For Clinical Electrophysiology of V. (2012). ISCEV standard for clinical multifocal electroretinography (mfERG) (2011 edition). *Documenta Ophthalmologica*, *124*(1), 1–13.
- Hu, F.-Y., J-k, L., Gao, F.-J., Qi, Y.-H., & Wu, J.-H. (2019). ABCA4 gene screening in a Chinese cohort with Stargardt disease: Identification of 37 novel variants. *Frontiers in Genetics*, *10*, 773–773.
- Hussain, R. M., Ciulla, T. A., Berrocal, A. M., Gregori, N. Z., Flynn, H. W., Jr., & Lam, B. L. (2018). Stargardt macular dystrophy and evolving therapies. *Expert Opinion on Biological Therapy*, *18*(10), 1049–1059.
- Hussain, R. M., Gregori, N. Z., Ciulla, T. A., & Lam, B. L. (2018). Pharmacotherapy of retinal disease with visual cycle modulators. *Expert Opinion on Pharmacotherapy*, *19*(5), 471–481.
- Jana, Z., Xie, Y., Carmen, A., Rosa, R. A., Miguel-Angel, L. M., Francesca, S., ... Mette, B. (2014). Analysis of the ABCA4 genomic locus in Stargardt disease. *Human Molecular Genetics*, *23*(25), 6797.
- Jiang, F., Pan, Z., Xu, K., Tian, L., & Li, Y. (2016). Screening of ABCA4 gene in a Chinese cohort with Stargardt disease or cone-rod dystrophy with a report on 85 novel mutations. *Investigative Ophthalmology & Visual Science*, *57*(1), 145–152.
- K S. (1909). Über familiäre, progressive Degeneration in der Maculagegend des Auges. *Graefes Archive for Clinical and Experimental Ophthalmology*, *71*, 534–550.
- Khan, K. N., Kasilian, M., Mahroo, O. A. R., Tanna, P., Kalitzeos, A., Robson, A. G., ... Michaelides, M. (2018). Early patterns of macular degeneration in ABCA4-associated retinopathy. *Ophthalmology*, *125*(5), 735–746.
- Kong, X., Fujinami, K., Strauss, R. W., Munoz, B., West, S. K., Cideciyan, A. V., ... ProgStar Study, G. (2018). Visual acuity change over 24 months and its association with foveal phenotype and genotype in individuals with Stargardt disease: ProgStar Study report no. 10. *JAMA Ophthalmology*, *136*(8), 920–928.

- Kong, X., Strauss, R. W., Michaelides, M., Cideciyan, A. V., Sahel, J. A., Munoz, B., ... ProgStar, S. G. (2016). Visual acuity loss and associated risk factors in the retrospective progression of Stargardt disease Study (ProgStar report no. 2). *Ophthalmology*, 123(9), 1887–1897.
- Kubota, R., Boman, N. L., David, R., Mallikarjun, S., Patil, S., & Birch, D. (2012). Safety and effect on rod function of ACU-4429, a novel small-molecule visual cycle modulator. *Retina*, 32(1), 183–188.
- Kubota, R., Calkins, D. J., Henry, S. H., & Linsenmeier, R. A. (2019). Emixustat reduces metabolic demand of dark activity in the retina. *Investigative Ophthalmology & Visual Science*, 60(14), 4924–4930.
- Lange, C., Feltgen, N., Junker, B., Schulze-Bonsel, K., & Bach, M. (2009). Resolving the clinical acuity categories "hand motion" and "counting fingers" using the Freiburg visual acuity test (FrACT). *Graefes Archive for Clinical and Experimental Ophthalmology*, 247(1), 137–142.
- Liu, X., Fujinami, Y. Y., Yang, L., Arno, G., & Fujinami, K. (2019). Stargardt disease in Asian population. In *Advances in vision research* (Vol. II, pp. 279–295). Singapore: Springer.
- Lois, N., Holder, G. E., Bunce, C., Fitzke, F. W., & Bird, A. C. (2001). Phenotypic subtypes of Stargardt macular dystrophy-fundus flavimaculatus. *Archives of Ophthalmology*, 119(3), 359–369.
- Maeda, A., Maeda, T., Golczak, M., & Palczewski, K. (2008). Retinopathy in mice induced by disrupted all-trans-retinal clearance. *The Journal of Biological Chemistry*, 283(39), 26684–26693.
- McBain, V. A., Townend, J., & Lois, N. (2012). Progression of retinal pigment epithelial atrophy in stargardt disease. *American Journal of Ophthalmology*, 154(1), 146–154.
- McCulloch, D. L., Marmor, M. F., Brigell, M. G., Hamilton, R., Holder, G. E., Tzekov, R., & Bach, M. (2015a). Erratum to: ISCEV standard for full-field clinical electroretinography (2015 update). *Documenta Ophthalmologica*, 131(1), 81–83.
- McCulloch, D. L., Marmor, M. F., Brigell, M. G., Hamilton, R., Holder, G. E., Tzekov, R., & Bach, M. (2015b). ISCEV standard for full-field clinical electroretinography (2015 update). *Documenta Ophthalmologica*, 130(1), 1–12.
- Mehat, M. S., Sundaram, V., Ripamonti, C., Robson, A. G., Smith, A. J., Borooah, S., ... Bainbridge, J. W. B. (2018). Transplantation of human embryonic stem cell-derived retinal pigment epithelial cells in macular degeneration. *Ophthalmology*, 125(11), 1765–1775.
- Molday, L. L., Rabin, A. R., & Molday, R. S. (2000). ABCR expression in foveal cone photoreceptors and its role in Stargardt macular dystrophy. *Nature Genetics*, 25(3), 257–258.
- Molday, R. S. (2015). Insights into the molecular properties of ABCA4 and its role in the visual cycle and Stargardt disease. *Progress in Molecular Biology and Translational Science*, 134, 415–431.
- Molday, R. S., Zhong, M., & Quazi, F. (2009). The role of the photoreceptor ABC transporter ABCA4 in lipid transport and Stargardt macular degeneration. *Biochimica et Biophysica Acta*, 1791(7), 573–583.
- Quazi, F., Lenevich, S., & Molday, R. S. (2012). ABCA4 is an N-retinylidene-phosphatidylethanolamine and phosphatidylethanolamine importer. *Nature Communications*, 3, 925.
- Rahman, N., Georgiou, M., Khan, K. N., & Michaelides, M. (2020). Macular dystrophies: Clinical and imaging features, molecular genetics and therapeutic options. *The British Journal of Ophthalmology*, 104(4), 451–460.
- Richards, S., Aziz, N., Bale, S., Bick, D., Das, S., Gastier-Foster, J., ... Committee, A. L. Q. A. (2015). Standards and guidelines for the interpretation of sequence variants: A joint consensus recommendation of the American College of Medical Genetics and Genomics and the Association for Molecular Pathology. *Genetics in Medicine*, 17(5), 405–424.
- Rosenfeld, P. J., Dugel, P. U., Holz, F. G., Heier, J. S., Pearlman, J. A., Novack, R. L., ... Kubota, R. (2018). Emixustat hydrochloride for geographic atrophy secondary to age-related macular degeneration: A randomized clinical trial. *Ophthalmology*, 125(10), 1556–1567.
- Sasso, P., Scupola, A., Silvestri, V., Amore, F. M., Abed, E., Calandriello, L., ... Caporossi, A. (2017). Morpho-functional analysis of Stargardt disease for reading. *Canadian Journal of Ophthalmology*, 52(3), 287–294.
- Schonbach, E. M., Strauss, R. W., Ibrahim, M. A., Janes, J. L., Birch, D. G., Cideciyan, A. V., ... ProgStar study g. (2020). Faster sensitivity loss around dense scotomas than for overall macular sensitivity in Stargardt disease: ProgStar report no. 14. *American Journal of Ophthalmology*, 216, 219–225.
- Schonbach, E. M., Wolfson, Y., Strauss, R. W., Ibrahim, M. A., Kong, X., Munoz, B., ... ProgStar Study, G. (2017). Macular sensitivity measured with microperimetry in Stargardt disease in the progression of atrophy secondary to Stargardt disease (ProgStar) study: Report no. 7. *JAMA Ophthalmology*, 135(7), 696–703.
- Schulz, H. L., Grassmann, F., Kellner, U., Spital, G., Ruther, K., Jagle, H., ... Stohr, H. (2017). Mutation spectrum of the ABCA4 gene in 335 Stargardt disease patients from a multicenter German cohort-impact of selected deep intronic variants and common SNPs. *Investigative Ophthalmology & Visual Science*, 58(1), 394–403.
- Schwartz, S. D., Hubschman, J. P., Heilwell, G., Franco-Cardenas, V., Pan, C. K., Ostrick, R. M., ... Lanza, R. (2012). Embryonic stem cell trials for macular degeneration: A preliminary report. *Lancet*, 379(9817), 713–720.
- Schwartz, S. D., Regillo, C. D., Lam, B. L., Elliott, D., Rosenfeld, P. J., Gregori, N. Z., ... Lanza, R. (2015). Human embryonic stem cell-derived retinal pigment epithelium in patients with age-related macular degeneration and Stargardt's macular dystrophy: Follow-up of two open-label phase 1/2 studies. *Lancet*, 385(9967), 509–516.
- Singh, R., Fujinami, K., Chen, L. L., Michaelides, M., & Moore, A. T. (2014). Longitudinal follow-up of siblings with a discordant Stargardt disease phenotype. *Acta Ophthalmologica*, 92(4), e331–e332.
- Strauss, R. W., Ho, A., Munoz, B., Cideciyan, A. V., Sahel, J. A., Sunness, J. S., ... Progression of Stargardt Disease Study G. (2016). The natural history of the progression of atrophy secondary to Stargardt disease (ProgStar) studies: Design and baseline characteristics: ProgStar report no. 1. *Ophthalmology*, 123(4), 817–828.
- Strauss, R. W., Kong, X., Ho, A., Jha, A., West, S., Ip, M., ... ProgStar Study, G. (2019). Progression of Stargardt disease as determined by fundus autofluorescence over a 12-month period: ProgStar report no. 11. *JAMA Ophthalmology*, 137, 1134.
- Strauss, R. W., Munoz, B., Ho, A., Jha, A., Michaelides, M., Cideciyan, A. V., ... ProgStar Study, G. (2017a). Progression of Stargardt disease as determined by fundus autofluorescence in the retrospective progression of Stargardt disease Study (ProgStar report no. 9). *JAMA Ophthalmology*, 135(11), 1232–1241.
- Strauss, R. W., Munoz, B., Ho, A., Jha, A., Michaelides, M., Mohand-Said, S., ... ProgStar Study, G. (2017b). Incidence of atrophic lesions in Stargardt disease in the progression of atrophy secondary to Stargardt disease (ProgStar) study: Report no. 5. *JAMA Ophthalmology*, 135(7), 687–695.
- Tanna, P., Georgiou, M., Aboshiha, J., Strauss, R. W., Kumaran, N., Kalitzeos, A., ... Michaelides, M. (2018). Cross-sectional and longitudinal assessment of retinal sensitivity in patients with childhood-onset Stargardt disease. *Translational Vision Science & Technology*, 7(6), 10.
- Tanna, P., Georgiou, M., Strauss, R. W., Ali, N., Kumaran, N., Kalitzeos, A., ... Michaelides, M. (2019). Cross-sectional and longitudinal assessment of the ellipsoid zone in childhood-onset Stargardt disease. *Translational Vision Science & Technology*, 8(2), 1.
- Tanna, P., Strauss, R. W., Fujinami, K., & Michaelides, M. (2017). Stargardt disease: Clinical features, molecular genetics, animal models and therapeutic options. *The British Journal of Ophthalmology*, 101(1), 25–30.

- Testa, F., Melillo, P., Di Iorio, V., Orrico, A., Attanasio, M., Rossi, S., & Simonelli, F. (2014). Macular function and morphologic features in juvenile stargardt disease: Longitudinal study. *Ophthalmology*, *121*(12), 2399–2405.
- Tsybovsky, Y., Molday, R. S., & Palczewski, K. (2010). The ATP-binding cassette transporter ABCA4: Structural and functional properties and role in retinal disease. *Advances in Experimental Medicine and Biology*, *703*, 105–125.
- Xin, W., Xiao, X., Li, S., Jia, X., Guo, X., & Zhang, Q. (2015). Identification of genetic defects in 33 Proband with Stargardt disease by WES-based bioinformatics gene panel analysis. *PLoS One*, *10*, e0132635.

SUPPORTING INFORMATION

Additional supporting information may be found online in the Supporting Information section at the end of this article.

How to cite this article: Liu X, Meng X, Yang L, et al. Clinical and genetic characteristics of Stargardt disease in a large Western China cohort: Report 1. *Am J Med Genet Part C*. 2020;184C:694–707. <https://doi.org/10.1002/ajmg.c.31838>



RESEARCH ARTICLE

RP2-associated retinal disorder in a Japanese cohort: Report of novel variants and a literature review, identifying a genotype–phenotype association

Kaoru Fujinami^{1,2,3,4} | Xiao Liu^{1,2,5} | Shinji Ueno⁶ | Atsushi Mizota⁷ | Kei Shinoda^{7,8} | Kazuki Kuniyoshi⁹ | Yu Fujinami-Yokokawa^{1,3,10,11} | Lizhu Yang^{1,2} | Gavin Arno^{1,3,4,12} | Nikolas Pontikos^{1,3,4} | Shuhei Kameya¹³ | Taro Kominami⁶ | Hiroko Terasaki⁶ | Hiroyuki Sakuramoto⁹ | Natsuko Nakamura^{1,7,14} | Toshihide Kurihara² | Kazuo Tsubota² | Yozo Miyake^{1,15,16} | Kazutoshi Yoshiake¹⁷ | Takeshi Iwata¹⁷ | Kazushige Tsunoda¹ | Japan Eye Genetics Consortium Study Group

¹Laboratory of Visual Physiology, Division of Vision Research, National Institute of Sensory Organs, National Hospital Organization Tokyo Medical Center, Tokyo, Japan

²Department of Ophthalmology, Keio University School of Medicine, Tokyo, Japan

³UCL Institute of Ophthalmology, London, UK

⁴Moorfields Eye Hospital, London, UK

⁵Southwest Hospital/Southwest Eye Hospital, Third Military Medical University (Army Medical University), Chongqing, China

⁶Department of Ophthalmology, Nagoya University Graduate School of Medicine, Nagoya, Japan

⁷Department of Ophthalmology, Teikyo University, Tokyo, Japan

⁸Department of Ophthalmology, Saitama Medical University, Moroyama Campus, Saitama, Japan

⁹Department of Ophthalmology, Kindai University Faculty of Medicine, Osaka-Sayama, Japan

¹⁰Department of Health Policy and Management, Keio University School of Medicine, Tokyo, Japan

¹¹Division of Public Health, Yokokawa Clinic, Suita, Japan

¹²North East Thames Regional Genetics Service, UCL Great Ormond Street Institute of Child Health, NHS Foundation Trust, London, UK

¹³Department of Ophthalmology, Nippon Medical School Chiba Hokusoh Hospital, Inzai, Japan

¹⁴Department of Ophthalmology, The University of Tokyo, Tokyo, Japan

¹⁵Aichi Medical University, Nagakute, Japan

¹⁶Next vision, Kobe Eye Center, Kobe, Japan

¹⁷Division of Molecular and Cellular Biology, National Institute of Sensory Organs, National Hospital Organization Tokyo Medical Center, Tokyo, Japan

Correspondence

Kaoru Fujinami, Laboratory of Visual Physiology, Division for Vision Research, National Institute of Sensory Organs, National Hospital Organization Tokyo Medical Center, No. 2-5-1, Higashigaoka, Meguro-ku, Tokyo

Abstract

The retinitis pigmentosa 2 (*RP2*) gene is one of the causative genes for X-linked inherited retinal disorder. We characterized the clinical/genetic features of four patients with *RP2*-associated retinal disorder (*RP2*-RD) from four Japanese families in

Kaoru Fujinami and Xiao Liu are joint first authors of this study.

This is an open access article under the terms of the Creative Commons Attribution-NonCommercial-NoDerivs License, which permits use and distribution in any medium, provided the original work is properly cited, the use is non-commercial and no modifications or adaptations are made.

© 2020 The Authors. *American Journal of Medical Genetics Part C: Seminars in Medical Genetics* published by Wiley Periodicals LLC.

152-8902 Japan.
Email: k.fujinami@ucl.ac.uk

Funding information

FOUNDATION FIGHTING BLINDNESS ALAN LATIES CAREER DEVELOPMENT PROGRAM, Grant/Award Number: CF-CL-0416-0696-UCL; Grant-in-Aid for Scientists to support international collaborative studies of the Ministry of Education, Culture, Sports, Science and Technology, Japan, Grant/Award Number: 16KK01930002; Grant-in-Aid for Young Scientists (A) of the Ministry of Education, Culture, Sports, Science and Technology, Japan, Grant/Award Number: 16H06269; Great Britain Sasakawa Foundation Butterfield Awards; Health Labour Sciences Research Grant, The Ministry of Health Labour and Welfare, Grant/Award Number: 201711107A; National Hospital Organization Network Research Fund, Grant/Award Number: H30-NHO-Sensory Organs-03; Novartis Research Grant; Grants-in-Aid for Scientific Research, Japan Society for the Promotion of Science, Japan, Grant/Award Number: H26-26462674; Ministry of Health, Labor and Welfare, Grant/Award Number: 18ek0109282h0002; Japan Agency for Medical Research and Development (AMED); ROHTO Pharmaceutical Co., Ltd.; Santen Pharmaceutical Co. Ltd.; Novartis Pharmaceuticals; Kowa Company, Ltd.; Kirin Company, Ltd.; Fuji Xerox Co., Ltd.; Tsubota Laboratory, Inc.; UCL Institute of Ophthalmology; Great Britain Sasakawa Foundation Butterfield Award; UCL Institute of Child Health; Great Ormond Street Hospital; Moorfields Eye Hospital; Ministry of Education, Culture, Sports, Science and Technology, Grant/Award Number: 18K16943

a nationwide cohort. A systematic review of *RP2*-RD in the Japanese population was also performed. All four patients were clinically diagnosed with retinitis pigmentosa (RP). The mean age at examination was 36.5 (10–47) years, and the mean visual acuity in the right/left eye was 1.40 (0.52–2.0)/1.10 (0.52–1.7) in the logarithm of the minimum angle of resolution unit, respectively. Three patients showed extensive retinal atrophy with macular involvement, and one had central retinal atrophy. Four *RP2* variants were identified, including two novel missense (p.Ser6Phe, p.Leu189Pro) and two previously reported truncating variants (p.Arg120Ter, p.Glu269CysfsTer3). The phenotypes of two patients with truncating variants were more severe than the phenotypes of two patients with missense variants. A systematic review revealed additional 11 variants, including three missense and eight deleterious (null) variants, and a statistically significant association between phenotype severity and genotype severity was revealed. The clinical and genetic spectrum of *RP2*-RD was illustrated in the Japanese population, identifying the characteristic features of a severe form of RP with early macular involvement.

KEYWORDS

inherited retinal disorder, retinitis pigmentosa, *RP2* gene, X-linked recessive

1 | INTRODUCTION

Inherited retinal disorder (IRD) is one of the major causes of blindness in developed countries in both children and the working population (Liew, Michaelides, & Bunce, 2014; Sohocki et al., 2001; Solebo, Teoh, & Rahi, 2017). Retinitis pigmentosa (RP) represents a heterogeneous group of RDs characterized by progressive bilateral degeneration of rod and cone photoreceptors, which affects approximately 1:3000 individuals (Boughman, Conneally, & Nance, 1980; Chizzolini et al., 2011; Lyraki, Megaw, & Hurd, 2016; Prokisch, Hartig, Hellinger, Meitinger, & Rosenberg, 2007). Various inheritance patterns have been identified in RP and allied disorders, including autosomal dominant, autosomal recessive (AR), X-linked recessive (XL), mitochondrial inheritance, and others (Wright, Chakarova, Abd El-Aziz, & Bhattacharya, 2010).

XLRP is observed in approximately 10 to 20% of RP cases (Breuer et al., 2002; Fishman, 1978; Haim, 1992; Prokisch et al., 2007; Wright et al., 2010) and is associated with the most severe form of the disease (Fishman, 1978). Three causative genes for XLRP are the RP GTPase regulator (*RPGR*; OMIM: 312610), the retinitis pigmentosa

2 (*RP2*; OMIM: 312600), and orofacioidigital syndrome 1 (*OFD1*; OMIM: 300170) genes. *RGPR* and *RP2* account for 70–90% and 7–18% of XLRP cases, respectively (Hardcastle et al., 1999; Neidhardt et al., 2008; Pelletier et al., 2007; Sahel, Marazova, & Audo, 2014; Vervoort et al., 2000).

RP2 was first identified by linkage analysis and encodes the *RP2* protein, which consists of 350 residues (Schwahn et al., 1998). The *RP2* protein is localized to the plasma membrane of rod/cone photoreceptors, the retinal pigment epithelium (RPE), and other retinal cells in human (Grayson et al., 2002), as well as in the Golgi complex, the primary cilia, and the basal body of the connecting cilium in mice (Evans et al., 2010; T. Hurd et al., 2010; T. W. Hurd, Fan, & Margolis, 2011; Lyraki et al., 2016). *RP2* goes through dual acylation at the extreme N-terminus, and this modification is crucial for plasma membrane localization and connecting cilium targeting (Chapple et al., 2000; Chapple, Hardcastle, Grayson, Willison, & Cheetham, 2002; Evans et al., 2010; T. Hurd et al., 2010; Lyraki et al., 2016). Cone-dominated retinal degeneration was reported in mouse models (Li et al., 2013; Li, Rao, & Khanna, 2019; H. Zhang et al., 2015).

Since the discovery of *RP2* as a causative gene for RP, 133 disease-associated variants have been identified, including 43 missense variants, 14 nonsense variants, 15 splice site alterations, 50 small insertions/deletions, nine gross deletions, one gross insertion, and others (HGMD; <https://portal.biobase-international.com>; Supporting Information), and patients with *RP2*-associated retinal disorder (*RP2*-RD) often present a severe and "atypical" form for RP, with early macular involvement causing central visual loss (Andreasson et al., 2003; Carss et al., 2017; Dandekar et al., 2004; Hosono et al., 2018; Jayasundera et al., 2010; Ji et al., 2010; Jin, Liu, Hayakawa, Murakami, & Nao-i, 2006; Maeda et al., 2018; Mashima et al., 2000; Mashima, Saga, Akeo, & Oguchi, 2001; Mears et al., 1999; Miano et al., 2001; Prokisch et al., 2007; Sharon et al., 2000; Sharon et al., 2003; Vorster et al., 2004; Wada, Nakazawa, Abe, & Tamai, 2000; Wang et al., 2014; Yang et al., 2014). A number of studies have been published about *RP2*-RD, especially in the European population; however, only a limited number of case reports/series have described the clinical and genetic features of *RP2*-RD in the East Asian population (Dan, Huang, Xing, & Shen, 2020; Hosono et al., 2018; Ji et al., 2010; Jiang et al., 2017; Jin et al., 2006; Kim et al., 2019; Koyanagi et al., 2019; Kurata et al., 2019; Lim, Park, Lee, & Taek Lim, 2016; Maeda et al., 2018; Mashima et al., 2001; Mashima et al., 2000; Pan et al., 2014; Wada et al., 2000; Xu et al., 2019; J. Zhang et al., 2019).

Therefore, the purpose of this study was to characterize the clinical and genetic features of patients with *RP2*-RD in a large nationwide Japanese cohort. A systematic review of *RP2*-RD in the Japanese population was also performed to clarify the genetic background and establish a genotype–phenotype association.

2 | METHODS

The protocol of this study adhered to the tenets of the Declaration of Helsinki and was approved by the Ethics Committee of the participating institutions of the Japan Eye Genetics Consortium (JEGC; <http://www.jegc.org/>). The principal institute is National Institute of Sensory Organs (NISO), National Hospital Organization Tokyo Medical Center (Reference: R18-029) (World Medical Association, 2013).

2.1 | Participants

Patients with a clinical diagnosis of IRD and available whole-exome sequencing (WES) genetic data were studied between 2008 and 2018. A total of 1,294 subjects from 730 families for whom genotype–phenotype association studies were completed, were surveyed, including 47 families with XLRP and 141 families with sporadic RP (Fujinami et al., 2016; Fujinami et al., 2019; Fujinami-Yokokawa et al., 2019; Fujinami-Yokokawa et al., 2020; Kameya et al., 2019; Katagiri et al., 2020; Kondo et al., 2019; Maeda-Katahira et al., 2019; Mawatari et al., 2019; Mizobuchi et al., 2019; Nakamura et al., 2019; Nakanishi et al., 2016; Pontikos et al., 2020; Xiao Liu et al., 2020; Yang et al., 2020).

2.2 | Clinical examinations

Clinical information is available in the NISO online database, including ethnicity, medical and family history, chief complaints of visual symptoms, onset of disease (of when the visual loss was first noted by the patient or when an abnormal retinal finding was first detected), measurement of refractive errors, best-corrected decimal visual acuity (BCVA) converted to the logarithm of the minimum angle of resolution (LogMAR) unit, fundus photographs, fundus autofluorescence (FAF) images, spectral-domain optical coherence tomographic (SD-OCT) images, kinetic visual fields, and electrophysiological responses recorded in accordance with the international standards of the International Society for Clinical Electrophysiology of Vision (ISCEV) (McCulloch et al., 2015a, 2015b).

2.3 | Variant detection

Genomic DNA was extracted from all affected subjects and unaffected family members (where available) for co-segregation analysis. WES with target sequence analysis of 301 retinal disease-associated genes mainly listed in a public database (RetNet <https://sph.uth.edu/retnet/home.htm>) was performed (Fujinami et al., 2016; Xiao Liu et al., 2020). The called variants were filtered based on the allele frequencies in the general Japanese population (less than 1%) of the Human Genetic Variation Database (HGVD; <http://www.hgvd.genome.med.kyoto-u.ac.jp/>). Hypomorphic variants with high allele frequencies (>1%) were analyzed for three particular genes (*EYS*, *ABCA4*, *USH2A*) (Yang et al., 2020). Depth and coverage for the target areas were assessed using the integrative Genomics Viewer (<http://www.broadinstitute.org/igv/>). Sanger bi-direct sequencing was performed to confirm the detected *RP2* variants and to conduct co-segregation analysis. Primer sequences are provided in Table S1.

Together with the clinical features (phenotype categorization) and the patterns of inheritance, disease-causing variants were determined from the detected/filtered variants in the retinal disease-associated genes (Fujinami-Yokokawa et al., 2020; Xiao Liu et al., 2020).

2.4 | In silico molecular genetic analysis

The allele frequencies of all called variants for the Japanese, East Asian, South Asian, European, and African populations were established based on the HGVD (Japanese), Integrative Japanese Genome Variation (iJGVD 3.5k, 4.7k; <https://jmorp.megabank.tohoku.ac.jp/ijgvd/>; Japanese), 1,000 Genomes (<http://www.internationalgenome.org/>; total), and the Genome Aggregation Database (gnomAD; <http://gnomad.broadinstitute.org/>; East Asian, South Asian, European [non-Finish], and African).

All detected variants in the *RP2* gene were analyzed with general and functional prediction programs: MutationTaster (<http://www.mutationtaster.org/>), FATHMM (<http://fathmm.biocompute.org.uk/9/>), Combined Annotation Dependent Depletion (CADD; <https://cadd.gs.washington.edu/>), SIFT (<https://www.sift.co.uk/>), PROVEAN ([-151-](http://</p>
</div>
<div data-bbox=)

provean.jcvi.org/index.php), Polyphen 2 (<http://genetics.bwh.harvard.edu/pph2/>), and Human Splicing Finder (<http://www.umd.be/HSF3/>). The evolutionary conservation scores were evaluated with the UCSC database (<https://genome.ucsc.edu/index.html>).

The location of the detected *RP2* variants was analyzed with a schematic genetic and protein structure of *RP2* (ENST00000218340.3), and multiple alignments of eight species of *RP2* were performed with the Clustal Omega program (<https://www.ebi.ac.uk/Tools/msa/clustalo/>). Molecular modeling of missense variants was performed with YASARA software (<http://www.yasara.org/>) based on a Swiss model (O75695; XRP2_HUMAN; <https://swissmodel.expasy.org/>).

The variant classification was performed for all detected variants, according to the guidelines of the American College of Medical Genetics and Genomics (ACMG) (Richards et al., 2015).

2.5 | A systematic review of *RP2*-RD

A systemic review of peer-reviewed articles that describe Japanese cases with *RP2*-RD was performed. A public search engine (PubMed; <https://www.ncbi.nlm.nih.gov/pubmed/>) was used to identify articles, and clinical and genetic information was collected. For the previously reported *RP2* variants, in silico molecular genetic analyses were performed in the same way as in the current study.

2.6 | Analysis of genotype–phenotype association

Patients in the current study and previously reported cases were classified into two genotype groups based on the presence of null *RP2* variants such as nonsense variants, frameshift variants, and splice site alterations: genotype group A with null variants and genotype group B with missense variants. For the purpose of this analysis, probands in the current cohort and previous publications were classified into two phenotype groups based on disease onset and BCVA: (a) a mild phenotype group showing both late-onset (≥ 10 years) and moderate or better VA (between 0.22 and 1.0 LogMAR unit in the better eye) and (b) a severe phenotype group with both early-onset (< 10 years) and severe VA (1.0 LogMAR unit or worse in the better eye). Patients who did not meet any of the two criteria were classified into an intermediate phenotype group. Probands with available data in families were selected for the further analyses and patients with unavailable data of either onset or VA were excluded.

An association between the genotype group classification and the phenotype severity group classification was investigated with Cochran-Armitage Test. A *p* value $< .05$ was considered statistically significant.

3 | RESULTS

3.1 | Demographics

Four affected males from four families who had a clinical diagnosis of IRD and were harboring *RP2* variants were identified. The detailed

demographics are described in Table 1. All four patients were clinically diagnosed with RP by attending doctors. The pedigrees of the four families are presented in Figure 1. All four families were originally from Japan and any mixture with other ethnicity was not reported. XL family history was clearly reported or possible in three families (Families #2, #3, and #4), and no affected subjects except for the proband were reported in one family (Family #1). One patient had a medical history of severe uveitis in the left eye (Patient 2), and retinal imaging, visual field testing and electrophysiological assessment were unavailable due to the dense corneal opacity. Cataracts were reported in two patients (Patients 2 and 4), and one patient underwent cataract surgery in the right eye (Patient 2). The mean age at the latest examination of four patients was 32.5 years (range, 10–47).

3.2 | Onset, chief complaint, refraction, and visual acuity

The mean age of onset was 11.3 (range, 3–28) years in the three patients with available records. Two of these three patients had early-onset of 3 years (Patients 1 and 2). Chief complaints at the initial visit of four patients with available records were night blindness in two patients (Patients 2 and 3), photophobia in one (Patient 1), and reduced visual acuity in one (Patient 4).

The mean spherical equivalent of the refractive errors of three phakic patients with available records was -2.17 diopter (-6.0 to 0.0) in the right eye and -2.33 diopter in the left eye (-6.0 to -0.50). Two patients had high myopia (Patients 2 and 4). One patient had an intraocular lens in the right eye (Patient 2). The median values of BCVA in the right and left eyes of the four patients with available records were 1.27 (0.52–2.00), and 1.12 (0.52–1.70) LogMAR units, respectively. There were three patients with severe VA (1.0 or worse LogMAR units in the better eye) (Patients 1, 2, and 4), and one with moderate VA (between 0.22 and 1.0 LogMAR unit in the better eye) (Patient 3).

3.3 | Retinal images and morphological findings

Fundus photographs were obtained in all four patients, and FAF images were available in one patient (Patient 1). The representative images are presented in Figure 2, and the detailed findings are described in Table 2. Extensive atrophic changes were observed in two patients (Patients 1 and 2). There was one patient with peripheral atrophy (Patient 3) and one with atrophic changes at the posterior pole (Patient 4). Preserved foveal appearance was shown in two patients (Patients 1 and 3), and preserved peripheral appearance was found in one patient (Patient 4). Bone spicule pigmentation at the periphery was identified in one patient (Patient 2), and macular pigmentation was detected in two patients (Patients 2 and 4). Retinal vessel attenuation was observed in three patients (Patients 1–3), and optic disc pallor was shown in two patients (Patients 2 and 3).

SD-OCT was obtained in four patients (Patients 1–4). Representative images are presented in Figure 3. Loss of photoreceptor layers

TABLE 1 Demographics and detected variants of four Japanese patients with RP2-associated retinal disorder (RP2-RD)

| Family no | Patient no | Patient ID | Inheritance | Sex | Age (at latest examination) | Onset | Chief complaint/ other symptoms | Refractive errors | | BCVA in the LogMAR unit | | Phenotype severity group | Genotype group |
|------------|---------------------|------------|-------------|-----|-----------------------------|-------|--|-------------------|--------------|-------------------------|------|------------------------------------|----------------|
| | | | | | | | | RE (diopter) | LE (diopter) | RE | LE | | |
| 1 (TMC-01) | 1-II:1 (patient 1) | 1-II:3 | Sporadic | M | 10 | 3 | Photophobia/poor VA/ night blindness | 0.0 | -0.5 | 1.3 | 1.15 | C.358C>T, p.Arg120Ter | A |
| 2 (NU-01) | 2-II:3 (patient 2) | 2-II:3 | XL | M | 35 | 3 | Night blindness/poor VA/ peripheral visual field defect | -6.0 | NA | 2 | NLP | c.801_804del, p.Glu269CysfsTer3 | A |
| 3 (TU-01) | 3-III:1 (patient 3) | 3-III:1 | XL | M | 38 | 28 | Night blindness | -0.5 | -0.5 | 0.52 | 0.52 | c.17C>T, p.Ser6Phe | B |
| 4 (KDU-01) | 4-II:1 (patient 4) | 4-II:1 | XL | M | 47 | NA | Reduced visual acuity | -6.0 | -6.0 | 1.7 | 1.7 | c.566T>C, p.Leu189Pro | NA |

Note: Age was defined the age when the latest examination was performed. The age of onset was defined as either the age at which visual loss was first noted by the patient or when an abnormal retinal finding was first detected. Severe post-uveitic changes with dense corneal opacity (invisible fundus) were found in the left eye of patient 2. Cataracts were reported in two patients (patients 2 and 4), and one patient underwent cataract surgery in the right eye (patient 2). RP2 transcript ID: NM_006915.2. Whole-exome sequencing with target analysis of 301 retinal disease-associated genes mainly listed on a public database (RetNet <https://sph.uth.edu/retnet/home.htm>) was performed. Genotype A: Null variants, severe group; genotype B: Missense variants, mild group. Abbreviations: AR, autosomal recessive; BCVA, best corrected deimal visual acuity converted to the logarithm of the minimum angle of resolution (LogMAR) unit; F, female; LE, left eye; M, male; NA, not available; NLP, no light perception; no. number; RE, right eye; XL, x-linked recessive.

was observed at the entire retina in three patients (Patients 1, 2, and 4) and at the peripheral retina in one patient (Patient 3). Relatively preserved foveal structure, including slight changes of fluid in the inner layers were identified in one patient (Patient 3).

3.4 | Visual fields and electrophysiological findings

Visual field testing was performed in four patients with Goldmann kinetic perimetry (Table 2). Peripheral visual field loss with central scotoma was observed in two patients (Patients 1 and 3). There was one patient with an entire visual field defect (Patient 2) and one with a large central scotoma and preserved peripheral field (Patient 4). Electrophysiological assessment was performed in four patients (Patients 1-4) (Table 2). Extinguished responses in both dark-adapted and light-adapted conditions were recorded in three patients (Patients 1-3). Relatively preserved responses in both dark-adapted and light-adapted conditions were observed in one patient (Patient 4).

3.5 | RP2 variants

Four affected probands (males) were tested with WES with target analysis of 301 retinal disease-associated genes: 1-II:1 (Patient 1), 2-II:3 (Patient 2), 3-III:1 (Patient 3), and 4-II:1 (Patient 4). In addition, two unaffected family members from Family 1 and two unaffected family members in Family 3 were examined for segregation: 1-I:1 (father of Patient 1), 1-I:2 (mother of Patient 1), 3-II:7 (father of Patient 3), and 3-II:8 (mother of Patient 3) (Figure 1, Table S2). Two mothers from two families (Families 1 and 3) were proved to be carriers: 1-I:2 (mother of Patient 1) and 3-II:8 (mother of Patient 3).

Variants data of four patients are summarized in Table 1 and Figure 1. Four hemizygous RP2 variants were identified: c.17C>T (p.Ser6Phe); c.358C>T (p.Arg120Ter); c.566T>C (p.Leu189Pro); and c.801_804del (p.Glu269CysfsTer3) (NM_006915.2). Two variants have been previously reported: p.Arg120Ter in eight articles (Carss et al., 2017; Hardcastle et al., 1999; Jin et al., 2006; Kurata et al., 2019; Mashima et al., 2001; Mears et al., 1999; Vorster et al., 2004; Wang et al., 2014) and p.Glu269CysfsTer3 in one article (Pelletier et al., 2007). The other two variants have never been reported: c.17C>T (p.Ser6Phe) and c.566T>C (p.Leu189Pro).

A schematic of the RP2 protein structure showing the positions of the four detected variants in the current study is presented in Figure 4. There was one missense variant located in exon 1 (p.Ser6Phe), one nonsense variant (p.Arg120Ter), and one missense variant (p.Leu189Pro) in exon 2, and one frameshift variant in exon 3 (p.Glu269CysfsTer3).

3.6 | In silico molecular genetic analysis

The detailed results of *in silico* molecular genetic analyses for the four detected RP2 variants in the current study are provided in Table 3.

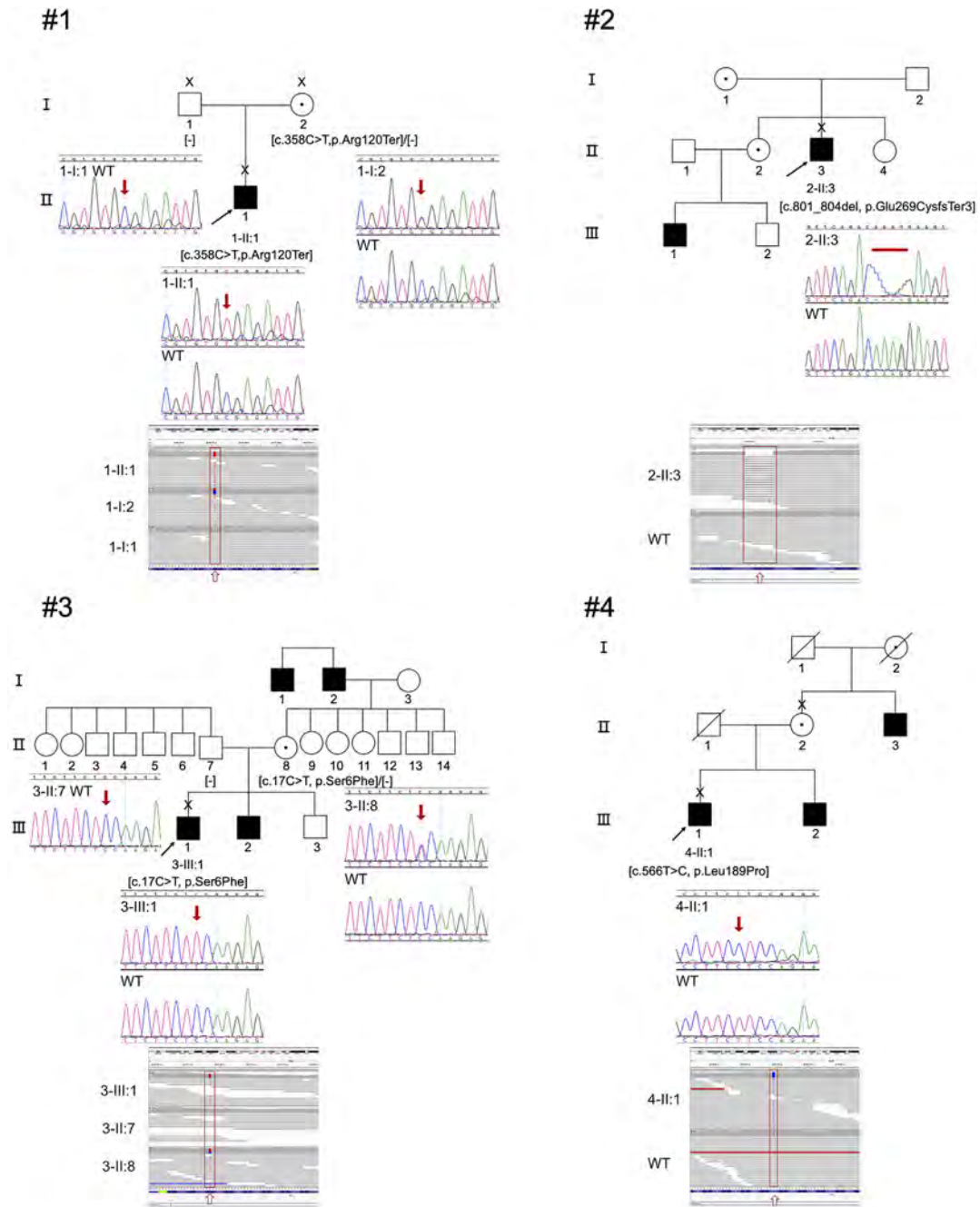


FIGURE 1 Pedigrees of four Japanese families with retinitis pigmentosa harboring hemizygous *RP2* variants. The affected males are represented by solid squares (men), and unaffected family members are represented by white icons. The slash symbol indicates deceased individuals. The generation is numbered on the left. The probands and the clinically examined individuals are marked by an arrow and a cross, respectively. Depth and coverage for the target areas by next-generation sequencing were assessed using the integrative Genomics Viewer (<http://www.broadinstitute.org/igv/>). Sanger bi-direct sequencing was also performed to confirm each variant

These four *RP2* variants were well-covered with WES, but no subjects in the general population had these variants, which confirmed the rarity of these detected variants (Table 3, Table S3).

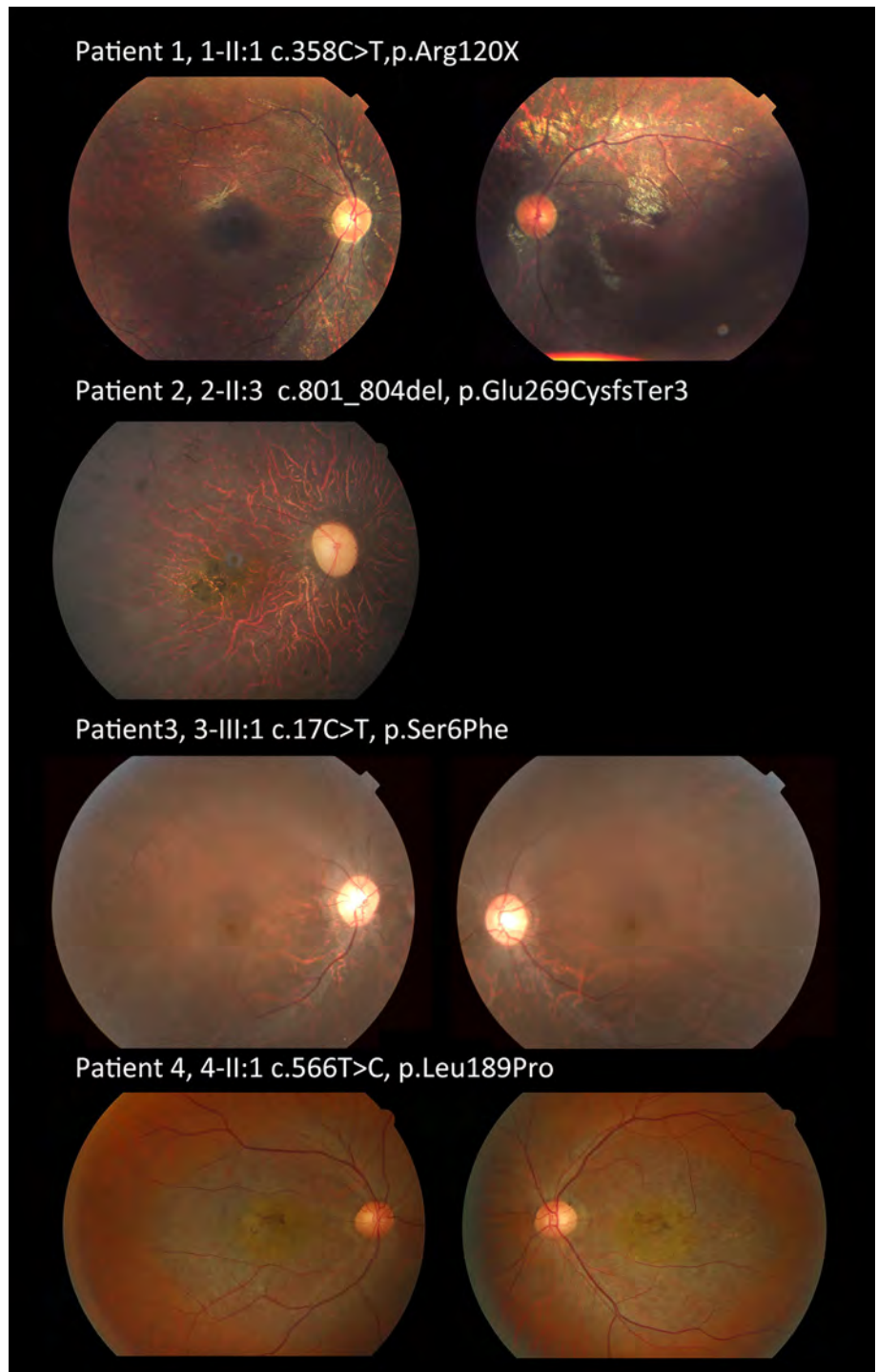
Three general (MutationTaster, FATHMM, CADD) and three functional (SIFT, PROVEAN, Polyphen2) prediction programs were applied for two missense variants (p.Ser6Phe, p.Leu189Pro), and all programs predicted disease-causing/damaging effects. The evolutionary conservation scores obtained with the UCSC database indicated high

conservation of the two missense variants (Figure 5). Molecular modeling of these missense variants is shown in Figure S1. Pathogenicity classifications, according to the ACMG guidelines, were pathogenic for the two truncating variants (p.Glu269CysfsTer3, p.Arg120Ter), likely pathogenic for the one missense variant (p.Ser6Phe), and uncertain significance for the one missense variant (p.Leu189Pro).

Overall, given the inheritance and the phenotype, two disease-causing variants (p.Glu269CysfsTer3, p.Arg120Ter) and two putative

FIGURE 2 Fundus photographs and fundus autofluorescence images of *RP2*-associated retinal disorder (*RP2*-RD).

Patient 1: Extensive retinal atrophic changes with relatively preserved foveal appearance and vessel attenuation.
 Patient 2: Extensive retinal atrophic changes with bone spicule pigmentation at the periphery and patchy pigmentation at the macula, vessel attenuation, and disc pallor.
 Patient 3: Atrophic changes at the peripheral retina with relatively preserved foveal appearance, vessel attenuation, and disc pallor.
 Patient 4: Atrophic changes at the posterior pole with pigmentation at the macula



disease-causing variants (p.Ser6Phe, p.Leu189Pro) were determined in four families with XLRP.

3.7 | Nineteen cases from 14 Japanese families with *RP2*-RD in previous reports

There are eight previous reports of *RP2*-RD in the Japanese population (Hosono et al., 2018; Jin et al., 2006; Koyanagi et al., 2019;

Kurata et al., 2019; Maeda et al., 2018; Mashima et al., 2000; Mashima et al., 2001; Wada et al., 2000). The summarized data are presented in Table 4. Nineteen affected males from 14 families were reported in total. There were 17 patients with RP and two patients with Leber congenital amaurosis (LCA).

The mean age at the latest examination among the 16 patients with available data was 31.2 (16–61) years, and the mean age at onset of the eight patients with available data was 5.75 (3–11) years. Other descriptions about the age of onset were as follows: in the first

TABLE 2 Retinal, morphological, visual field, and electrophysiological findings of four Japanese patients with RP2-RD

| Patient no | Fundus/FAF findings | SD-OCT findings | Visual field | Electrophysiological assessment |
|------------|--|---|--|---|
| 1 | Extensive retinal atrophic changes with relatively preserved foveal appearance and vessel attenuation. | Loss of photoreceptor layers at the entire retina with relatively preserved other sensory retinal layers and RPE layer. | Peripheral visual field loss with central scotoma. | Extinguished responses in both dark-adapted and light-adapted conditions. |
| 2 | Extensive retinal atrophic changes with bone spicule pigmentation at the periphery and patchy pigmentation at the macula, vessel attenuation, and disc pallor. | Loss of photoreceptor layers at the entire retina with thinned RPE. | Entire visual field loss. | Extinguished responses in both dark-adapted and light-adapted conditions. |
| 3 | Atrophic changes at the peripheral retina with relatively preserved foveal appearance, vessel attenuation, and disc pallor. | Loss of photoreceptor layers at the peripheral retina with relatively preserved foveal structure including slight changes of fluid in the inner layers. | Peripheral visual field loss with central scotoma. | Extinguished responses in both dark-adapted and light-adapted conditions. |
| 4 | Atrophic changes at the posterior pole with pigmentation at the macula. | Loss of photoreceptor layers at the entire retina with thinned RPE. | Large central scotoma with preserved peripheral field. | Relatively preserved responses in both dark-adapted and light-adapted conditions. |

Note: Retinal imaging, visual field testing, and electrophysiological assessment were unavailable due to the dense corneal opacity after severe uveitis in the left eye of Patient 2.

Abbreviations: FAF, fundus autofluorescence; LE, left eye; RE, right eye; RPE, retinal pigment epithelium; SD-OCT, spectral-domain optical coherence tomography.

decade (two patients), early teens (one patient), within 1 year (one patient), and childhood (one patient). Night blindness was noticed as the chief complaint in 10 out of the 12 patients (10/12, 83%) with available data. The mean spherical equivalent of refractive errors of 10 patients with available data was -6.6 diopter (-12.0 – 0.75) in the right eye and -6.1 diopter in the left eye (-10.0 – 0.50). The mean BCVA in the right and left eyes of 12 patients with available data was 1.14 (0.70–1.52) and 1.25 (0.52–1.70) LogMAR units, respectively. There were five eyes with hand motion, three eyes with light perception, and one eye with non-light perception. Electrophysiological responses were undetectable in 12 patients with available data.

The detailed results of *in silico* molecular genetic analyses for the 12 RP2 variants in the previous Japanese reports are provided in Table 3. There were four frameshift variants, three nonsense variants, two splice site alterations, and three missense variants: c.87G>A (p.Trp29Ter); c.102+1G>A; c.217delT (p.Tyr73IlefsTer18); c.353G>A (p.Arg118His); c.358C>T (p.Arg120Ter); c.413A>G (p.Glu138Gly); c.677delG (p.Gly226ValfsTer12); c.685C>T (p.Gln229Ter); c.758T>G (p.Leu253Arg); c.769-2A>G; c.882delA (p.Gly295ValfsTer14); and c.831_832dupTC (p.Gln278LeufsTer16). Eight variants are unique in the Japanese population. With regard to four variants, there are reports from other populations: c.102+1G>A; p.Arg118His; p.Arg120Ter; and p.Glu138Gly. One common variant (p.Arg120Ter) was identified in three Japanese families in the previous reports (Jin et al., 2006; Kurata et al., 2019; Mashima et al., 2001).

3.8 | Genotype–phenotype association

For the analysis, a total of 10 probands with available onset age and BCVA were studied: three from the current study and seven from previously reported cases. There were eight patients in genotype group A (null variants) and two in genotype group B (non-null variants) (Table S4). Seven patients had a severe phenotype with earlier onset of the disease and severe VA loss, and three had a mild phenotype with later onset and moderate VA loss. A statistically significant association between genotype group classification and phenotype severity classification was revealed ($p < .05$).

4 | DISCUSSION

The clinical and genetic spectrum of RP2-RD was documented in a nationwide cohort of the Japanese population, detecting four variants, two of which have never been reported. A severe RP phenotype with early macular involvement causing central visual loss was identified and a genotype–phenotype association based on the presence of null variants was illustrated.

In the present study, RP2-RD accounted for 6.4% of XLRP families (3/47 families with XLRP) and 0.7% of sporadic RP cases (1/141 families with sporadic RP) in the JEGC cohort with IRD. Koyanagi et al. reported genetic results of a large cohort of 1,209 patients with RP and revealed that three of 18 patients (3/18, 16.7%) with a family

FIGURE 3 Optical coherence tomographic images of RP2-RD. Patient 1: Loss of photoreceptor layers at the entire retina with relatively preserved other sensory retinal layers and retinal pigment epithelial (RPE) layer. Patient 2: Loss of photoreceptor layers at the entire retina with thinned RPE. Patient 3: Loss of photoreceptor layers at the peripheral retina with relatively preserved foveal structure, including slight changes of fluid in the inner layers. Patient 4: Loss of photoreceptor layers at the entire retina with thinned RPE

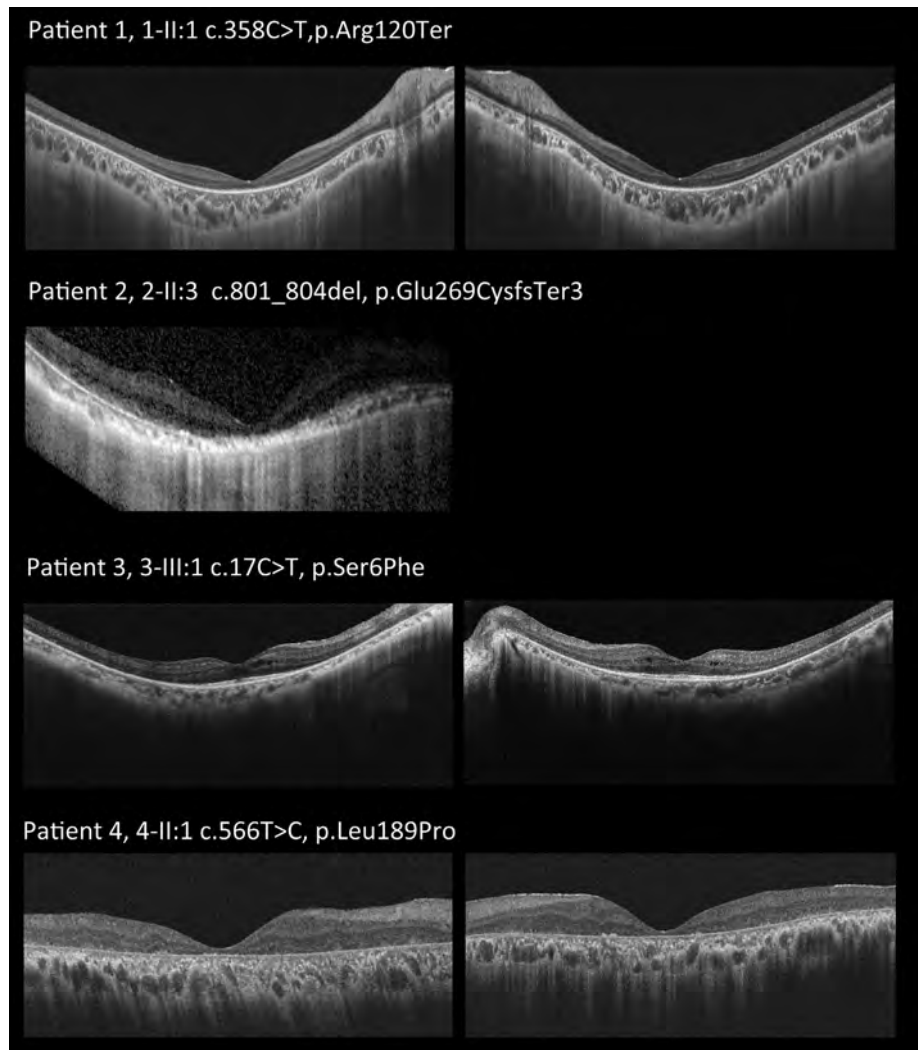


FIGURE 4 A schematic genetic and protein structure of RP2 and the location of the detected variants. The RP2 gene (ENST00000218340.3) contains five exons that encode a 350 amino acid protein containing a myristoylation part, a cofactor C (Arl3 binding) domain, and a ferredoxin-like domain (Jayasundera et al., 2010). Four variants detected in the current study are underlined (c.17C>T (p.Ser6Phe); c.358C>T (p.Arg120Ter); c.566T>C (p.Leu189Pro); and c.801_804del (p.Glu269CysfsTer3)), and previously reported variants in the Japanese populations are shown without an underline. Two detected variants (p.Ser6Phe, p.Leu189Pro), which have never been reported, are shown in *italic*

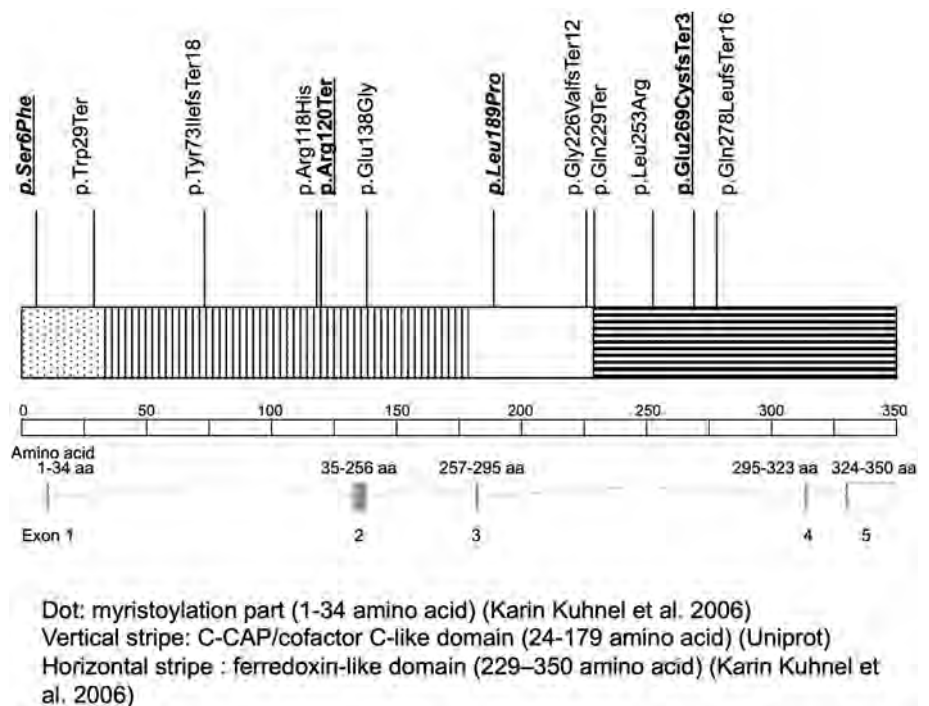


TABLE 3 *In silico* molecular genetic analysis results for four detected variants in the current study and 10 previously reported variants in Japanese patients with RP2-RD

| Nucleotide change | Amino acid change/ effect | Position | Coding impact | Location | dbSNP ID | IJGVD | | | | | Allele frequency (genome) | | | | | |
|---------------------------|------------------------------|----------|------------------------|--|-------------|-------|------|------|-------------|------------|---------------------------|---------|------------------------|-------|------|----|
| | | | | | | HGVD | 3.5K | 4.7K | 1000 genome | East Asian | South Asian | African | European (Non-Finnish) | Total | Male | |
| c.17C>T | p.Ser6Phe | 46696552 | Missense | Exon 1 of 5 position 75 of 160 (coding) | NA | NA | NA | NA | NA | NA | NA | NA | NA | NA | NA | NA |
| c.87G>A | p.Trp29Ter | 46696622 | Nonsense | Exon 1 of 5 position 145 of 160 (coding, NMD) | NA | NA | NA | NA | NA | NA | NA | NA | NA | NA | NA | NA |
| c.102+1G>A | Splice site alteration | 46696638 | Splice site alteration | Intron 1 of 4 position 1 of 16273 (splicing-ACMG, splicing, intronic) | NA | NA | NA | NA | NA | NA | NA | NA | NA | NA | NA | NA |
| c.217delT | p.Tyr73IlefsTer18 | 46713025 | Frameshift | Exon 2 of 5 position 115 of 666 (coding, NMD) | NA | NA | NA | NA | NA | NA | NA | NA | NA | NA | NA | NA |
| c.353G>A | p.Arg118His | 46713161 | Missense | Exon 2 of 5 position 251 of 666 (coding) | rs28933687 | NA | NA | NA | NA | NA | NA | NA | NA | NA | NA | NA |
| c.358C>T, p. Arg120Ter | p.Arg120Ter | 46713166 | Nonsense | Exon 2 of 5 position 256 of 666 (coding, NMD) | rs104894927 | NA | NA | NA | NA | NA | NA | NA | NA | NA | NA | NA |
| c.413A>G | p.Glu138Gly | 46713221 | Missense | Exon 2 of 5 position 311 of 666 (coding) | NA | NA | NA | NA | NA | NA | NA | NA | NA | NA | NA | NA |
| c.566T>C | p.Leu189Pro | 46713374 | Missense | Exon 2 of 5 position 464 of 666 (coding) | NA | NA | NA | NA | NA | NA | NA | NA | NA | NA | NA | NA |
| c.677delG | p.Gly226ValfsTer12 | 46713485 | Frameshift | Exon 2 of 5 position 575 of 666 (coding, NMD) | NA | NA | NA | NA | NA | NA | NA | NA | NA | NA | NA | NA |
| c.685C>T | p.Gln229Ter | 46713493 | Nonsense | Exon 2 of 5 position 583 of 666 (coding, NMD) | NA | NA | NA | NA | NA | NA | NA | NA | NA | NA | NA | NA |
| c.758T>G | p.Leu253Arg | 46713566 | Missense | Exon 2 of 5 position 656 of 666 (coding) | NA | NA | NA | NA | NA | NA | NA | NA | NA | NA | NA | NA |
| c.769-2A>G | Splice site alteration | 46719421 | Splice site alteration | Intron 2 of 4 position 5845 of 5846 (splicing-ACMG, splicing, intronic) | NA | NA | NA | NA | NA | NA | NA | NA | NA | NA | NA | NA |
| c.801_804delAAAG | p.Glu269CysfsTer3 | 46719455 | Frameshift | Exon 3 of 5 position 33-36 of 115 (coding, NMD) | NA | NA | NA | NA | NA | NA | NA | NA | NA | NA | NA | NA |

TABLE 3 (Continued)

| Nucleotide change | Amino acid change/ effect | Position | Coding impact | Location | dbSNP ID | iGVGD | | | | Allele frequency (genome) | | | | | | |
|---------------------------|------------------------------|------------------------------|---------------|--|------------|--------|------------------------|-------|-------------|---------------------------|-------------|---------|------------------------|-------|------------|---|
| | | | | | | HGVD | 3.5K | 4.7K | 1000 genome | East Asian | South Asian | African | European (Non-Finnish) | Total | Male | |
| c.831_832dupTC | p.Gln278LeufsTer16 | 46719484 | Frameshift | Exon 3 of 5 before position 65 of 115 (coding, NMD) | NA | NA | NA | NA | NA | NA | NA | NA | NA | NA | NA | |
| c.882delA | p.Gly295ValfsTer14 | 46719536 | Frameshift | Exon 3 of 5 position 114 of 115 (splicing-ACMG, splicing, coding, NMD) | NA | NA | NA | NA | NA | NA | NA | NA | NA | NA | NA | |
| General prediction | | | | | | | | | | | | | | | | |
| MutationTaster | | | | | | | | | | | | | | | | |
| Functional prediction | | | | | | | | | | | | | | | | |
| SIFT | | | | | | | | | | | | | | | | |
| CADD | | | | | | | | | | | | | | | | |
| FATHMM | | | | | | | | | | | | | | | | |
| Human Splice Finder 3.0 | | | | | | | | | | | | | | | | |
| Nucleotide change | Amino acid change/ effect | Prediction | Accuracy | Converted rankscore | Prediction | Score | Converted rankscore | Score | Prediction | Score | Prediction | Score | Prediction | Score | Prediction | Human Splice Finder 3.0 |
| c.17C>T | p.Ser6Phe | Disease causing | 0.9993 | 0.4646 | Damaging | -2.81 | 0.9113 | 24 | Damaging | 24 | Damaging | 24 | Damaging | 24 | Damaging | Probably no impact on splicing |
| c.87G>A | p.Trp29Ter | Disease causing automatic | 1 | 0.81 | Damaging | 0.936 | 0.5866 | 37 | NA | NA | NA | NA | NA | NA | NA | Potential alteration of splicing |
| c.102+1G>A | Splice site alteration | Disease causing | 1 | 0.81 | Damaging | 0.9426 | 0.6059 | 33 | NA | NA | NA | NA | NA | NA | NA | Most probably affecting splicing |
| c.217delT | p.Tyr73IlefsTer18 | NA | NA | NA | NA | NA | NA | 26.5 | NA | NA | NA | NA | NA | NA | NA | Probably no impact on splicing |
| c.353G>A | p.Arg118His | Disease causing | 1 | 0.81 | Damaging | -2.73 | 0.9068 | 29.1 | Damaging | 29.1 | Damaging | 29.1 | Damaging | 29.1 | Damaging | Potential alteration of splicing |
| c.358C>T, p. Arg120Ter | p.Arg120Ter | Disease causing automatic | 1 | 0.81 | Damaging | 0.7834 | 0.3863 | 34 | NA | NA | NA | NA | NA | NA | NA | Potential alteration of splicing |
| c.413A>G | p.Glu138Gly | Disease causing | 1 | 0.81 | Damaging | -2.81 | 0.9113 | 27.8 | Damaging | 27.8 | Damaging | 27.8 | Damaging | 27.8 | Damaging | Potential alteration of splicing |
| c.566T>C | p.Leu189Pro | Disease causing | 1 | 0.81 | Damaging | -3.01 | 0.9221 | 27.1 | Damaging | 27.1 | Damaging | 27.1 | Damaging | 27.1 | Damaging | Potential alteration of splicing |
| c.677delG | p.Gly226ValfsTer12 | NA | NA | NA | NA | NA | NA | 27.5 | NA | NA | NA | NA | NA | NA | NA | Potential alteration of splicing |
| c.685C>T | p.Gln229Ter | Disease causing automatic | 1 | 0.81 | Damaging | 0.947 | 0.6204 | 36 | Damaging | 36 | Damaging | 36 | Damaging | 36 | Damaging | Potential alteration of splicing |
| c.758T>G | p.Leu253Arg | Disease causing | 0.9998 | 0.4908 | Tolerated | -1.12 | 0.7759 | 24.7 | Damaging | 24.7 | Damaging | 24.7 | Damaging | 24.7 | Damaging | This mutation has probably no impact on splicing. |
| c.769-2A>G | Splice site alteration | NA | NA | NA | NA | NA | NA | 34 | NA | NA | NA | NA | NA | NA | NA | Most probably affecting splicing |
| c.801_804delAAAAG | p.Glu269CysfsTer3 | NA | NA | NA | NA | NA | NA | 11.53 | NA | NA | NA | NA | NA | NA | NA | Potential alteration of splicing |
| c.831_832dupTC | p.Gln278LeufsTer16 | NA | NA | NA | NA | NA | NA | NA | NA | NA | NA | NA | NA | NA | NA | NA |
| c.882delA | p.Gly295ValfsTer14 | NA | NA | NA | NA | NA | NA | NA | NA | NA | NA | NA | NA | NA | NA | Potential alteration of splicing |

(Continues)

| Nucleotide change | Amino acid change/effect | Conservation | | | | Conservation | | | | ACMG Classification | | | | | References in the Japanese population | References in other population | | | | | |
|-------------------|--------------------------|---------------------|---------------------|----------------------|----------------------|---------------------|---------------------|----------------------|----------------------|---------------------------------|---------|---------|------------------------|---------|---------------------------------------|--------------------------------|-----|-----|-----|---|---|
| | | PhastCons46way | | PhyloP100way | | PhastCons100way | | PhyloP100way | | Identified classification rules | | | | | | | | | | | |
| | | Mammalian rankscore | Mammalian rankscore | vertebrate rankscore | vertebrate rankscore | Mammalian rankscore | Mammalian rankscore | vertebrate rankscore | vertebrate rankscore | Factor1 | Factor2 | Factor3 | Factor4 | Factor5 | | | | | | | |
| c.17C>T | p.Ser6Phe | 2.072 | NA | 1 | NA | 2.226 | 0.4261 | 1 | 0.7164 | 1 | NA | 0.7164 | Likely pathogenic | PM2 | PP1 | PP2 | PP3 | PP3 | NA | This study | NA |
| c.87G>A | p.Trp29Ter | 2.134 | NA | 1 | NA | 4.5009 | 0.6011 | 1 | 0.7164 | 1 | NA | 0.7164 | Pathogenic | PV51 | PM2 | PP3 | PP3 | PP3 | NA | Koyanagi et al., 2019 | NA |
| c.102+1G>A | Splice site alteration | 2.134 | NA | 0.994 | NA | 4.5009 | 0.6011 | 1 | 0.7164 | 1 | NA | 0.7164 | Pathogenic | PV51 | PP1 | PM2 | PP3 | PP3 | NA | Kurata et al., 2019 | Sharon et al., 2000 |
| c.217delT | p.Tyr73IlefsTer18 | 4.494 | NA | 1 | NA | NA | NA | NA | NA | NA | NA | NA | Pathogenic | PV51 | PP1 | PM2 | PP3 | PP3 | NA | Kurata et al., 2019 | NA |
| c.353G>A | p.Arg118His | 5.5 | NA | 1 | NA | 9.4499 | 0.9677 | 1 | 0.7164 | 1 | NA | 0.7164 | Likely Pathogenic | PM2 | PM5 | PP2 | PP3 | PP5 | PP5 | Koyanagi et al., 2019 | Schwahn et al., 1998 and others |
| c.358C>T | p.Arg120Ter | NA | NA | NA | NA | 0.8289 | 0.271 | 0.8659 | 0.3072 | 0.8659 | 0.271 | 0.3072 | Pathogenic | PV51 | PP1 | PM2 | PP3 | PP5 | PP5 | This study, Mashima et al., 1999 and others | Mears et al., 2001; Jin et al., 2006; Kurata et al., 2019 |
| c.413A>G | p.Glu138Gly | 2.134 | NA | 0.994 | NA | 8.805 | 0.9154 | 1 | 0.7164 | 1 | NA | 0.7164 | Likely pathogenic | PM2 | PP1 | PP2 | PP3 | PP5 | PP5 | Kurata et al., 2019 | Miano et al., 2001 |
| c.566T>C | p.Leu189Pro | 4.5 | NA | 1 | NA | 7.5549 | 0.8117 | 1 | 0.7164 | 1 | NA | 0.7164 | Uncertain Significance | PM2 | PP3 | PP3 | PP3 | PP3 | PP3 | This study | NA |
| c.677delG | p.Gly226ValfsTer12 | 5.506 | NA | 1 | NA | NA | NA | NA | NA | NA | NA | NA | Pathogenic | PV51 | PM2 | PP3 | PP3 | PP3 | PP3 | Koyanagi et al., 2019 | NA |
| c.685C>T | p.Gln229Ter | 3.8 | NA | 1 | NA | 4.504 | 0.6014 | 1 | 0.7164 | 1 | NA | 0.7164 | Pathogenic | PV51 | PP1 | PM2 | PP3 | PP3 | PP3 | Kurata et al., 2019 | NA |
| c.758T>G | p.Leu259Arg | 4.542 | NA | 1 | NA | 7.5549 | 0.8117 | 1 | 0.7164 | 1 | NA | 0.7164 | Likely pathogenic | PS3 | PM2 | PP1 | PP3 | PP5 | PP5 | Wada et al., 2000 | NA |
| c.769-2A>G | Splice site alteration | 4.319 | NA | 1 | NA | 8.211 | 0.8971 | 1 | 0.7164 | 1 | NA | 0.7164 | Pathogenic | PV51 | PM2 | PP1 | PP3 | PP3 | PP3 | Hosono et al., 2018 | NA |
| c.801_804delAAAG | p.Glu269CysfsTer3 | 4.319 | NA | 1 | NA | NA | NA | NA | NA | NA | NA | NA | Pathogenic | PV51 | PM2 | PP3 | PP3 | PP3 | PP3 | This study | Pelletier et al., 2007 |
| c.831_832dupTC | p.Gln278LeufsTer16 | NA | NA | NA | NA | NA | NA | NA | NA | NA | NA | NA | Pathogenic | PV51 | PM2 | PP1 | PP3 | PP3 | PP3 | Mashima et al., 2000 | NA |
| c.882delA | p.Gly295ValfsTer14 | NA | NA | NA | NA | NA | NA | NA | NA | NA | NA | NA | Pathogenic | PV51 | PM2 | PP3 | PP3 | PP3 | PP3 | Maeda et al., 2018 | NA |

Note: Chr—chromosome; Het—heterozygous; ND—not detected. Reference: NM_006915.2, ENST00000218340.3, GRCh37.p13. The allele frequency of all called variants for Japanese, East Asian, South Asian, European, and African was established based on the HGVD (Japanese), Integrative Japanese Genome Variation (IJGV) 3.5k, 4.7k; <https://jgvp.megabank.tohoku.ac.jp/ijgv/>; Japanese), 1000 genome (<http://www.internationalgenome.org/>; total), and the genome aggregation database (gnomAD; <http://gnomad.broadinstitute.org/>; East Asian, South Asian, European (non-Finish), and African). All detected variants in

the *RP2* gene were analyzed with general and functional prediction programs; MutationTaster (<http://www.mutationtaster.org>), FATHMM (<http://fathmm.biocompute.org.uk/>), Combined Annotation Dependent Depletion (CADD; <https://cadd.gs.washington.edu/>), SIFT (<https://www.sift.co.uk/>), PROVEAN (<http://provean.jcvi.org/index.php>), Polyphen 2 (<http://genetics.bwh.harvard.edu/pph2/>), and Human Splicing Finder (<http://www.umd.be/HSF3/>). Evolutionary conservation score was evaluated with the UCSC database (<https://genome.ucsc.edu/index.html>). Classification of predictions by the American College of Medical Genetics and Genomics (ACMG) was also applied for all detected variants; PVS1 (Null variant (nonsense, frameshift, canonical ± 1 or 2 splice sites, initiation codon, single or multiexon deletion) in a gene where loss of function is a known mechanism of disease); PS3 (Well-established in vitro or in vivo functional studies supportive of a damaging effect on the gene or gene product); PM2 (pathogenicity moderate); absent from controls in Exome Sequencing Project, 1000 Genomes Project, or Exome Aggregation Consortium); PM5 (Novel missense change at an amino acid residue where a different missense change determined to be pathogenic has been seen before); PP1 (Cosegregation with disease in multiple affected family members in a gene definitively known to cause the disease.); PP3 (Multiple lines of computational evidence support a deleterious effect on the gene or gene product (conservation, evolutionary, splicing impact, etc.); PP4 (Patient's phenotype or family history is highly specific for a disease with a single genetic etiology); PP5 (pathogenicity supporting 5; reputable source recently reports variant as pathogenic, but the evidence is not available to the laboratory to perform an independent evaluation).

history of XL harbored pathogenic *RP2* variants (Koyanagi et al., 2019). The prevalence of *RP2*-RD in Japan can be slightly lower than that in Europe (21.6% in Denmark; 15.9% in France) (Pelletier et al., 2007; Prokisch et al., 2007). In total, four out of 287 families with RP with any inheritance (4/287, 1.4%) were diagnosed with *RP2*-RD in the JEGC cohort, and this proportion was lower than that in the United States (18/611, 2.9%) (Jayasundera et al., 2010).

In the current study, three patients presented extensive/peripheral retinal atrophy with macular involvement, and one had constricted retinal atrophic changes at the posterior pole. Thus, the characteristic clinical findings of an "atypical" form of early macular involvement were identified, as reported previously (Dandekar et al., 2004; Jayasundera et al., 2010). High myopia (≤ -6.0 diopters) was identified in a half (50%) of our four Japanese patients and its prevalence is similar to that of *RP2*-RD in a different cohort (12/25, 48.0%) (Jayasundera et al., 2010). This prevalence of high myopia in *RP2*-RD was much higher than that of the general Japanese population (5.8–11.8%) reported in previous reports (Ueda et al., 2019; Yotsukura et al., 2019). Central visual loss was also found in all four patients, which was likely caused by macular dysfunction in *RP2*-RD. Although the onset of disease was variable, it is notable that the presence of macular involvement is crucial for the impairment of visual acuity in *RP2*-RD.

Two novel and two previously reported variants were identified in four Japanese families in the current study. Two truncating variants (p.Arg120Ter, p.Glu269CysfsTer3) are located in exons 2 and 3, and functional loss of the *RP2* protein was predicted. One missense variant (p.Leu189Pro) was located in the ARL3 binding domain, and the other missense variant (p.Ser6Phe) was located in the myristoylation region of the *RP2* protein (Figure 4) (Jayasundera et al., 2010; Pelletier et al., 2007; Schwahn et al., 1998). Although functional analysis has not been performed, the clinical findings and the suggested inheritance highly support the disease causation with the XL recessive inheritance.

Mashima et al. reported detailed clinical findings of a patient with p.Arg120Ter: a 24-year-old Japanese male presented a severe form of RP with early macular involvement (Mashima et al., 2001). Similar clinical findings were observed in our patient with p.Arg120Ter (Patient 1). Likewise, Kurata et al. reported the severe phenotype of a patient with this variant. Although there are four reports from other populations, a founder effect should be considered for this allele in the Japanese population, given the high prevalence of this allele (4/18 families; 22.2%) in patients with *RP2*-RD.

The current study and literature search of *RP2*-RD in the Japanese population revealed a high proportion of null variants (11/15; 73.3%), which is in keeping with the findings among the European and North American populations (9/13; 69.2% in France; 11/17; 64.8% in the United States). This finding supports that the complete loss of function is the main mechanism of *RP2*-RD shared between the Japanese and European populations.

Ten unique *RP2* variants in the Japanese population were analyzed: two variants detected in the current study and eight previously reported variants. This high proportion (10/15, 66.7%) of unique

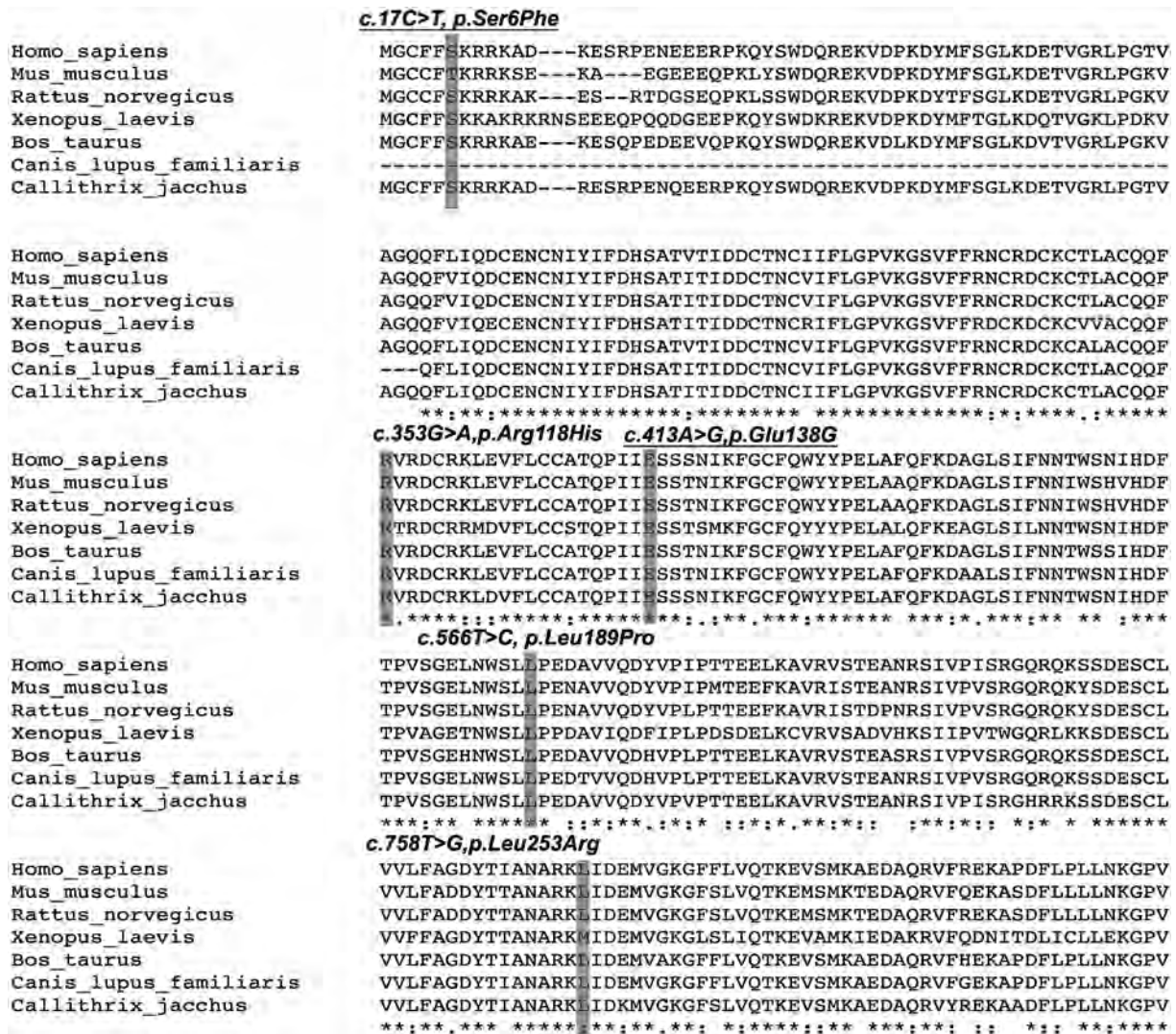


FIGURE 5 Multiple alignments of eight species of *RP2*. The alignment was performed with the Clustal Omega program (<https://www.ebi.ac.uk/Tools/msa/clustalo/>), and the amino acid sequence alignment is numbered in accordance with the *Homo sapiens* *RP2* sequence (ENST00000218340.3). An asterisk indicates complete conservation across the eight species. The positions of variant residues are highlighted with a gray background; c.17C>T (p.Ser6Phe) and c.566T>C (p.Leu189Pro) detected in the current study and c.353G>A (p.Arg118His); c.566T.C (p.Leu189Pro); and c.758T>G (p.Leu253Arg) from previous reports

variants suggests the distinct genetic background of the Japanese population with regard to the *RP2* gene.

A genotype–phenotype association based on the presence of null variants was revealed in the current study. A more severe phenotype with early-onset disease was associated with a severe genotype with null variants, while a milder phenotype with relatively preserved visual acuity was associated with a mild genotype with missense variants. This genotype–phenotype association is in keeping with that reported in the previous literature, and such information should be useful in predicting disease prognosis (Jayasundera et al., 2010; Pelletier et al., 2007).

There are limitations in the current study. First, the clinical assessments of mothers (carriers) of the probands were unavailable and cosegregation analysis was not performed in two families. Additional analysis of mothers of the proband both in regard to clinical and genetic aspects could further validate the clinical and molecular

genetic diagnosis of *RP2*-RD. Second, the molecular disease-causing mechanisms of the novel two variants are not yet known; therefore, further functional analysis is needed to elucidate the nature of novel variants. Third, the data obtained by the literature search were not standardized, and it could be difficult to compare the data with each other. Last, the sample size for genotype–phenotype association analysis in the current study was still small, so further studies in larger cohorts could help to elucidate the disease mechanism.

In conclusion, phenotypic and genotypic characteristics of *RP2*-RD were illustrated in the Japanese population. A distinct genetic background in the Japanese population was identified; however, a significant genotype–phenotype association was confirmed, as in other populations. This information should be helpful to monitor and counsel patients, as well as to in selecting patients for future therapeutic trials.

TABLE 4 Clinical information of 19 patients from 14 Japanese families with RP2-RD

| Patient ID in the original article | RP2 variants | Phenotype | Inheritance | Sex | Age (at latest examination) | Onset | Chief complaint | Refractive errors | | | BCVA in the LogMAR unit | | | Electrophysiological assessment | | | Phenotype severity group | Genotype group | References |
|------------------------------------|--------------|-----------|-------------|-----|-----------------------------|-------------|--|-------------------|--------------|--------------------------|--------------------------|--|--|--|-------------------------|------------------------|--------------------------|-----------------------|------------|
| | | | | | | | | RE (dioptor) | LE (dioptor) | LE | RE | LE | LE | Dark-adapted condition | Light-adapted condition | Dark-adapted condition | | | |
| c.87G>A,p.Trp29Ter | YWC-116 | RP | XL | M | 24 | NA | NA | NA | NA | NA | NA | NA | NA | NA | NA | NA | A | Koyanagi et al., 2019 | |
| c.102+1G>A, splice site alteration | F8-P8 | RP | XL | M | 16 | 11 | Night blindness | -8.5 | -4.5 | 0.82 | 0.52 | 0.52 | Non-recordable | NA | NA | Mild | A | Kurata et al., 2019 | |
| c.217delT, p.Tyr73IlefsTer18 | F9-P9 | RP | XL | M | 30 | 9 | Night blindness | -7 | -6.5 | 1.52 | 1.7 | 1.7 | Non-recordable | Non-recordable | Severe | A | Kurata et al., 2019 | | |
| c.359G>A,p.Arg118His | N-212 | RP | XL | M | 61 | NA | NA | NA | NA | NA | NA | NA | NA | NA | NA | B | Koyanagi et al., 2019 | | |
| c.358C>T, p.Arg120Ter | I-III-1 | RP | XL | M | 24 | 5 | Night blindness | -3 | -3 | 1.15 | 1.15 | 1.15 | NA | NA | Severe | A | Mashima et al., 2001 | | |
| c.358C>T, p.Arg120Ter | I-II-2 | RP | XL | M | 48 | <10 years | Night blindness | NA | NA | LP | LP | LP | NA | NA | Severe | A | Mashima et al., 2001 | | |
| C.358C>T, p.Arg120Ter | I-II-3 | RP | XL | M | 44 | <10 years | Night blindness/ poor vision | NA | NA | LP | HM | HM | NA | NA | Severe | A | Mashima et al., 2001 | | |
| c.358C>T, p.Arg120Ter | E-3 | RP | XL | M | NA | Childhood | Night blindness | NA | NA | NA | NA | NA | Non-recordable | Non-recordable | NA | A | Jin et al., 2006 | | |
| 0.358C>T, p.Arg120Ter | F10-P10 | RP | XL | M | 17 | 6 | Visual loss | 0.75 | 0.5 | 1.1 | 1.3 | 1.3 | Non-recordable | Non-recordable | Severe | A | Kurata et al., 2019 | | |
| c.413A>G,p.Glu138Gly | F11-P11 | RP | XL | M | 41 | NA | Night blindness/ poor visual acuity | -12 | -10 | HM | HM | HM | Non-recordable | NA | NA | B | Kurata et al., 2019 | | |
| c.413A>G,p.Glu138Gly | F11-P12 | RP | XL | M | 38 | NA | NA | -10 | -8.5 | 1.15 | 1.15 | 1.15 | Non-recordable | NA | NA | B | Kurata et al., 2019 | | |
| c.677delG, p.Gly226ValfsTer12 | OPH-619 | RP | XL | M | 36 | NA | NA | NA | NA | NA | NA | NA | NA | NA | NA | A | Koyanagi et al., 2019 | | |
| c.685C>T,p.Gln229Ter | F12-P13 | RP | XL | M | 30 | 3 | Visual loss | -5.25 | -5.75 | 1.52 | 1.7 | 1.7 | Non-recordable | Non-recordable | Severe | A | Kurata et al., 2019 | | |
| c.758T>G,p.Leu253Arg | III-4 | RP | XL | M | 29 | 6 | Night blindness/ poor visual acuity | NA | NA | NA | NA | NA | NA | NA | NA | B | Wada et al., 2000 | | |
| c.758T>G,p.Leu253Arg | III-1 | RP | XL | M | NA | Early teens | NA | -6.5 | -9 | 0.7 | 1.22 | 1.22 | Non-recordable | Non-recordable | Mild | B | Koyanagi et al., 2019 | | |
| c.769-2A>G | NA | LCA | NA | M | NA | <1 year | NA | NA | NA | Severe visual impairment | Severe visual impairment | Severely reduced or non-detectable ERG | Severely reduced or non-detectable ERG | Severely reduced or non-detectable ERG | Severe | A | Hosono et al., 2018 | | |
| c.882delA, p.Gly295ValfsTer14 | 40 | RP | XL | M | 25 | NA | NA | NA | NA | NA | NA | NA | NA | NA | NA | A | Maeda et al., 2018 | | |
| c.831_832dupTC, p.Gln278LeufsTer16 | IV-1 | RP | XL | M | 19 | 3 | Night blindness/ photophobia | -6.75 | -7.0 | HM | HM | HM | NA | NA | Severe | A | Mashima et al., 2000 | | |
| c.831_832dupTC, p.Gln278LeufsTer16 | IV-2 | LCA | XL | M | 17 | 3 | Night blindness/ photophobia | -8 | -8 | 1.15 | 1.3 | 1.3 | NA | NA | Severe | A | Mashima et al., 2000 | | |

Note: A systematic review of peer-reviewed articles which describe Japanese cases with RP2-RD was performed.

Abbreviations: ERG, electroretinogram; ID, identification; LCA, Leber congenital amaurosis; RP, retinitis pigmentosa.

English proofreading: English proofreading has been conducted by the Springer Nature Author Services (<https://authorservices.springernature.com/>).

ACKNOWLEDGMENTS

The authors would like to thank The Japan Eye Genetics Study (JEGC) Group. The JEGC Study Group members are as follows: Chair's Office: National Institute of Sensory Organs, Takeshi Iwata, Kazushige Tsunoda, Kaoru Fujinami, Shinji Ueno, Kazuki Kuniyoshi, Takaaki Hayashi, Mineo Kondo, Atsushi Mizota, Nobuhisa Naoi, Kei Shinoda, Shuhei Kameya, Hiroyuki Kondo, Taro Kominami, Hiroko Terasaki, Hiroyuki Sakuramoto, Satoshi Katagiri, Kei Mizobuchi, Natsuko Nakamura, Go Mawatari, Toshihide Kurihara, Kazuo Tsubota, Yoza Miyake, Kazutoshi Yoshitake, Toshihide Nishimura, Yoshihide Hayashizaki, Nobuhiro Shimozawa, Masayuki Horiguchi, Shuichi Yamamoto, Manami Kuze, Shigeki Machida, Yoshiaki Shimada, Makoto Nakamura, Takashi Fujikado, Yoshihiro Hotta, Masayo Takahashi, Kiyofumi Mochizuki, Akira Murakami, Hiroyuki Kondo, Susumu Ishida, Mitsuru Nakazawa, Tetsuhisa Hatase, Tatsuo Matsunaga, Akiko Maeda, Kosuke Noda, Atsuhiko Tanikawa, Syuji Yamamoto, Hiroyuki Yamamoto, Makoto Araie, Makoto Aihara, Toru Nakazawa, Tetsuju Sekiryu, Kenji Kashiwagi, Kenjiro Kosaki, Carninci Piero, Takeo Fukuchi, Atsushi Hayashi, Katsuhiko Hosono, Keisuke Mori, Kouji Tanaka, Koichi Furuya, Keiichiro Suzuki, Ryo Kohata, Yasuo Yanagi, Yuriko Minegishi, Daisuke Iejima, Akiko Suga, Brian P. Rossmiller, Yang Pan, Tomoko Oshima, Mao Nakayama, Megumi Yamamoto, Naoko Minematsu, Daisuke Mori, Yusuke Kijima, Kentaro Kurata, Norihiro Yamada, Masayoshi Itoh, Hideya Kawaji, Yasuhiro Murakawa, Ryo Ando, Wataru Saito, Yusuke Murakami, Hiroaki Miyata, Lizhu Yang, Yu Fujinami-Yokokawa, Xiao Liu, Gavin Arno, Nikolas Pontikos, Kazuki Yamazawa, Satomi Inoue, and Takayuki Kinoshita.

Kaoru Fujinami is supported by grants from Grant-in-Aid for Young Scientists (A) of the Ministry of Education, Culture, Sports, Science and Technology, Japan (16H06269), grants from Grant-in-Aid for Scientists to support international collaborative studies of the Ministry of Education, Culture, Sports, Science and Technology, Japan (16KK01930002), grants from National Hospital Organization Research Fund (H30-NHO-Sensory Organs-03), grants from Foundation Fighting Blindness Alan Latics Career Development Program (CF-CL-0416-0696-UCL), grants from Health Labour Sciences Research Grant, The Ministry of Health Labour and Welfare (201711107A), and grants from Great Britain Sasakawa Foundation Butterfield Awards.

Yu Fujinami-Yokokawa is supported by grants from Grant-in-Aid for Young Scientists of the Ministry of Education, Culture, Sports, Science and Technology, Japan (18K16943).

Gavin Arno is supported by a Fight for Sight (UK) Early Career Investigator Award, NIHR-BRC at Moorfields Eye Hospital and the UCL Institute of Ophthalmology, NIHR-BRC at Great Ormond Street Hospital and UCL Institute of Child Health, and Great Britain Sasakawa Foundation Butterfield Award, UK.

Nikolas Pontikos is funded by a Moorfields Eye Charity Career Development Award (R190031A), the NIHR-BRC at Moorfields Eye Hospital and the UCL Institute of Ophthalmology.

Toshihide Kurihara is supported by Tsubota Laboratory, Inc., Fuji Xerox Co., Ltd., Kirin Company, Ltd., Kowa Company, Ltd., Novartis Pharmaceuticals, Santen Pharmaceutical Co. Ltd., and ROHTO Pharmaceutical Co., Ltd.

Takeshi Iwata is supported by Japan Agency for Medical Research and Development (AMED) (18ek0109282h0002).

Kazushige Tsunoda is supported by AMED, the Ministry of Health, Labor and Welfare, Japan (18ek0109282h0002), Grants-in-Aid for Scientific Research, Japan Society for the Promotion of Science, Japan (H26-26462674), grants from National Hospital Organization Network Research Fund, Japan (H30-NHO-Sensory Organs-03), and Novartis Research Grant (2018).

The funding sources had no role in the design and conduct of the study; collection, management, analysis, and interpretation of the data; preparation, review, or approval of the manuscript; and decision to submit the manuscript for publication.

CONFLICT OF INTEREST

All authors have completed and submitted the ICMJE Form for disclosure of potential conflicts of interest. Individual investigators who participate in the sponsored project(s) are not directly compensated by the sponsor but may receive a salary or other support from the institution to support their effort on the project(s).

Kaoru Fujinami is a paid Consultant for Astellas Pharma Inc., Kubota Pharmaceutical Holdings Co., Ltd., Acucela Inc., Novartis AG, Janssen Pharmaceutica, Sanofi Genzyme, NightstaRx Limited; reports personal fees from Astellas Pharma Inc., Kubota Pharmaceutical Holdings Co., Ltd., Acucela Inc., Novartis AG, Santen Company Limited, Foundation Fighting Blindness, Foundation Fighting Blindness Clinical Research Institute, Japanese Ophthalmology Society, Japan Retinitis Pigmentosa Society; reports grants from Astellas Pharma Inc. (NCT03281005), outside the submitted work.

Toshihide Kurihara is an investor in Tsubota Laboratory, Inc. and RestoreVision, Inc. Toshihide Kurihara reports grants and personal fees from ROHTO Pharmaceutical Co., Ltd., Tsubota Laboratory, Inc., Fuji Xerox Co., Ltd., Kowa Company, Ltd., Santen Pharmaceutical Co. Ltd., outside the submitted work.

Kazuo Tsubota reports grants and personal fees from Santen Pharmaceutical Co., Ltd., grants and personal fees from Otsuka Pharmaceutical Co., Ltd., grants and personal fees from Wakamoto Pharmaceutical Co., Ltd., grants from ROHTO Pharmaceutical Co., Ltd., grants from R-Tech Ueno, personal fees from Laboratoires Thea, grants from Alcon Japan, investor of Tear Solutions, grants and investor of Tsubota Laboratory, Inc., outside the submitted work.

ORCID

Kaoru Fujinami  <https://orcid.org/0000-0003-4248-0033>

Gavin Arno  <https://orcid.org/0000-0002-6165-7888>

Nikolas Pontikos  <https://orcid.org/0000-0003-1782-4711>

REFERENCES

Andreasson, S., Breuer, D. K., Eksandh, L., Ponjavic, V., Frennesson, C., Hirianna, S., ... Swaroop, A. (2003). Clinical studies of X-linked

- retinitis pigmentosa in three Swedish families with newly identified mutations in the RP2 and RPGR-ORF15 genes. *Ophthalmic Genetics*, 24(4), 215–223. <https://doi.org/10.1076/opge.24.4.215.17228>
- Boughman, J. A., Conneally, P. M., & Nance, W. E. (1980). Population genetic studies of retinitis pigmentosa. *American Journal of Human Genetics*, 32(2), 223–235.
- Breuer, D. K., Yashar, B. M., Filippova, E., Hiriyanna, S., Lyons, R. H., Mears, A. J., ... Swaroop, A. (2002). A comprehensive mutation analysis of RP2 and RPGR in a north American cohort of families with X-linked retinitis pigmentosa. *American Journal of Human Genetics*, 70(6), 1545–1554. <https://doi.org/10.1086/340848>
- Carss, K. J., Arno, G., Erwood, M., Stephens, J., Sanchis-Juan, A., Hull, S., ... Raymond, F. L. (2017). Comprehensive rare variant analysis via whole-genome sequencing to determine the molecular pathology of inherited retinal disease. *American Journal of Human Genetics*, 100(1), 75–90. <https://doi.org/10.1016/j.ajhg.2016.12.003>
- Chapple, J. P., Hardcastle, A. J., Grayson, C., Spackman, L. A., Willison, K. R., & Cheetham, M. E. (2000). Mutations in the N-terminus of the X-linked retinitis pigmentosa protein RP2 interfere with the normal targeting of the protein to the plasma membrane. *Human Molecular Genetics*, 9(13), 1919–1926.
- Chapple, J. P., Hardcastle, A. J., Grayson, C., Willison, K. R., & Cheetham, M. E. (2002). Delineation of the plasma membrane targeting domain of the X-linked retinitis pigmentosa protein RP2. *Investigative Ophthalmology & Visual Science*, 43(6), 2015–2020.
- Chizzolini, M., Galan, A., Milan, E., Sebastiani, A., Costagliola, C., & Parmeggiani, F. (2011). Good epidemiologic practice in retinitis pigmentosa: From phenotyping to biobanking. *Current Genomics*, 12(4), 260–266. <https://doi.org/10.2174/138920211795860071>
- Dan, H., Huang, X., Xing, Y., & Shen, Y. (2020). Application of targeted panel sequencing and whole exome sequencing for 76 Chinese families with retinitis pigmentosa. *Molecular Genetics & Genomic Medicine*, 8(3), e1131. <https://doi.org/10.1002/mgg3.1131>
- Dandekar, S. S., Ebenezer, N. D., Grayson, C., Chapple, J. P., Egan, C. A., Holder, G. E., ... Hardcastle, A. J. (2004). An atypical phenotype of macular and peripapillary retinal atrophy caused by a mutation in the RP2 gene. *The British Journal of Ophthalmology*, 88(4), 528–532. <https://doi.org/10.1136/bjo.2003.027979>
- Evans, R. J., Schwarz, N., Nagel-Wolfrum, K., Wolfrum, U., Hardcastle, A. J., & Cheetham, M. E. (2010). The retinitis pigmentosa protein RP2 links pericentriolar vesicle transport between the Golgi and the primary cilium. *Human Molecular Genetics*, 19(7), 1358–1367. <https://doi.org/10.1093/hmg/ddq012>
- Fishman, G. A. (1978). Retinitis pigmentosa. Genetic percentages. *Archives of Ophthalmology*, 96(5), 822–826.
- Fujinami-Yokokawa, Y., Pontikos, N., Yang, L., Tsunoda, K., Yoshitake, K., Iwata, T., ... Japan Eye Genetics Consortium. (2019). Prediction of causative genes in Inherited Retinal disorders from spectral-domain optical coherence tomography utilizing deep learning techniques. *Journal of Ophthalmology*, 2019, 1691064. <https://doi.org/10.1155/2019/1691064>
- Fujinami-Yokokawa, Y., Kuniyoshi, K., Hayashi, T., Ueno, S., Mizota, A., Shinoda, K., ... Japan Eye Genetics Consortium. (2020). Clinical and genetic characteristics of 18 patients from 13 Japanese families with CRX-associated Retinal disorder: Identification of genotype-phenotype associations. *Scientific Reports*, in press, 10, 9531.
- Fujinami, K., Kameya, S., Kikuchi, S., Ueno, S., Kondo, M., Hayashi, T., ... Tsunoda, K. (2016). Novel RP11L1 variants and genotype-phenotype microstructural phenotype associations in cohort of Japanese patients with occult macular dystrophy. *Investigative Ophthalmology & Visual Science*, 57(11), 4837–4846. <https://doi.org/10.1167/iovs.16-19670>
- Fujinami, K., Yang, L., Joo, K., Tsunoda, K., Kameya, S., Hanazono, G., ... East Asia Inherited Retinal Disease Society Study Group. (2019). Clinical and genetic characteristics of east Asian patients with occult macular dystrophy (Miyake disease): East Asia occult macular dystrophy studies report number 1. *Ophthalmology*, 126(10), 1432–1444. <https://doi.org/10.1016/j.ophtha.2019.04.032>
- Grayson, C., Bartolini, F., Chapple, J. P., Willison, K. R., Bhamidipati, A., Lewis, S. A., ... Cheetham, M. E. (2002). Localization in the human retina of the X-linked retinitis pigmentosa protein RP2, its homologue cofactor C and the RP2 interacting protein Arl3. *Human Molecular Genetics*, 11(24), 3065–3074.
- Haim, M. (1992). Prevalence of retinitis pigmentosa and allied disorders in Denmark. III. Hereditary pattern. *Acta Ophthalmologica*, 70(5), 615–624.
- Hardcastle, A. J., Thiselton, D. L., Van Maldergem, L., Saha, B. K., Jay, M., Plant, C., ... Bhattacharya, S. (1999). Mutations in the RP2 gene cause disease in 10% of families with familial X-linked retinitis pigmentosa assessed in this study. *American Journal of Human Genetics*, 64(4), 1210–1215.
- Hosono, K., Nishina, S., Yokoi, T., Katagiri, S., Saito, H., Kurata, K., ... Hotta, Y. (2018). Molecular diagnosis of 34 Japanese families with Leber congenital Amaurosis using targeted next generation sequencing. *Scientific Reports*, 8(1), 8279. <https://doi.org/10.1038/s41598-018-26524-z>
- Hurd, T., Zhou, W., Jenkins, P., Liu, C. J., Swaroop, A., Khanna, H., ... Margolis, B. (2010). The retinitis pigmentosa protein RP2 interacts with polycystin 2 and regulates cilia-mediated vertebrate development. *Human Molecular Genetics*, 19(22), 4330–4344. <https://doi.org/10.1093/hmg/ddq355>
- Hurd, T. W., Fan, S., & Margolis, B. L. (2011). Localization of retinitis pigmentosa 2 to cilia is regulated by importin beta2. *Journal of Cell Science*, 124(Pt 5), 718–726. <https://doi.org/10.1242/jcs.070839>
- Jayasundera, T., Branham, K. E., Othman, M., Rhoades, W. R., Karoukis, A. J., Khanna, H., ... Heckenlively, J. R. (2010). RP2 phenotype and pathogenetic correlations in X-linked retinitis pigmentosa. *Archives of Ophthalmology*, 128(7), 915–923. <https://doi.org/10.1001/archophthol.128.7.915>
- Ji, Y., Wang, J., Xiao, X., Li, S., Guo, X., & Zhang, Q. (2010). Mutations in RPGR and RP2 of Chinese patients with X-linked retinitis pigmentosa. *Current Eye Research*, 35(1), 73–79. <https://doi.org/10.3109/02713680903395299>
- Jiang, J., Wu, X., Shen, D., Dong, L., Jiao, X., Hejtmancik, J. F., & Li, N. (2017). Analysis of RP2 and RPGR mutations in five X-linked Chinese families with retinitis pigmentosa. *Scientific Reports*, 7, 44465. <https://doi.org/10.1038/srep44465>
- Jin, Z. B., Liu, X. Q., Hayakawa, M., Murakami, A., & Nao-i, N. (2006). Mutational analysis of RPGR and RP2 genes in Japanese patients with retinitis pigmentosa: Identification of four mutations. *Molecular Vision*, 12, 1167–1174.
- Kameya, S., Fujinami, K., Ueno, S., Hayashi, T., Kuniyoshi, K., Ideta, R., ... Japan Eye Genetics, C. (2019). Phenotypical characteristics of POC1B-associated retinopathy in Japanese cohort: Cone dystrophy with normal fundus appearance. *Investigative Ophthalmology & Visual Science*, 60(10), 3432–3446. <https://doi.org/10.1167/iovs.19-26650>
- Katagiri, S., Hayashi, T., Nakamura, M., Mizobuchi, K., Gekka, T., Komori, S., ... Nakano, T. (2020). RDH5-related fundus Albipunctatus in a large Japanese cohort. *Investigative Ophthalmology & Visual Science*, 61(3), 53. <https://doi.org/10.1167/iovs.61.3.53>
- Kim, M. S., Joo, K., Seong, M. W., Kim, M. J., Park, K. H., Park, S. S., & Woo, S. J. (2019). Genetic mutation profiles in Korean patients with Inherited Retinal diseases. *Journal of Korean Medical Science*, 34(21), e161. <https://doi.org/10.3346/jkms.2019.34.e161>
- Kondo, H., Oku, K., Katagiri, S., Hayashi, T., Nakano, T., Iwata, A., ... Iwata, T. (2019). Novel mutations in the RS1 gene in Japanese patients with X-linked congenital retinoschisis. *Human Genome Variation*, 6, 3. <https://doi.org/10.1038/s41439-018-0034-6>
- Koyanagi, Y., Akiyama, M., Nishiguchi, K. M., Momozawa, Y., Kamatani, Y., Takata, S., ... Sonoda, K. H. (2019). Genetic characteristics of retinitis

- pigmentosa in 1204 Japanese patients. *Journal of Medical Genetics*, 56(10), 662–670. <https://doi.org/10.1136/jmedgenet-2018-105691>
- Kurata, K., Hosono, K., Hayashi, T., Mizobuchi, K., Katagiri, S., Miyamichi, D., ... Hotta, Y. (2019). X-linked retinitis pigmentosa in Japan: Clinical and genetic findings in male patients and female carriers. *International Journal of Molecular Sciences*, 20(6), 1518–1518. <https://doi.org/10.3390/ijms20061518>
- Li, L., Khan, N., Hurd, T., Ghosh, A. K., Cheng, C., Molday, R., ... Khanna, H. (2013). Ablation of the X-linked retinitis pigmentosa 2 (Rp2) gene in mice results in opsin mislocalization and photoreceptor degeneration. *Investigative Ophthalmology & Visual Science*, 54(7), 4503–4511. <https://doi.org/10.1167/iovs.13-12140>
- Li, L., Rao, K. N., & Khanna, H. (2019). Structural but not functional alterations in cones in the absence of the Retinal disease protein retinitis Pigmentosa 2 (RP2) in a cone-only retina. *Frontiers in Genetics*, 10, 323. <https://doi.org/10.3389/fgene.2019.00323>
- Liew, G., Michaelides, M., & Bunce, C. (2014). A comparison of the causes of blindness certifications in England and Wales in working age adults (16–64 years), 1999–2000 with 2009–2010. *BMJ Open*, 4(2), e004015. <https://doi.org/10.1136/bmjopen-2013-004015>
- Lim, H., Park, Y. M., Lee, J. K., & Taek Lim, H. (2016). Single-exome sequencing identified a novel RP2 mutation in a child with X-linked retinitis pigmentosa. *Canadian Journal of Ophthalmology*, 51(5), 326–330. <https://doi.org/10.1016/j.cjco.2016.03.017>
- Lyraki, R., Megaw, R., & Hurd, T. (2016). Disease mechanisms of X-linked retinitis pigmentosa due to RP2 and RPGR mutations. *Biochemical Society Transactions*, 44(5), 1235–1244. <https://doi.org/10.1042/BST20160148>
- Maeda-Katahira, A., Nakamura, N., Hayashi, T., Katagiri, S., Shimizu, S., Ohde, H., ... Tsunoda, K. (2019). Autosomal dominant optic atrophy with OPA1 gene mutations accompanied by auditory neuropathy and other systemic complications in a Japanese cohort. *Molecular Vision*, 25, 559–573.
- Maeda, A., Yoshida, A., Kawai, K., Arai, Y., Akiba, R., Inaba, A., ... Takahashi, M. (2018). Development of a molecular diagnostic test for retinitis Pigmentosa in the Japanese population. *Japanese Journal of Ophthalmology*, 62(4), 451–457. <https://doi.org/10.1007/s10384-018-0601-x>
- Mashima, Y., Saga, M., Akeo, K., & Oguchi, Y. (2001). Phenotype associated with an R120X nonsense mutation in the RP2 gene in a Japanese family with X-linked retinitis pigmentosa. *Ophthalmic Genetics*, 22(1), 43–47.
- Mashima, Y., Saga, M., Hiida, Y., Imamura, Y., Kudoh, J., & Shimizu, N. (2000). Novel mutation in RP2 gene in two brothers with X-linked retinitis pigmentosa and mtDNA mutation of leber hereditary optic neuropathy who showed marked differences in clinical severity. *American Journal of Ophthalmology*, 130(3), 357–359. [https://doi.org/10.1016/s0002-9394\(00\)00553-5](https://doi.org/10.1016/s0002-9394(00)00553-5)
- Mawatari, G., Fujinami, K., Liu, X., Yang, L., Yokokawa, Y. F., Komori, S., ... JEGC Study Group. (2019). Clinical and genetic characteristics of 14 patients from 13 Japanese families with RPGR-associated retinal disorder: Report of eight novel variants. *Human Genome Variation*, 6, 34. <https://doi.org/10.1038/s41439-019-0065-7>
- McCulloch, D. L., Marmor, M. F., Brigell, M. G., Hamilton, R., Holder, G. E., Tzekov, R., & Bach, M. (2015a). Erratum to: ISCEV standard for full-field clinical electroretinography (2015 update). *Documenta Ophthalmologica*, 131(1), 81–83. <https://doi.org/10.1007/s10633-015-9504-z>
- McCulloch, D. L., Marmor, M. F., Brigell, M. G., Hamilton, R., Holder, G. E., Tzekov, R., & Bach, M. (2015b). ISCEV standard for full-field clinical electroretinography (2015 update). *Documenta Ophthalmologica*, 130(1), 1–12. <https://doi.org/10.1007/s10633-014-9473-7>
- Mears, A. J., Gieser, L., Yan, D., Chen, C., Fahrner, S., Hirianna, S., ... Swaroop, A. (1999). Protein-truncation mutations in the RP2 gene in a north American cohort of families with X-linked retinitis pigmentosa. *American Journal of Human Genetics*, 64(3), 897–900. <https://doi.org/10.1086/302298>
- Miano, M. G., Testa, F., Filippini, F., Trujillo, M., Conte, I., Lanzara, C., ... Ciccocioppa, A. (2001). Identification of novel RP2 mutations in a subset of X-linked retinitis pigmentosa families and prediction of new domains. *Human Mutation*, 18(2), 109–119. <https://doi.org/10.1002/humu.1160>
- Mizobuchi, K., Hayashi, T., Katagiri, S., Yoshitake, K., Fujinami, K., Yang, L., ... Nakano, T. (2019). Characterization of GUCA1A-associated dominant cone/cone-rod dystrophy: Low prevalence among Japanese patients with inherited retinal dystrophies. *Scientific Reports*, 9(1), 16851. <https://doi.org/10.1038/s41598-019-52660-1>
- Nakamura, N., Tsunoda, K., Mizuno, Y., Usui, T., Hatase, T., Ueno, S., ... Miyake, Y. (2019). Clinical stages of occult macular Dystrophy based on optical coherence tomographic findings. *Investigative Ophthalmology & Visual Science*, 60(14), 4691–4700. <https://doi.org/10.1167/iovs.19-27486>
- Nakanishi, A., Ueno, S., Hayashi, T., Katagiri, S., Kominami, T., Ito, Y., ... Terasaki, H. (2016). Clinical and genetic findings of autosomal recessive Bestrophinopathy in Japanese cohort. *American Journal of Ophthalmology*, 168, 86–94. <https://doi.org/10.1016/j.ajo.2016.04.023>
- Neidhardt, J., Glaus, E., Lorenz, B., Netzer, C., Li, Y., Schambeck, M., ... Berger, W. (2008). Identification of novel mutations in X-linked retinitis pigmentosa families and implications for diagnostic testing. *Molecular Vision*, 14, 1081–1093.
- Pan, X., Chen, X., Liu, X., Gao, X., Kang, X., Xu, Q., ... Zhao, C. (2014). Mutation analysis of pre-mRNA splicing genes in Chinese families with retinitis pigmentosa. *Molecular Vision*, 20, 770–779.
- Pelletier, V., Jambou, M., Delphin, N., Zinovieva, E., Stum, M., Gigarel, N., ... Rozet, J. M. (2007). Comprehensive survey of mutations in RP2 and RPGR in patients affected with distinct retinal dystrophies: Genotype-phenotype correlations and impact on genetic counseling. *Human Mutation*, 28(1), 81–91. <https://doi.org/10.1002/humu.20417>
- Pontikos, N., Murphy, C., Moghul, I., Arno, G., Fujinami, K., Fujinami, Y., ... UK Inherited Retinal Dystrophy Consortium, Phenopolis Consortium. (2020). Phenogenon: Gene to phenotype associations for rare genetic diseases. *PLoS One*, 15(4), e0230587. <https://doi.org/10.1371/journal.pone.0230587>
- Prokisch, H., Hartig, M., Hellinger, R., Meitinger, T., & Rosenberg, T. (2007). A population-based epidemiological and genetic study of X-linked retinitis pigmentosa. *Investigative Ophthalmology & Visual Science*, 48(9), 4012–4018. <https://doi.org/10.1167/iovs.07-0071>
- Richards, S., Aziz, N., Bale, S., Bick, D., Das, S., Gastier-Foster, J., ... Committee, A. L. Q. A. (2015). Standards and guidelines for the interpretation of sequence variants: A joint consensus recommendation of the American College of Medical Genetics and Genomics and the Association for Molecular Pathology. *Genetics in Medicine*, 17(5), 405–424. <https://doi.org/10.1038/gim.2015.30>
- Sahel, J. A., Marazova, K., & Audo, I. (2014). Clinical characteristics and current therapies for inherited retinal degenerations. *Cold Spring Harbor Perspectives in Medicine*, 5(2), a017111. <https://doi.org/10.1101/cshperspect.a017111>
- Schwahn, U., Lenzner, S., Dong, J., Feil, S., Hinzmann, B., van Duijnhoven, G., ... Berger, W. (1998). Positional cloning of the gene for X-linked retinitis pigmentosa 2. *Nature Genetics*, 19(4), 327–332. <https://doi.org/10.1038/1214>
- Sharon, D., Bruns, G. A., McGee, T. L., Sandberg, M. A., Berson, E. L., & Dryja, T. P. (2000). X-linked retinitis pigmentosa: Mutation spectrum of the RPGR and RP2 genes and correlation with visual function. *Investigative Ophthalmology & Visual Science*, 41(9), 2712–2721.
- Sharon, D., Sandberg, M. A., Rabe, V. W., Stillberger, M., Dryja, T. P., & Berson, E. L. (2003). RP2 and RPGR mutations and clinical correlations in patients with X-linked retinitis pigmentosa. *American Journal of Human Genetics*, 73(5), 1131–1146. <https://doi.org/10.1086/379379>
- Sohocki, M. M., Daiger, S. P., Bowne, S. J., Rodriguez, J. A., Northrup, H., Heckenlively, J. R., ... Sullivan, L. S. (2001). Prevalence of mutations

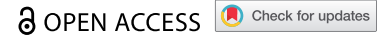
- causing retinitis pigmentosa and other inherited retinopathies. *Human Mutation*, 17(1), 42–51. [https://doi.org/10.1002/1098-1004\(2001\)17:1<42::AID-HUMU5>3.0.CO;2-K](https://doi.org/10.1002/1098-1004(2001)17:1<42::AID-HUMU5>3.0.CO;2-K)
- Solebo, A. L., Teoh, L., & Rahi, J. (2017). Epidemiology of blindness in children. *Archives of Disease in Childhood*, 102(9), 853–857. <https://doi.org/10.1136/archdischild-2016-310532>
- Ueda, E., Yasuda, M., Fujiwara, K., Hashimoto, S., Ohno-Matsui, K., Hata, J., ... Sonoda, K. H. (2019). Trends in the prevalence of myopia and myopic Maculopathy in a Japanese population: The Hisayama study. *Investigative Ophthalmology & Visual Science*, 60(8), 2781–2786. <https://doi.org/10.1167/iovs.19-26580>
- Vervoort, R., Lennon, A., Bird, A. C., Tulloch, B., Axton, R., Miano, M. G., ... Wright, A. F. (2000). Mutational hot spot within a new RPGR exon in X-linked retinitis pigmentosa. *Nature Genetics*, 25(4), 462–466. <https://doi.org/10.1038/78182>
- Vorster, A. A., Rebello, M. T., Coutts, N., Ehrenreich, L., Gama, A. D., Roberts, L. J., ... Greenberg, L. J. (2004). Arg120stop nonsense mutation in the RP2 gene: Mutational hotspot and germ line mosaicism? *Clinical Genetics*, 65(1), 7–10. <https://doi.org/10.1111/j.2004.00163.x>
- Wada, Y., Nakazawa, M., Abe, T., & Tamai, M. (2000). A new Leu253Arg mutation in the RP2 gene in a Japanese family with X-linked retinitis pigmentosa. *Investigative Ophthalmology & Visual Science*, 41(1), 290–293.
- Wang, J., Zhang, V. W., Feng, Y., Tian, X., Li, F. Y., Truong, C., ... Wong, L. J. (2014). Dependable and efficient clinical utility of target capture-based deep sequencing in molecular diagnosis of retinitis pigmentosa. *Investigative Ophthalmology & Visual Science*, 55(10), 6213–6223. <https://doi.org/10.1167/iovs.14-14936>
- World Medical Association. (2013). World medical association declaration of Helsinki: Ethical principles for medical research involving human subjects. *JAMA*, 310(20), 2191–2194. <https://doi.org/10.1001/jama.2013.281053>
- Wright, A. F., Chakarova, C. F., Abd El-Aziz, M. M., & Bhattacharya, S. S. (2010). Photoreceptor degeneration: Genetic and mechanistic dissection of a complex trait. *Nature Reviews. Genetics*, 11(4), 273–284. <https://doi.org/10.1038/nrg2717>
- Xiao Liu, K. F., Kuniyoshi, K., Kondo, M., Ueno, S., Hayashi, T., Mochizuki, K., ... Consortium, J. E. G. (2020). Clinical and genetic characteristics of 15 affected patients from 12 Japanese families with GUCY2D-associated retinal disorder. *Translational Vision Science & Technology*, 9(6), 2.
- Xu, K., Xie, Y., Sun, T., Zhang, X., Chen, C., & Li, Y. (2019). Genetic and clinical findings in a Chinese cohort with Leber congenital amaurosis and early onset severe retinal dystrophy. *The British Journal of Ophthalmology*, 104, 932–937. <https://doi.org/10.1136/bjophthalmol-2019-314281>
- Yang, L., Fujinami, K., Ueno, S., Kuniyoshi, K., Hayashi, T., Kondo, M., ... JEGC Study Group. (2020). Genetic Spectrum of EYS-associated Retinal disease in a large Japanese cohort: Identification of disease-associated variants with relatively high allele frequency. *Scientific Reports*, 10(1), 5497. <https://doi.org/10.1038/s41598-020-62119-3>
- Yang, L., Yin, X., Feng, L., You, D., Wu, L., Chen, N., ... Ma, Z. (2014). Novel mutations of RPGR in Chinese retinitis pigmentosa patients and the genotype-phenotype correlation. *PLoS One*, 9(1), e85752. <https://doi.org/10.1371/journal.pone.0085752>
- Yotsukura, E., Torii, H., Inokuchi, M., Tokumura, M., Uchino, M., Nakamura, K., ... Tsubota, K. (2019). Current prevalence of myopia and Association of Myopia with Environmental Factors among Schoolchildren in Japan. *JAMA Ophthalmology*, 137, 1233. <https://doi.org/10.1001/jamaophthalmol.2019.3103>
- Zhang, H., Hanke-Gogokhia, C., Jiang, L., Li, X., Wang, P., Gerstner, C. D., ... Baehr, W. (2015). Mistrafficking of prenylated proteins causes retinitis pigmentosa 2. *The FASEB Journal*, 29(3), 932–942. <https://doi.org/10.1096/fj.14-257915>
- Zhang, J., Gao, F., Du, C., Wang, J., Pi, X., Guo, W., ... Cui, X. (2019). A novel RP2 missense mutation Q158P identified in an X-linked retinitis pigmentosa family impaired RP2 protein stability. *Gene*, 707, 86–92. <https://doi.org/10.1016/j.gene.2019.05.006>

SUPPORTING INFORMATION

Additional supporting information may be found online in the Supporting Information section at the end of this article.

How to cite this article: Fujinami K, Liu X, Ueno S, et al. RP2-associated retinal disorder in a Japanese cohort: Report of novel variants and a literature review, identifying a genotype–phenotype association. *Am J Med Genet Part C*. 2020;184C:675–693. <https://doi.org/10.1002/ajmg.c.31830>

RESEARCH REPORT



Long-term follow-up of a Chinese patient with *KCNV2*-retinopathy

Hongxuan Lie^{a,b*}, Gang Wang^{a,b*}, Xiao Liu^{a,b,c,d*}, Xiaohong Meng^{a,b}, Yanling Long^b, Jiayun Ren^{a,b}, Lizhu Yang^{c,d}, Yu Fujinami-Yokokawa^{c,e,f,g}, Toshihide Kurihara^d, Kazuo Tsubota^d, Kaoru Fujinami^b, and Shiyong Li^b

^aOphthalmology Department, Southwest Hospital, Army Medical University (Third Military Medical University), Chongqing, China; ^bKey Lab of Visual Damage and Regeneration & Restoration of Chongqing, Chongqing, China; ^cLaboratory of Visual Physiology, Division for Vision Research, National Institute of Sensory Organs, National Hospital Organization, Tokyo Medical Center, Tokyo, Japan; ^dDepartment of Ophthalmology, Keio University School of Medicine, Tokyo, Japan; ^eGraduate School of Health Management, Keio University, Tokyo, Japan; ^fDepartment of Genetics, UCL Institute of Ophthalmology, London, UK; ^gDivision of Inherited Eye Diseases, Moorfields Eye Hospital, London, UK

ABSTRACT

Purpose: To characterize and monitor the clinical and electrophysiological features of a Chinese patient with *KCNV2* retinopathy.

Methods: A 17-year-old Chinese male with the diagnosis of cone dystrophy with supernormal rod response (CDSRR) was followed-up for 5 years, with full ophthalmological examinations, including decimal best corrected visual acuity (BCVA), fundus photography, fundus autofluorescence (FAF) imaging, spectral-domain optical coherence tomography (SD-OCT), and full-field electroretinogram (ERG). Genetic screening was performed to detect the sequence variations in the retinal dystrophy associated genes in the patient and his parents.

Results: The patient demonstrated the characteristic full-field electroretinography (ERG) features of CDSRR, namely a profound enlargement of the dark-adapted ERG b-wave amplitude with increasing flash strength and a broadened a-wave trough; this case also had undetectable light-adapted ERGs. A BCVA of 0.15 was maintained over 5 years in both eyes; while progressive macular atrophy was identified. Molecular genetic analyses revealed two novel disease-causing *KCNV2* variants in compound heterozygous state: c.1408 G > C (p.Gly470Arg) and c.1500 C > G (p.Tyr500Ter).

Conclusions: This is the first long-term case study of an East Asian patient with molecularly confirmed CDSRR. The progressive atrophy with maintained VA demonstrated in this case will be valuable for increasing the understanding of the natural course of *KCNV2* retinopathy and it will help in counselling patients with this disease.

ARTICLE HISTORY

Received November 06, 2019

Revised October 24, 2020

Accepted November 29, 2020

KEYWORDS

Cone dystrophy with supernormal rod responses; *KCNV2*; longitudinal follow-up; electroretinogram; optical coherence tomography





Introduction

Cone dystrophy with supernormal rod response (CDSRR) is an autosomal recessive disorder first described by Gouras et al. in 1983 (1). Affected individuals usually present within the first two decades of life, with visual decline, photophobia, and nyctalopia in approximately 50% of case (2–8). Some patients present with color vision deficits, myopia, central scotoma, and, particularly in younger patients, nystagmus. Fundus findings are usually unremarkable in children, but adults frequently exhibit distinct macular changes or retinal pigment epithelial (RPE) atrophy (2–10).


The term CDSRR refers to the unique characteristics observed with full-field electroretinogram (ERG) (1). The scotopic ERG to a dim light strength (≤ 0.01 cd·s/m²) is typically markedly delayed and of subnormal amplitude. Small increments in flash strength produce disproportionately large increments in the rod-mediated ERG b-wave amplitude, leading to high-normal or supernormal values

with a standard flash ERG (3.0 cd·s/m²) (3–7,11). At flash strengths ≥ 3.0 cd·s/m², a broadened trough of the rod-mediated ERG a-wave is seen, and cone-mediated ERGs are reduced and delayed.

CDSRR is caused by biallelic sequence variations in the potassium voltage-gated channel modifier subfamily V member 2 (*KCNV2*) gene (MIM# 607604), leading to a functional defect of the encoded voltage-gated potassium channel subunit, Kv8.2 (12). Over 100 different disease-associated variations in the *KCNV2* gene have been reported, but the number of publications focusing on patients in the East Asian population is very limited (5,13). Moreover, only a few reports have described the electrophysiological and morphological natural history of *KCNV2* retinopathy (3–9,11–20). Here, we report the long-term follow-up of a Chinese patient with CDSRR caused by biallelic pathogenic *KCNV2* variants. These findings are important for counselling patients and designing therapeutic trials, particularly in the East Asian population.

CONTACT Kaoru Fujinami  k.fujinami@ucl.ac.uk  Laboratory of Visual Physiology, Division for Vision Research, National Institute of Sensory Organs, National Hospital Organization, Tokyo Medical Center, 2-5-1, Higashigaoka, Meguro-ku, Tokyo 152-8902, Japan; Shiyong Li  shiyong_li@126.com  Southwest Hospital/Southwest Eye Hospital, Third Military Medical University (Army Medical University), Chongqing 4000038, China.

*Co-first authors

 Supplemental data for this article can be accessed on the [publisher's website](#).

© 2020 The Author(s). Published with license by Taylor & Francis Group, LLC.

This is an Open Access article distributed under the terms of the Creative Commons Attribution-NonCommercial-NoDerivatives License (<http://creativecommons.org/licenses/by-nc-nd/4.0/>), which permits non-commercial re-use, distribution, and reproduction in any medium, provided the original work is properly cited, and is not altered, transformed, or built upon in any way.

Methods

Patient recruitment

A Chinese patient with CDSRR was recruited from the Outpatient Department of Southwest Eye Hospital, Third Military Medical University (Army Medical University), Chongqing, China. Informed consent for all procedures described here was obtained from the patient and his relatives who were also assessed, and agreement for publishing this case study was obtained. The study procedures were approved by the local ethics committee (Reference number: 73981486-2), and all procedures were performed under the Declaration of Helsinki principles on human research.

Clinical investigation

A detailed medical history was obtained from the patient, and comprehensive ophthalmological examinations were performed, including decimal best corrected visual acuity (BCVA), dilated ophthalmoscopy, color fundus photography recorded with a nonmydriatic retinal camera (a Nonmyd WX-3D; Kowa, Tokyo, Japan), fundus autofluorescence (FAF) imaging with a confocal scanning laser ophthalmoscope (HRA 2; Heidelberg Engineering, Heidelberg, Germany; excitation light, 488 nm; barrier filter, 500 nm; field of view, $30 \times 30^\circ$), spectral-domain optical coherence tomography (SD-OCT) using a Spectralis OCT platform (Heidelberg Engineering), static visual field testing (Humphrey field analyzer, Model 750i, Zeiss, Germany), microperimetry (Maia, CenterVue, Padova, Italy), and electrophysiological recordings.

Electrophysiology

Full-field ERGs were recorded according to the standard International Society for Clinical Electrophysiology of Vision (ISCEV) protocol with a ColorDome Ganzfeld stimulator (Diagnosys LLC, Lowell, MA, USA) using the 'minimum' and 'extended' protocols.

The minimum protocol included the following: (i) dark-adapted dim flash $0.01 \text{ cd}\cdot\text{s}\cdot\text{m}^{-2}$ (DA 0.01), (ii) dark-adapted bright flash $3.0 \text{ cd}\cdot\text{s}\cdot\text{m}^{-2}$ (DA 3.0), (iii) light-adapted $3.0 \text{ cd}\cdot\text{s}\cdot\text{m}^{-2}$ at 2 Hz (LA 3.0), and (iv) light-adapted $3.0 \text{ cd}\cdot\text{s}\cdot\text{m}^{-2}$ 30 Hz flicker ERG (LA 3.0 30 Hz) (21).

The extended protocol included DA ERGs elicited by flash strengths of 0.001, 0.003, 0.01, 0.03, 0.1, 0.3, 1.0, 3.0, 10.0, 20.0, and $30.0 \text{ cd}\cdot\text{s}\cdot\text{m}^{-2}$, as described in previous reports (3,5,7). Moreover, multifocal ERGs (mfERGs) were recorded with a VERIS Science 6.3.2 imaging system (EDI, San Mateo, CA, USA) under careful monitoring of fixation, according to the ISCEV standard protocol (22). mfERGs with stable fixation were selected for further analysis.

Mutation detection

DNA was extracted from the blood of the proband and his parents using previously described protocols (23), and 21 genes associated with macular dystrophy were sequenced (Supplementary Table 1). Polymerase chain reaction (PCR) amplification and bidirectional sequencing with a genetic

analyzer (ABI PRISM 3100 \times I; Applied Biosystems, Foster City, CA, USA) were performed to confirm the variants, and the co-segregation analysis was conducted.

Molecular genetic analysis

Molecular genetic analyses were conducted for all the detected variants in the *KCNV2* gene, according to a published protocol; URLs for the software and databases are available in a previous report (15). The pathogenicity of each variant was predicted using three different software programs: PolyPhen2, PROVEAN, and Mutation Taster. The allele frequency of each variant was calculated using the GnomAD database. The evolutionary conservation of the affected amino acid residues was assessed using PhastCons, phyloP, and Clustal Omega.

Results

Clinical course

A 17-year-old Chinese male (of Han ancestry) presented to the ophthalmology clinic with a history of photophobia and abnormal color vision since childhood. Ophthalmological examinations were conducted at presentation and subsequently at the ages of 19 and 22. No family history of ocular diseases, general health problems, or consanguinity was reported (Figure 1).

Ocular examination and retinal imaging

At the first visit, the BCVA was 0.15 in both eyes, and this acuity was maintained for 5 years. Fundus photography revealed de-pigmented atrophic changes in both maculae, with optic disk cupping in the right eye. FAF imaging revealed a ring of hyperautofluorescence at the perifovea in both eyes (Figure 2). Serial investigations during the follow-up term demonstrated disappearance of the ring, but clear enlargement of the atrophic areas of low AF density, with well-demarcated macular atrophy being observed in fundus photography by the age of 22 (Figure 2).

On the initial visit, SD-OCT demonstrated loss of photoreceptor layers at the maculae, with a relatively well-maintained RPE. Over the 5-year follow-up period, thinning of the sensory retinal layers was observed, along with clear loss of outer retinal structures and RPE atrophy at the maculae, corresponding to the atrophic area seen on funduscopic/FAF imaging (Figure 2).

The significantly thinned foveal thickness indicated a minimal change over the 5-year period.

Electrophysiological findings

At the first presentation at age 17 (baseline), the b-wave in the DA0.01 condition was delayed in the peak time and reduced in the amplitude (Figure 3a). As the flash strength increased, there was a profound and abnormal increase in the amplitude of the rod-mediated DA ERG b-wave. To the strongest flashes, the DA ERG a-wave was abnormally broad and delayed, and it was similar to a square wave but with a late negative component

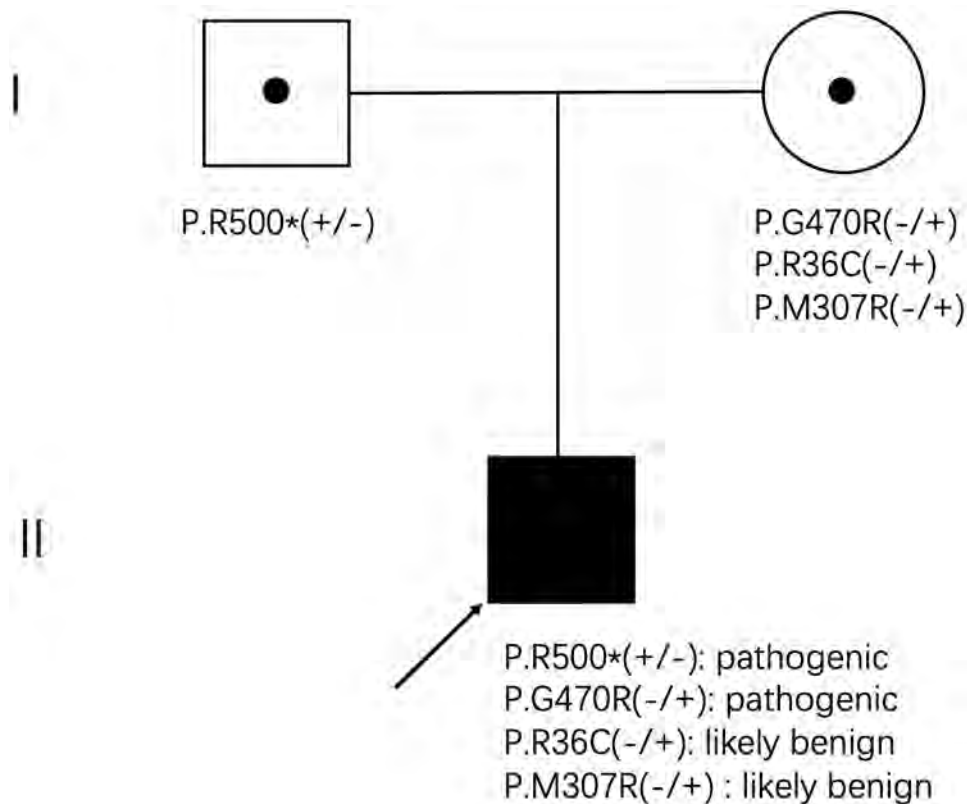


Figure 1. Pedigree and molecular status of a Chinese patient with CDSRR. Arrow indicates the proband. The filled shape indicates the affected individual and dots indicate carrier individuals. The codes indicate function-affecting sequence variations in KCNV2 versus the reference protein (p.) sequence. Amino acid substitutions are represented by one-letter amino acid codes, and an asterisk (*) is used to indicate a variation encoding a translation stopcodon. Square, male; circle, female. The generation number is shown on the left.

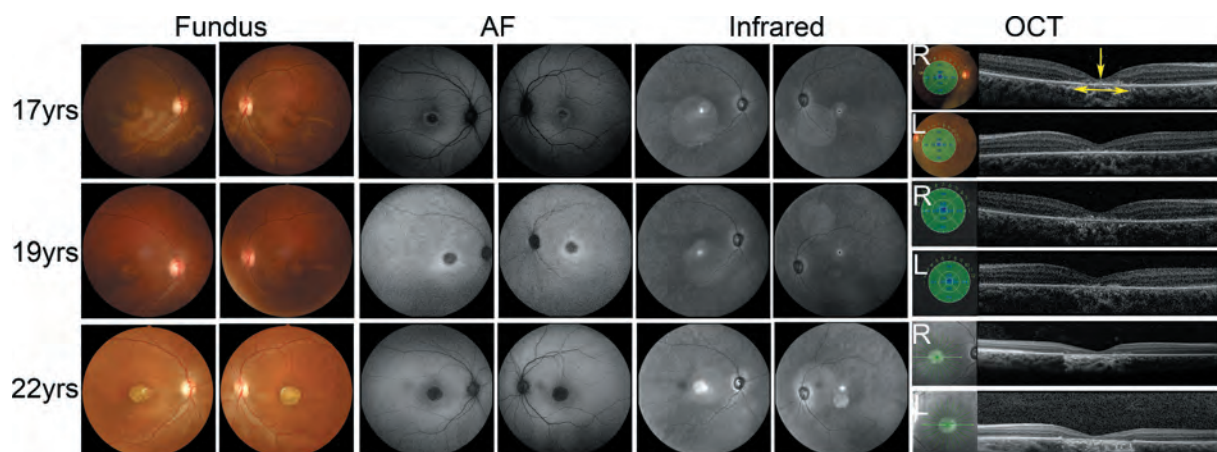


Figure 2. Retinal imaging of a Chinese patient with CDSRR. Serial fundus photographs, fundus autofluorescence (FAF) images, infrared (IR) images and spectral-domain optical coherence tomographic (SD-OCT) images of both eyes of the patient aged 17, 19, and 22 years. Fundus photography revealed a pronounced and well-demarcated area of atrophy which developed over 5 years. FAF imaging detected a corresponding hypo-autofluorescence (low-density) lesion at the initial presentation with a ring change of hyper-autofluorescence around, which developed into a pronounced well-demarcated area of low density. IR imaging revealed a corresponding lesion located at the fovea at the initial presentation, which progressed over the following years. SD-OCT at the initial presentation demonstrated loss of photoreceptor layers at the maculae with a maintained RPE. Over the 5-year follow-up, marked atrophy of the sensory retina and RPE at the macula were observed in a distribution corresponding to the atrophy detected in the other forms of imaging. Fovea is marked by a single-head yellow arrow, and atrophic macular areas are marked by a double-head yellow arrow.

(Figure 3a). No detectable ERG responses were observed in the LA conditions (LA 3.0 and LA 3.0 30 Hz; Figure 3a).

The DA stimulus-ERG response series of our patient were compared with those of age-matched healthy controls (Supplementary Table 2). The shapes of the DA stimulus-ERG

series for the a-waves and b-waves were abnormal at both baseline (age 17 years) and follow-up (19 and 22 years; Figure 3a). The baseline ERGs were undetectable to the dimmest flashes, but the b-waves exhibited abnormal enlargement as the stimulus strength increased (Figure 3a, b-e). In comparison to the control ERGs, the

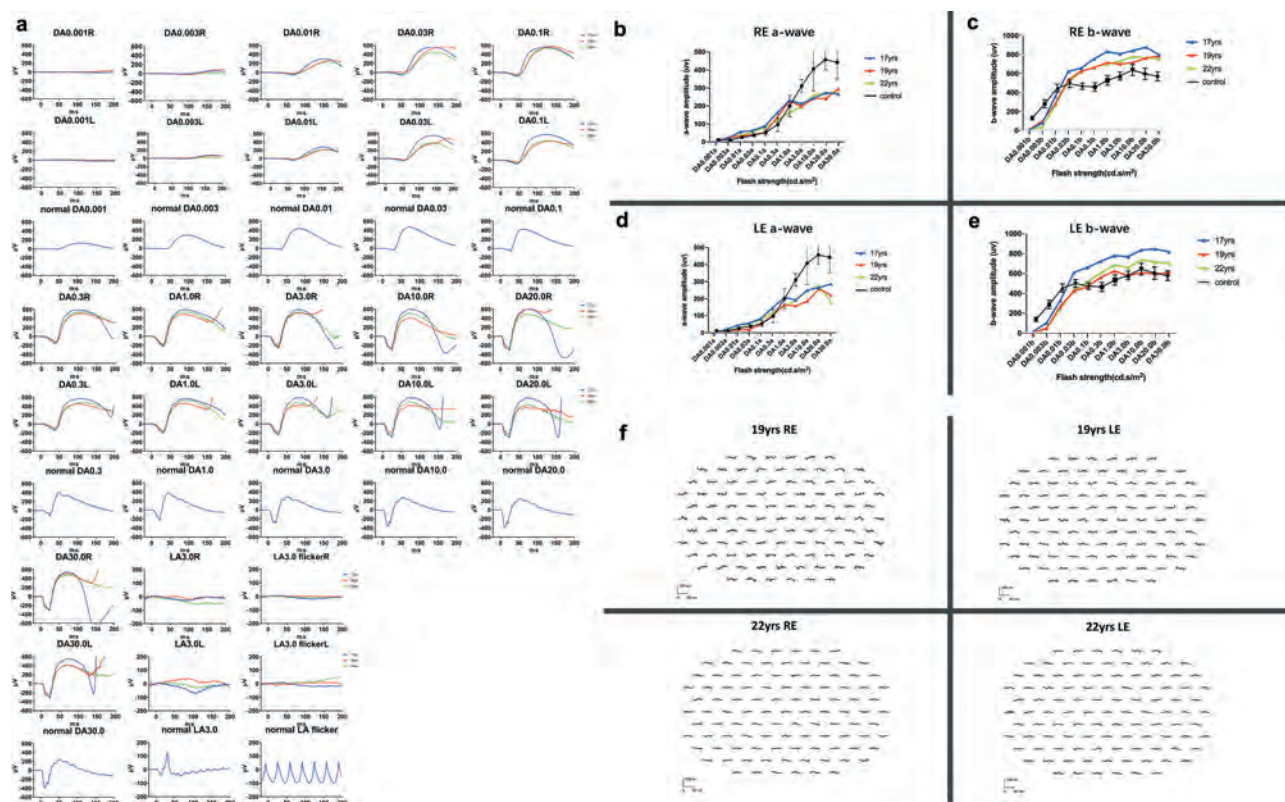


Figure 3. Full-field electroretinogram findings in a Chinese patient with CDSRR and comparison with healthy controls. A) Full-field electroretinograms (ERGs) to a range of flash strengths are shown for the right eye (R) and left eye (L) of the patient and are compared with control data from a representative age-matched individual without retinal disease (N; age 17 years). Patient traces obtained at the ages of 17, 19, and 22 years are shown in red, blue, and green, respectively. The corresponding DA ERG stimulus response series (B, C, D, and E) for the right eye (B, C) and the left eye (D, E). a- and b-waves are shown for each patient visit and compared with averaged control data from four healthy controls (age range 17–30 years); color coding of patient ages as in A); control data is presented in black. F) mfERG trace array for both eyes at the age of 19 and 22 years. mfERGs were undetectable or severely abnormal at both visits and at all eccentricities, consistent with severe widespread macular dysfunction.

baseline a-waves were smaller to flash strengths greater than 1.0 cd.s.m⁻² (Figure 3 b,d) and showed relative stability at follow-up visits, and baseline b-waves were larger to flash strengths greater than 0.03 cd.s.m⁻² (Figure 3 c, e). The follow-up ERG b-waves to the flashes >0.03 cd.s.m⁻² were slightly smaller than those at baseline; the right eye b-waves were similar at the ages of 19 and 22 (Figure 3c), whereas the left eye b-waves were smallest at the last visit (Figure 3e).

The mfERGs demonstrated gross abnormality (i.e. a severe generalised reduction of the traces across all hexagons), consistent with severe cone system dysfunction across the posterior pole (Figure 3F). The mfERGs revealed no significant progression, whereas the FAF images indicated an enlargement of hypoauto-fluorescence at the maculae from 19 to 22 years of age.

Detected variants and pathogenicity analysis

In consideration of the recessive inheritance and phenotypic findings (Figure 1), four rare *KCNV2* variants were listed as candidates for the disease causation, none of which have been previously reported. Co-segregation analysis with the parental samples revealed three maternal missense alleles (c.106 C > T (p.Arg36Cys); c.920 T > G (p.Met307Arg); c.1408 G > C (p.Gly470Arg)) and one paternal nonsense (premature stop codon) allele (c.1500 C > G (p.Tyr500Ter)).

To determine the most likely disease-causing variant in the three maternal variants of the proband, *in silico* (software-based) molecular genetic analysis was performed (Table 1 and Supplementary Table 3), c.1408 G > C (p.Gly470Arg) was considered the pathogenic maternal variant. Evolutional conservation (Supplementary Figure 1) and predicted protein damage based on protein structure (Supplementary Figure 2) of the two pathogenic variants were performed.

Discussion

The clinical and genetic features of a male Chinese patient with CDSRR were described in detail; specifically, *KCNV2* retinopathy and detailed *in silico* molecular genetic analysis. Our results revealed two likely disease-causing variants that have not been previously described in the East Asian population. The progressive atrophy at the macula with maintained VA observed in our case will be valuable for increasing the understanding of the natural course of *KCNV2* retinopathy and help in patient counselling.

The BCVA was well-maintained over this 5-year period. This suggests that the decline in VA, corresponding to the loss of foveal function, occurs early in the disease, and that this is followed by further expansion of macular atrophy. These findings are corresponding to the previous literature that suggests a slow progress of *KCNV2* retinopathy (3,7,9,13). The subjective

Table 1. Results of *In silico* molecular genetic analysis of pathogenic variants in the *KCNV2* gene.

| Exon | Nucleotide substitution | Amino acid change | Report | Polyphen 2 | | Mutation Taster | | Proven(v1,1,3) | | East Asian allele frequency observed by GnomAD | PhyloP | PhastCons | Reference |
|------|-------------------------|-------------------|------------|------------|---------------------|-----------------|-------------|----------------|----|--|--------|-------------|-----------|
| | | | | Prediction | Hum var score (0–1) | Prediction | Prediction | Score | | | | | |
| 2 | c.1408 G > C | p.Gly470Arg | This study | PRD | 1.000 | DC | Deleterious | –7.526 | ND | 6.107 | 1 | ND in dbSNP | |
| 2 | c.1500 C > G | p.Tyr500Ter | This study | NA | NA | DC | NA | NA | 0 | 3.411 | 1 | ND in dbSNP | |

PRD = probably damaging; ND = not detected; Disease causing = DC; NA = not available

Polyphen2(vision 2.2.6) appraises mutations qualitatively as Benign, Possibly Damaging or Probably Damaging based on the model's false positive rate.

Mutation taster (<http://www.mutationtaster.org/>) were used to predict the probable damaging effects of the mutant allele at splicing level and protein expression levels.

GenomAD denotes variants in the Genome Aggregation Database, Cambridge, MA (URL: <http://gnomad.broadinstitute.org>).

Conservation in the positions of the identified variants was evaluated with primate PhyloP and phastCons scores provided by UCSC based on the human genome 19 coordinates (<http://genome.ucsc.edu/cgi-bin/hgTrackUi?db=hg19&g=cons46way>; accessed on August 7th, 2018).

visual reduction detected by the VA measurement is also consistent with the macular dysfunction objectively detected by mfERGs, which is in keeping with the findings reported in previous studies showing undetectable pattern ERG responses in all patients with this disorder irrespective of the macular appearance, the presence of macular atrophy, or age (3).

FAF and SD-OCT were particularly effective for monitoring the disease progression. A hypo-autofluorescence area seen at baseline developed over 5 years into a remarkably well-demarcated area of low density. The ring enhancement at the perifovea disappeared during the development of macular atrophy, which agrees with the previously reported findings (3,9,11). The lack of correlation between serial mfERGs and progressive macular atrophy on FAF imaging likely reflects the severity of macular dysfunction at baseline and the limited spatial resolution of the mfERG technique. Notably, in this case, the DA ERGs only revealed possible borderline reductions over the 5-year period, suggesting the relative stability of peripheral retinal function. Preservation of peripheral retinal function may be crucial for retaining peripheral visual function, which is essential in patients with severe central vision impairment.

The electrophysiological features demonstrated in our case were characteristic of the diagnosis of CDSRR. These unique abnormalities were similar to those previously reported for other cases with *KCNV2* retinopathy (3,5,13). Zobor et al. (24) demonstrated that in six patients with *KCNV2* retinopathy, the a-wave amplitude slowly and continuously increased in strength (from 10^{-3} cd*s/m² to 1.0 cd*s/m²); in contrast, the b-wave amplitude remained low until the flash strength reached 2.5 log cd*s/m² (–0.03 cd*s/m²). In our study, a strong flash (DA10.0) was required to define the characteristic broad and delayed a-wave trough, not clearly visible in the DA3.0 ERG. The amplitude of the b-wave at the strong flash was larger at baseline than at the follow-up visits. At the ages of 19 and 22, mild interocular asymmetries in response to stronger flash strengths were noted, with minimal differences between the follow-up visits on the right eye and mild reduction between visits on the left eye. These asymmetries are unlikely to be clinically significant and they may relate to technical factors and inter-session variability, such as due to small changes in the patient's compliance during testing. Generally, during the follow-up visits, the rod function was stable. In healthy subjects, the DA strong flash ERGs are mixed rod and cone responses. The undetectable LA ERGs at baseline (Figure 3a) suggest that, in this unusual case, DA strong flash ERGs are likely to reflect selective

activation of the rod system, therefore highlighting the relatively high degree of peripheral rod system stability in this disorder.

We demonstrated that our patient is a compound heterozygote for the two novel alleles, p.Gly470Arg and p.Tyr500Ter. The *KCNV2* gene encodes for a 545 amino acid protein, structurally composed of an N-terminal A and B box (NAB), six transmembrane domains (S1–S6), and a pore loop (between S5 and S6) (Supplementary Figure 2). In the East Asian population, a relatively high number of pathogenic variants have been seen around the P loop between S5 and S6. Further population-based studies are required to provide useful ethnicity-based genotype–phenotype correlations.

Further follow-up of this patient and an investigation of other East Asian patients with CDSRR will help us provide better advice to patients regarding useful clinical testing, disease prognosis, and potential treatment of this disease. The sequence variants occurring in the East Asian population are different from those found in the European population; thus, different genetic backgrounds are assumed to be underlying. Although related articles about this disorder involve Asian patients, longitudinal studies are still lacking. A longitudinal clinical and genetic study of a large sample of patients and relatives from multiple ethnicities will be required to confirm if there is a difference based on ethnicity, but such results are particularly important for ethnicity-based education and counseling of patients regarding the likelihood of their children being affected.

In conclusion, this study documented detailed findings over 5 years in a Chinese patient with CDSRR caused by biallelic novel pathogenic *KCNV2* variants. Progressive macular atrophy with maintained VA was observed, with relatively preserved peripheral rod function. This information in the natural course of *KCNV2* retinopathy could help in diagnosing, counselling, and monitoring patients; it could also be beneficial for designing potential therapeutic trials in the East Asian population.

Declaration of interest

The authors report no conflicts of interest. The authors alone are responsible for the content and writing of this article.

Role of the funder

The funding sources had no role in the design and conduct of the study; collection, management, analysis, and interpretation of the data;

preparation, review, or approval of the manuscript; or decision to submit the manuscript for publication.

Funding

Shiyong Li is supported by grants from the National Nature Science Foundation of China (81974138), National Basic Research Program of China (2018YFA0107301), Chongqing Social and Livelihood Science Innovation grant (cstc2017shmsA130100). Kaoru Fujinami is supported by grants from Grant-in-Aid for Young Scientists (A) of the Ministry of Education, Culture, Sports, Science and Technology, Japan (16H06269), grants from Grant-in-Aid for Scientists to support international collaborative studies of the Ministry of Education, Culture, Sports, Science and Technology, Japan (16KK01930002), grants from National Hospital Organization Network Research Fund (H30-NHO-2-12), grants from the Foundation for Fighting Blindness – Alan Lattes Career Development Program (CF-CL-0416-0696-UCL), grants from Health Labor Sciences Research Grant, The Ministry of Health, Labor and Welfare (201711107A), and grants from the Great Britain Sasakawa Foundation Butterfield Awards. Yu Fujinami–Yokokawa is supported by grants from Grant-in-Aid for Young Scientists of the Ministry of Education, Culture, Sports, Science and Technology, Japan (18K16943).

ORCID

Yanling Long  <http://orcid.org/0000-0003-3442-3311>

Kaoru Fujinami  <http://orcid.org/0000-0003-4248-0033>

Shiyong Li  <http://orcid.org/0000-0001-9783-9520>

References

- Alexander KR, Fishman GA. Supernormal scotopic ERG in cone dystrophy. *Br J Ophthalmol*. 1984;68(2):69–78. doi:10.1136/bjo.68.2.69.
- Michaelides M, Holder GE, Webster AR, Hunt DM, Moore AT. A detailed phenotypic study of “cone dystrophy with supernormal rod ERG”. *Digest World Latest Med Information*. 2005;89(3):332–39.
- Robson AG, Webster AR, Michaelides M, Downes SM, Cowing JA, Hunt DM, Moore AT, Holder GE. Cone dystrophy with supernormal rod electroretinogram”: A comprehensive genotype/phenotype study including fundus autofluorescence and extensive electrophysiology. *Retina*. 2010;30(1):51–62. doi:10.1097/IAE.0b013e3181bfe24e.
- Sergouniotis PI, Holder GE, Robson AG, Michaelides M, Webster AR, Moore AT. High-resolution optical coherence tomography imaging in KCNV2 retinopathy. *Br J Ophthalmol*. 2012;96(2):213–17. doi:10.1136/bjo.2011.203638.
- Fujinami K, Tsunoda K, Nakamura N, Yu K, Miyake Y. Molecular characteristics of four Japanese cases with KCNV2 retinopathy: report of novel disease-causing variants. *Mol Vis*. 2013;19(19):1580–90.
- Ajoy V, Anthony R, Graham H. Pathognomonic (diagnostic) ERGs. A review and update. *Retina*. 2013;33(1):5–12. doi:10.1097/IAE.0b013e31827e2306.
- Vincent A, Wright T, Garcia-Sanchez Y, Kisilak M, Campbell M, Westall C, Héon E. Phenotypic characteristics including in vivo cone photoreceptor mosaic in KCNV2-Related “Cone dystrophy with supernormal rod electroretinogram. *Investigative Ophthalmol Visual Sci*. 2013. doi:10.1167/iops.12-10971.
- Stockman A, Henning GB, Michaelides M, Moore AT, Webster AR, Cammack J, Ripamonti C. Cone dystrophy with “Supernormal” Rod ERG: psychophysical testing shows comparable rod and cone temporal sensitivity losses with no gain in rod function. *Invest Ophthalmol Vis Sci*. 2014;55(2):832. doi:10.1167/iops.13-12919.
- Friedburg C, Wissinger B, Schambeck M, Bonin M, Kohl S, Lorenz B. Long-term follow-up of the human phenotype in three siblings with cone dystrophy associated with a homozygous p. G461R mutation of KCNV2. *Invest Ophthalmol Vis Sci*. 2011;52(12):8621–29. doi:10.1167/iops.11-8187.
- Guimaraes TACD, Georgiou M, Robson AG, Michaelides M. KCNV2 retinopathy: clinical features, molecular genetics and directions for future therapy. *Ophthalmic Genet*. 2020;41(19):1–8. doi:10.1080/13816810.2020.1766087.
- Grigg JR, Holder GE, Billson FA, Korsakova M, Jamieson RV. The importance of electrophysiology in revealing a complete homozygous deletion of KCNV2. *J Am Asso Pediatric Ophthalmol Strabismus*. 2013;17(6):641–43. doi:10.1016/j.jaapos.2013.08.006.
- Wu H, Cowing JA, Michaelides M, Wilkie SE, Jeffery G, Jenkins SA, Mester V, Bird AC, Robson AG, Holder GE. Mutations in the gene KCNV2 encoding a voltage-gated potassium channel subunit cause “Cone dystrophy with supernormal rod electroretinogram” in humans. *Am J Hum Genet*. 2006;79(3):0–579. doi:10.1086/507568.
- Kutsuma T, Katagiri S, Hayashi T, Yoshitake K, Iejima D, Gekka T, Kohzaki K, Mizobuchi K, Baba Y, Terauchi R, et al. Novel allelic loss-of-function KCNV2 variants in cone dystrophy with supernormal rod responses. *Doc Ophthalmol*. 2019;138(3):229–239. doi:10.1007/s10633-019-09679-6
- Kaoru F, Shuhei K, Sachiko K, Shinji U, Mineo K. Novel RP11L variants and genotype-photoreceptor microstructural phenotype associations in cohort of Japanese patients with occult macular dystrophy. *Invest Ophthalmol Vis Sci*. 2016;57(11):4837–4846. doi:10.1167/iops.16-19670.
- Huang L, Xiao X, Li S, Jia X, Wang P, Sun W, Xu Y, Xin W, Guo X, Zhang Q, et al. Molecular genetics of cone-rod dystrophy in Chinese patients: new data from 61 probands and mutation over-view of 163 probands. *Exp Eye Res*. 2016;146:252–58.
- Zelinger L, Wissinger B, Eli D, Kohl S, Banin E. Cone dystrophy with supernormal rod response: novel KCNV2 mutations in an underdiagnosed phenotype. *Ophthalmology*. 2013;120(11):2338–43. doi:10.1016/j.ophtha.2013.03.031.
- Ritter M, Vodopituz J, Lechner S, Moser E, Janecke AR. Coexistence of KCNV2 associated cone dystrophy with supernormal rod electroretinogram and MFRP related oculopathy in a Turkish family. *Br J Ophthalmol*. 2013;97(2):169–73. doi:10.1136/bjophthalmol-2012-302355.
- Wissinger B, Dangel S, Ja’gle H, Hansen L, Baumann B, Rudolph G, Wolf C, Bonin M, Koeppen K, Ladewig T. Cone dystrophy with supernormal rod response is strictly associated with mutations in KCNV2. *Invest Ophthalmol Vis Sci*. 2008;49(2):751. doi:10.1167/iops.07-0471.
- Salah SB, Kamei S, Séné-Hal A, Lopez S, Bazalgette C, Bazalgette C, Eliaou CM, Zanlonghi X, Hamel CP. Novel KCNV2 mutations in cone dystrophy with supernormal rod electroretinogram. 2008;145(6):1099–106. doi:10.1016/j.jao.2008.02.004.
- McCulloch DL, Marmor MF, Brigell MG, Hamilton R, Holder GE, Tzekov R, Bach M. ISCEV Standard for full-field clinical electroretinography (2015 update). *Documenta ophthalmologica*. 2015;130(1):1–12. doi:10.1007/s10633-011-9296-8.
- Hood DC, Bach M, Brigell M, Keating D, Kondo M, Lyons JS, Marmor MF, McCulloch DL, Palmowski-Wolfe AM, Vision FtiSFCEo. ISCEV standard for clinical multifocal electroretinography (mfERG) (2011 edition). *Documenta Ophthalmol*. 2012;124(1):1–13. doi:10.1007/s10633-011-9296-8.
- Nasiri H, Forouzandeh M, Rasaei M, Rahbarizadeh F. Modified salting-out method: high-yield, high-quality genomic DNA extraction from whole blood using laundry detergent. *J Clin Lab Anal*. 2005;19(6):229–32. doi:10.1002/jcla.20083.
- Ditta Z, Susanne K, Bernd W, Eberhart Z, Herbert JG, Den HAI. Rod and Cone Function in Patients with KCNV2 Retinopathy. *Plos One*. 2012;7(10):e46762. doi:10.1371/journal.pone.0046762.
- Otschytch N, Raes A, Van Hoorick D, Snyders DJ. Obligatory heterotetramerization of three previously uncharacterized Kv channel γ -subunits identified in the human genome. *Proc Natl Acad Sci U S A*. 2002;99(12):7986–91. doi:10.1073/pnas.122617999.